A GENERALIZED THEORY FOR FLY ASH MODIFIED SOILS

A dissertation presented to

the faculty of the

the Fritz J. and Dolores H. Russ

College of Engineering and Technology of Ohio University

In partial fulfillment

of the requirements for the degree

Doctor of Philosophy

Kwame Adu-Gyamfi

March 2006

This dissertation entitled

A GENERALIZED THEORY FOR FLY ASH MODIFIED SOILS

by

KWAME ADU-GYAMFI

has been approved for

the Department of Civil Engineering

and the Russ College of Engineering and Technology by

L. Sebastian Bryson

Assistant Professor of Civil Engineering

Dennis Irwin

Dean, Fritz J. and Dolores H. Russ College of Engineering and Technology

A B S T R A C T

ADU-GYAMFI, KWAME. Ph.D. March 2006. Civil Engineering

A Generalized Theory for Fly Ash Modified Soils (247 pp.)

Director of Dissertation: L. Sebastian Bryson

The disposal of fly ash (particularly class F fly ash) is increasingly becoming a problem, and the way to solve this problem safely and economically is by utilization. Due to the unique behavior of fly ashes, it has not been widely used in soil modification applications. To improve or increase fly ash utilization, this study seeks to develop a generalized theory that can adequately predict the behavior of fly ash modified soils and to quantify the uncertainties in the behavior of the ash, which hinders its wide application in soil modification.

For this study, laboratory tests were performed on mixtures made from three different fly ashes of different chemical compositions. The laboratory tests were designed such that all the necessary properties needed for the analyses were addressed as well as data gaps observed in the literature. The laboratory testing provided engineering (index, deformation, and strength) properties and the necessary physicochemical properties of mixtures at various fly ash percentages for all the mixtures were determined.

Three mixture theory models were used to predict engineering properties based on the properties of individual constituents. The predictive accuracies of three models were assessed, and the model that best predicted actual results was selected for modification. The need for modification is because of deviations in the model predictions. The selected model was that of Voigt (1889).

Upon physicochemical analysis, it was observed that the chemical composition of the fly ashes play a significant role in the behavior of the modified soils, particularly that of calcium oxide (CaO). A relationship was found between CaO and the sum of oxides (SiO_2+Al_2O_3+Fe_2O_3) in the fly ashes. As a result, the selected model was modified based on the two chemical components (CaO and the sum of oxides) of the fly ashes. A modification term (α) was defined as a ratio between the CaO and the sum of oxides raised to an experimental index (*x*). The α term varied with respect to engineering properties. The variation was found to be dependent on the experimental index (*x*). The modified model performed well in predictions of laboratory data and data from the literature.

Due to the improvements observed in the modified model's predictions, it is believed that it can be widely applicable to a wide variety of fly ash-modified soils.

Approved:

L. Sebastian Bryson

Assistant Professor of Civil Engineering

To My Family and Friends and

All My Teachers (both past and present).

TABLE OF CONTENTS

LIST OF TABLES

TABLE PAGE

LIST OF FIGURES

FIGURE PAGE

CHAPTER 1 : INTRODUCTION

1.1 INTRODUCTION

Coal is used in generating electricity in many parts of the world. Increasing demand of electricity from coal-burning power stations causes an increase in the generation of coal combustion by-products (CCPs). Coal combusted by-products include fly ash, bottom ash, boiler slag, and Flue Gas Desulphurized (FGD) materials.

According to the American Coal Ash Association (ACAA) survey (http://www.acaa-usa.org/PDF/2004_CCP_Survey(9-9-05.pdf)), CCP produced in the U.S. in the year 2004 was estimated to be 122.5 million tons. Fly ash is the most generated CCP in the country and poses the most significant disposal problems. It constituted 70.8 million tons (57.8%) of the total CCP produced in 2004, of which 39.7% was utilized in various engineering and agricultural applications. The remaining CCP produced went to landfill sites.

Coal power stations account for about 90% of coal consumed in Ohio and supply about 90% of the state's electricity. The state produces about 10 million tons of CCP per year, and almost half of the CCP produced is fly ash. Of the fly ash produced in Ohio, less than 20% is utilized beneficially in various engineering applications. Again, the remaining fly ash goes to landfills in the state and surrounding regions. The disposal of this material in an economical and environmentally acceptable manner has become a public concern. The most desirable alternative to disposal is utilization, which provides the economic benefit of cost reduction by replacing traditional civil engineering building materials, and mitigates possible adverse environmental effects associated with land filling. If treated and applied correctly,

these materials have various properties that make them suitable raw material for many uses ranging from highway/civil engineering to agricultural applications.

In particular, the focus of this research is on fly ash-modified soils. There are two main types of fly ash, Class F and Class C, according to the American Society of Testing Materials (ASTM) C 618. Class C fly ash has calcium oxide content greater than 20% and is self-cementing in the presence of water. Class C fly ash is mostly utilized in concrete due to its self-cementing properties. Class F fly ash typically has less than 10% calcium oxide and is almost not self-cementing in the presence of water. Fly ash with calcium oxide between 10% and 20% is classified as low Class C. This research specifically deals with Class F fly ash. This type (Class F) is the most generated and the least utilized among the two fly ashes and poses the greatest disposal problems.

The concept of soil stabilization or modification through the addition of additives to improve the engineering properties of soft soils has been around for a long time. With the scarcity of conventional aggregates and reduced capacity in landfills, attention has drifted onto turning some waste products into beneficial use. The highway and transportation industry has used fly ash for the purpose of soil stabilization. Some primary highway applications of the fly ash-modified soils include soil stabilization for increased stability of embankment and foundation systems (i.e. soil mixing applications), and soil stabilization to improve soft subgrade (i.e. road embankment applications). However, fly ash-modified soils have traditionally not been widely used. One of the main reasons for the limited use of fly ash-modified soils is that the chemical and mechanical properties of the fly ash are batch-specific. It has been found that even fly ash generated from the same coal source at different

times from the same plant behaves differently (Naik, 2002; Tsimas, 2005). Consequently, there is poor understanding of the behavior of fly ash-modified soils. Also, lack of a unified theoretical framework for characterizing and modeling soil mixtures contributes to the reason why the behavior of fly ash-modified soils has not been fully understood.

It has been observed that a wide range of theories in soil mechanics are response-based and mainly involve the basic soil types: clays and sands. Most constitutive models for soils are also applicable to pure sands and clays. These concepts usually fall short in addressing the problems involving soil mixtures. Soil mixtures by definition are materials consisting of two or more different soil types. As a result it becomes difficult to predict the effects of soil constituent variations on soil mixtures. This is because variations in the soil components can alter the mixture in such a way that it behaves as an entirely different material. There is therefore the need to improve the fundamental understanding of the behavior of the constituents of soil mixtures when they are combined and how the constituent properties influence the overall behavior of the soil mixture. Researchers (Vallejo and Mawby, 2000; Kumar and Wood, 1997; Stovall et al, 1996; Fragaszy et al., 1992) have conducted both theoretical and experimental studies on soil mixtures to analyze strengths, density, deformation, permeability, etc. Their studies revealed that the behavior of soil mixtures is complex. Often researchers present the experimental results of the soil mixtures, but do not present data pertaining to the individual constituents of the mixtures. Consequently, the effects of the constituents on the mixture are not adequately evaluated. The behavior of one mixture cannot reliably be compared to the behavior of another mixture, unless the contribution of the individual constituents is ascertained.

It is commonly acknowledged that the properties of fly ash depend on the source of coal and the burning technique. However, there has not been any known attempt in the literature to develop generalized theory to predict the unique engineering behavior of fly ash-modified soils. It is necessary to understand the unique behavior of fly ashes. This will aid in soil modification applications with limited known properties of the fly ash and soil type, hence the focus of this research. This research investigates behavior of fly ash-modified soils and develops a model which will be applicable to a range of fly ash-modified soils.

For this research, the behavior of soil mixtures derived from three different fly ashes is considered. Predictive models relying on individual constituents are used in assessing the behavior of the ash mixtures. These models are then modified based on the predictive accuracy and the physical and chemical interaction between the ash and the clay particles. The modified models are then validated with data from literature to ensure a wide range of applicability. The intent of this predictive model is to reduce uncertainties surrounding the behavior of fly ash in fly ash-modified soils, which has hindered its wide application in soil stabilization. It is believed that this will contribute to an increase in the use of fly ash in soil stabilization by optimizing the quantity of ash required to achieve better engineering properties.

1.2 RESEARCH OBJECTIVES

The focus of this study is on fly ash-modified soils with emphasis on Class F fly ash. The goal is to develop a generalized theory that can be used to predicting the behavior of a wide

range of fly ash-modified soil mixtures. The following are the objectives leading to the achievement of the set goal of the study:

1. Perform comprehensive literature review to ascertain the state-of-the-art mixture theory and fly ash-modified soils. From this, three of the most promising the mixture models will be selected to assess their predictive capabilities on fly ash-modified soils.

2. Extract data from literature for mixture theory modeling and physicochemical interaction assessment of fly ash-modified soils. This will help in analyzing trends and any nuances associated with the models.

3. Conduct laboratory experiments on mixtures of four different fly ashes and clay to obtain engineering properties. Also, obtain the chemical composition of each fly ash to help in physicochemical assessment.

4. Evaluate the effect of fly ash proportion in mixtures consisting of various proportions of fly ash the mixtures in terms of volume fractions.

5. Assess the predictability of the mixture theory models and the influence of fly ash chemical composition on the mixtures using laboratory results. The trends will be compared to the assessment with literature data.

6. Based on the mixture theory models predictions, select the model with the best predicted results for modification.

7. Develop an improved mixture model based on the chemical composition of the fly ashes, which incorporates physicochemical effects into mixture theory model predictions to improve predictability.

8. Validate the improved model using data from literature.

9. Transform data from the improved model and laboratory test results into a critical state model, which can be used in predicting behavior with little information on the mixtures.

It is believed that the generalized model that emerges from the study will be applicable to a wide variety of fly ash modified soils.

1.3 OUTLINE OF DISSERTATION

The general pattern of presentation in the subsequent chapters is as follows: Chapter 2 will present the background of this study including a general presentation of mixture theory. Also presented in this chapter are results from similar studies found in the literature. In Chapter 3, data from literature are analyzed using various mixture models, and their strengths and limitations are discussed. Presentation and analyses of laboratory data from this study is presented in Chapter 4. This will attempt to address the data gaps found in Chapter 2. Chapter 5 assesses the predictive abilities of the models on research data. Based on the performance of the models, modifications will be made to a specific model to enhance their predicting abilities, based on physicochemical interaction. The modified model will be validated using the data from literature. The model modification and validation will

be presented in Chapter 6. Conclusion based on the findings of this study and recommendation for further research will be presented in Chapter 7.

CHAPTER 2 : RESEARCH BACKGROUND

2.1 MIXTURE THEORY MODELS

2.1.1 INTRODUCTION

Mixture theory is the study of composite material behavior, often referred to as mixtures, where the interaction of individual constituents are examined on a microscopic scale and is used to predict and define the behavior of the heterogeneous composite material. A mixture theory model predicts the properties of the composite mixtures from the properties and volume fractions of the individual constituents (Tien et al., 2004). The theory considers a mixture to consist of at least two interacting and interpenetrating continua. Continuum mechanics is usually applied to solve many discrete media problems.

The concept of mixture theory concentrates on the mass balance, momentum, and entropy of the mixtures. Some good references on the subject include papers by Bedford and Drumheller (1983), Hansen (1989), and Hansen et al. (1991). In recent years, the theory has been used in various field of application such as modeling and evaluation of mechanical properties of asphaltic concrete (Wang et al., 2004; Krishnan and Rao, 2001, 2000), evaluation of dental materials (Braem et al., 1987; Chantler et al., 1999; and Sakaguchi et al., 2004), flow through porous media (Morland et al., 2004; 1978, Passman, 1977), and soil stabilization (Tien et al., 2004; Omine et al., 1998).

2.1.2 GENERAL MIXTURE THEORY MODEL FORMULATION

Mixture theory considers the microstructure of the constituent materials in a mixture. The concept of mixture theory was originally proposed for modeling fluid mixtures and granular flow properties. Many different theories based on the concept of mixture theory have been developed over the years. The foundation of the mixture theory concept is that, all properties of the mixture must be the mathematical consequences of the properties of the constituents. Of all the many mixture theories that have been proposed (Dorban, 1985; Drumheller and Bedford, 1980; Twiss, 1975; Twiss and Eringen, 1974; Muller, 1968), the underlying philosophy of thermodynamics and conservation laws governing the behavior of the mixtures remains the same. Volume fraction-based mixture theory is considered to be well suited for solid state and granular materials (Passman, 1977; Goodman and Cowin, 1971, 1972; Hansen et al., 1991).

An important variable in volume fraction-based mixture theory is the volume fractions of the constituents and their gradients. The general derivation of the volume fraction mixture theory is based on work done by Hansen et al. (1991). Consider the deformation of a particle of each jth constituent in a mixture of n constituents to be given by

$$x_j = \chi(X_j, t) \tag{2.1}$$

where x_j and X_j represents the coordinates of the deformed and reference configuration of the jth particle. The velocity ($\dot{x}_j$), acceleration ($\ddot{x}_j$), and the velocity gradient (L_j) are given as:

$$\dot{x}_j = \frac{\partial \chi(X_j, t)}{\partial t} \tag{2.2}$$

$$\ddot{x}_j = \frac{\partial^2 \chi(X_j, t)}{\partial t^2} \tag{2.3}$$

$$L_j = \frac{\partial \dot{x}_j}{\partial x} \tag{2.4}$$

If ρ_j is the density of the j[th] particle, then it follows that the density of the mixture, ρ can be expressed as

$$\rho = \sum_j \rho_j \tag{2.5}$$

The velocity of the mixture can therefore be expressed as

$$\rho \dot{x} = \sum_j \rho_j \dot{x}_j \tag{2.6}$$

The balance equations for mass, momentum and energy are given by

Balance of mass:

$$c_j = \dot{\rho}_j + (\nabla \rho_j \dot{x}_j) \tag{2.7}$$

Balance of linear momentum:

$$\rho_j \ddot{x}_j = \nabla t_j + \rho_j b_j + p_j \tag{2.8}$$

Balance of angular momentum:

$$m_j = t_j - t_j^T \tag{2.9}$$

Balance of energy:

$$\rho_j J_j = tr\left(t_j^T L_j\right) - \nabla \cdot q_j + \rho_j r_j \tag{2.10}$$

where c_j = mass supplied, p_j = linear momentum, m_j = angular momentum, ρ_j = partial density, t_j = partial stress tensor, and b_j = body force. The subscript, refers to the j[th] constituent. The energy terms $J_j, q_j,$ r_j denotes internal energy, heat flux, and heat supplied, respectively. The superscript T in Equations 2.9 and 2.10 denotes the transpose of the matrix of the stress tensor in three dimensional space, and the term *tr* denotes the trace of the matrix. The partial density, ρ_j, of the j[th] constituent can be expressed in terms of volumetric fraction and the true density of the constituent. This is explained in equation form as

$$\rho_j = \frac{m_j}{V} \tag{2.11}$$

$$\gamma_j = \frac{m_j}{V_j} \tag{2.12}$$

where m_j is the mass of the j^{th} constituent, and γ_j is the true density of the j^{th} constituent. Combining Equations 2.11 and 2.12 gives an expression of partial density in terms of

volume fraction and true density as can be seen in Equation 2.13. The volume fraction is defined as the ratio of the volume of the individual constituent to that of the total volume of the mixture. This is given in equation form as

$$\rho_j = f_j \gamma_j \tag{2.13}$$

$$f_j = \frac{V_j}{V} \tag{2.14}$$

where V is the total volume of the mixture, and V_j is the volume of the jth constituent. According to Equation 2.14, in the absence of constituent j, the volume fraction f_j will be equal to zero. Similarly if the mixture consists solely of constituent j then the volume fraction f_j will be equal to one. This therefore implies that the volume fraction ranges between 0 and 1, by definition (i.e. $0 \leq f_j \leq 1$). For a number of constituents forming the mixture and occupying the mixture volume, the total volume of the mixture is given by

$$V = \sum_{j=1}^{n} V_j \tag{2.15}$$

and the sum of volume fractions of all constituents in the mixture is given by

$$\sum_{j=1}^{n} f_j = 1 \tag{2.16}$$

Volume fraction can also be expressed in gravimetric form as the ratio of individual weights of the constituents to the total weight of the mixture.

Hansen et al. (1991) pointed out that a significant aspect of the volume fraction theory is the restrictions imposed on the supply terms. These are given as:

$$\sum_j c_j = 0 \tag{2.17}$$

$$\sum_j p_j = 0 \tag{2.18}$$

$$\sum_j m_j = 0 \tag{2.19}$$

$$\sum_j J_j = 0 \tag{2.20}$$

The restrictions represents interaction between constituents, and implies that constituent A acting on constituent B is the negative of the effect of constituent B acting on constituent A. These results hold for all mixtures, and are valid for exchanges of mass, momentum, and energy.

The behavior of the mixture is governed by the sum of the constituent equations. From Equation 2.13, the total density of the mixture can be expressed as

$$\rho = \sum_{j=1}^{n} f_j \gamma_j = \sum_{j=1}^{n} \rho_j \tag{2.21}$$

The implicit presence of volume fraction leads to the mixture definition of the terms describing the constituent particles. In the case of the stress tensor, the partial stress traction is influenced by the area fraction of the particular constituent. According to Hansen et al.

(1991), quantitative stereology shows that area fraction of a randomly distributed mixture is identical to volume fraction; hence partial stress is also scaled by volume fraction. The definitions of the parameters governing the behavior of the mixture can therefore be expressed in terms of volume fractions and are given in equation form as follows:

$$\dot{x} = \sum_{j=1}^{n} f_j \dot{x}_j \qquad 2.22$$

$$\sum_{j=1}^{n} \rho_j \ddot{x}_j = \sum_{j=1}^{n} f_j \gamma_j \ddot{x}_j \qquad 2.23$$

$$t = \sum_{j=1}^{n} f_j t_j \qquad 2.24$$

$$J = \sum_{j=1}^{n} f_j J_j \qquad 2.25$$

$$q = \sum_{j=1}^{n} f_j q_j \qquad 2.26$$

where $\dot{x}$ = velocity, $\ddot{x}$ = acceleration, q = heat flux, ρ = density, J = internal energy, and t = stress tensor. The subscript refers to the jth constituent.

In general, the relationship for determining the effective properties of mixtures using the concept of volume fraction can be illustrated in equation form as

$$y = \sum_{j=1}^{n} f_j y_j \qquad 2.27$$

where y is the effective property of the mixture and y_j is that property of the j^{th} individual constituents forming the mixture.

Consider a binary mixture of two non-reactive materials with no mass transfer. A binary mixture consists of two different materials where the primary material is termed the matrix and the secondary material called inclusion. The inclusion is usually distributed randomly in the matrix. For binary mixtures, Equation 2.27 becomes

$$y = f_1 y_1 + f_2 y_2 \tag{2.28}$$

Subscripts 1 and 2 in Equation 2.28 can be replaced by i and m, denoting inclusion and matrix shown in Equations 2.29 and 2.30, respectively

$$y = f_i y_i + f_m y_m \tag{2.29}$$

and

$$f_i + f_m = 1 \tag{2.30}$$

From Equations 2.29 and 2.30 the basic form of mixture theory for binary mixtures can be rewritten as

$$y = f_i y_i + (1 - f_i) y_m \tag{2.31}$$

2.2 MIXTURE THEORY APPLIED TO SOILS

Most experimental and theoretical analyses of soil behavior has typically assumed ideal soils such as pure clays or uniform sands. However, many natural soils consist of coarse granular particles in a matrix of finer particles or vice versa. The properties of natural or

man-made mixtures are expected to be intermediate between that of the individual constituent materials. The estimate of these properties can be done using mixture theory models.

2.2.1 EFFECT OF INCLUSIONS ON MIXTURE BEHAVIOR

The behavior of soil mixtures is expected to be influenced by both the particle size and other index properties of the materials present. Void ratio is an index used to characterize the degree of packing of soils with different fines content or particle sizes. The effective void ratio of a soil mixture can be determined by the volume fractions and void ratios of the individual constituents. This is given by the equation

$$e_{eff} = e_c f_c + e_f f_f \tag{2.32}$$

where e_{eff} = effective void ratio; and subscripts *c*, and *f* denotes coarse and fine, respectively. The shape and surface roughness of particles affects the porosity and the effective packing void ratio of multi-sized particles. The maximum and minimum void ratios of spherical particles are lower in packing than that of angular shaped particles. The fractions of individual constituents in mixtures also tend to influence the properties of the mixture, but the optimum percentage required to significantly alter the mixture properties is the question. This is important to achieve the desired engineering properties for mixtures such as fly ash-modified soils, which are used in this research.

2.2.1.1 COARSE MATRIX, FINE INCLUSIONS

For binary mixtures of coarse and fine particle sizes, a minimum porosity is reached at a volume fraction of the small particles at approximately between 30% and 40% (Santamarina, 2001, and Vallejo et al., 2000). Santamarina (2001) indicated that the higher the disparity in particle sizes (i.e. high coefficient of uniformity) the lower the void ratio in the mixture. This is illustrated in Figure 2.1 where R_d represents the size ratio between the larger particle and fine particle sizes forming the mixture.

A similar behavior was reported by Vallejo (2001). He used small and large beads to represent sand and gravel in his laboratory experiment. A relation for porosity of the mixture was given by

$$n_{mix} = \frac{V_0 - \left(\frac{W_c}{\gamma_c} + \frac{W_f}{\gamma_f}\right)}{V_0} \qquad 2.33$$

where V_0 is the bulk volume of the mixture after a 24-hour application of normal stress; W is the weight, γ is the unit weight, and the subscripts *c* and *f* denotes coarse and fine, respectively. The concentration by weight of the coarse particles, ω_c, was also given by the relation

$$\omega_c = \frac{W_c}{W_c + W_f} \qquad 2.34$$

It was observed that n_{mix} was dependent on ω_c, and that the porosity of the individual constituents was higher than the porosity of the mixture. The theoretical minimum porosity was also given by the relation

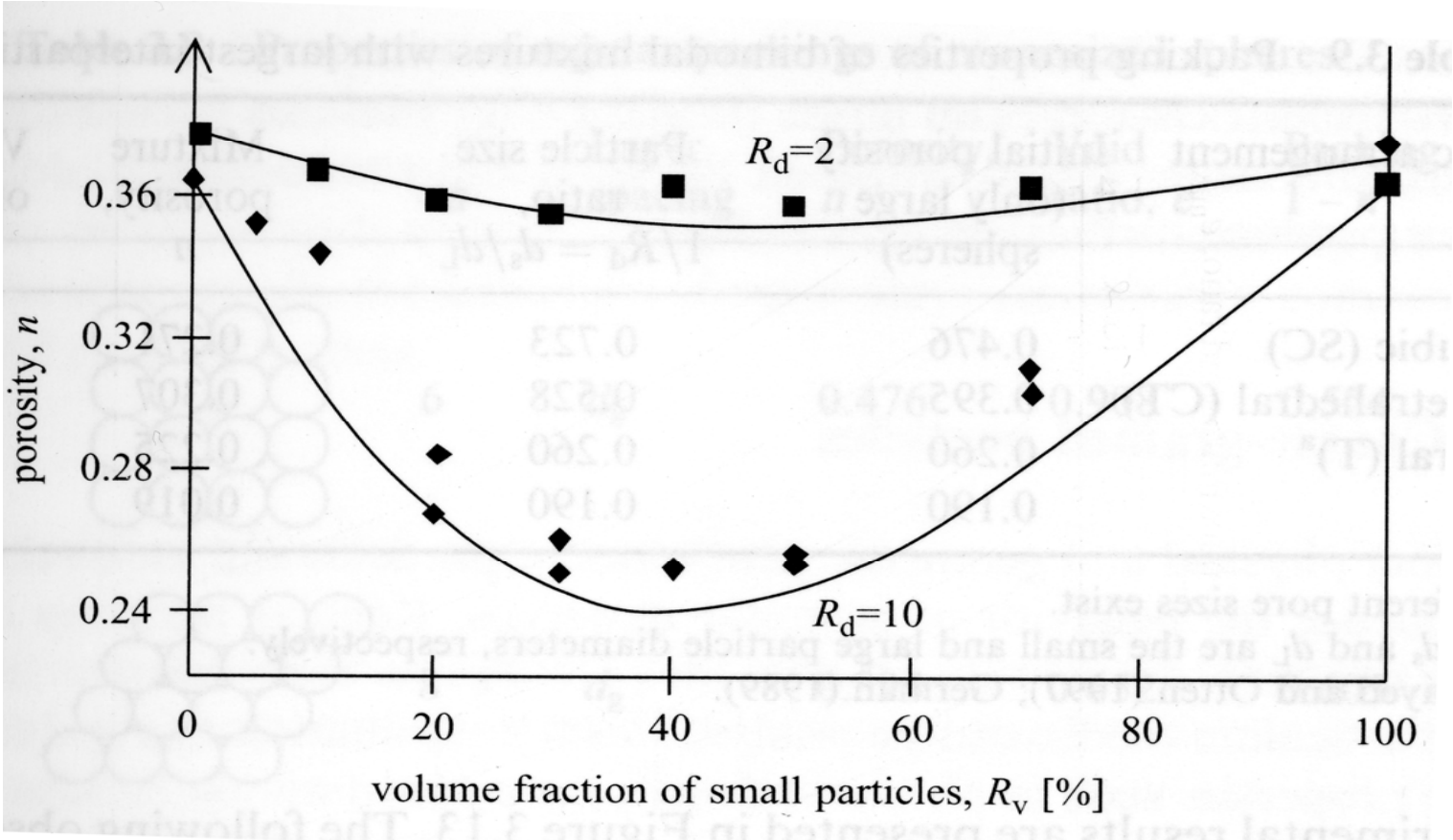

Figure 2.1 Effect of Ratio of Particle Sizes and Volume Fraction on the Porosity of a Binary Mixture (Satamarina, 2001)

$$n_{mix-\min} = n_f n_c \tag{2.35}$$

The concentration of coarse grains at minimum porosity is also governed by

$$\omega_{c-\min} = \frac{(1-n_c)\gamma_c}{n_c(1-n_f)\gamma_f + (1-n_c)\gamma_c} \tag{2.36}$$

Figure 2.2 present data reported by Vallejo (2001). In the figure, two points of transition (*d* and *f*) were observed. It can be observed in Figure 2.2 that the laboratory minimum porosity occurs within the range of 20% to 40% of the volume fraction of the fine particles, while the theoretical minimum occurs at 25%. The laboratory results reported by Vallejo (2001) are in accordance with data reported by Santamarina (2001). The transition range (20% to 40%) observed in Figure 2.2 coincides with a trend change in the peak shear strengths of the mixtures as seen in Figure 2.3 at the different normal stresses.

The properties (porosity and shear strength) of the mixture are controlled partially by the constituents of the binary mixture within the points of transition. Beside this region the properties are controlled fully by either constituent depending on the weight concentration.

A minimum porosity was observed in the study, and this represents the point that separates coarse grain controlled structure and partially fine grain controlled structure. It was found that behavior change in the coarse grained control, partially coarse-fine grained controlled, and fine grained controlled regions are similar in both porosity and shear strength determination according to the study.

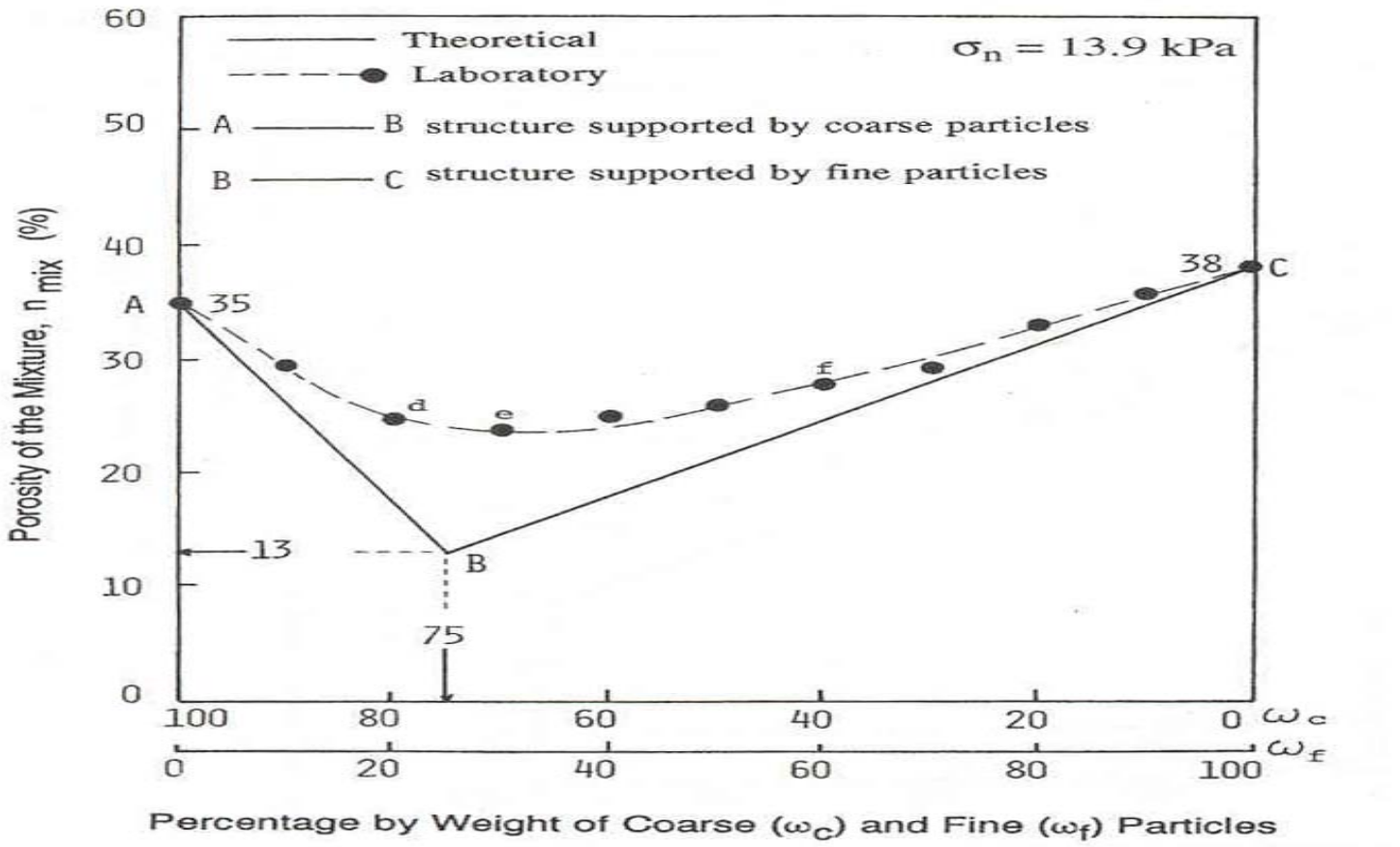

Figure 2.2 Effect of Volume Fraction on the Porosity of a Binary Mixture (Vallejo, 2001)

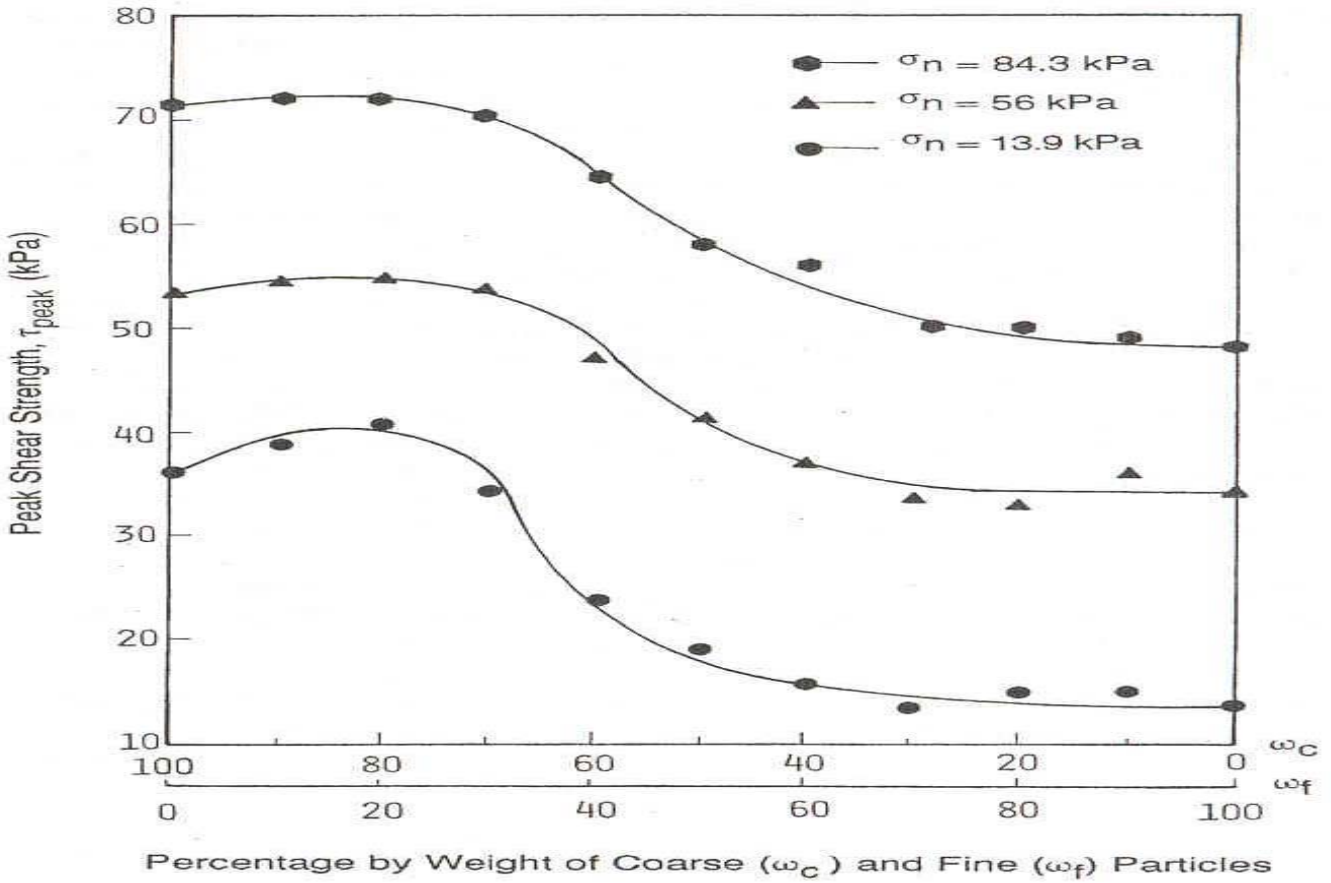

Figure 2.3 Effect of Volume Fraction on Peak Shear Strength of a Binary Mixture (Vallejo, 2001)

2.2.1.2 FINE MATRIX, COARSE INCLUSIONS

Kumar and Wood (1997) conducted a study on mixtures of clay with increasing proportions of coarse sand. The two materials were different in both particle size and mineral character; this is similar to the case of fly ash-modified soils.

Tests performed by Kumar and Wood (1997) on the mixtures included liquid limit, permeability, one dimensional compression and consolidated drained (CD) and consolidated undrained (CU) triaxial compression. They observed a behavior change after 20% of the clay content. Figure 2.4 shows change in the trend of permeability after 20% clay content. Considering that the particles of the fly ash are coarser than the clay particles, Kumar and Wood's (1997) study can be applied to fly ash-modified soils.

Georgiannou et al. (1990) conducted a similar test by adding kaolin clay to river sand. It was determined that the mechanical behavior of the sand began to be affected when the clay content of the mixture reached about 30%. The above discussion gives an idea on the effect of proportional changes in individual constituents in binary mixtures on engineering properties. This concept will be investigated in the study of fly ash-modified soils.

2.3 EXISTING MIXTURE THEORY MODELS

Several phenomenological models have been developed based on mixture theory discussed above to help predict mechanical properties of mixtures. There has been several modifications of the theories based on different principles, however, only the models relevant to this study are discussed here. The most relevant to this study are models with underlying principles based on the concept of volume fractions discussed in Section 2.1.2.

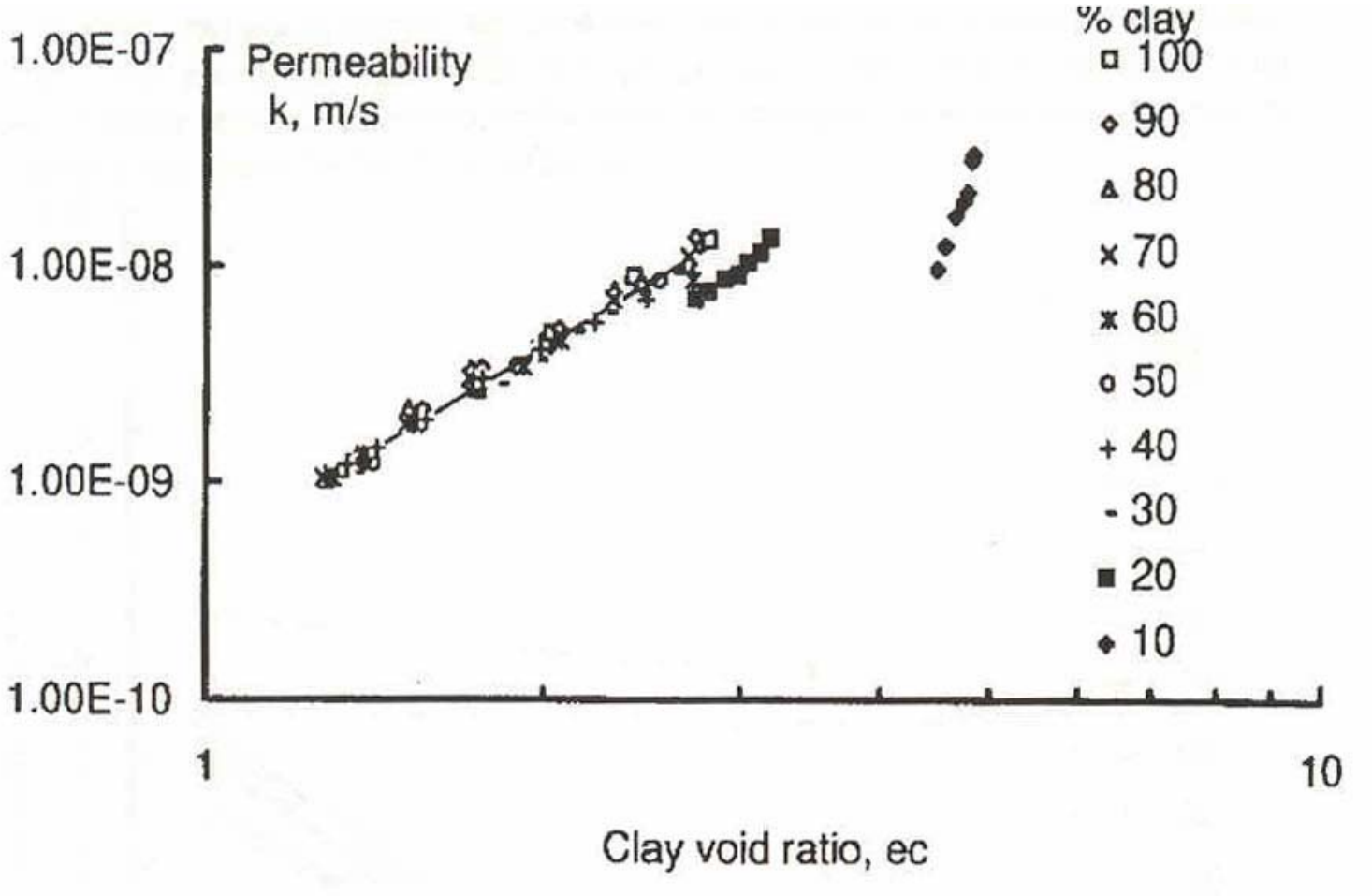

Figure 2.4 Effect of Clay Void Ratio on Permeability (Kumar and Wood, 1997)

Among the earlier models are the upper and lower bound of the mixture rules developed by Voigt (1889) and Reuss and Angew (1929). Voigt (1889) developed a model on the assumption that all elements constituting the mixture are subjected to the same uniform strain. The equation is given as

$$K_{mix} = f_i K_i + (1 - f_i) K_m \tag{2.37}$$

K is the bulk modulus of the material and the subscripts *i*, *m*, and *mix* represents inclusion, matrix, and mixture, respectively and *f* is the volume content of the constituent. The above relation can also be used in determining other material properties of the mixture such as elastic and shear moduli.

The Reuss and Angew (1929) model assumed that all elements in the mixture were subjected to a uniform stress equal to the applied stress. The resulting equation is given by

$$K_{mix} = \frac{1}{\frac{f_i}{K_i} + \frac{(1 - f_i)}{K_m}} \tag{2.38}$$

The above equation can also be used in determining other elastic parameters of the mixture.

Voigt's (1889) approximation gives the upper bounds and Reuss and Angew's (1929) approximation gives the lower bounds of the elastic moduli of the mixtures. Both models give fairly accurate predictions when the difference between the elastic moduli of the two constituent materials is very small.

Hashin and Shtrikman (1962) model is an improvement upon Voigt (1889) and Reuss and Angew's (1929) models and is most applicable when the elastic moduli disparity is very large. Hashin and Shtrikman (1962) developed a model for both upper and lower bounds elastic moduli of the mixtures based on variational principle and verified the validity with experimental results. The method was expanded to incorporate mixtures with different types of inclusions. Hashin and Shtrikman's equation for bulk modulus is given by

$$K_L = K_m + \frac{f_i}{\frac{1}{K_i - K_m} + \frac{3(1-f_i)}{3K_m + 4G_m}} \tag{2.39}$$

$$K_U = K_i + \frac{1-f_i}{\frac{1}{K_m - K_i} + \frac{3f_i}{3K_i + 4G_i}} \tag{2.40}$$

where subscripts L and U denotes lower, and upper bounds, respectively. G is the shear modulus of the material. Watt and O'Connel (1980) confirmed the application of the Hashin and Shtrikman method on different mixtures.

Omine et. al. (1998) developed a relation that was an improvement upon earlier work on the subject of elastic moduli of mixtures. The formula was based on the principle that the stress experienced by the mixture (σ_{mix}) was based on the weighted averages of the stresses experienced by the individual constituents. Thus, the averages can be obtained from the relations; $\sigma_{mix} = f_i\sigma_i + (1-f_i)\sigma_m$. Similar assumption was made for strains experienced by

the mixture (ε_{mix}) as well. This is in accordance with Voigt's (1889) equation. The resulting incremental stress-strain relationship is given as

$$\varepsilon_{mix} = \frac{f_i b C_i + (1 - f_i) C_m}{(b-1) f_i + 1} \sigma_{mix} \tag{2.41}$$

where C is the coefficient related to the material properties; and b is a stress distribution parameter (which represents the average stress ratio of inclusion to matrix). The concept is used to obtain the elastic moduli of two-phase mixtures from specific stress conditions. For example, Young's modulus under one-dimensional stress conditions is given by

$$E_{mix} = \frac{(b-1) f_i + 1}{\frac{f_i b}{E_i} + \frac{(1 - f_i)}{E_m}} \tag{2.42}$$

where

$$b = \left(\frac{E_i}{E_m} \right)^{1/2} \tag{2.43}$$

A similar relation applies to both bulk (K) and shear (G) moduli. Omine et al. (1998) compared his relation to earlier developed relations using experimental data to validate the results. The resulting plots are given in Figures 2.5 to 2.7. It is noted that the f_s used in the figures is the same as f_i used in the aforementioned derivations and equations.

From Figures 2.5 and 2.6, it can be seen that the upper and lower bounds of the Hashin-Shtrikman (1962) equation predicted the bulk modulus of the tungsten carbide more closely than Voigt (1889) and Reuss and Angew's (1929) relations, depicting an improvement on the

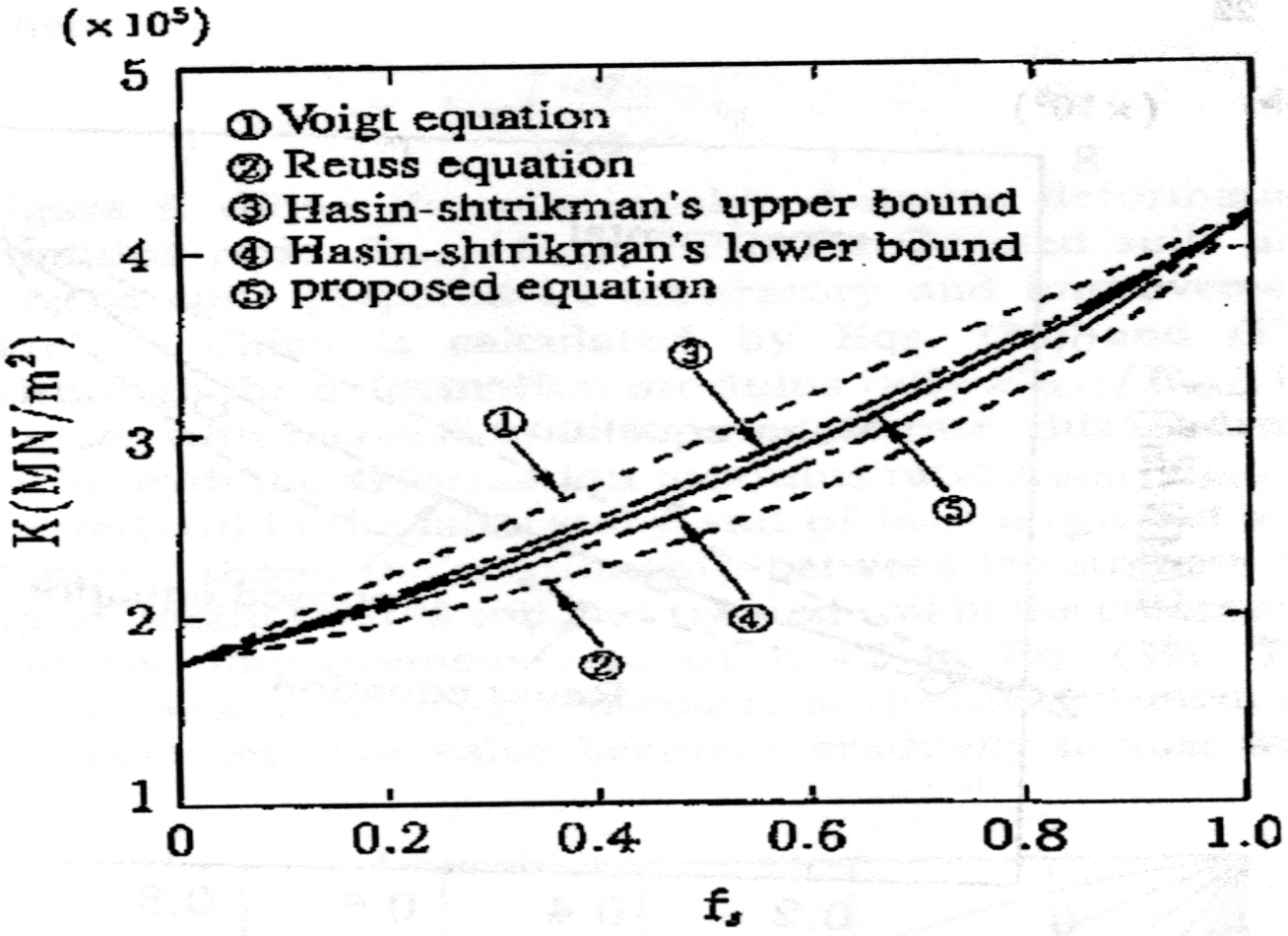

Figure 2.5 Relationship between Bulk Moduli, K, of Mixtures and Volume Fraction of Tungsten Carbide f_s (Omine et al., 1998)

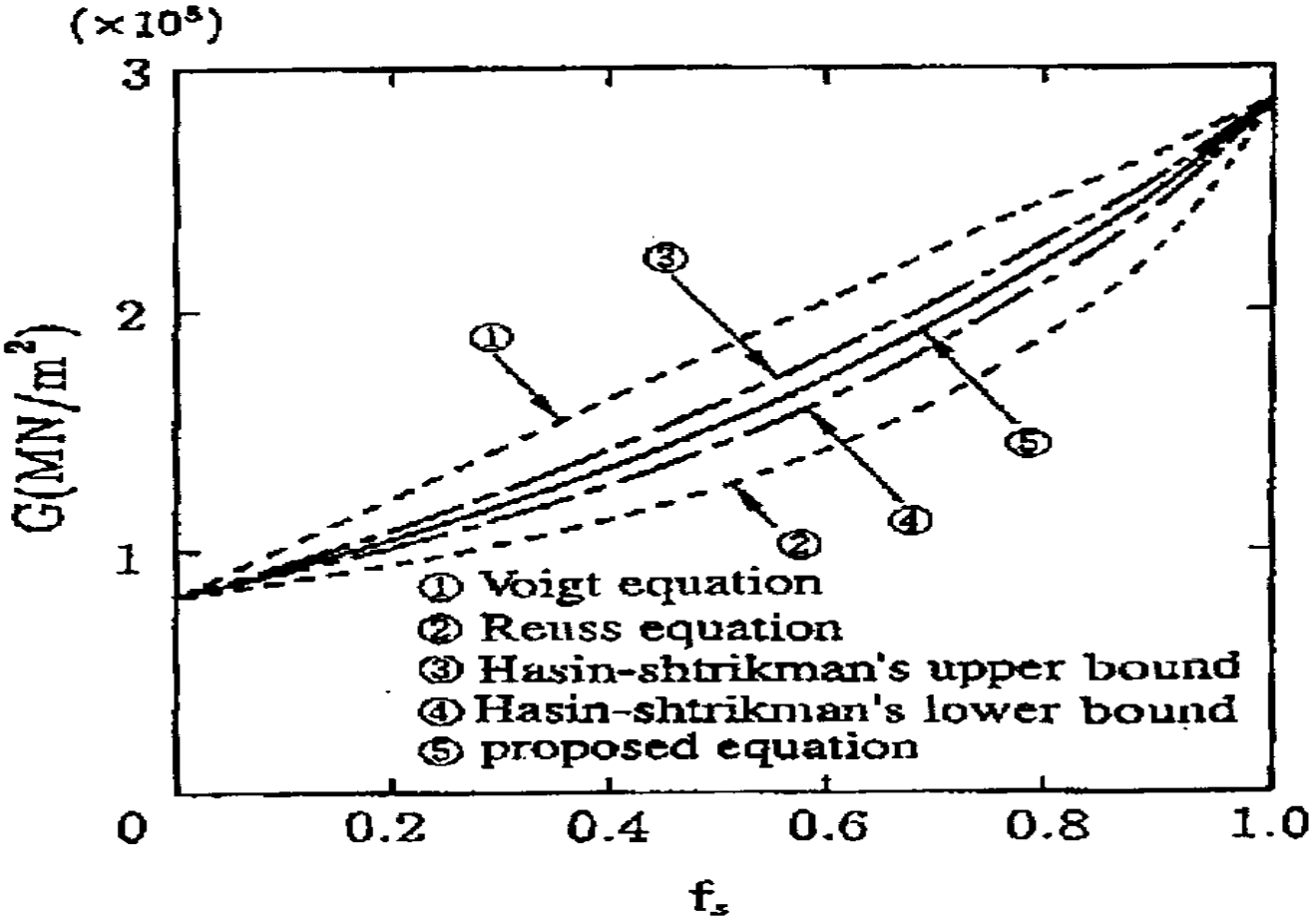

Figure 2.6 Relationship between Shear Moduli, G, of Mixtures and Volume Fraction of Tungsten Carbide f_s (Omine et al., 1998)

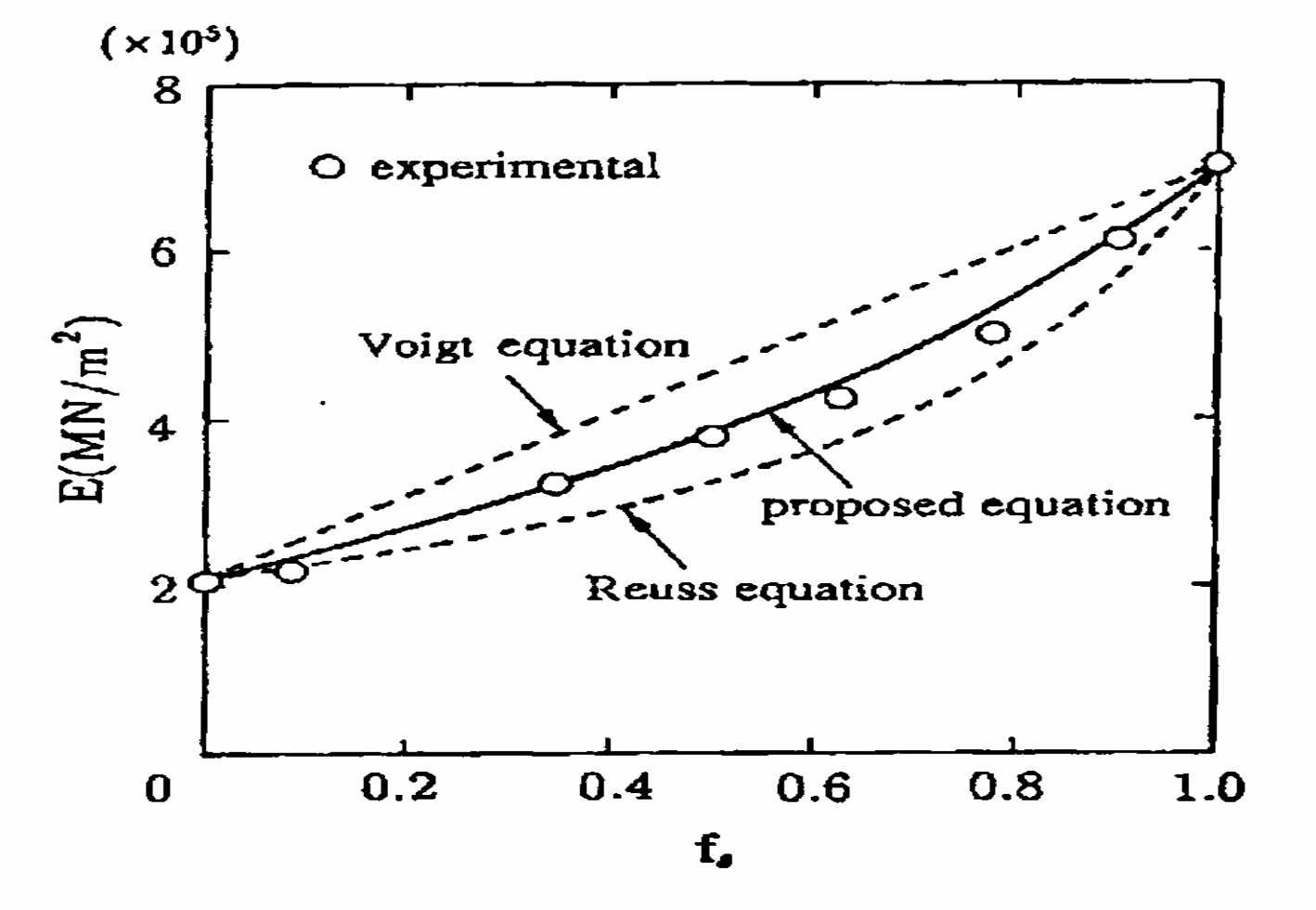

Figure 2.7 Relationship between Young's Moduli, E, of Mixtures and Volume of Tungsten Carbide f_s (Omine et al., 1998)

latter. From the figures (Figures 2.5 and 2.6), the equation developed by Omine et al. (1998) gives intermediate values between the lower and upper bounds of the Hashin-Shtrikman (1962) equation. It can therefore be inferred that Omine's (1998) equation closely predicts the laboratory results better than the rest, making it more effective in predicting the elastic moduli of isotropic elastic two-phase mixtures. The Braem et al. (1987) model is based on the linear mixing of the log of the elastic modulus of the matrix and inclusion of the mixture. It was also a modification of the rule of mixtures earlier proposed by Voigt (1889), and Reuss and Angew (1929). The equation is given as

$$E_{mix} = E_m \left(\frac{E_i}{E_m} \right)^x \qquad 2.44$$

where the subscripts *mix*, *m*, and *i* denotes mixture, matrix, and inclusion, respectively. The parameter *x* is the volume fraction of the inclusion. The Braem et al. (1987) model is applicable to inclusion particles that are homogeneously embedded in the matrix such that the composite can be considered to be isotropic. Braem et al. (1987) noted that, for small particle sizes of inclusion (filler) the Young's modulus of a composite is less dependent on particles size than on the maximum packing volume fraction. Figures 2.8 and 2.9 show how Beam et al. (1987) model best fits laboratory data and compare to earlier models. Figure 2.9 shows the curve fitting of Braem's model to 57 data points of mixtures investigated by Bream et al. (1987). This yielded a correlation of 94.8%. They further compared the model to two of the earlier models, Voigt (1889) and Reuss and Angew (1929), and this is shown in Figure 2.9.

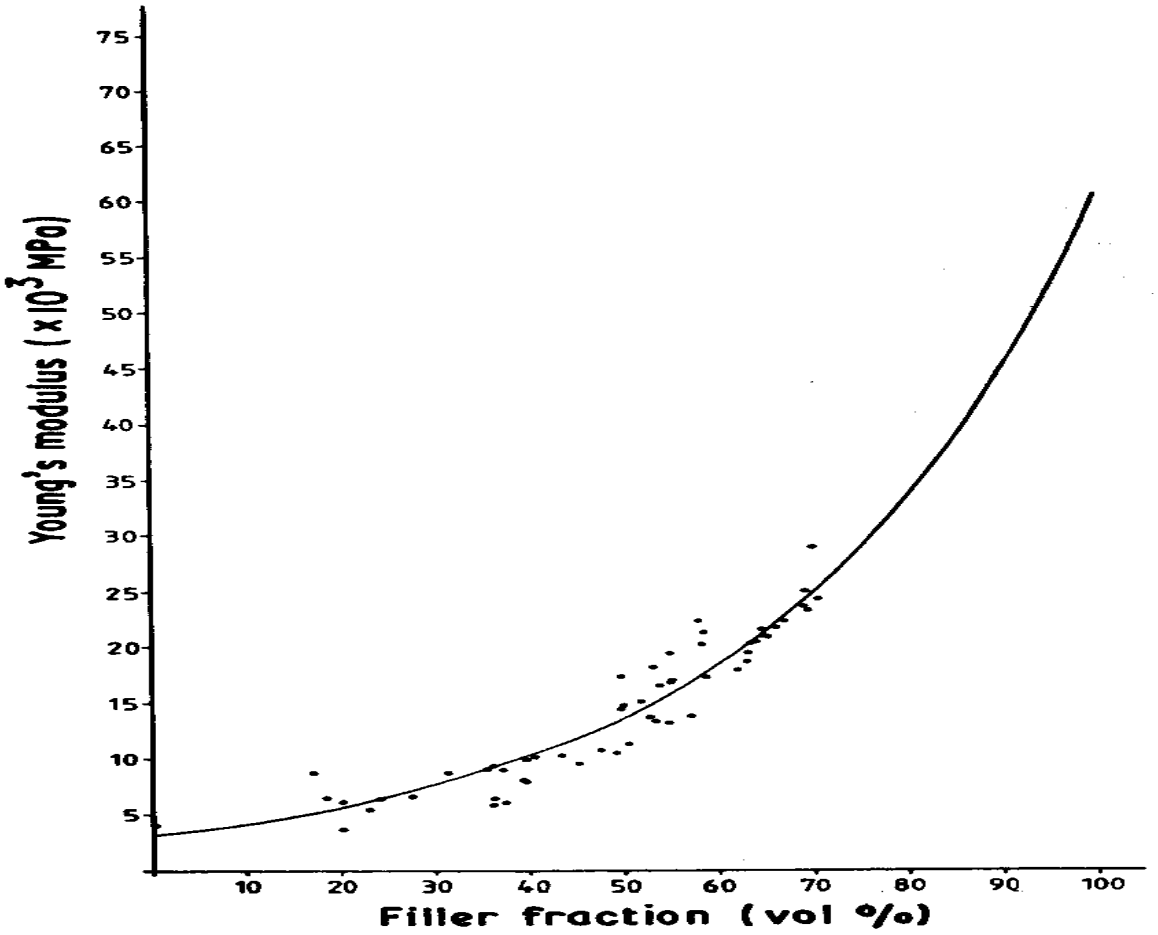

Figure 2.8 Curve Fitting of Braem's (1987) Model for Data Points of 57 Investigated Mixtures (Braem et al., 1987)

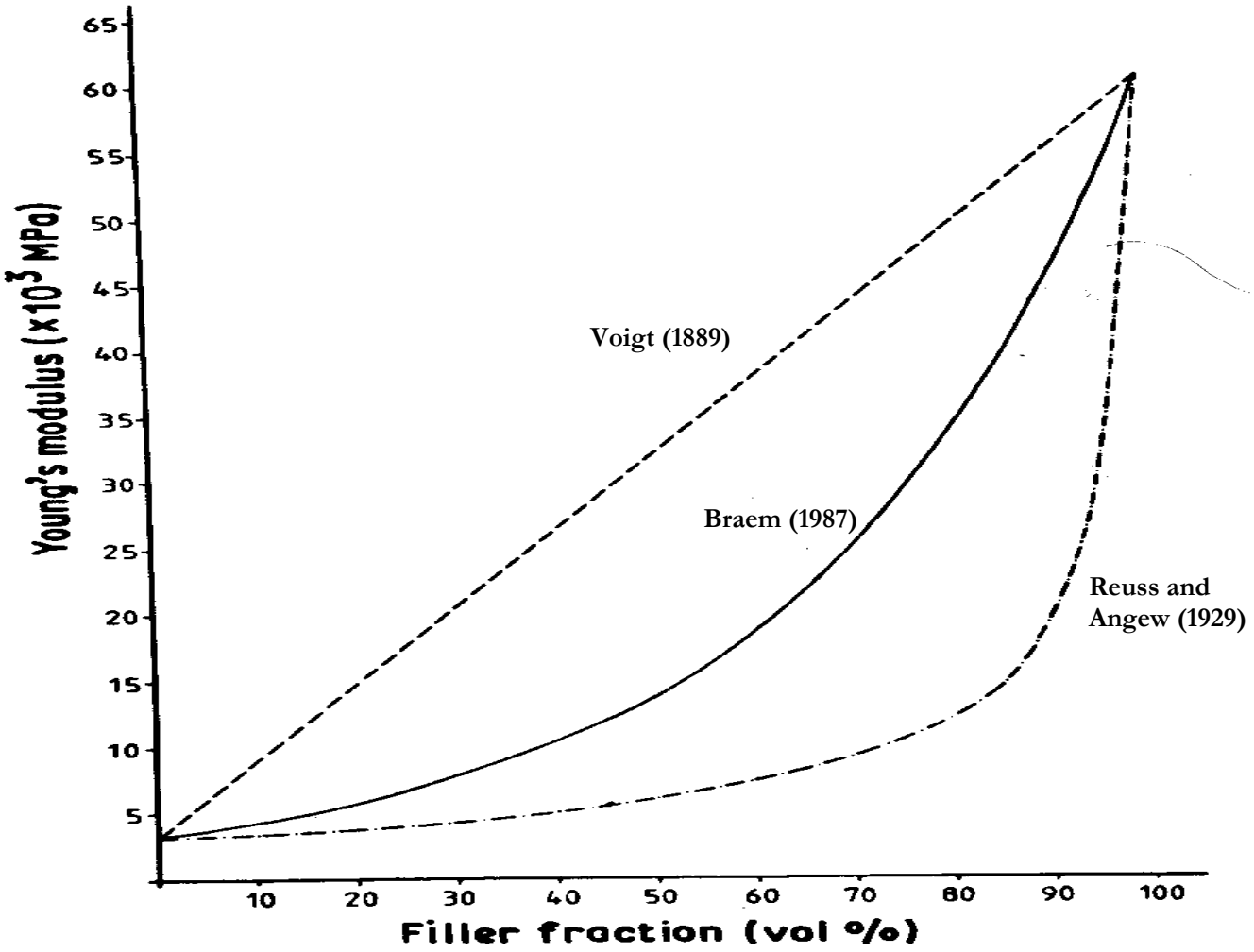

Figure 2.9 Comparison of Braem's (1987) Model to Voigt (1889) and Reuss and Angew's (1929) Models (Braem et al., 1987)

With the aforementioned models, it is the intent of this research to modify or develop a simple predictive model based on the existing mixture models that will accurately predict mixture properties of fly ash-modified soils.

The models mentioned earlier can be transposed to clay fly-ash mixture based on the basic mixture model concept, which relies on volume fractions to predict material properties. An existing model that best predicts the behavior of the fly ash-modified soils, based on experimental results will then be modified where necessary to improve upon its predictive capabilities.

2.4 FLY ASH-MODIFIED SOILS

In engineering, situations arise where soil improvement becomes necessary to be able to bear the load of a structure on it. These improvements have been done through soil stabilization techniques and reinforcements. Admixing techniques in soils are effective and relatively easy in soil improvements (Prabakar et al., 2004). Fly ash has been used in various applications including soil modification. It is relatively cheap to use fly ash for soil improvement since it is a coal combustion by-product and is typically available at a low cost.

Kumar et al. (2004) conducted a study on the effect of fly ash on engineering properties of expansive soils. The soil used was classified as high plasticity clay (CH) with a liquid limit (LL) of 80 and plasticity index (PI) of 52. The soil had a free swelling index (FSI) of 250%. The fly ash used had a calcium oxide (CaO) content of 2.21% and the sum of silica, alumina, and ferric oxide was 90.44%. According to the chemical composition of the fly ash, it is classified as Class F in accordance to ASTM C 618. All tests conducted on the fly ash, and

fly ash-expansive soil blends conforms to ASTM standards. The effects of fly ash on consistency, compaction, hydraulic conductivity, and shear strength on the expansive soil were evaluated. The investigation considered fly ash-soil mixtures with 0, 5, 10, 15, and 20% fly ash contents on a dry weight basis. Table 2.1 shows results of some of the tests conducted.

Table 2.1 Effect of Fly Ash on Index Properties, Swelling, Compaction, and Hydraulic Conductivity (Kumar et al., 2004)

Property	Fly ash content (%)				
	0	**5**	**10**	**15**	**20**
Liquid limit (%)	80	77	75	73	70
Plastic limit (%)	28	31	35	40	44
Plasticity Index (%)	52	46	40	33	26
Free swell index	250	200	165	140	125
Swell potential (%)	10.8	8.75	7.2	6.0	5.5
Swelling pressure (kPa)	90	72	60	50	45
Optimum moisture content (%)	40	38	35	33	31
Maximum dry unit weight (kN/m^3)	13.75	13.91	14.05	14.19	14.30
Hydraulic conductivity, *k* (cm/s)	9.70×10^{-7}	Not tested	6.02×10^{-7}	Not tested	3.95×10^{-7}

It was observed that, liquid limit, swell potential, optimum moisture content (OMC), and hydraulic conductivity decreases with increasing fly ash content. Maximum dry density (MDD) and plastic limit were found to increase with increasing fly ash content. An increase in MDD and a decrease in OMC with the addition of fly ash are synonymous to an increase in compactive effort in Proctor test.

This indicates an improvement in stability of the soil with the addition of fly ash. Undrained shear strength was determined from unconfined compression tests at different moisture contents. It was observed that the undrained shear strength increased with increasing fly ash content, but decreased with increasing moisture content in all the mixtures (see Figure 2.10). it was also observed that the FSI of the soil was reduced by 50% with the addition of 20% fly ash.

Prabakar et al. (2004) conducted a study on the influence of Class F fly ash on strength behavior of soils. In their study, three different soil samples and one fly ash were used. The soil samples used were classified as low plasticity clay (CL), low plasticity organic silty clay (OL), and inorganic silt (MH). The major consideration was the effect of fly ash on strength behavior of different soil types. All tests were performed at OMC conditions. The percentage of fly ash varied from 0% to 46%. The investigation revealed a decrease in MDD and an increase in OMC with increasing fly ash content in all the soil types.

Prabakar et al. (2004) inferred that the reduction in MDD with increasing fly ash content may have been due to a decrease in specific gravity of the mixtures as the fly ash content increases. With regards to shear strength parameters, it was observed that cohesion (c)

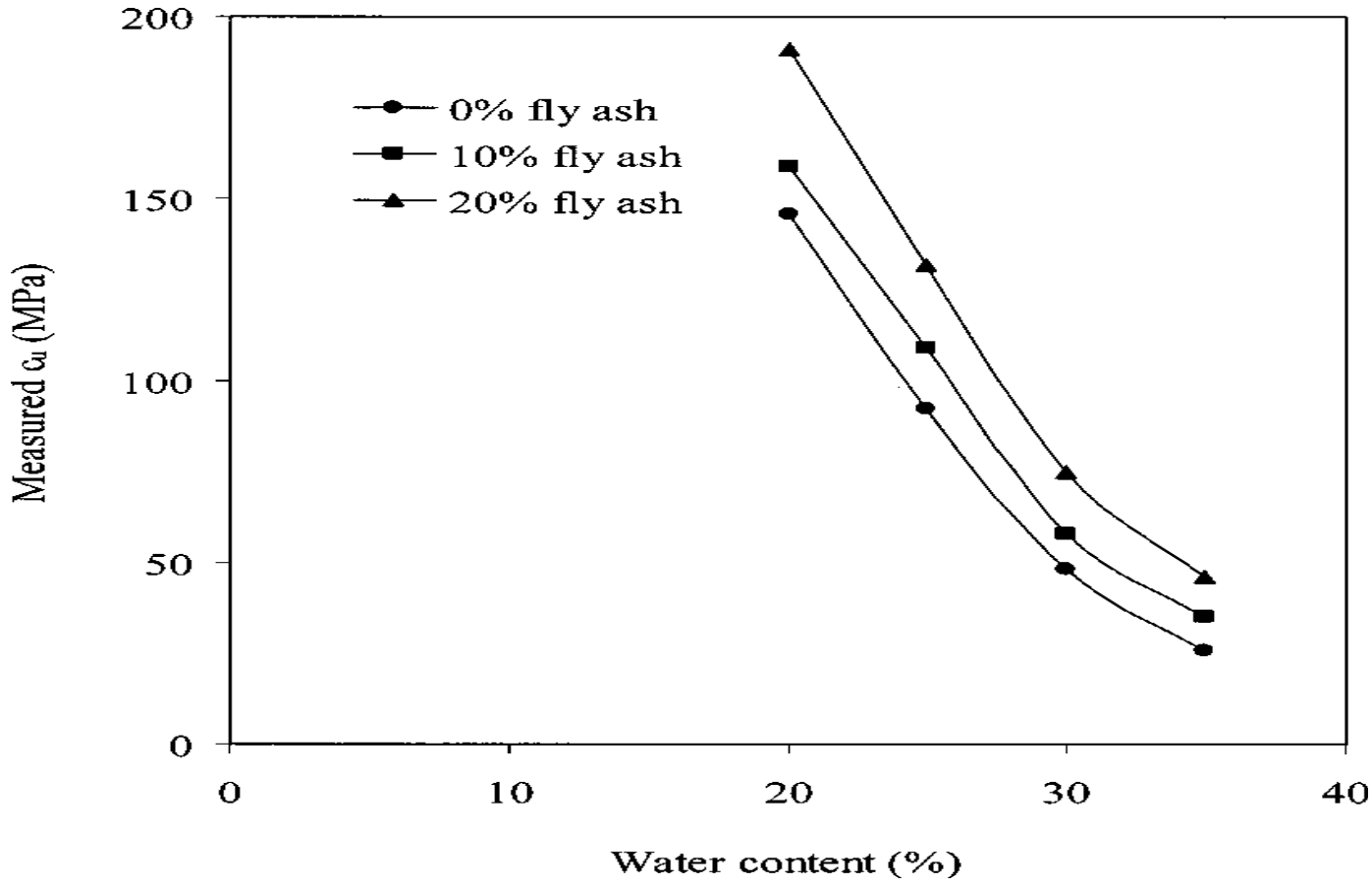

Figure 2.10 Variation of Undrained Shear Strength with Percent Fly Ash and Moisture Content (Kumar et al., 2004)

increased with increasing fly ash content. This trend was observed in the CL and OL soil types with the exception of the MH soil type. In MH soil, cohesion decreased with increasing fly ash content with no specific trend observed. Generally, the angle of internal friction also increased with increasing amount of fly ash in all soil types, with MH experiencing the biggest increase (see Table 2.2).

Table 2.2 Effect of Fly Ash Concentration on Strength Parameters of Soils (Prabakar et al., 2004)

% Fly Ash	Cohesion (Kg/cm^2)			Angle of Internal Friction (degrees)		
	Soil-A	Soil-B	Soil-C	Soil-A	Soil-B	Soil-C
0 %	0.250	0.185	0.530	30.25	17.17	25.53
9.0 %	0.250	0.280	0.523	31.60	24.22	20.43
20.0 %	0.270	0.300	0.475	33.02	25.20	21.97
28.5 %	0.310	0.300	0.500	35.60	28.30	23.25
35.5 %	0.340	0.330	0.480	34.20	29.63	26.28
41.2 %	0.370	0.370	0.440	32.10	29.88	27.37
46.0 %	0.395	0.380	0.395	28.63	30.63	27.93
100.0 %	–	0.150	–	29.35	29.35	29.35

An increase in the shear strength parameters of the mixture with increasing fly ash content could be due to the type of soil and the fly ash characteristics. Also the addition of fly ash can increase cohesion in soils with low plasticity (Prabakar, 2004). The increments observed in the strength parameters were nonlinear with all the soil types. Again, increase in fly ash resulted in an increase in the California Bearing Ratio (CBR) value in all the soil types. The improvement of soil strength in CBR due to the addition of fly ash is a function of soil and fly ash interlocking phenomena (Prabakar, 2004). As the fly ash content increases, the number of interlocking particles increases thereby increasing the stability of the soil mixture, hence the CBR of the mixture.

Cocka (2001) investigated the uses of various stabilizers in the stabilization of an expansive soil (see Table 2.3). The soil was prepared in the laboratory with 85% koalinite and 15% bentonite, and was classified according to the unified soil classification system (USCS) as CH (high plasticity clay). Among the stabilizers used was a low calcium Class C fly ash with an 18.98% CaO content (Soma fly ash). Cocka (2001) also used a Class F fly ash (Tuncbilck fly ash) according to ASTM C 618. The sum of the silicate, aluminate, and ferric oxide percentages for this fly ash was 70.72% with CaO content of 2.18%. The percentages of the fly ashes used in preparing the mixtures are 0, 3, 5, 8, 10, 15, 20, and 25%. It was observed that grain size distribution of the soil was altered by the addition of the stabilizers. Increasing amount of fly ash shifted the distribution curve to the coarser side. This was mainly a result of addition of silt size particles, and also due to chemical reactions that caused flocculation of clay size particles (Cokca, 2001).

In Table 2.3, Sample A denotes the expansive soil, SFA is Soma fly ash, TFA is Tuncbilck fly ash, and the numbers preceding the letters denotes the percentages of each ash mixed with soil Sample A. It can be seen in the table that the liquid limit and the plasticity index of the soil decreased with increasing fly ash content. The addition of the fly ashes generally decreased the specific gravity of the mixture, as the specific gravities of the ashes are lower than that of the expansive soil. The addition of the fly ashes to the soil decreased the swell potential as the fraction of the silt sized particles increased, while the percentage of the clay sized particle decreased. This resulted in a general reduction in activity of the soil. It was observed that cation exchanges, which could result in flocculation due to the addition of fly ash, also decreased the surface area and water adsorption, thereby reducing swell potential (Cokca, 2001).

Swelling potential also decreased with time, and this can be attributed to time-dependent pozzolanic reactions with the fly ash and the soil minerals. Cocka (2001) concluded that, both high-calcium and low-calcium fly ashes are suitable stabilizers for expansive soils.

Nalbantoglu (2004) also investigated the effectiveness of fly ash as a stabilizer for expansive soils. Two soils classified as CH (clay with high plasticity) and CL (clay with low plasticity) according to USCS were used in the study. A Class C fly ash with CaO content of 14.8% was used as the stabilizer in the study. The study was conducted on mixtures of soil and 0, 15, and 25% fly ash by weight. It was observed that an increase in fly ash decreased the plasticity index of both soils. The reduction in plasticity index due to fly ash treatment was observed to be greater in the high plasticity soil than in the low plasticity soil

Table 2.3 Effect of Fly Ashes on Index Properties of Soil (Cokca, 2001)

	Clay	Silt	*Gs*	Atterbergs Limits			Soil Classification	Activity
				LL	PL	PI		PI/Percent
Sample	(%)	(%)		(%)	(%)	(%)		Clay
A	48	50	2.65	74	22	52	CH	1.08
3SFA	47	51	2.64	49	24	25	CL	0.53
5SFA	45	51.5	2.63	48	26	22	CL	0.49
8SFA	44	51.5	2.62	47	26	21	CL	0.48
10SFA	44	52	2.62	47	28	19	ML	0.43
15SFA	43	53	2.60	45	29	16	ML	0.37
20SFA	43	53	2.59	44	32	12	ML	0.28
25SFA	38	54	2.53	42	29	13	ML	0.34
3TFA	46	50	2.59	54	19	35	CH	0.76
5TFA	45	51	2.62	53	21	32	CH	0.71
8TFA	44.5	51.5	2.62	52	21	31	CH	0.69
10TFA	44.5	50.5	2.61	50	22	28	CH-CL	0.63
15TFA	41	47	2.54	49	22	27	CL	0.66
20TFA	40	54	2.53	47	21	26	CL	0.65
25TFA	36	54	2.47	46	20	26	CL	0.72

Note: Soil classification is according to Unified Soil Classification System

(see Figure 2.11).

Nalbantoglu (2004) reported that the liquid limit may decrease or increase depending on the type of soil, but the overall plasticity index decreased with increasing fly ash content. The swell potential was also found to reduce drastically in the high plasticity soil than the low plasticity soil with the treatment of fly ash. The effect can be attributed to the smaller particle size, high specific surface area, and less crystallinity of the clay minerals in the high plasticity soil compared to that of the low plasticity soil. Rapid hydration processes and cation exchange between fly ash and clay particles lead to flocculation of the clay particles. This caused the clay size fraction of the soil to decrease in the mixture. Soils with larger specific surface areas usually have higher cation exchange capacity (CEC), higher surface activity and consequently higher water adsorption potential (Nalbantoglu, 2004).

The study revealed a decrease in the CEC in the soils with the treatment of fly ash (see Figure 2.12) which promoted flocculation. This explains why the treatment of fly ash causes the soils to become more granular (due to flocculation), thereby resulting to lower surface activity and less water adsorption potential. Figure 2.13 shows the increase in particle size with increase in fly ash content. The increase in particle sizes was also observed with increase in time as well.

The aforementioned results from researchers indicate that fly ash addition to clay increases strength. The researchers attributed various factors to this behavior of fly ash-modified soils. The factors will be analyzed in this study with respect to the proportions of fly ash used as well as the composition of the ashes and the soil.

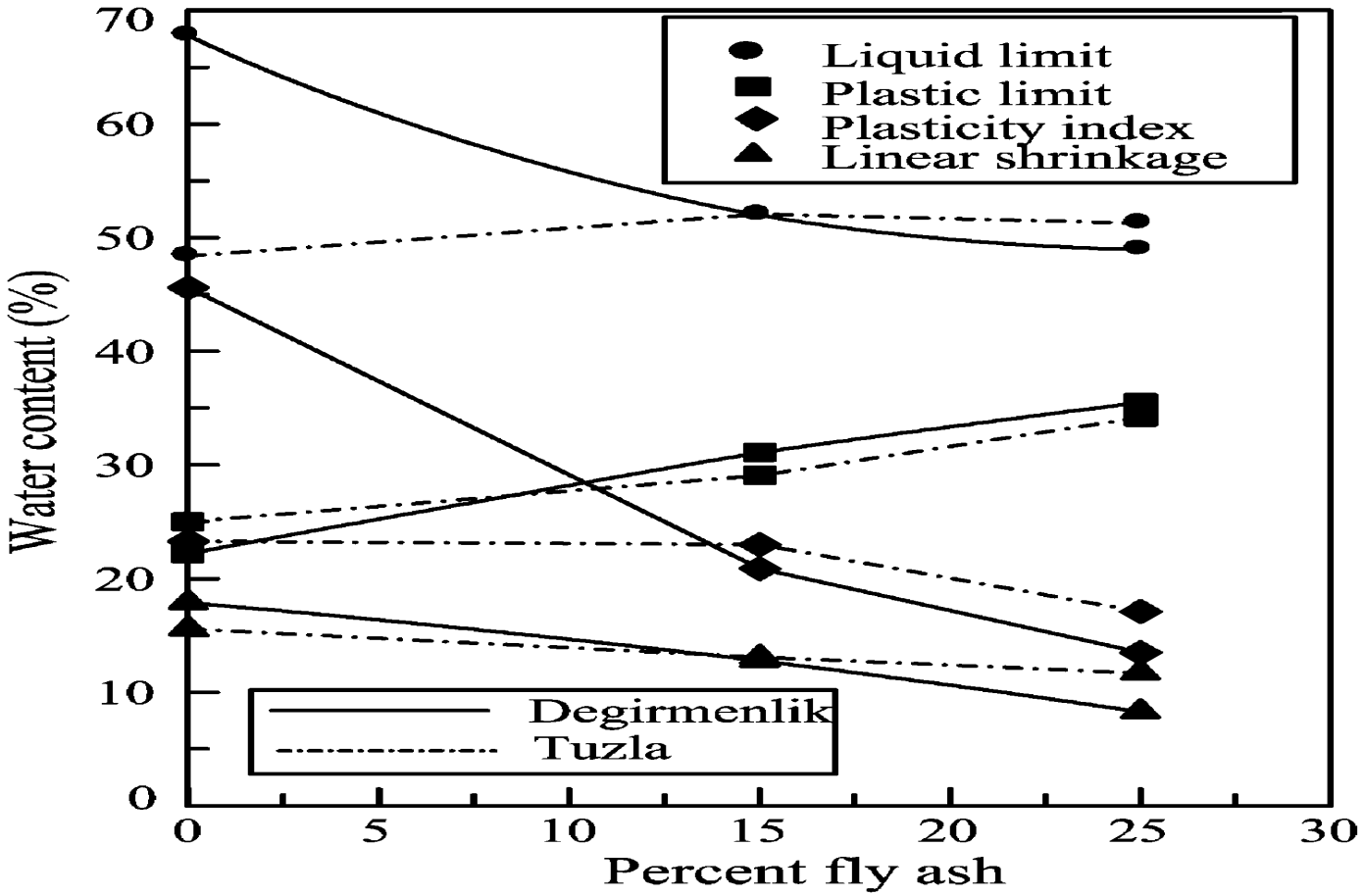

Figure 2.11 Effect of Fly Ash on the Consistency of Low and High Plasticity Clays (Nalbantoglu, 2004)

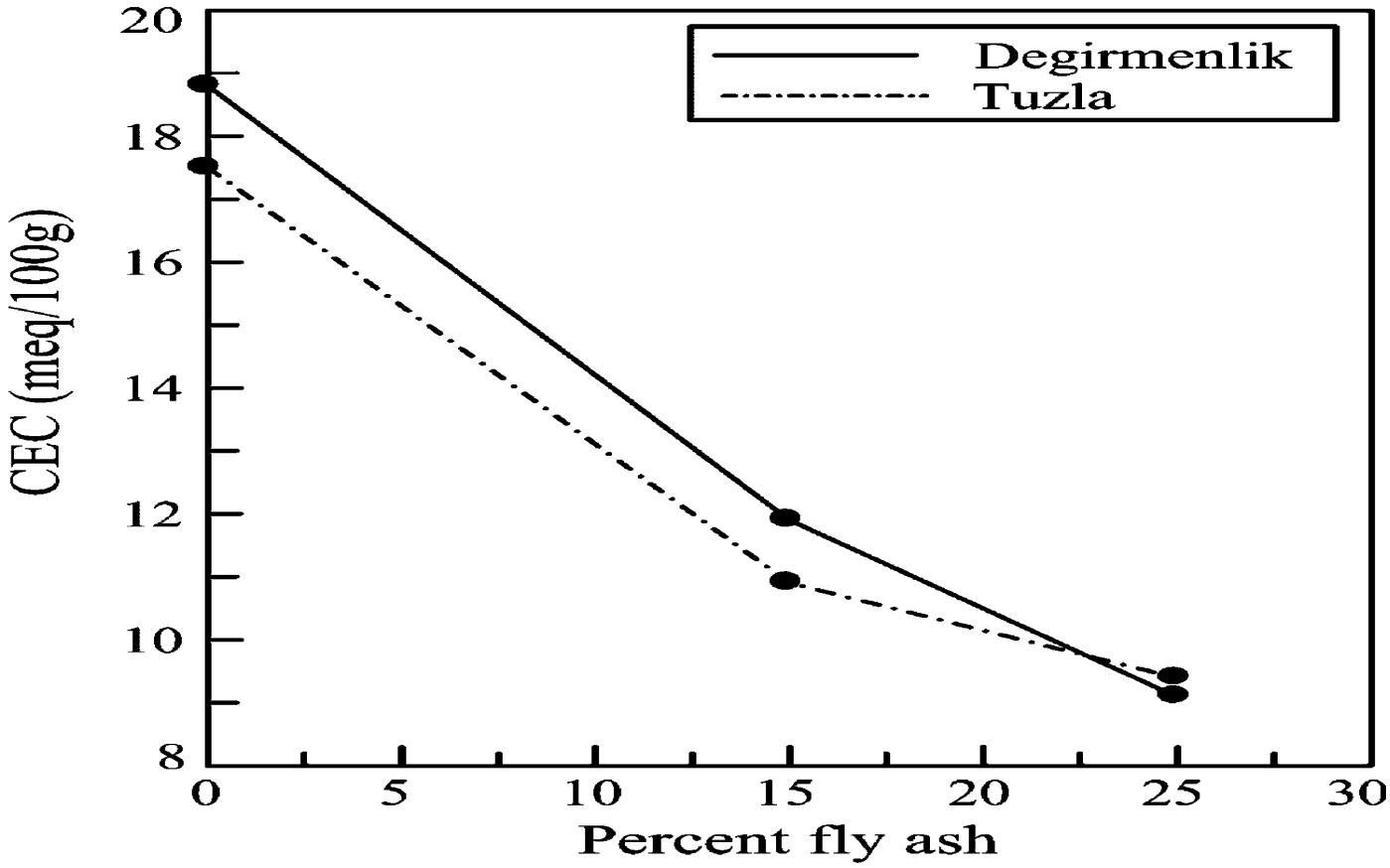

Figure 2.12 Effect of Fly Ash on Cation Exchange Capacity of Low and High Plasticity Clays (Nalbantoglu, 2004)

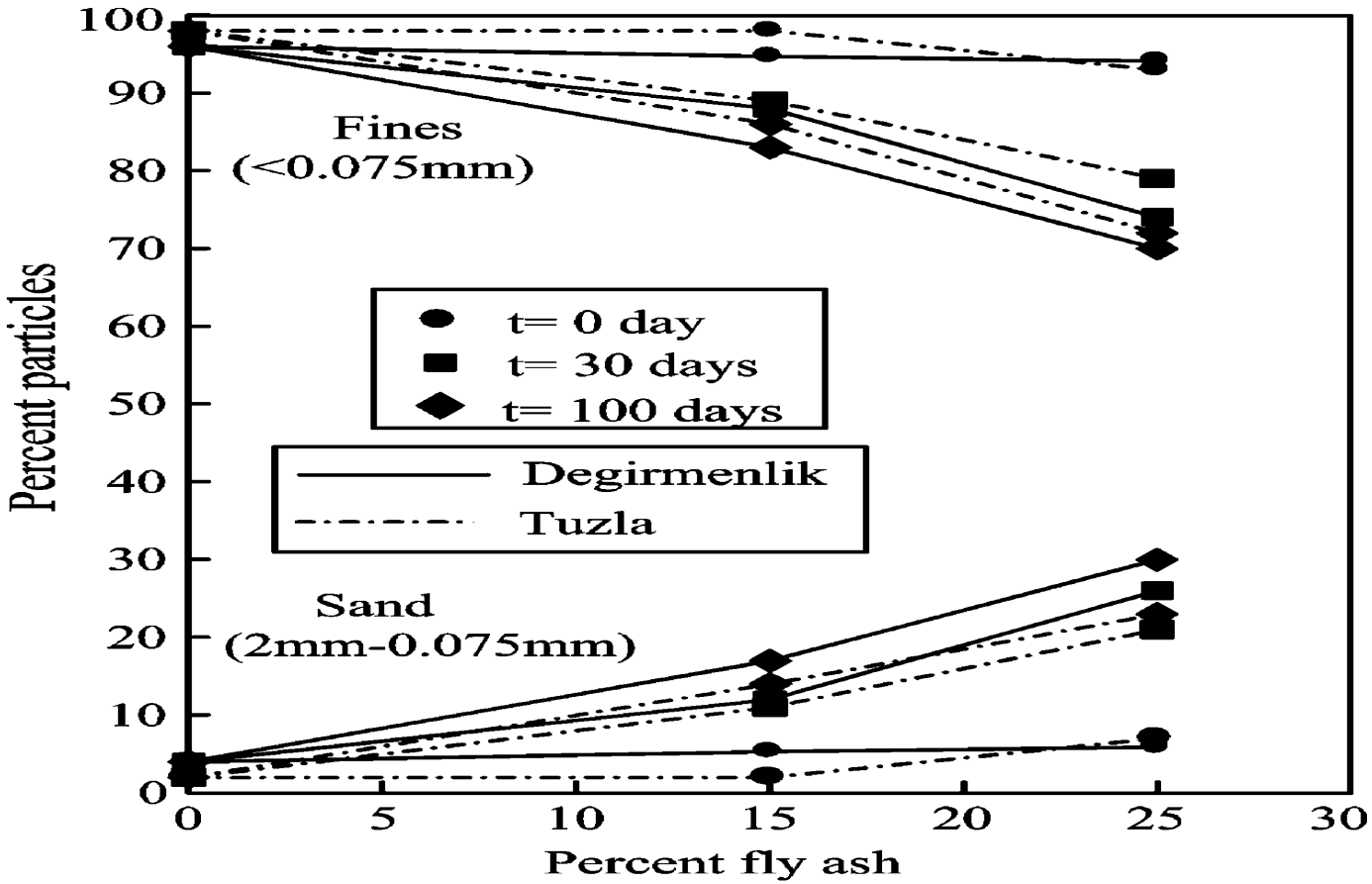

Figure 2.13 Effect of Fly Ash on Particle Sizes (Nalbantoglu, 2004)

2.5 PHYSICOCHEMICAL INFLUENCE ON MIXTURES

Fly ash-soil modification relies partly on the physical properties and the interactions between the minerals present in the soil and the fly ash. Currently, it is known that fly ash from the same source behaves differently, which makes predicting the behavior of fly ash-modified soils unreliable.

This unique behavior has been one of the setbacks in its wide application in the engineering sector. Physicochemical and mechanical theories for relating composition to engineering properties are necessary to understand the behavior of fly ash-modified soil mixtures.

2.5.1 PHYSICOCHEMICAL INFLUENCE ON ENGINEERING PROPERTIES

The mechanical and chemical characteristics of fly ash are highly dependent on the type and source of the coal as well as the burning technique. There are variations of the engineering properties of fly ash-modified soils due to the variation in the fly ash characteristics. Physical and chemical interactions may occur between different constituents within soil mixtures. Several studies have highlighted the influence of physicochemical factors on engineering properties of saturated clays (Narasimha and Mathew, 1995; Mitchell, 1993; Sridharan et al., 1986; Mesri and Olson, 1971). These factors influence the engineering properties of fly ash-modified soils as well. As mentioned earlier, the addition of fly ash to clay particles causes the clay particles to reduce and the silt sized particles to increase. This was found to be due to chemical reactions that caused flocculation of the clay size particles as explained by Cokca (2001). This phenomenon tends to reduce the specific surface of the

clay particles leading to a reduction in the plasticity index and an increase in the shear strength of the mixture.

Physicochemical mechanism influences a wide range of soil engineering properties such as consistency, consolidation, hydraulic conductivity, and shear strength (Mitchell, 1993). Calcium oxide, which is a key constituent in fly ash, dissociates in the presence of water to form calcium cations and hydroxide anions. The availability of the calcium cations depends on the degree of crystallinity of the calcium oxide. The less crystallized the calcium oxide, the more calcium cations present upon dissociation in the presence of water.

2.5.2 INFLUENCE OF CATION EXCHANGE CAPACITY

Cation exchange is an important reaction responsible for improvements in clay soil characteristics. Cation exchange capacity (CEC) is the quantity of exchangeable cations required to balance the charge differential on the surface of the clay particles. Some clay properties such as surface activity and water absorption potential are directly proportional to CEC. Fly ash has the potential of providing multivalent cations (Ca^{2+}, Al^{3+}, Fe^{3+}, etc), which promotes flocculation of clay particles by cation exchange. In solution, negatively charged ions are attached to the clay surface where the positively charged ions (cations) are attracted to them. An electrical force attracts the cations in solution to the anions on the surface of the clay particles, while the diffusive forces tend to repel the cations away from the clay surface. The balance between the electrical forces and the diffusive forces causes a distribution of cations in solution adjacent to anions on the clay surface. This distribution of opposite charged ions is called the diffuse double layer. The plasticity of clayey soils is due to

the existence of double-layer water. The innermost layer of double-layer water is very strongly held by the clay particle; it is referred to as absorbed water. The distribution of opposite charged ions promotes CEC with the introduction of more cations in solution from the fly ash in fly ash-soil (clay) mixtures.

2.5.3 POZZOLANIC REACTIONS

The calcium cations react with other ions of chemical compounds found on most clay surfaces to form cementitious materials. The non calcium oxides in fly ash usually act as inert oxides; however, in the presence of enough calcium cations, these oxides can also react to form cementitious bonds.

$$Ca^{++} + 2(OH)^{-} + SiO_2 \rightarrow CaO.SiO_2.H_2O \qquad 2.45$$

$$Ca^{++} + 2(OH)^{-} + Al_2O_3 \rightarrow CaO.Al_2O_3.H_2O \qquad 2.46$$

The reaction of SiO_2 and Al_2O_3 in fly ash depends on the amount of $Ca(OH)_2$ present. The rate of pozzolanic reaction depends on the $Ca(OH)_2$ concentration and it is a function of time (Hwang et al., 2004). Reactions between calcium cations and hydroxide ions from the fly ash and the clay silica and alumina are pozzolanic which leads to the formation of calcium-silicate-hydrate (Equation 2.45) and calcium-alumina-hydrate (Equation 2.46), respectively (Nalbantoglu, 2004; Wartman and Riemer, 2002; Usmen and Bowers, 1990). These two products are responsible for the cementitious properties in the fly ash-clay mixtures. A secondary pozzolanic reaction between hydrated CaO and silica and alumina

from the fly ash and clay minerals leads to additional cementation. This contributes to increase in shear strength with increasing fly ash content.

Hwang et al. (2004) reported that with fly ash used in cement the contribution of the fly ash to the pozzolanic activity (α) is expressed as a function of time. This contribution was quantified and expressed mathematically as

$$\alpha = k_1 \exp[k_2 (FA/C)] \qquad 2.47$$

where k_1 and k_2 are experimental constants and are time dependent. The FA and C are the proportion of fly ash and cement in the mixture, respectively. This idea could be applicable in modifying the mixture theory models described above to improve the predictive capabilities of the models.

Due to the effect of physicochemical interactions on mixture properties of fly ash-soil mixtures, predictions of mixture properties may not be directly interpreted from mixture proportions of the individual constituents alone. The subject of physicochemical interactions between constituents of fly ash-soil mixtures therefore needs to be considered when predicting the engineering properties together with any applicable theory where necessary. However, this research will not focus on chemical reactions that take place in pozzolanic activity of fly ash because the focus of this research is on Class F fly ash. This class of fly ash typically has little to no pozzolanic properties.

2.6 CRITICAL STATE MODEL

2.6.1 INTRODUCTION

It is rarely possible to perform the analyses required to obtain complete and accurate knowledge of the engineering behavior of the material. This is particularly true for goematerials. Better understanding of real problems can be achieved if intelligent simplifications (models) of the reality are made. The objective of using conceptual models is to focus attention on the important features of a problem, leaving the irrelevant features. A critical state model (CSM) is a simplification and idealization of soil behavior, and it captures the behavior of soils that are of great importance to the geotechnical engineer.

Critical state in soil mechanics is the ultimate condition in which plastic shearing could continue indefinitely without changes in volume or effective stresses. Critical state soil mechanics (CSSM) model provides a framework that helps to describe, interpret, and anticipate soil response (behavior) to various loadings. The model is used to provide generalized understanding of soil behavior. Generally, when soil consolidates under higher stresses, the increase in shear strength is dependent on the soil, the loading conditions (drained or undrained), and the stress path. All this is interrelated and can be linked together by critical state soil mechanics. The CSSM model may be considered as an empirical relation that unifies strength and deformation properties of soils, particularly shear and compression properties (Kirby, 1998). The fundamental concept of CSM is that a unique failure surface exists, which defines failure of a soil irrespective of the history of the loading or the stress path. The model serves as a tool in estimating soil responses in situations where sufficient

soil tests cannot be conducted to completely characterize the soil, or when the soil response from various loading regimes need to be predicted during and after construction. Some of the properties the model helps in estimating are failure stresses and strains, stress-strain characteristics of soils from few parameters obtained from soil tests, and to evaluate possible soil stress states and failure if loadings on a geotechnical system were to change.

2.6.2 KEY CRITICAL STATE RELATIONS

Critical state parameters can be obtained from consolidation and triaxial test results. In the *ln(v) : ln(p')* plane, the slope of isotropic normally consolidated line (iso-ncl) is given as λ, and that of the recompression line is given as κ. At critical state, a soil behaves as a viscous fluid and is governed by the following equations:

$$q = Mp' \tag{2.48}$$

where

$$q = \sigma_1' - \sigma_3' \tag{2.49}$$

and

$$p' = \frac{\sigma_1' - 2\sigma_3'}{3} \tag{2.50}$$

$$v = \Gamma - \lambda \ln p' \tag{2.51}$$

Under axisymmetric loading conditions *q, p'* and *v* are deviatoric stress, effective mean stress, and specific volume, respectively. In triaxial compression test, σ_1' is the total effective stress and σ_3' is the effective confining stress. M, Γ, κ, and λ, are the critical state parameters and are material constants for a particular soil.

At failure (or critical state) for remolded or normally consolidated soils, the slope of the isotropic normally consolidated line (iso-ncl) from Equations 2.48 through 2.50 gives

$$M = \frac{3\left(\frac{\sigma_1^{'}}{\sigma_3^{'}} - 1\right)}{\left(\frac{\sigma_1^{'}}{\sigma_3^{'}} + 2\right)} \qquad 2.52$$

But

$$\left(\frac{\sigma_1^{'}}{\sigma_3^{'}}\right) = \frac{1+\sin\phi_{cs}}{1-\sin\phi_{cs}} \qquad 2.53$$

Combining Equations 2.52 and 2.53 gives a relationship between friction angle at critical state and the slope of the critical state line (for soil compression). This is given as

$$M = \frac{6\sin\phi_{cs}^{'}}{3-\sin\phi_{cs}^{'}} \qquad 2.54$$

where $\phi_{cs}^{'}$ is the critical state friction angle. In *p'-q* plane, the intersection of critical state line and the stress path defines failure condition. From that, the *p'* at failure can be calculated and the remaining critical state parameters can be obtained from the above equations. The slope of Mohr-Coulomb failure plane in normal stress (σ), shear strength (τ) space is ϕ_{cs} while the slope of critical state or failure line in (*p', q*) space is M. The scenario is presented in Figure 2.14.

Pore pressure parameters can also be related to shear strength using a critical state model. Under undrained conditions, soil volume and void ratio remain constant. According

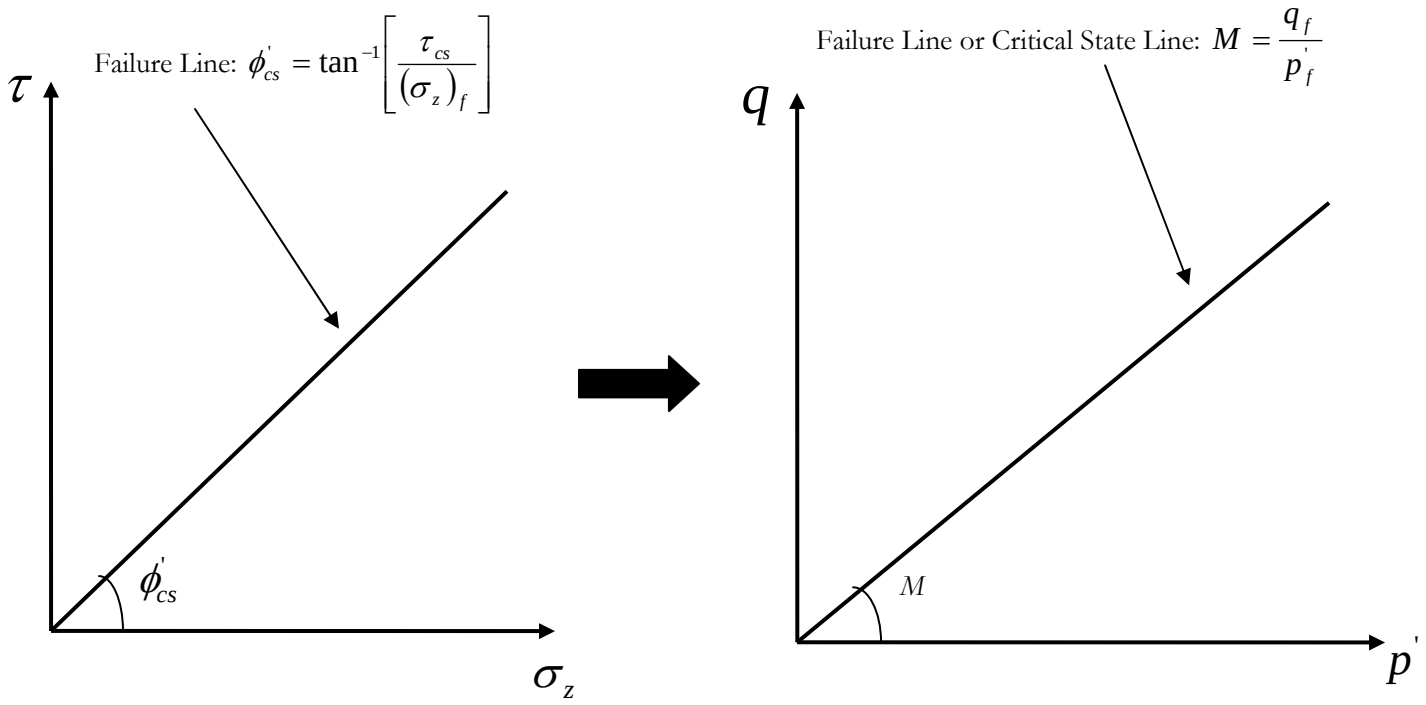

Figure 2.14 Mapping of Failure Plane in (σ, τ) space into (p', q) Space (after Budhu, 2000)

to CSSM, under undrained conditions at failure the following relation exists

$$p_f^{'} = \exp\left(\frac{e_\Gamma - e_0}{\lambda}\right) \qquad 2.55$$

where $p_f^{'}$ is effective stress at failure, e_0 is initial void ratio, e_Γ is void ratio on the critical state line (csl) when $\ln p' = 1$, and λ is the compression index of the soil plotted in *v : ln(p')* space. Considering undrained shear strength (S_u) at failure to be half the deviatoric stress in undrained triaxial test, and combining Equations 2.48 and 2.55, the undrained shear strength can be related to void ratio and critical state parameters as

$$S_u = \frac{M}{2}\exp\left(\frac{e_\Gamma - e_0}{\lambda}\right) \qquad 2.56$$

Changes in deviator stress and mean effective stress are related by the pore pressure parameter at failure (a_f). Considering that the slope of the total stress path (TSP) in conventional triaxial compression equals 3, the excess pore pressure (U_f) can therefore be related to undrained shear strength as

$$U_f = 2S_u\left(\frac{1}{3} - a_f\right) \qquad 2.57$$

where the shear strength can be obtained from the critical state parameters as in Equation 2.56.

2.6.3 YIELD SURFACE

Yield surface refers to the boundary between stress states elastic and elasto-plastic behavior of the soil material. The yield surface for a normally consolidated soil from an undrained triaxial compression test is shown in Figure 2.15. Deformations at the initial yield state and beyond in soils tend to increase significantly than the region below the yield surface (Figure 2.15). The intersection between the initial yield surface and the effective stress path (ESP; c.f. total stress path, TSP) gives the yield stresses of the material. The yield surface expands with load increments beyond the initial yield surface. The expansion continues with increasing load till the surface coincides with the point where the critical state line intersects with the effective stress path. The coordinates of this point gives the failure stresses.

The size of the initial yield surface is governed by the pre-consolidated mean effective stress ($p_c^{'}$). The yield surface assumes an elliptical shape and this was found to be a reasonable approximation for soils (Wong and Mitchell, 1975). The equation for the yield surface is given by

$$(p')^2 - p'\,p'_c + \frac{q^2}{M^2} \qquad 2.58$$

During incremental loading, deformation within the yield surface can be quantified based on stiffness of the soil under the concept of critical state by the shear modulus (G). This is given by

$$G = \frac{1.5\,p'(1+e_0)(1-2\nu')}{\kappa(1+\nu')} \qquad 2.59$$

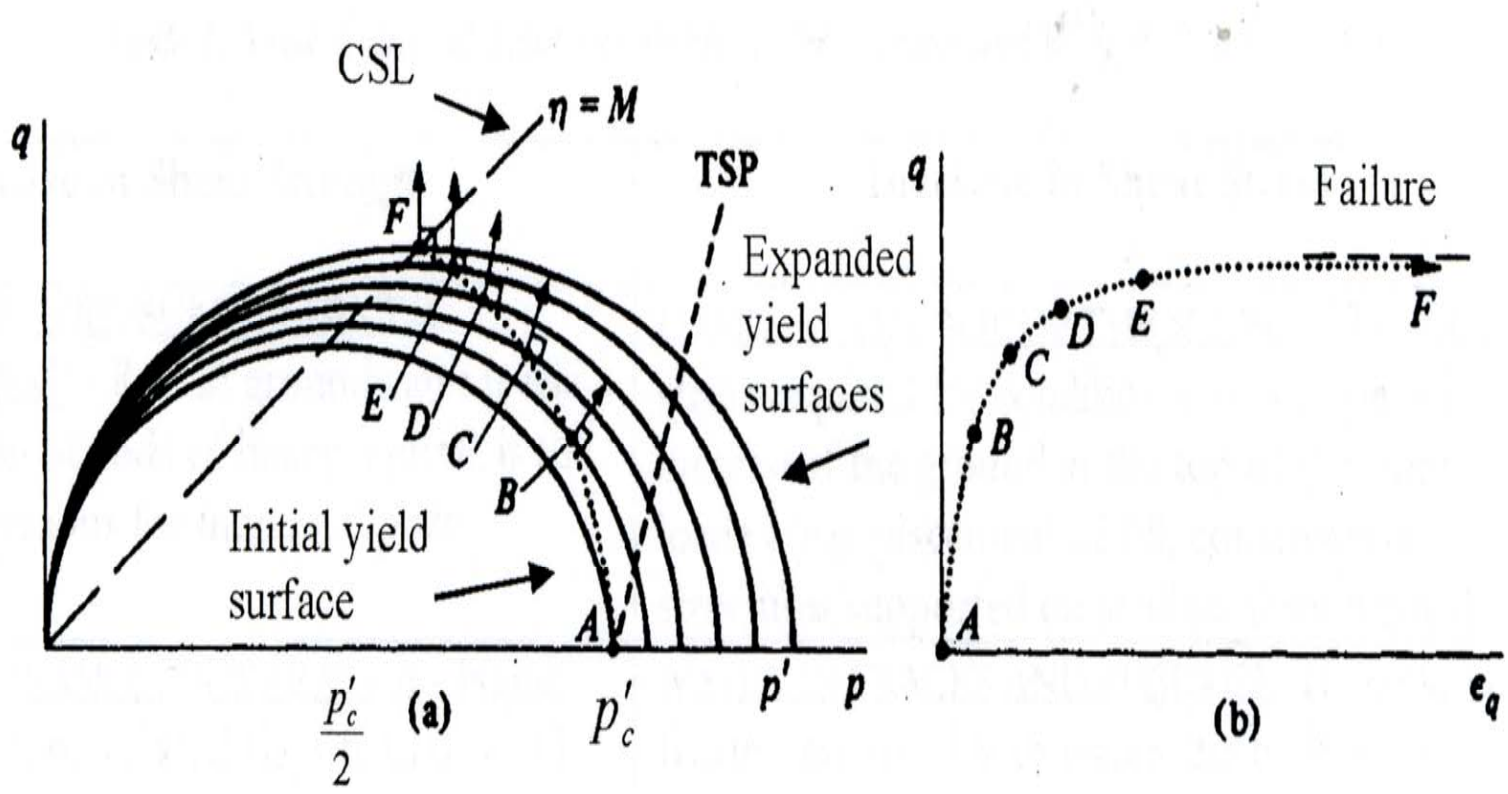

Figure 2.15 Expansion of the Yield Surfaces: (a) Critical State Concept, (b) Stress-strain plot (after Wood, 1990)

where ν' is the Poisson's ratio.

The CSM is not intended to replicate all the details of the behavior of soils, but to serve as a simple framework from which the important features of soil behavior can be interpreted and understood. Wood and Wroth (1978) and Wood (1990) through CSM correlated results from Atterberg limits with various engineering properties (undrained shear strength, compressibility indices, etc.) with fine grained soils. An example of some of the relationships is given as

$$\lambda = \frac{(PI)G_s}{\ln R} \tag{2.60}$$

where

$$R = \frac{s_P}{s_L} \tag{2.61}$$

PI is the plasticity index of the soil; G_s is the specific gravity; s_P and s_L are the undrained shear strengths of the soil at water contents equal to their plastic and liquid limits, respectively. The λ is the compressibility of the soil in the compression plane in critical state soil mechanics. A relationship between λ and C_c of remolded soils is given as

$$C_c = 2.303\lambda \tag{2.62}$$

2.6.4 SOME CRITICAL STATE APPLICATIONS

Bouckovalas et al. (2003) reported that the effect of fines in soils (in their case, silty sand) causes the critical state line (csl) to rotate about a pivot which is roughly dependent on the mean effective stress and a corresponding void ratio (Figure 2.16). It was further revealed

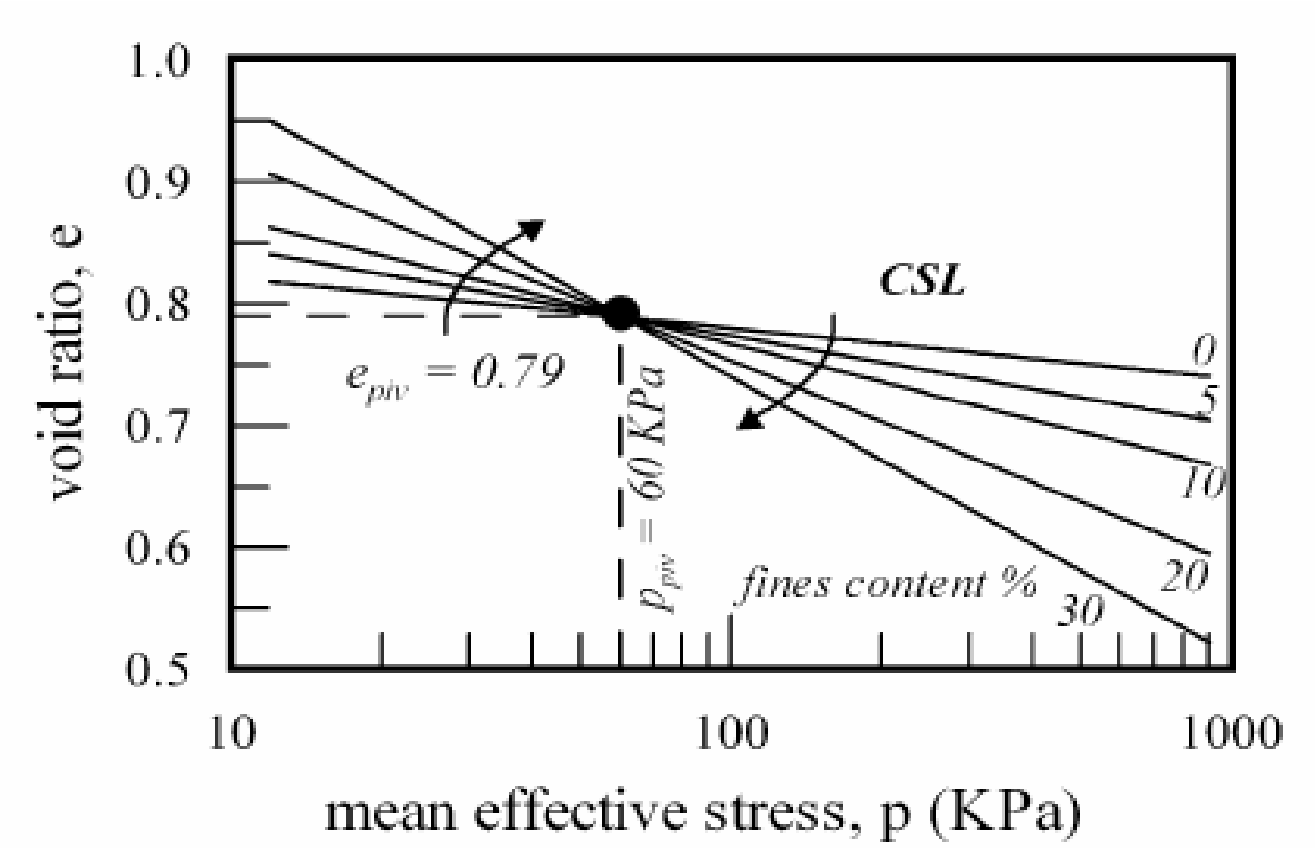

Figure 2.16 The Effect of Fines on Critical State Line (CSL) in e - lnp' Space (after Bouckovalas et al., 2003)

that both λ and Γ increases with fines content whereas M remains constant. Empirical relations were developed between the critical state parameters and fines content (see Figure 2.17). A combination of two of the relations were combined and that led to a direct relation between λ and Γ, and is given as

$$\Gamma = 0.79 + 4.1\lambda \qquad 2.63$$

The equation (Equation 2.63) fits well with the raw data (Figure 2.18) and was considered to be reliable for a wide range of silty sands.

In an evaluation of mechanical behavior of clay soils using triaxial tests, Eko (2004) observed that the distance between the normally consolidated line (ncl) and the critical state line (csl) may be soil type dependent after comparing results with other researchers such as Kirby (1998), Adams and Wulfsohn (1996), and O'Sullivan et al. (1996). The uniqueness of both the critical state and the normally consolidated line was demonstrated in the study as all the data points from different tests lined up on the same line (Figure 2.19). Uniqueness referred to as the independence of the critical state line from testing conditions such as drainage, sample preparation method and strain rate.

Kumar et al. (1997) utilized critical state soil mechanics in expressing relations on the mechanical behavior of kaolinite and coarse sand. It was found that clay void ratio plotted against vertical effective stress in the one dimensional compression test shows a unique relationship until clay content is down to about 30% (i.e. sand content about 70%) where the sand particles interacts sufficiently to affect the one-dimensional compression relationship

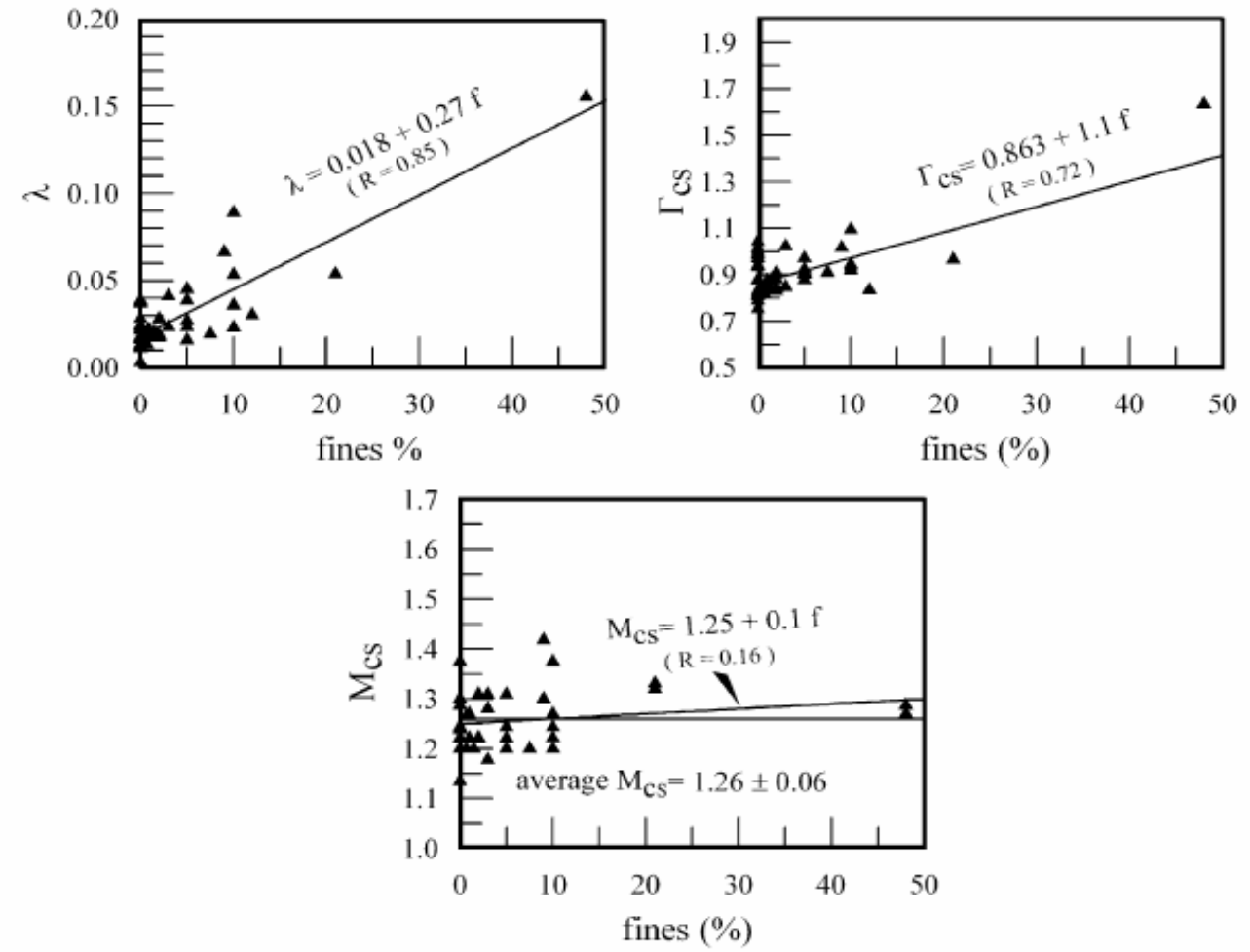

Figure 2.17 Evaluation of the Effect of Fines Content on Critical State Parameters Γ, λ and M (after Bouckovalas et al., 2003)

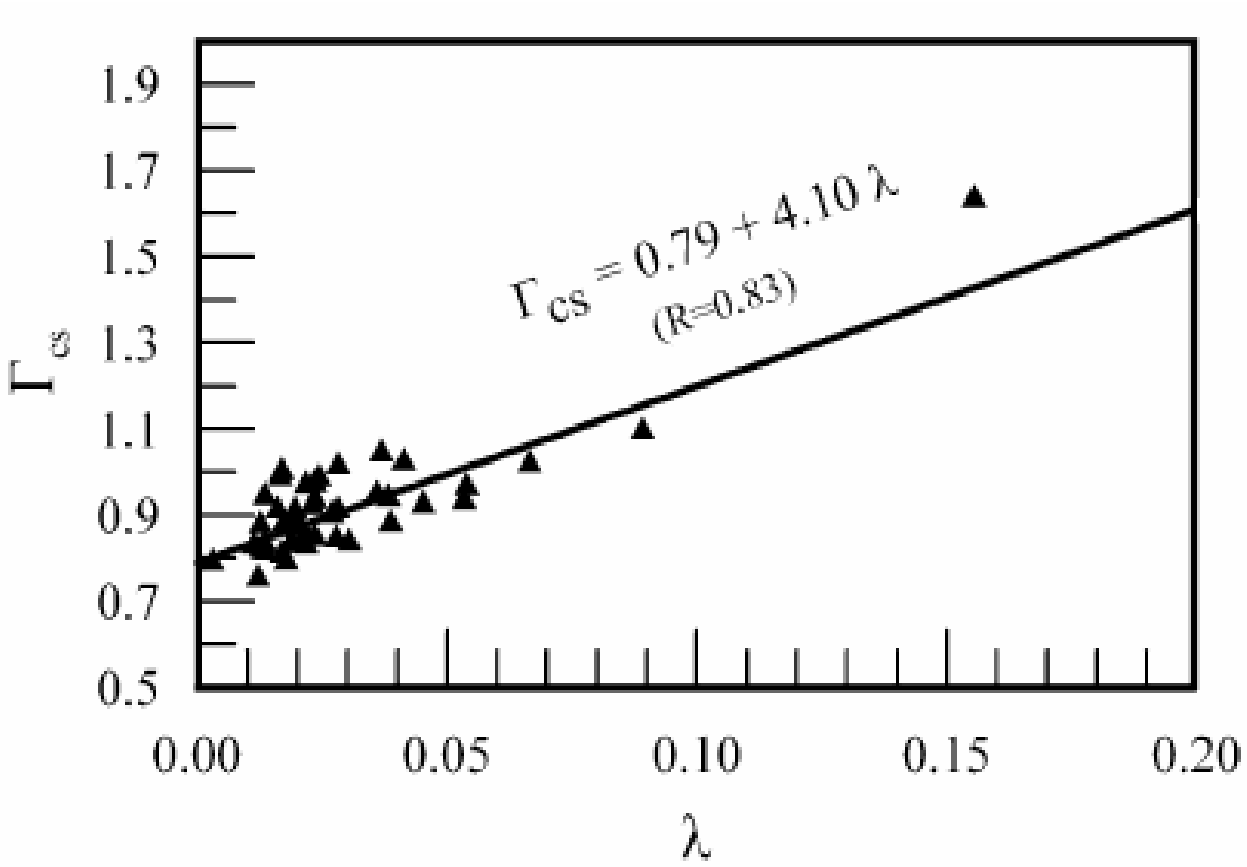

Figure 2.18 Correlation between Critical State Parameters Γ and λ (after Bouckovalas et al., 2003)

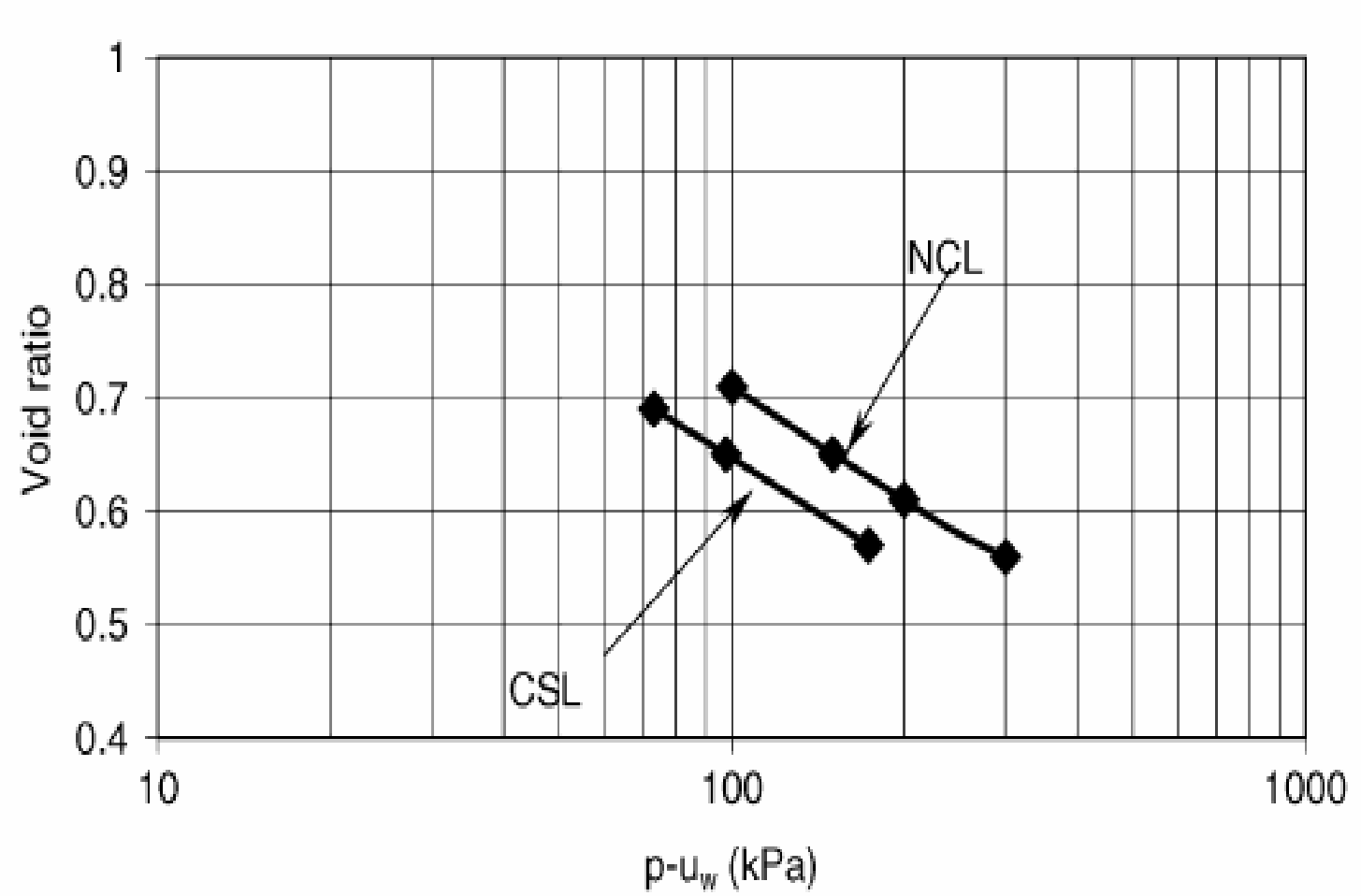

Figure 2.19 Normally Consolidated Line (NCL) and Critical State Line (CSL) of Sainte-Rosalie Clay (after Eko, 2005)

(see Figure 2.20). Much higher stresses (about 15580 kPa) confirm that the effect of the presence of granular materials is negligible for clay contents higher than 40%. The relationship obtained is given as

$$\ln v_c = \ln K - \lambda \ln \sigma_v^{'} \qquad 2.64$$

where K is a reference value of clay specific volume for vertical effective stress $\sigma_v^{'} = 1kPa$. From the above equation, a relationship was established between vertical effective stresses, clay content (C), and granular specific volume (v_g) as

$$\sigma_v^{'} = \left[\left(\frac{1-C}{C} \right) \left(\frac{v_g - 1}{K} \right) \right]^{-\frac{1}{\lambda}} \qquad 2.65$$

Triaxial compression tests were performed on samples with isotropic overconsolidation ratios of 1.33 and 4. The results of undrained compression tests indicated that, shear stress and shear strain as well as pore pressure and shear strain relationships were independent of clay content down to about 30% (see Figures 2.21 and 2.22).

With clay content of 40% and above, the pore pressure response shows typical over consolidated clays while below that percentage it shows a pore pressure response more typical of loose sand. A similar pattern was observed in the drained compression tests as well. A clear distinction similar to the undrained condition is observed when clay volumetric strain instead of volumetric strain is plotted against shear strain. It was then concluded that for clay contents above 30%, the behavior of the mechanical properties of the mixtures is

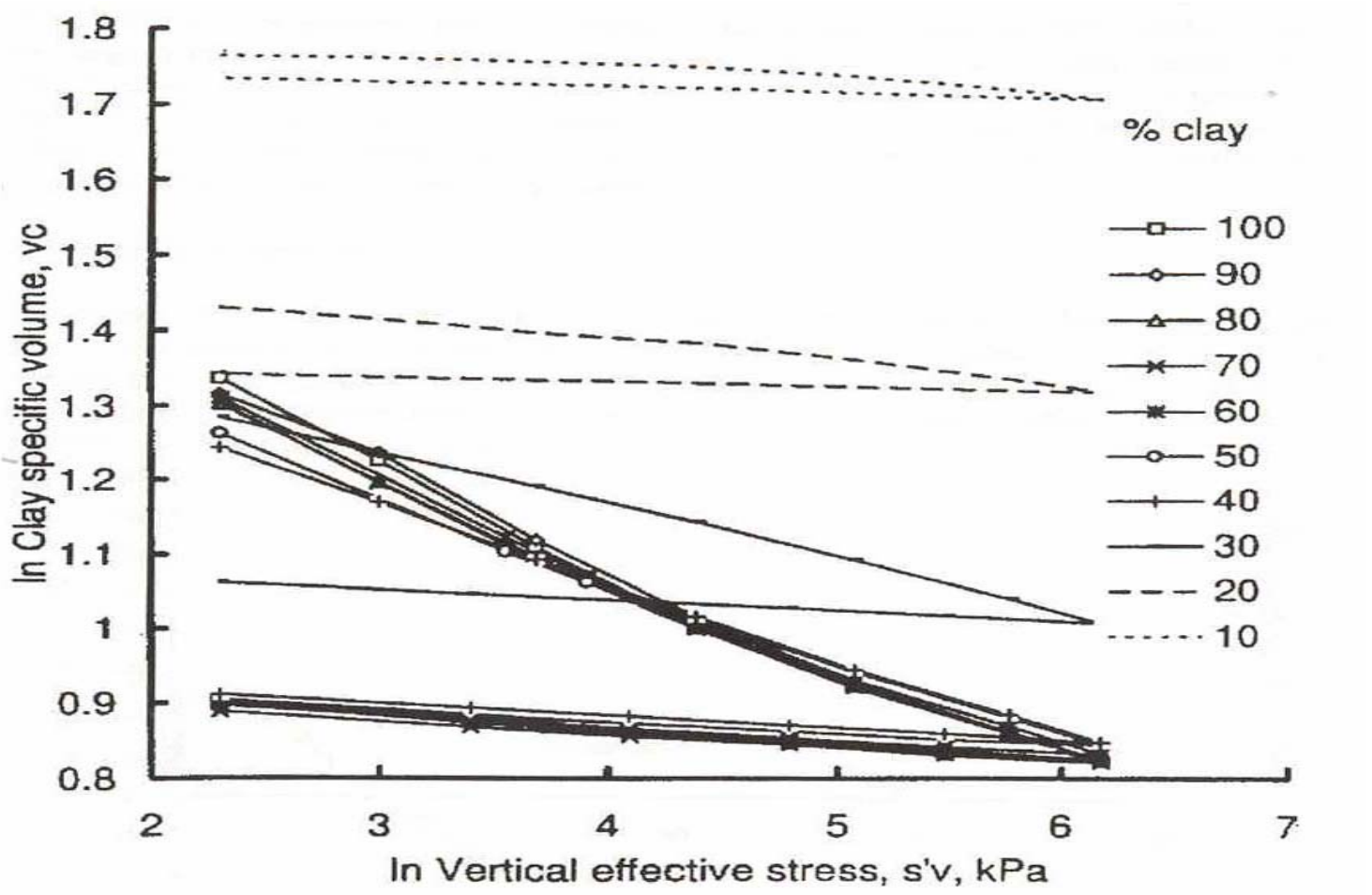

Figure 2.20 One-Dimensional Compression of Mixtures: Vertical Effective Stress vs Clay Specific Volume (Kumar and Wood, 1997)

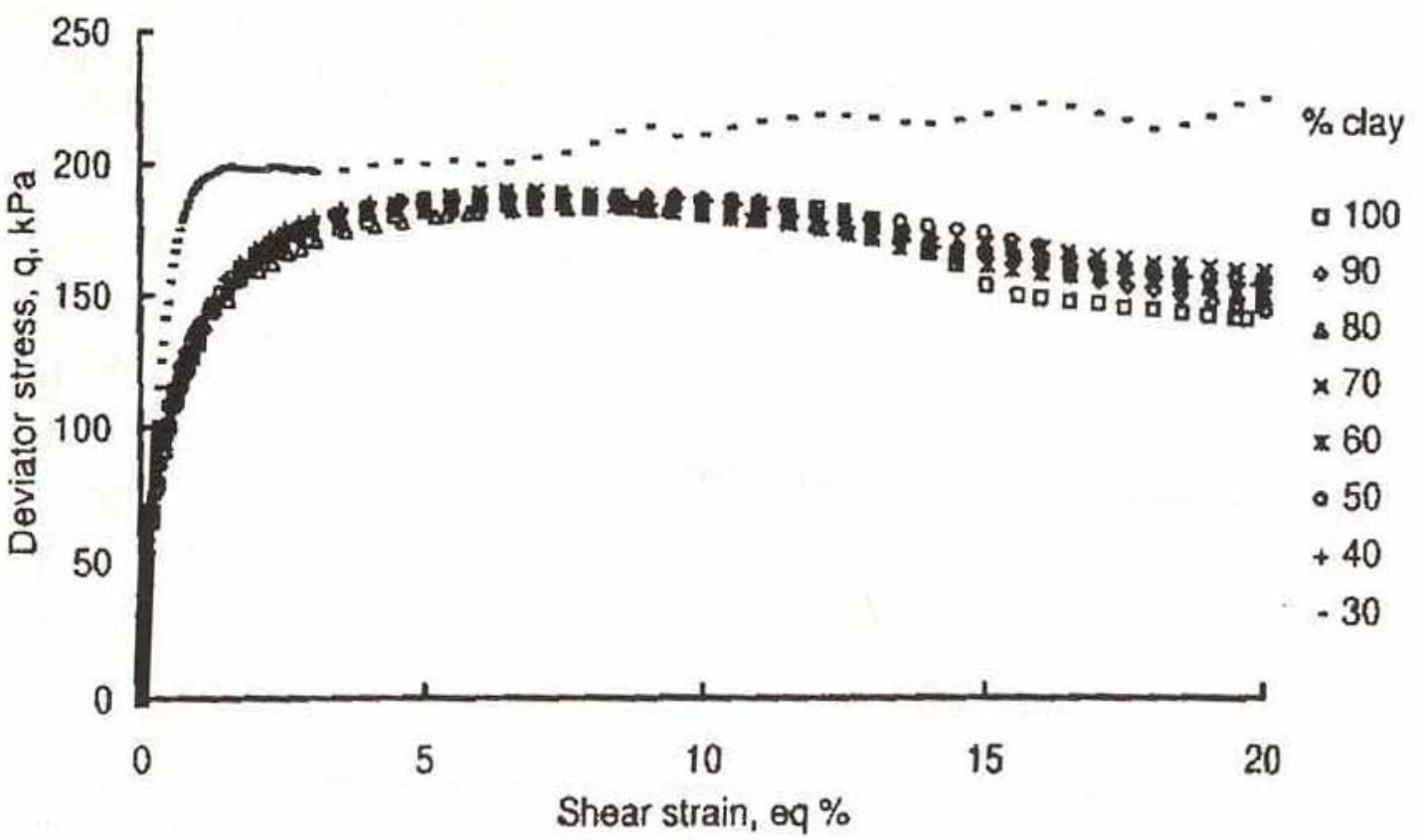

Figure 2.21 Undrained Triaxial Compression of Mixtures: Stress-Strain Response of Normally Consolidated Samples (Kumar and Wood, 1997)

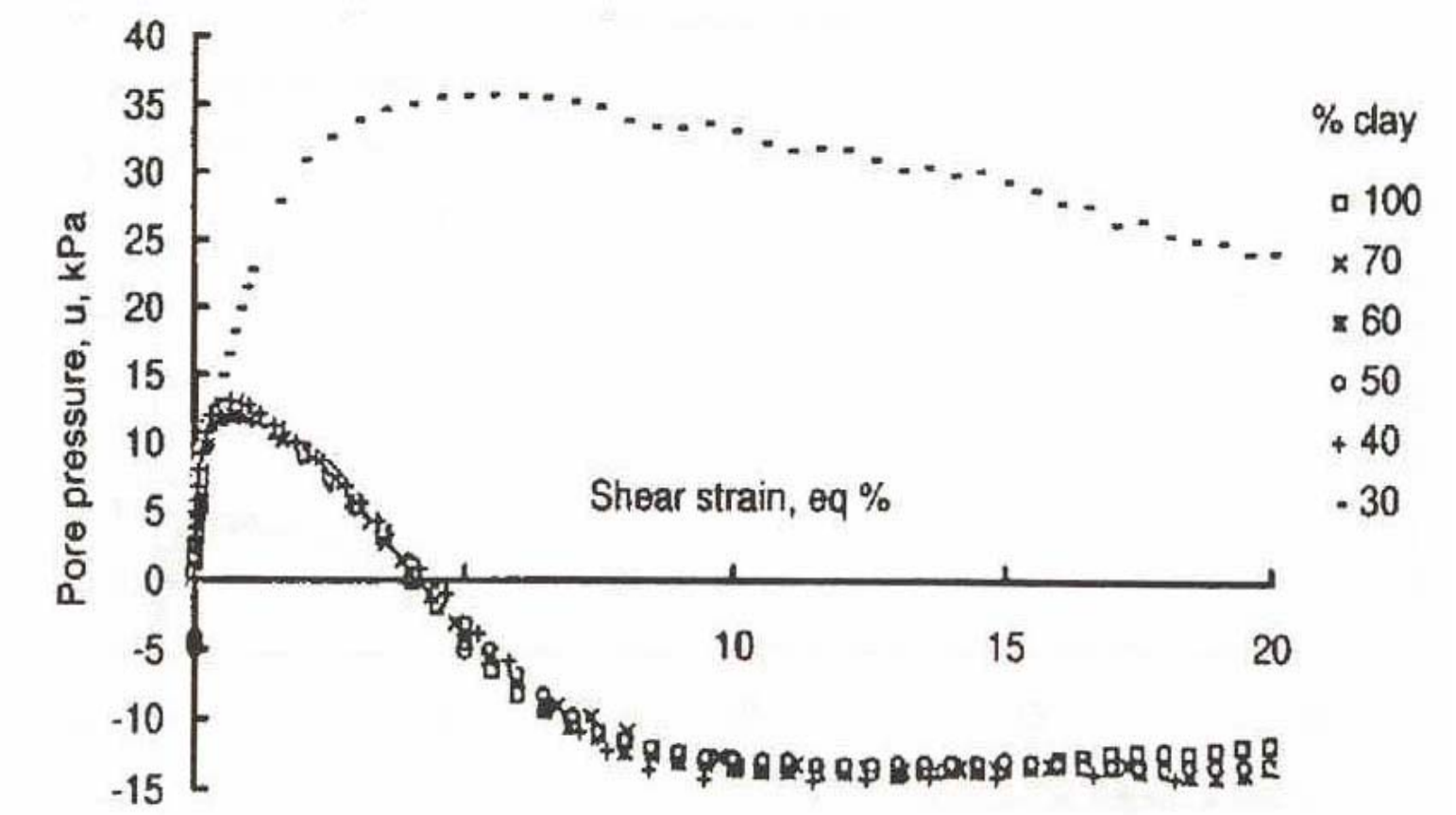

Figure 2.22 Undrained Triaxial Compression of Mixtures: Pore Pressure Response of Samples with Over-consolidation Ratio = 4 (Kumar and Wood, 1997)

controlled by the properties of the clay phase alone.

Based on this knowledge, the generalized model or theory that will emerge from the combination of mixture theory and the physicochemical properties of the fly ash-modified soils (taking into consideration the time effect on cementation) will therefore be transformed into a critical state model. This will make it easier in predicting the behavior of fly ash modified soils with limited known properties. The possibility of this is the premise on which the CSM is based upon. The model will help engineers in predicting the properties of soil mixtures based on the constituents before actually preparing them.

2.7 SUMMARY

The discussion above presents ideas and theories that are applicable to fly ash-modified soils. The formulation of the mixture theory model is based on the basic principles of thermodynamic and conservation laws. From the formulation, it is observed that the concept is primarily based on the properties of the individual constituents and their respective volume or gravimetric fractions. The theory can therefore be used to predict any property in any mixture regardless of the nature of the materials as long as those properties of the individual constituents are known. Different forms and modifications of the mixture theories were observed and have been used in different applications by different authors successfully.

It was also observed that, in binary mixtures, a minimum porosity or void ratio is reached where maximum or minimum engineering properties of the mixture are realized. This minimum porosity or void ratio is dependent on the shape of the materials constituting

the binary mixture and usually occurs within 20% to 40% of the inclusion in the mixture. This phenomenon is always realized regardless of whether the inclusion is coarse and the matrix is fine or vice versa as demonstrated by Santamarina (2001), Vallejo (2000), and Kumar and Wood (1997).

Research of fly ash-modified soils has thrown light on the effect of CaO on the engineering properties of the soil mixture. Findings revealed that regardless of soil type, fly ash is capable of improving engineering properties of fly ash-modified soils. Results from literature indicate that fly ash addition can improve index and strength properties of fly ash-modified soils. There were no reports on deformation properties in literature.

The improvement in engineering properties of fly ash modified soils is partially attributed to physicochemical interactions between the fly ash and the soil. The extent of improvement could be dependent on the chemical composition of the fly ash or the soil type, or both. Chemical properties such as cation exchange capacity of soils are also influenced by the addition of fly ash. The ability to exchange cations among soil and fly ash particles depending on the chemical compositions lead to pozzolanic reactions, which contributes to the improvement in strength and index properties.

Laboratory results can be transformed into critical state terms. The rationale behind this transformation is that predictions can be made based with limited data available on the soil or soil mixture. This is because critical state soil mechanics is an idealization and simplification of soil behavior and captures the salient aspects needed by the geotechnical

engineer. It can be used to predict yield and failure stresses. Critical state parameters are unique to each soil type and can be obtained from laboratory test results.

Due to the difference in particle sizes in the materials considered in this study, mixture theory models are suitable for predictions in mixtures from these materials. The concept of minimum porosity or void ratio can also be analyzed due to difference in particle sizes. The materials considered are fly ash and clay, and due to their chemical compositions, physicochemical activities can be analyzed and compared to results from literature.

CHAPTER 3 : ANALYSES OF LITERATURE DATA

3.1 ASSESSMENT OF MIXTURE THEORY MODELS

The predictive accuracy of the models discussed in Chapter 2, as applied to fly ash-modified soils is assessed here. This assessment consisted of using some of the more established mixture theory models to predict several engineering properties of mixtures from individual constituents. The specific models considered are Voigt (1889), Omine et al. (1998), and Braem et al. (1987). The Hashin-Shtrikman model was not used because it requires more than one property of the individual constituents to predict one property of the mixture. Also, the model predicts upper and lower bounds, but this study seeks to predict closer to the actual results. The properties considered include optimum moisture content (OMC), maximum dry density (MDD), cohesion intercept, internal friction angle (ϕ), and California bearing ratio (CBR). The influence of physicochemical interactions on the predictive accuracy of the mixture theory models are also analyzed and discussed.

Most of the work reported in the literature on fly ash modified soils involves high calcium Class C fly ash, lime, or cement in addition to the fly ash. This research is focused on fly ash modified soils that used mainly Class F and low calcium oxide Class C fly ash with no lime or cement admixtures.

3.1.1 MOISTURE-DENSITY PARAMETERS

Soil compaction is important in geotechnical engineering for many reasons. It uses a compactive effort to render the soil configuration into a denser material, which increases strength and stability. As a result of compaction, compressibility and percolation through the

soil mass is reduced. Usually, the maximum properties are realized at the optimum moisture content. At optimum moisture content, void ratio is said to be minimum leading to the maximum dry density in the soil. The improved properties of the soil due to compaction make it suitable for geotechnical applications such as embankments and subgrades. Mixture theory models have been used in predicting and comparing moisture-density relationships from other researchers. Figure 3.1 presents the maximum dry density of actual data from soil mixtures made from different soil types and Class F fly ash are plotted against their respective optimum moisture content, and then compared with predicted maximum dry density from mixture theory models. It can be observed in Figure 3.1 that the maximum dry density decreases with increasing optimum moisture content although the mixtures are different in each case with respect to fly ash content. It appears that the soil type had no effect on the trend between the dry densities and the moisture content. The mixture theory models predictions followed similar trends as the actual and they predict closely to the actual data as well. The results in Figure 3.1 show a similar trend with all the data from Prabakar (2001), and Kumar and Sharma (2000). A similar relation between maximum dry density and optimum moisture content with two different clay types (CL and CH) and a Class C fly ash from Misra (2000) is presented in Figure 3.2. The trend observed in maximum dry density with respect to optimum moisture content is reversed as compared to those in the Class F mixtures in Figure 3.1. This could be due to the chemical composition of the fly ashes. The models predicted closely to the actual in the CH soil mixture, but were not the case in all the data points in the CL soil mixture.

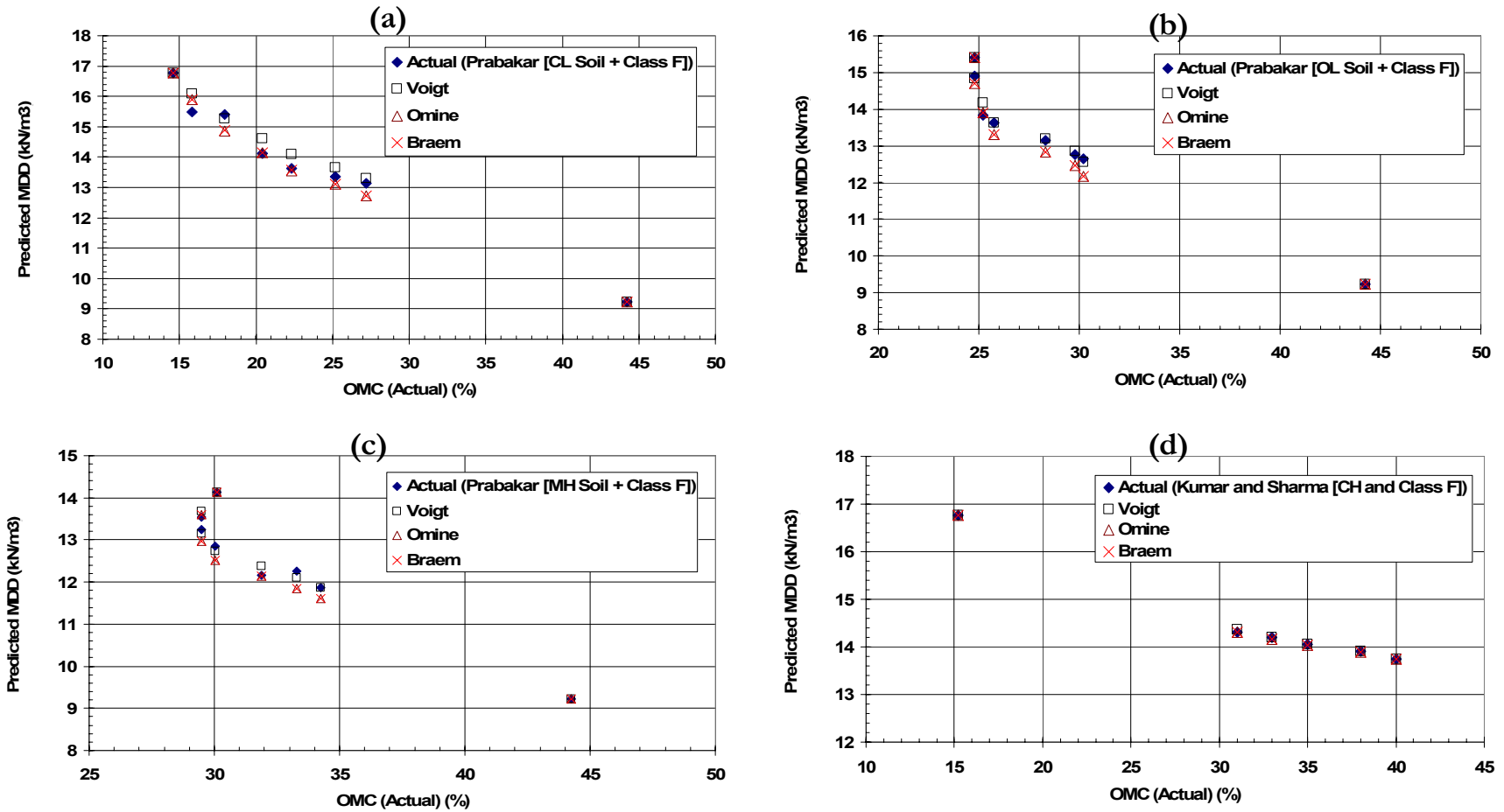

Figure 3.1 Comparing Actual and Predicted Maximum Dry Density (MDD) of Class F Fly Ash Mixtures

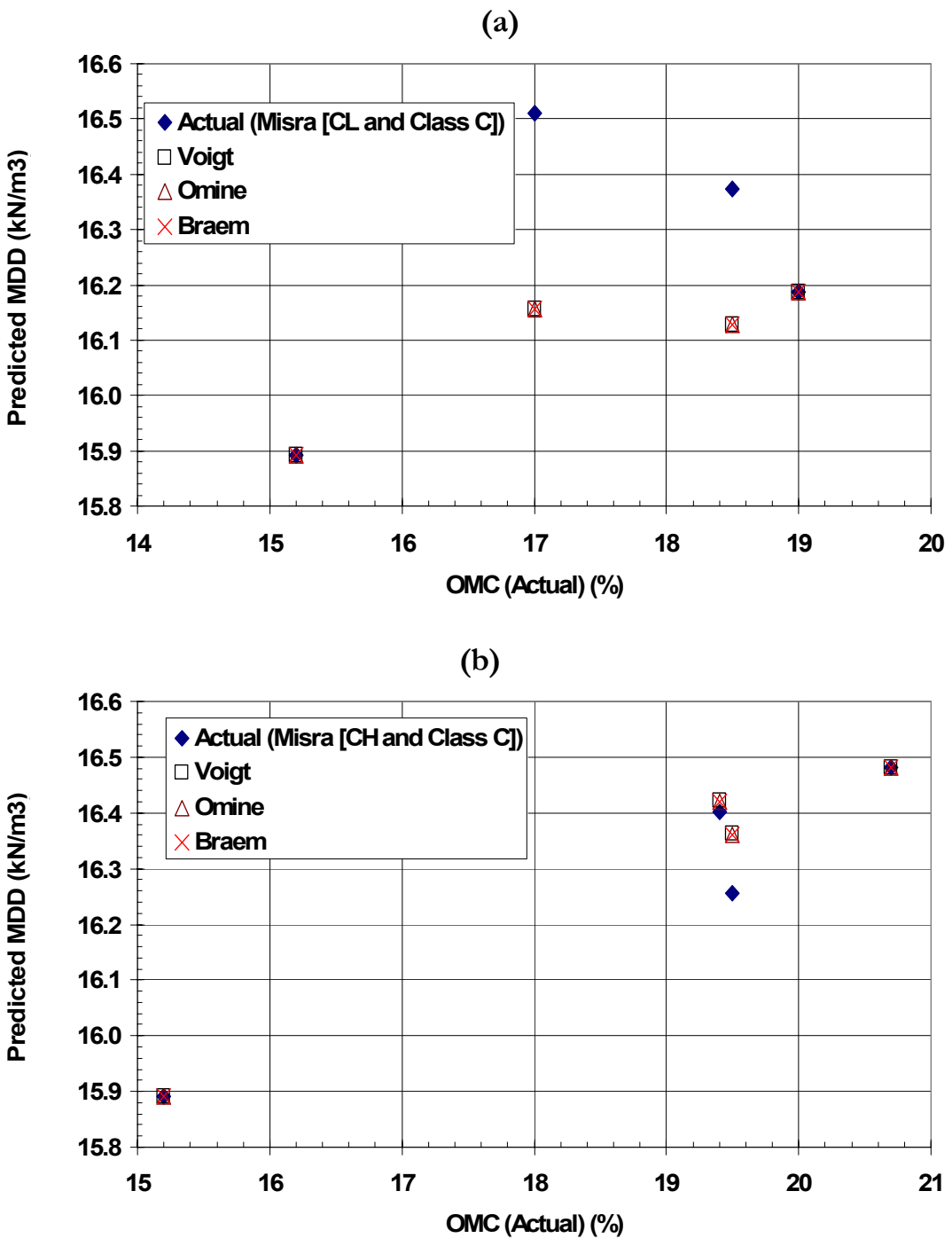

Figure 3.2 Comparing Actual and Predicted Maximum Dry Density (MDD) of Class C Fly Ash Mixtures

Figure 3.3 relates the actual and predicted moisture-density parameters to index properties. According to Figures 3.3 (a) and (b), the optimum moisture content increases with increasing liquid limit (LL) and plasticity index (PI). The models proposed by Braem et al. (1987) and Omine (1998) predicted closely to each other and both predicted better with respect to the actual than that of Voigt (1889). In Figure 3.3 (c), it is observed that maximum dry density decreases with increasing plasticity index. All the models predicted well with respect to the actual data and relatively closer to each other as well.

3.1.2 COMPARING ACTUAL PARAMETERS TO PREDICTED RESULTS

To further assess the predictive accuracy of the models, actual results of engineering parameters of fly ash modified-soil mixtures from literature are compared with the same parameters predicted from individual constituents using the mixture theory models. The actual and predicted data can be found in Appendix A.

Figure 3.4 shows moisture-density parameters from various researchers presented in Section 3.1.1. From the figure, optimum moisture content and maximum dry density predictions with the models gives a fairly good correlation between predicted and actual results with all the data. The data showed that regardless of the type of soil or fly ash the models can fairly predict moisture-density parameters well.

The three different soil types used by the researcher (Prabakar, 2004) in his investigation of fly ash contribution to strength parameters of soil mixtures are compared here. The soil types used were clay of low to medium plasticity (CL), an organic silty-clay of low plasticity (OL), and inorganic silts (MH). The fly ash used in the mixtures is classified as Class F. The

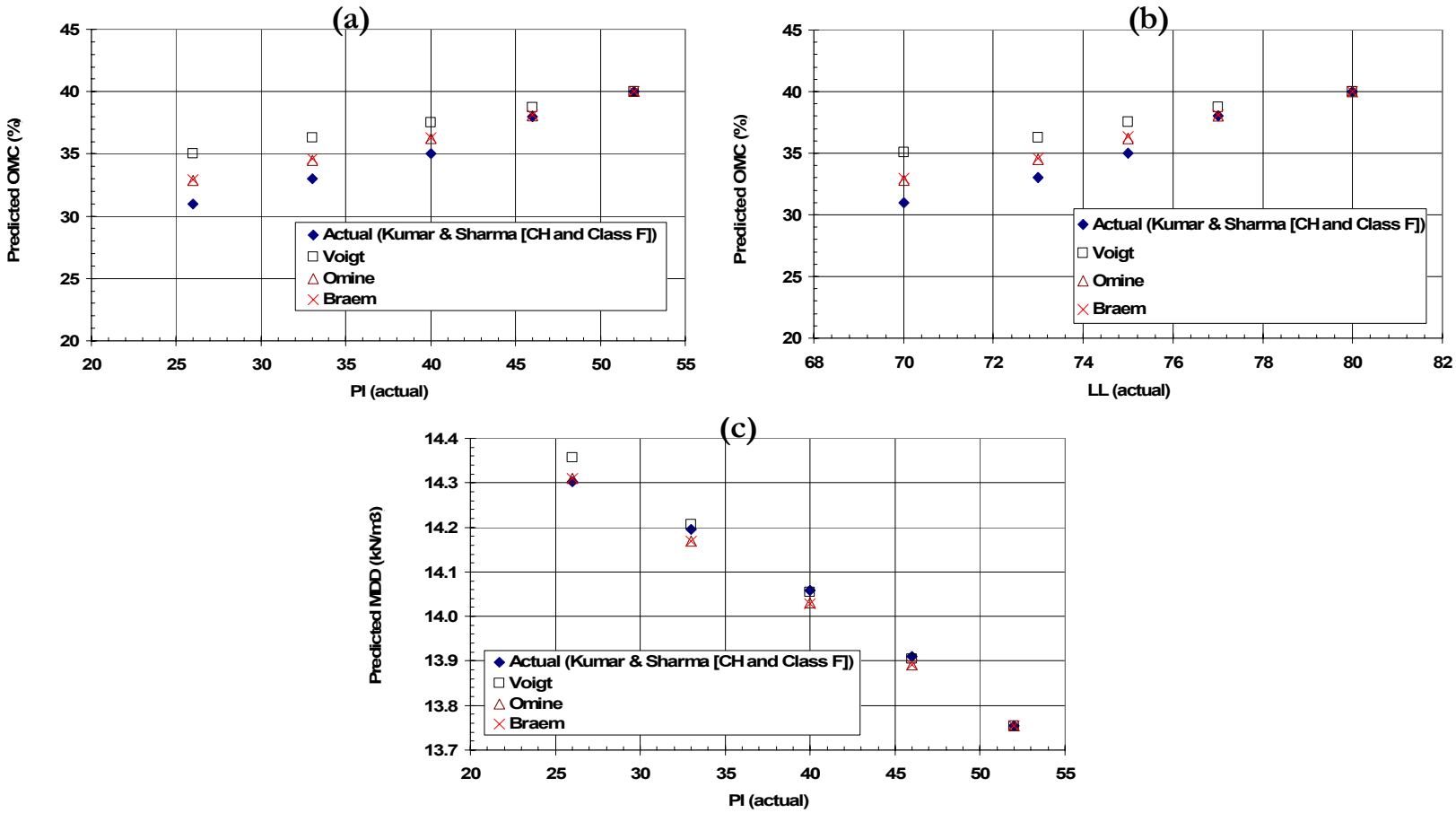

Figure 3.3 Relating Consistency Limits to Moisture-Density Parameters and Comparing Actual to Predicted

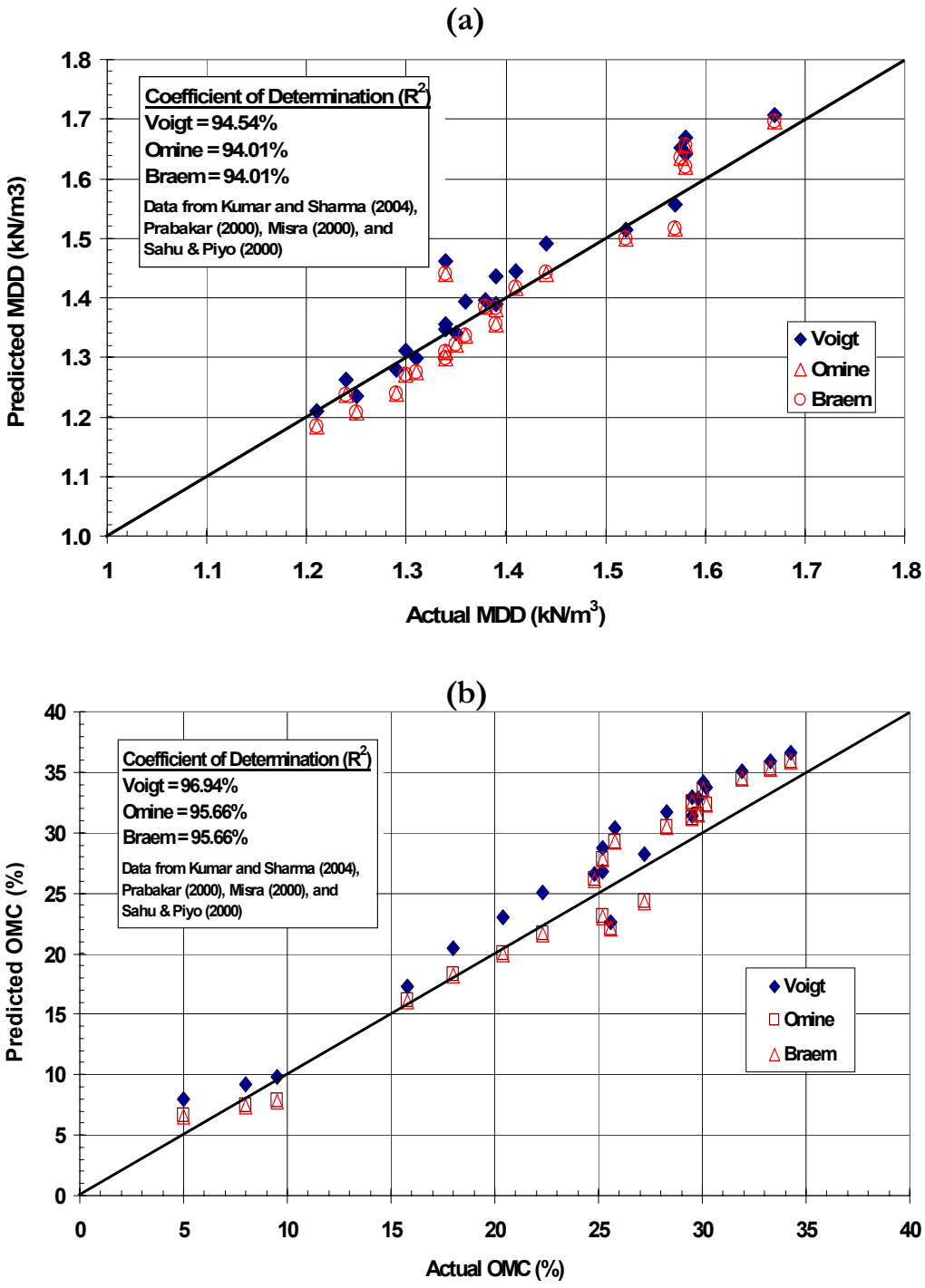

Figure 3.4 Comparisons of Predicted and Actual Maximum Dry Density and Optimum Moisture Content

correlation between predicted and actual data, although skewed, was very good in the strength parameters considered. It can be seen in Figure 3.5(a) that predictions with all the models were strongly correlated with respect to cohesion in both CL and OL soils. Omine (1998) and Braem et al. (1987) models predicted very close to each other in the inorganic silts (MH) compared to that of Voigt (1889); however, Voigt seem to predict better in that soil. The coefficient of determination is summarized in Table 3.1. It can be seen that, in general, Voigt's model predicts better than the other models.

Table 3.1 Determination Coefficient (R^2)

	Cohesion		
Model	CL	OL	MH
Voigt	97.3%	87.2%	73.2%
Omine	96.4%	87.2%	68.9%
Braem	96.4%	87.2%	68.9%
	Friction Angle		
	CL	OL	MH
Voigt	8.3%	95.1%	96.5%
Omine	8.3%	94.7%	96.5%
Braem	8.3%	94.7%	96.5%
	CBR		
	CL	OL	MH
Voigt	97.2%	93.6%	97%
Omine	97.0%	96.2%	98.5%
Braem	97.0%	96.2%	98.5%

The trend in cohesion of the clayey soils was found to be different from that of the inorganic silt. Depending on the chemical compositions of the soil and the fly ash constituting the mixture, relatively different types of chemical interactions can take place.

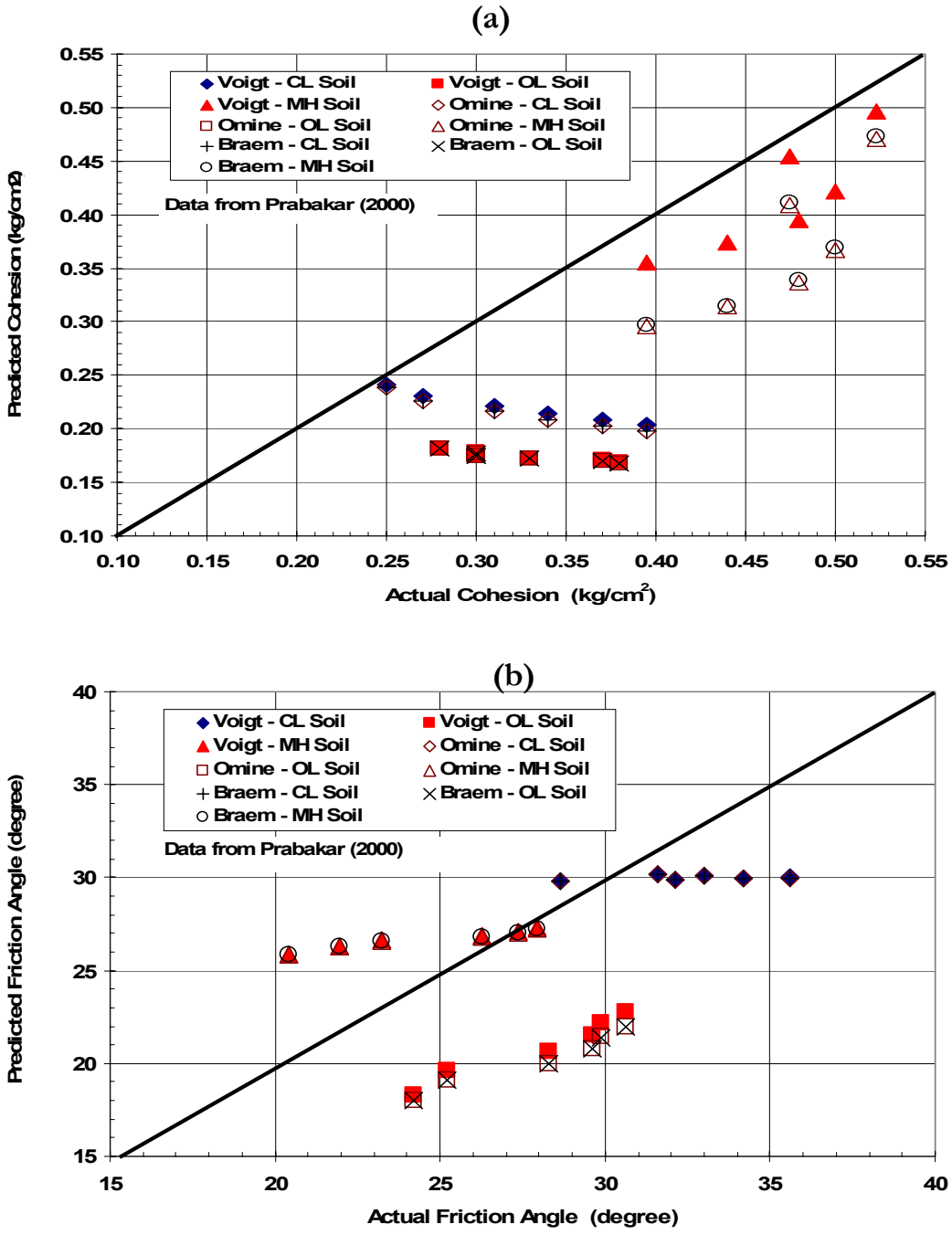

Figure 3.5 Comparisons of Predicted and Actual Cohesion and Friction Angle

The difference in trends among the soil types as seen in Figure 3.5 could be due to different chemical interactions that takes place between the different soil types and the fly ash. A similar trend was observed with friction angle in all the soil types as well [see Figure 3.5(b)]. This further explains why strength predictions might not be accurate using properties from the individual constituents alone. Unlike the predictions in cohesion, all the model predictions in friction angle were very close to each other in all the soil types. With the exception of friction angles in the inorganic silts, which all the models overpredict, the rest of the strength parameters in all the soil types are underpredicted by the models. The California bearing ratio (CBR) of the soil mixtures were also underpredicted by all the models according to Figure 3.6. The soil type of which predictions were very close to the actual data is the inorganic silts. This could be attributed to the fact that there were minimal or no reactions between the silts particles and the fly ash particles. Fly ashes consist mainly of silt sized particles and therefore in the absence of chemical or physicochemical interactions, they replace similar sized particles in the inorganic silt-fly ash mixtures. This could, therefore, be the reason why the predictions in the inorganic silt mixtures are better than that of the clay soil mixtures. The skewness in the trends observed in the models predictions need to be modified to yield well correlated results comparable to the actual data. This could be rectified by analyzing the physicochemical behavior of the soil and the fly ash interactions.

Most data reported in literature, depending on the focus of the research, has concentrated on the effect of fly ash on either consistency limits or moisture-density parameters with very few investigating the effects of fly ash on strength properties. Lack of

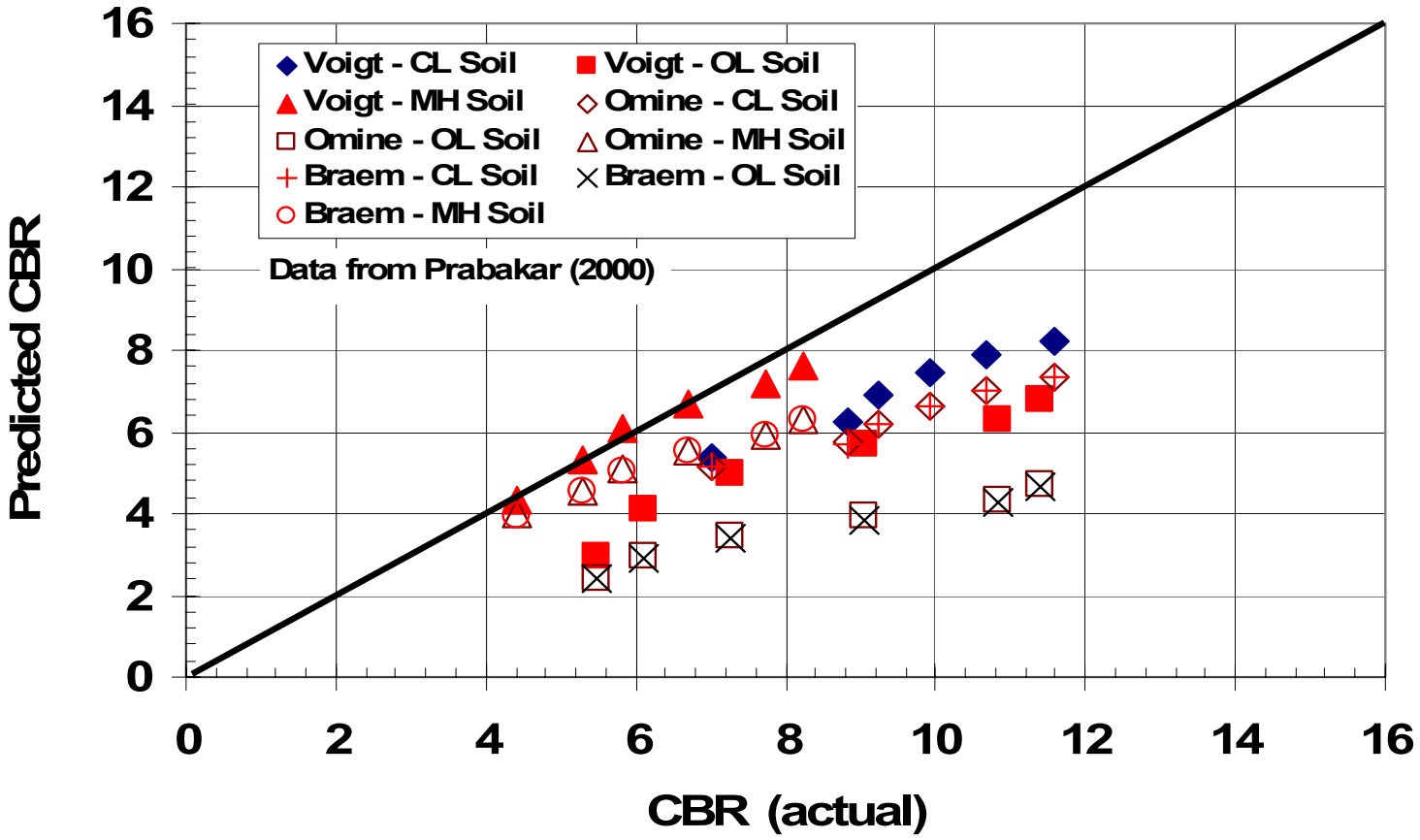

Figure 3.6 Comparison of Models Prediction of CBR for CL, OL and MH Soil Mixtures

data on investigating all the engineering properties mentioned above on the same mixtures make it difficult to have a good assessment of the models. The models rely basically on individual properties constituting the mixtures to predict the mixture properties. Since most of the study in literature is usually based on one of the engineering properties and in most cases either the properties of the soil or the fly ash alone is not reported, it becomes difficult applying the mixture theory models to predict the mixture properties. In situations where the individual properties are not available, it will be difficult and probably inaccurate to extrapolate the properties from the mixtures. It would also not be a good idea in using data from one researcher and compare or predict other engineering properties from other researchers since the soil types and the fly ashes used may not be the same, as well as the method used in obtaining the results. These data gaps call for detailed laboratory experiments on mixtures to aid in assessing the predictive accuracy of the models on soil mixtures.

3.2 PHYSICOCHEMICAL ANALYSIS OF LITERATURE DATA

One of the main distinguishing factors among the two types of fly ashes (Class C and Class F) is its physicochemical characteristics. It is therefore believed that the engineering properties of fly ash-soil mixtures can be linked to these factors. Developing and establishing relations for the influence of physicochemical properties on engineering behavior of fly ash-modified soils can be derived from literature data.

Data obtained from existing literature were examined for the influence of the physicochemical properties on some properties of fly ash modified soils. Properties of fly

ash soil mixtures such as liquid limits, plasticity index, maximum dry density, and unconfined compressive strengths were considered. Knowledge of index properties of fine-grained soil and soil mixtures are of great importance. Index properties are used in geotechnical engineering to describe, identify, classify, and as a basis for preliminary assessment of the soils mechanical behavior. There are well established relationships between soil composition and some physical properties of soils (Mitchell, 1993).

Figure 3.7(a) shows the effect of calcium oxide (CaO) content on liquid limits of high plasticity clayey soils. According to the figure, increase in fly ash content decreases the liquid limit of the soil. It was also observed that an increase in the CaO has a reduction effect on the liquid limits of the soil. A similar trend was observed with plasticity index of the soil as seen in Figure 3.7(b). This effect could be due to the chemical reactions between the CaO and the silica and alumina from the clay. Other factors such as specific surface, and CEC of the clay could contribute to this effect as well.

The effect of fly ash content on maximum dry density is illustrated in Figure 3.8. As can be seen in Figure 3.8, maximum dry density decreases with increasing fly ash content for all the data from different researchers with different soil types and fly ashes. According to the results from Kumar and Sharma (2004), the MDD tends to increase with increasing fly ash up to about 20% and then decreases. The decrease in the data from Misra et al. (2000) with both soil types is also not very much up to 20% fly ash content. Besides the interaction that takes place between the fly ash and clay particles, the decrease could be attributed to the hollow nature of the fly ash particles that make the material less dense as it replaces the clay

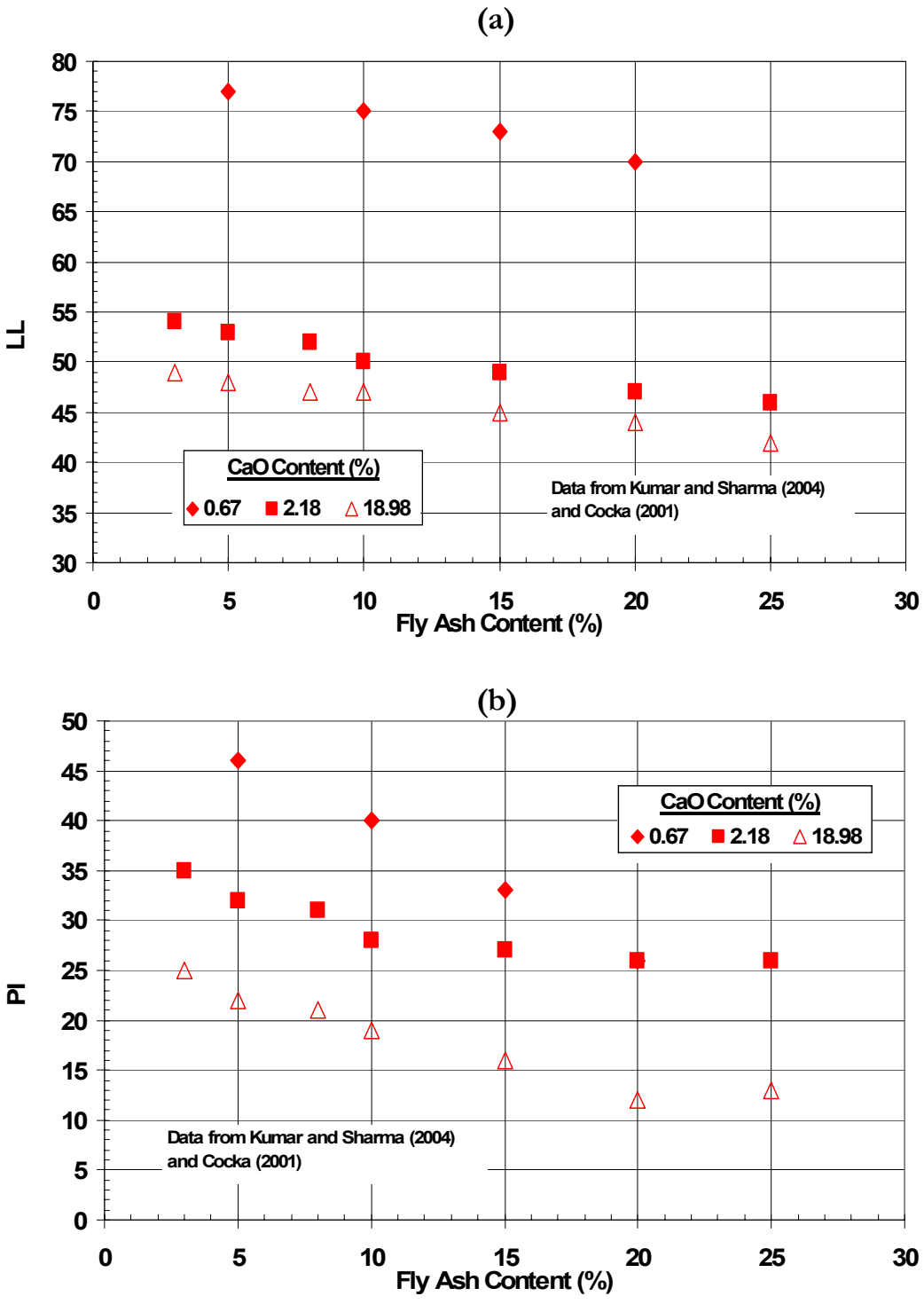

Figure 3.7 Effect of CaO on Liquid Limits (LL) and Plasticity Index (PI) on High Plasticity Clays (CH)

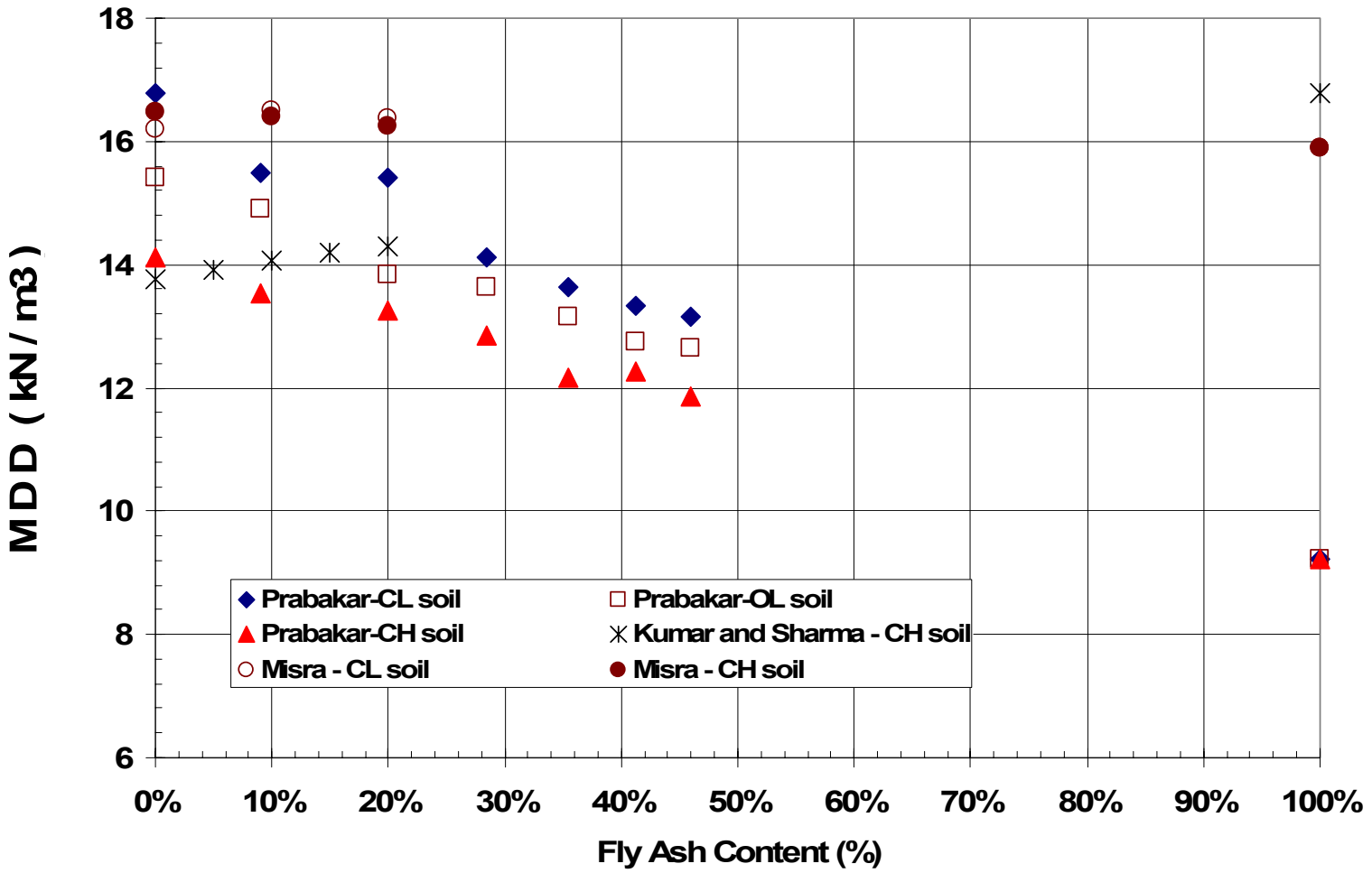

Figure 3.8 Effect of Fly Ash Content on Maximum Dry Density

material in the mixtures.

With respect to the amount of CaO content in the fly ash, the CaO content for Prabakar (2004) was 1.5%. The difference in the trends is due to the three different soil types used in the study, with CL having higher densities, followed by OL, and then the CH soil. The mixture with the highest CaO content is that of Misra et al. (2000), which gave higher densities in both soil types than the other mixtures from other researchers. It is also believed that the amount of Fe_2O_3 present in the fly ash accounts for the heaviness of the ash. This then follows that the ash with a high Fe_2O_3 content will result in high densities in their mixtures. Again, this phenomenon was observed in the densities obtained by all the researchers with the fly ash chemical compositions.

With unconfined compressive strengths, it can be seen in Figure 3.9 that as CaO content increases, strength increases. As the fly ash content increases, it is expected that the CaO available for physicochemical activity increases in each of the mixtures. This is seen in an increase in the strengths as the fly ash content increases. Similarly, as the CaO content increases in different fly ashes mixed with the clay samples, an increase in strengths was observed.

Analyses of mixtures with different fly ash percentages mixed with different soil types were considered in the case of strength properties. The results were found to trend with the amount of fly ash used in the mixtures. The variation in trends was observed to be between soil types. The effect of fly ash content on cohesion and internal friction angle in the mixtures is presented in Figure 3.10.

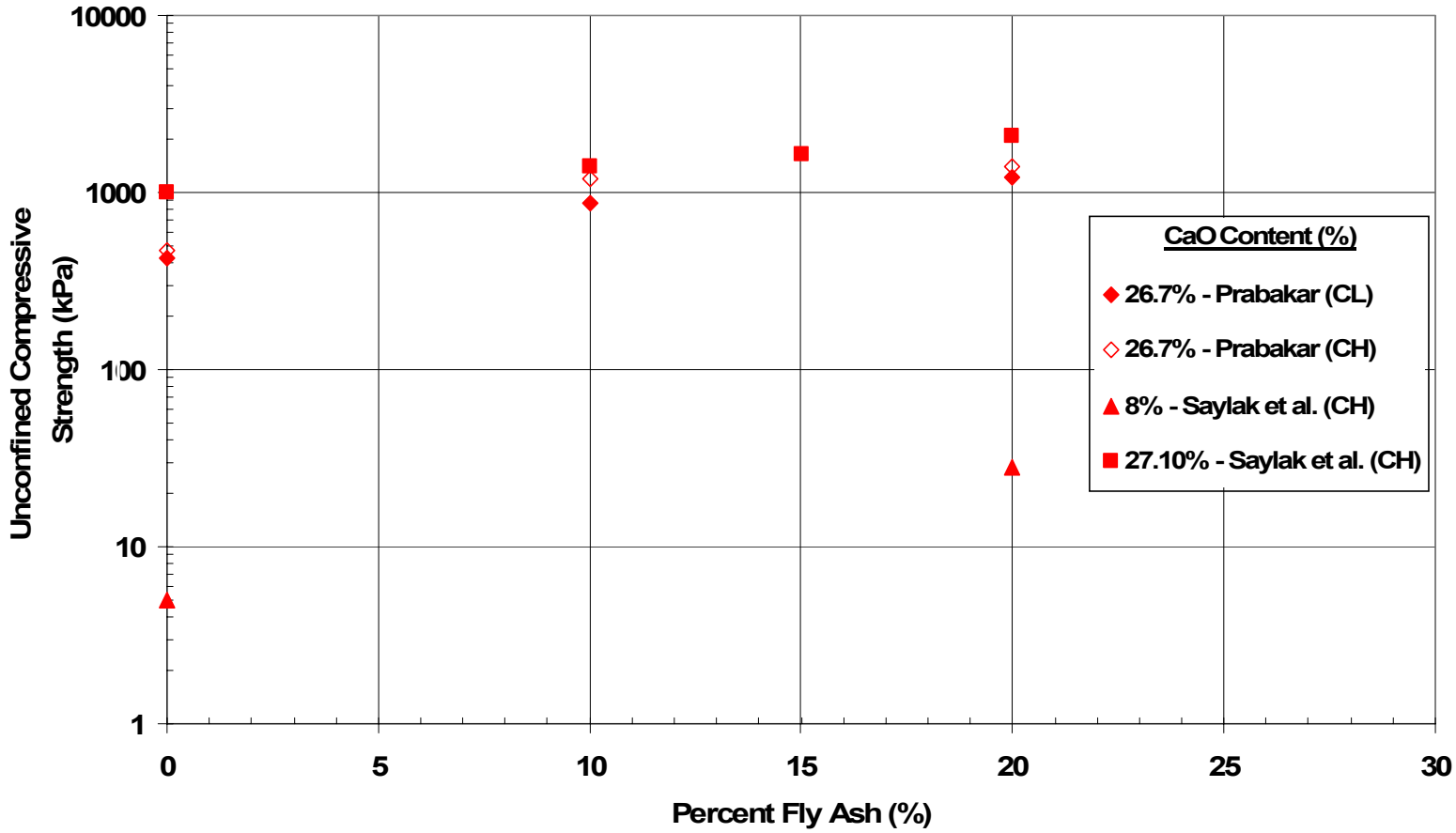

Figure 3.9 Effect of CaO Content from Fly Ashes on Unconfined Compression Strength on Clayey Soils

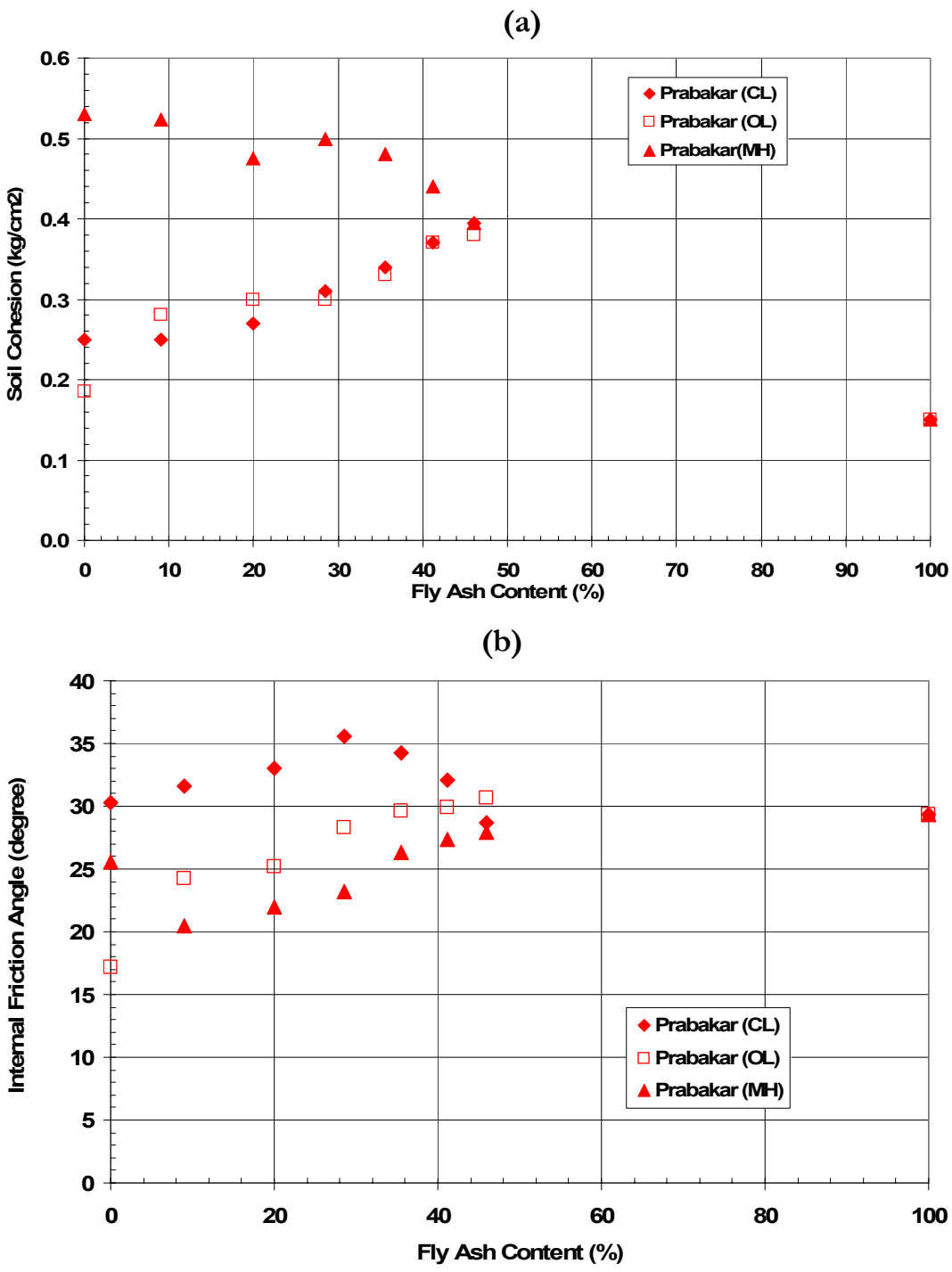

Figure 3.10 Effects of Fly Ash Content on Cohesion and Internal Friction Angle

It is observed from both Figures 3.10 (a) and (b) that, as the fly ash content increases, the cohesion as well as friction angle increases with the exception of the soil type MH. This might be due the chemical reactions between the MH soil and the fly ash used in the study. Mineralogical differences between the soil types could account for such behavior. The quantity of fly ash in fly ash soil mixtures affects the geotechnical properties of the mixtures. The effects can be seen in Figures 3.7 through 3.10. According to Figures 3.7 (a) and (b), the liquid limit and plasticity index of each of the mixtures decreases with increasing fly ash content. Compressive strength increases with fly ash content as the material becomes coarser. The internal friction angle increases as the materials becomes coarse which is due to the increase in fly ash content. This will in turn increase strength in the mixtures as the amount of fly ash increases.

3.3 SUMMARY OF OBSERVATIONS

It was observed that the mixture theory models can predict some of the geotechnical properties well. In certain cases, the models either overpredict or underpredict the actual results. This could be due to other factors that the models do not take into consideration such as the influence of chemical composition of the materials forming the mixtures and chemical reactions between particles. In terms of moisture-density parameters, the models' predictability was found to be independent of the soil type. Voigt's model predicted better in the case of maximum dry density than that of the other two models. There was a good trend in relating moisture-density parameters to consistency limits.

From literature, most data are presented on just the mixtures and not the individual constituents. This makes it difficult in applying the mixture theory models.

It was also observed that the amount of fly ash present influences the behavior of the mixtures and depending on the mineralogical composition of the ash, as well as the soil type, the mixtures behave differently. Fly ash content was found to decrease the maximum dry density of all the mixtures. This is attributed to the hollow nature of the fly ash particles which makes it lighter and therefore reduces the dry density when it replaces the clay particles. In general, the trends were similar among the different researchers presented above.

CaO was found to influence consistency limits. The higher the CaO, the lower the consistency limit for a given mixture of same fly ash proportion. Compressive strength is also found to increase with increasing fly ash content due to the chemical interaction that renders the particles to be coarser and also increasing bonding between particles.

It would therefore be prudent to combine the models with the physicochemical effect as a result of chemical interactions between the ashes and the soil types to improve upon the predictive capabilities of the models.

CHAPTER 4 : LABORATORY RESULTS

The results obtained from the experiments performed are presented in this chapter. The properties obtained from the experiments included index properties, deformation properties, and strength properties. All experiments were according to American Society of Testing Materials (ASTM) standards and were performed in duplicates and in some cases triplicates to ascertain repeatability of results. The results presented are the averages of the tests performed. All samples were tested immediately after preparation and therefore time effects were not considered in the entire study.

4.1 INDEX PROPERTIES

Index properties help classify and quantify the soil, fly ash, and soil mixtures in terms of grain sizes and distributions, consistency limits, and pore structure. The chemical compositions of the fly ashes as well as cation exchange capacities (CEC) were also analyzed. These properties were analyzed because they will be useful in determining the effects of fly ash quantities and chemical properties on the mixtures and help to relate them to geotechnical properties of the mixtures.

4.1.1 CHEMICAL COMPOSITION AND CATION EXCHANGE CAPACITY OF FLY ASH

Four fly ashes were analyzed by Sieg (2005) of Headwaters Resources Materials Testing and Research Facility. The original test results are presented in Appendix A. The chemical analyses were performed on dry ignited basis using a Burker S4 X-ray fluorescence spectrometer according to ASTM D4326. Carbon content was measured with a Leco

SC444DR Carbon/Sulfur analyzer. The LOI was performed according to ASTM C 311 (Standard Test Methods for Sampling and Testing Fly Ash or Natural Pozzolans for Use in Portland-Cement Concrete). The results of the chemical composition (ASTM C 311 / D 4326) of the fly ashes and cation exchange capacity for all soil mixtures are presented in Tables 4.1 and 4.2, respectively. The cation exchange capacity was performed according to Soil Survey Standard Test Method by ammonium chloride (NH_4Cl). The tests were performed in triplicates to ensure repeatability, and the averages of the results are presented in Table 4.2. Three of the ashes were classified as Class F and one as Class C fly ashes. The Class C ash was found to be within the low calcium oxide range (10% - 20%) according to ASTM C 618 classification.

Table 4.1 Chemical Composition of Fly Ashes

Sample Label	Fly Ash 1 (Class F)	Fly Ash 2 (Class F)	Fly Ash 3 C (Class F)	Class C
Silicon Dioxide, SiO_2	41.57 %	40.62 %	58.76 %	40.21 %
Aluminum Oxide, Al_2O_3	20.66 %	19.87 %	29.14 %	21.74 %
Iron Oxide, Fe_2O_3	29.97 %	27.06 %	3.81 %	9.08 %
Sum of SiO_2, Al_2O_3, Fe_2O_3	92.20 %	87.55 %	91.71 %	71.03 %
Sulfur Trioxide, SO_3	0.78 %	2.33 %	0.13 %	2.15 %
Calcium Oxide, CaO	3.04 %	4.04 %	0.89 %	16.99 %
Sodium Oxide, Na_2O	0.41 %	0.38 %	0.24 %	1.22 %
Magnesium Oxide, MgO	0.64 %	2.86 %	0.85 %	4.52 %
Potassium Oxide, K_2O	1.67 %	1.66 %	2.82 %	1.41 %
Phosphorus Pentoxide, P_2O_5	0.24 %	0.21 %	0.10 %	1.30 %
Titanium Dioxide, TiO_2	1.03 %	0.97 %	1.70 %	1.33 %
Carbon	1.19 %	0.63 %	2.13 %	2.19 %
Loss on Ignition	1.45 %	1.86 %	2.70 %	2.89 %

According to Table 4.2, the CEC decreases with increasing fly ash content in all the fly ash types. This trend of decrease in CEC as a result of increasing fly ash content was also observed by Nalbantoglu (2004) in an investigation on the use of fly ash as an expansive soil stabilizer (see Figure 2.11).

Table 4.2 Cation Exchange Capacity of Soil Mixtures

Sample Description	Percent Fly Ash (%)	Cation Exchange Capacity (CEC) – meq/100g
CLAY	0%	57.18
Fly Ash 1	10%	43.45
	20%	38.68
	40%	33.25
	100%	4.21
Fly Ash 2	10%	47.22
	20%	45.87
	40%	34.92
	100%	6.35
Fly Ash 3	10%	52.76
	20%	36.80
	40%	33.68
	100%	12.13
Class C	10%	53.49
	20%	29.21
	40%	22.88
	100%	2.66

He found similar trends with two different soil types, clay with high plasticity (CH) and a low to medium plasticity clayey soil (CL). Nalbantoglu (2004) attributed the trend to specific

area and surface activity. He pointed out that CEC is associated with higher specific area and surface activity. The addition of fly ash, which is mainly silt-sized particles, reduces the specific surface area and activity of the soil mixture, leading to a decrease in CEC. Specific surface and activity are related to the clay fraction ($< 2\,\mu m$) of the soil. As can be seen in Figure 4.1, as the clay fraction of the soil mixtures decreases, the CEC also decreases in all the soil types except in the Class C ash where the addition of fly ash did not affect the clay fraction in two of the mixtures. The trends shown in the Figure 4.1 supports the statement made by Nalbantoglu (2004). It is observed that the decrease in CEC in Class C mixtures as the ash content increases was found to be greater compared to the Class F ashes in this study. Cocka (2001) mentioned that the potential of fly ashes providing multivalent cations promote flocculation of clay particles by cation exchange capacity. As a result, the greater decrease in CEC in Class C fly ash compared to that of Class F could be due to the significant difference in CaO contents.

4.1.2 GRAIN SIZE DISTRIBUTION

Particle size distributions on all the mixtures were analyzed to help classify the soil mixtures. The hydrometer method was used in analyzing the particle size distribution according to ASTM D 422-63 (Standard Test Method for Particle-Size Analysis of Soils). The grain size distribution tests were performed in duplicates to ensure consistency. The averages of the results were used for the particle size distribution curves. The particle size distribution curves in all the fly ash mixtures indicate that as the fly ash content increases the mixture becomes

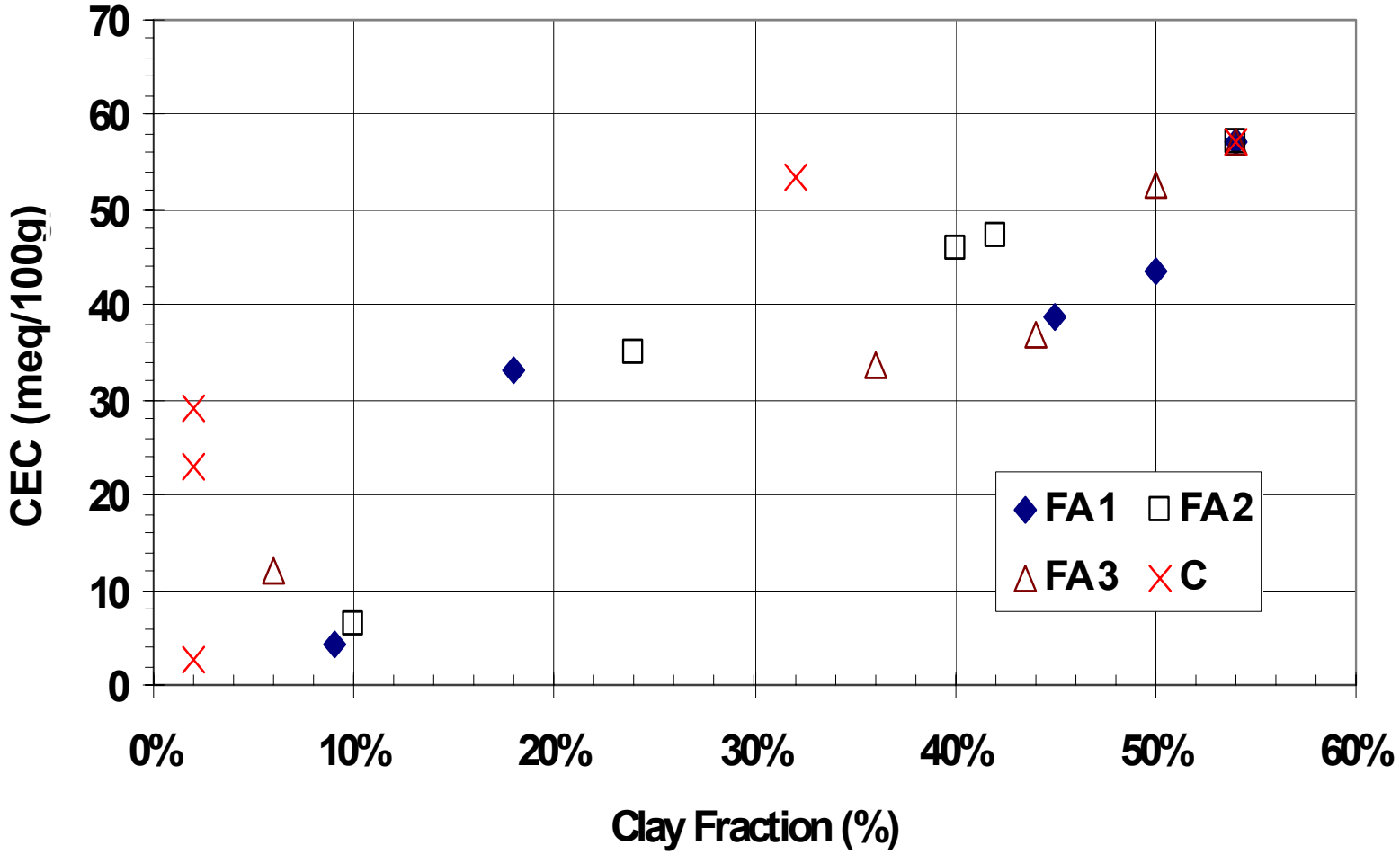

Figure 4.1 Effect of Clay Fraction on Cation Exchange Capacity (CEC)

coarser. The fly ash replaces the clay sized particles making the resulting mixture coarser compared to the pure clay soil. Figure 4.2 shows the distribution curves of all the ashes and their mixtures. Lu and Zhu (2004) indicated that fly ash alters the grain size distribution of clay soils making it coarser, which in turn affects the physical properties of the soil mixture. This is the case with most researchers such as Kim et al. (2005), Lu and Zhu (2004), Nalbantoglu (2004), Cocka (2001), and Ferguson (1993) on the subject.

4.1.3 SPECIFIC GRAVITY AND ATTERBERGS LIMITS

Specific gravity is used in determining moisture-density related properties of materials. ASTM D 854-00 (Standard Test Methods for Specific Gravity of Soil Solids by Water Pycnometer) was the method used in determining the specific gravity of the fly ash-soil mixtures and were performed in duplicates. Specific gravity of the mixtures was found to decrease with increasing fly ash content in all the fly ashes. In general, the specific gravity of fly ash-soil mixtures decreases with increasing fly ash content due to the low specific gravity of fly ashes compared to that of soils (Cocka, 2001). The observed trend in this study can be seen in Figure 4.3 where the effect of fly ash content on specific gravity is presented. The behavior of specific gravity with fly ash content from Figure 4.3 is in agreement with Cocka (2001). The low specific gravity of fly ashes could be due to the hollow shaped sized particles of fly ashes which makes it lighter in weight. A summary of the results of the specific gravity can be seen in Table 4.3. It can be observed that the specific gravity increases with increasing iron oxide (Fe_2O_3) content (see Table 4.1) in the fly ashes. This is because the iron oxide partly accounts for the weight of the fly ash, therefore the higher that component in the fly ash, the heavier the resulting mixture.

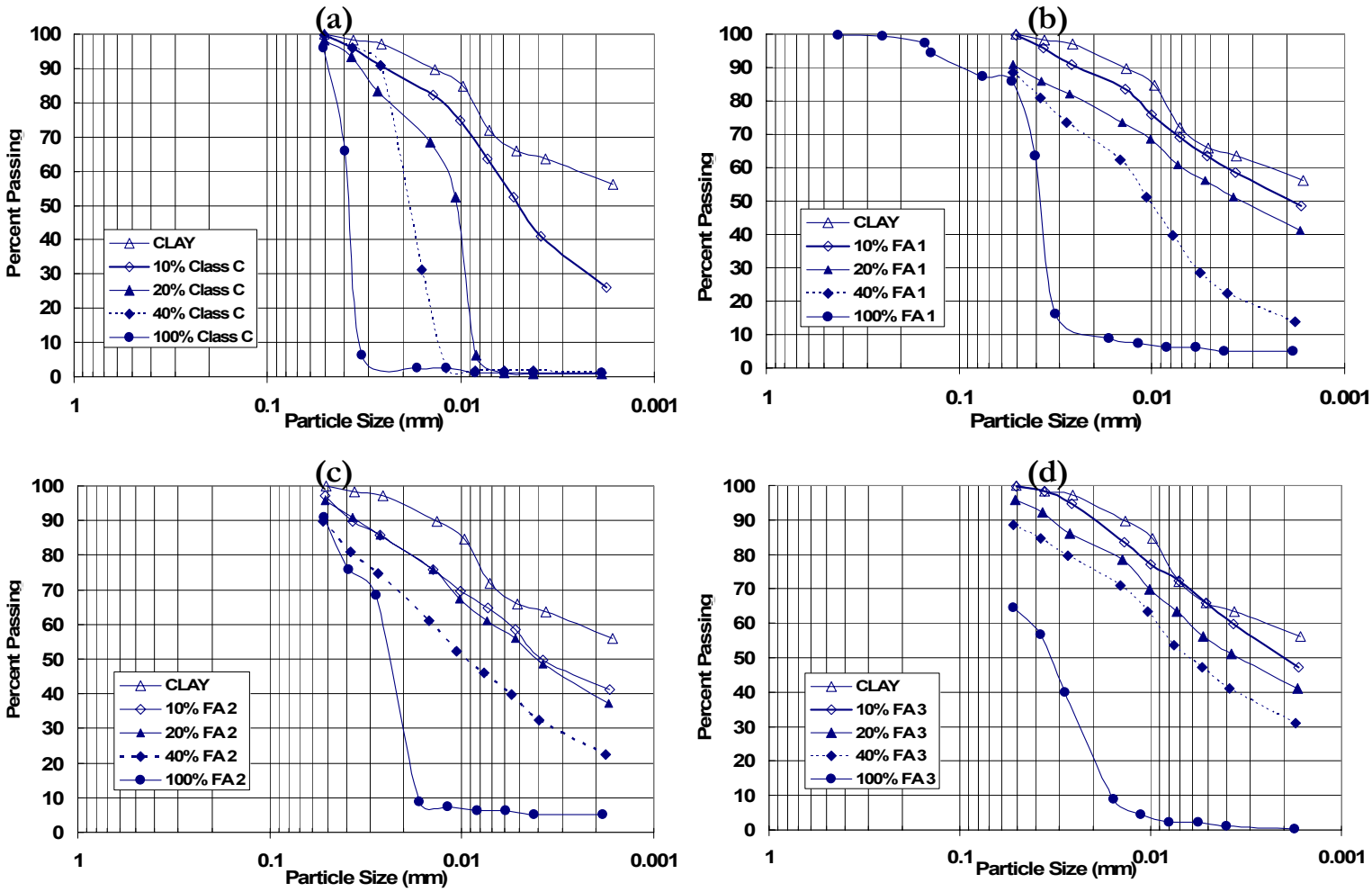

Figure 4.2 Particle Size Distributions of Various Fly Ash Soil Mixtures

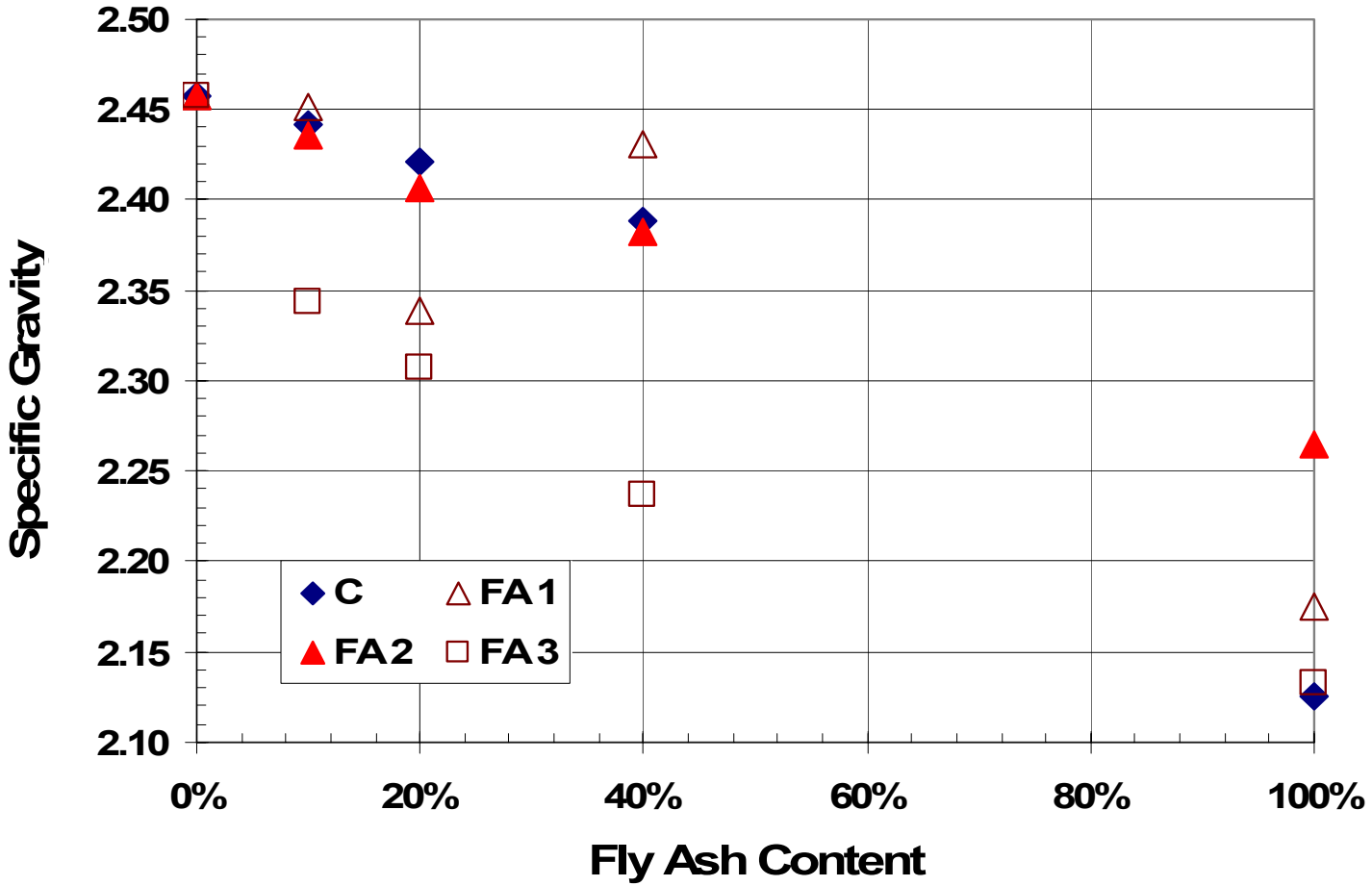

Figure 4.3 Effect of Fly on Specific Gravity of Fly Ash-Soil Mixtures

Table 4.3 Summary of Specific Gravity and Atterbergs Limits

Sample Description	Percent Fly Ash	Specific Gravity	Liquid Limit (LL)	Plasticity Index (PI)
CLAY	0%	2.46	44.95	17.90
	10%	2.45	45.58	22.10
	20%	2.34	44.02	24.90
	40%	2.43	34.95	12.45
Fly Ash 1	100%	2.18	-	-
	10%	2.44	42.89	22.07
	20%	2.41	42.07	32.26
	40%	2.38	41.24	7.91
Fly Ash 2	100%	2.26	-	-
	10%	2.34	50.99	28.11
	20%	2.31	47.03	28.69
	40%	2.24	40.21	25.93
Fly Ash 3	100%	2.13	-	-
	10%	2.44	46.50	21.60
	20%	2.42	47.58	25.08
	40%	2.39	42.89	23.99
Class C	100%	2.13		

The Casagrande method of determining consistency limits was used in the liquid limits, plastic limits, and plasticity indices of the mixtures. The test was according to ASTM D 4318-00 (Standard Test Methods for Liquid Limit, Plastic Limit, and Plasticity Index of Soils). These tests were performed in triplicates and the averages were taken to ensure consistency of the results. From Table 4.2, the liquid limit (LL) of the mixtures tends to decrease as the fly ash content increases. The Class F fly ashes are non-plastic and therefore

the consistency limits were not determined. An increase in plasticity index (PI) of all the mixtures from 10% to 20% fly ash was observed [Figure 4.4 (b)]. The PI then decreases after 20% fly ash content in all cases. The effect of fly ash on the consistency limits in this study is similar to observations made by Cocka (2001), Kumar and Sharma (2004), and Nalbantoglu (2004), which was discussed in Chapter 2. Lingling et al. (2005) also found that PI decreases as fly ash content increases in clay-fly ash mixtures. As mentioned earlier, as particle size increases, activity and specific surface decreases. Plasticity of soils is a function of activity and specific surface, and therefore as these properties decreases with increasing fly ash content, it is expected that the plasticity also decreases accordingly. As explained by Nalbantoglu (2004), the PI of fly ash soil mixtures decreases due to an increase in plastic limit of the mixtures as fly ash content increases. He further explained that liquid limit may increase or decrease depending on soil type but the increase in plastic limit offsets an increase in liquid limit in soils where an increase in liquid limit is observed, thereby resulting in a decrease in the plasticity index. This might explain the increase in PI in the soil mixtures up to 20% of the mixtures. Even though there is a decrease in liquid limit in all the mixtures as can be seen in Figure 4.4 (a), the change in plastic limits were inconsistent with the change in liquid limit as the fly ash content increases resulting in the behavior observed in Figure 4.4 (b). Also, as explained in Section 2.2.1, mixture behavior changes around 20% to 40% of inclusion as a result the mixture achieving minimum porosity. This idea, coupled with physicochemical interactions taking place at the minimum possible porosity in the mixture could be the reason for a behavior change in the plasticity of the soil.

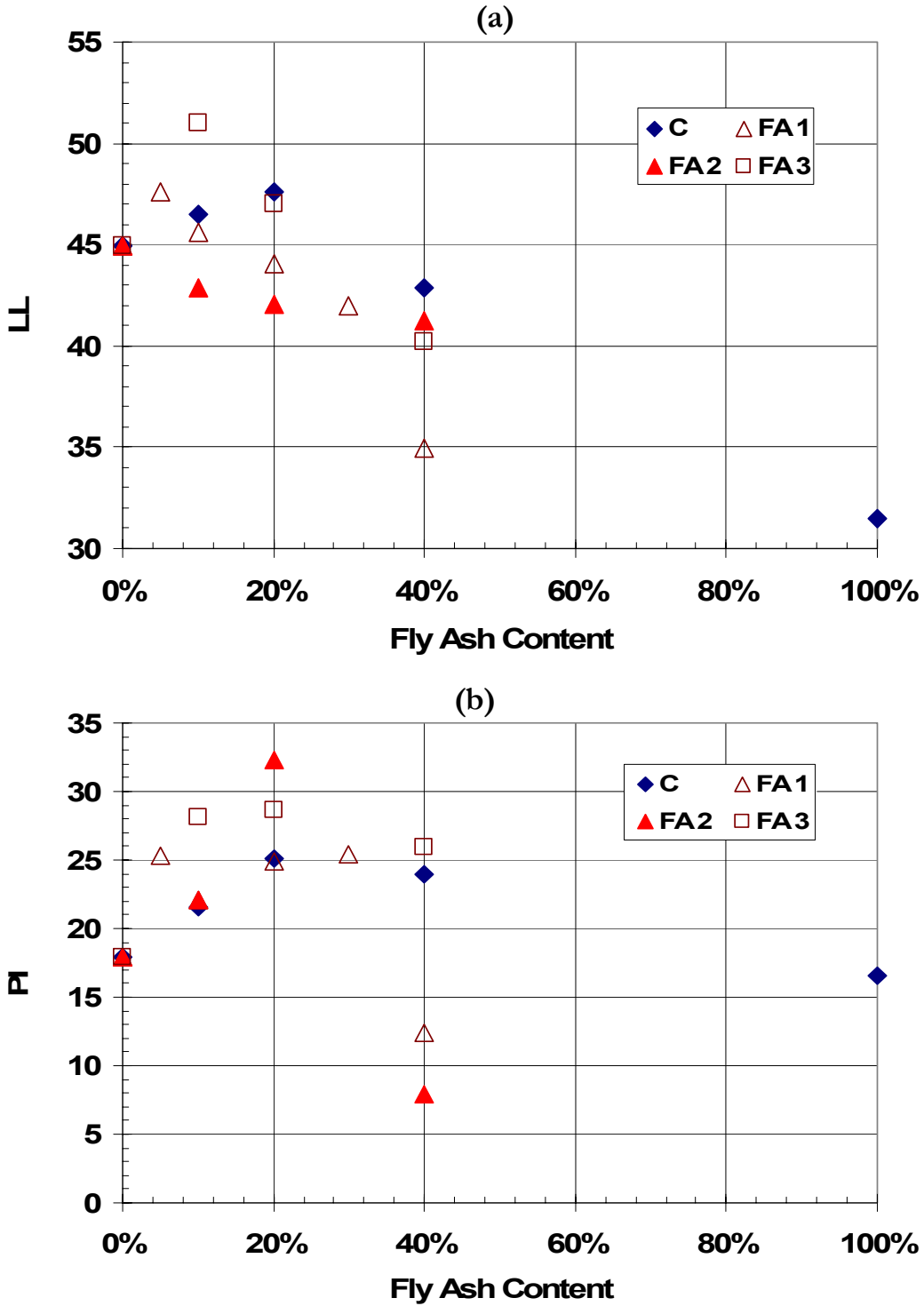

Figure 4.4 Consistency Limits and Fly Ash (FA) Content of Fly Ash-Soil Mixtures

4.1.4 STANDARD PROCTOR (COMPACTION) TESTS

The standard proctor method of compaction according to ASTM D 698-00a (Standard Test Methods for Laboratory Compaction Characteristics of Soil Using Standard Effort [12,400 ft-lb/ft^3 (600 kN-m/m^3)] was used in this study. Soil and fly ashes were mixed at different fly ash percentages. Soil compaction followed immediately without delay after water was added to the mixtures and mixed thoroughly. This was done to eliminate time effect on the results. For consistency in results, tests were performed in duplicates and the averages taken. This test was performed because almost all the data reported in the literature used the standard proctor so it would serve as a common basis in comparing results. A graphical presentation of the standard proctor results of optimum moisture contents and maximum dry densities of all mixtures varying with fly ash content can be seen in Figures 4.5.

The optimum moisture content (OMC) was found to decrease with increasing fly ash content in all mixtures, except in the case of pure Fly Ash 3 (FA 3), which showed an increase [Figure 4.5 (a)]. There was a slight increase in optimum moisture content between 10% and 20% in all the mixtures except in Fly Ash 1 (FA 1).

Maximum dry density (MDD) of all the soil mixtures were found to increase up to 20% of the fly ash content and then decrease afterwards, except in FA 1 where an increase was observed up to 40% before decreasing. The density is expected to increase as coarse particles are added to fine particles. This increase in density is due to the fine particles filling in void spaces in the coarse particles making the mixture dense. The density is expected to increase

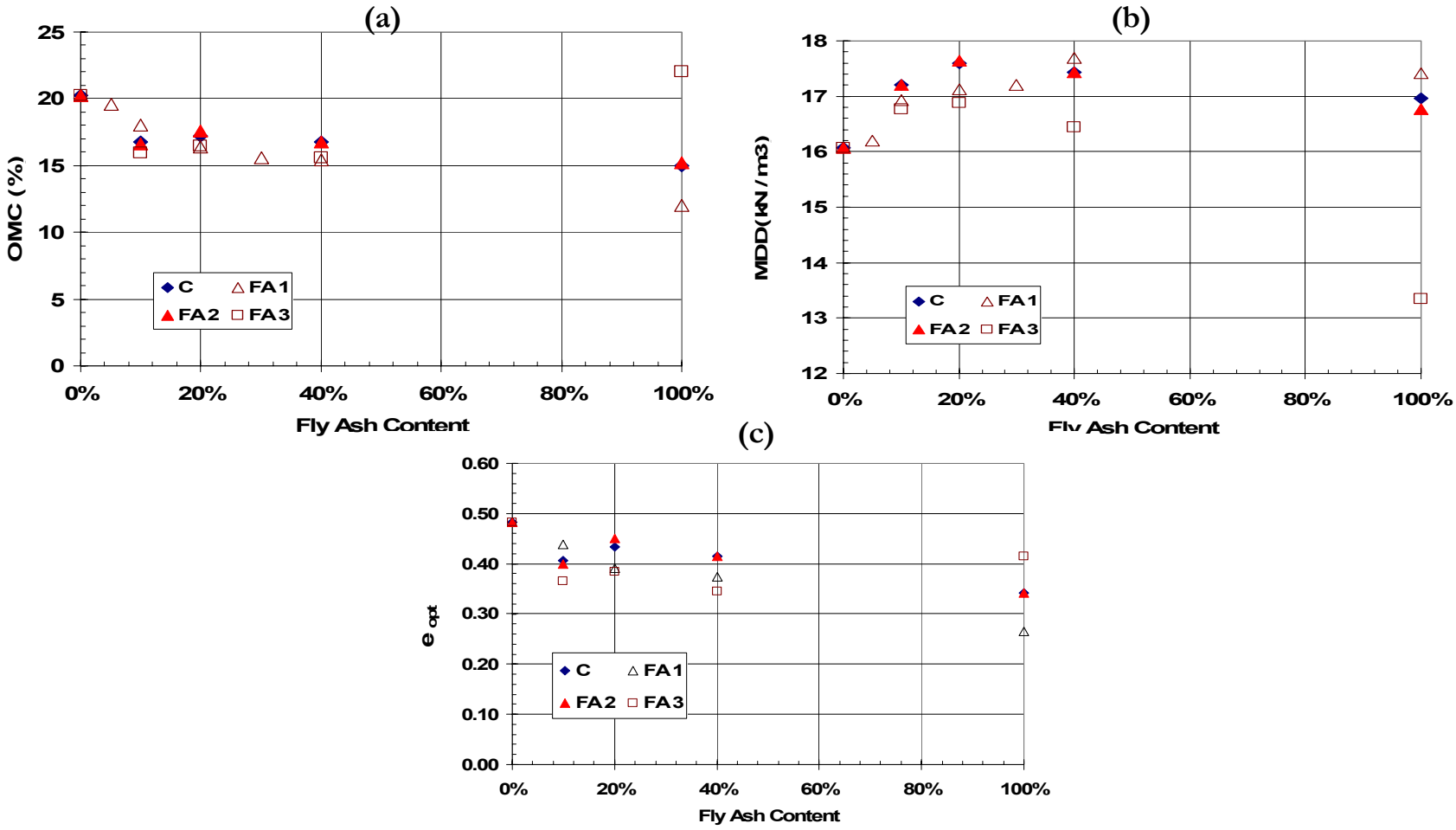

Figure 4.5 Effect of Fly Ash (FA) Content on Compaction Parameters of Various Fly Ashes

with increase in coarse particle content up to a point where the fine particles will not be sufficient enough to fill in all the available void spaces adequately. This will then lead to a decrease in the density of the mixture. In the case of this experiment, the percentage of fly ash at which the density starts to decrease is at around 20% of the fly ash content in the mixture. As the voids are filled with fine materials or vice versa, there is less void space left for water, hence the decrease in moisture content as the density increases.

With the exception of 100% FA 3 where the optimum void ratio (e_{opt}) increases with respect to 40% FA 3, all the mixtures showed a decreases in optimum void ratio with increasing fly ash content [Figure 4.5 (c)]. A slight increase in the optimum void ratios was from 10% to 20% fly ash content was observed in all the mixtures. This behavior is similar to the effective void ratio and minimum porosity concept in soil mixtures discussed in Section 2.2.1. It goes to strengthen the similar behavior observed in both MDD and OMC at around the same fly ash contents.

Misra (2000), Kumar and Sharma (2004), and Zachary (2002) reported an increase in maximum dry density and a decrease in optimum moisture content as fly ash content increases. Kumar and Sharma pointed out that, at given moisture content dry density increases with increasing fly ash content, making an increase in fly ash content in fly ash-soil mixtures synonymous to an increase in compaction energy. Kaniraj and Havangi (2001) mentioned that fly ash shows a wide variation in optimum moisture content and maximum dry density because of their specific gravity which is dependent on iron oxide (Fe_2O_3) and carbon contents. A summary of the standard proctor results is also presented in Table 4.4.

Table 4.4 Summary of Standard Proctor Test

Sample Description	Percent Fly Ash	OMC (%)	MDD (kN/m^3)	Optimum Void Ratio (e_{opt})
CLAY	0%	20.25	16.07	**0.48**
Fly Ash 1	10%	18.00	16.92	**0.44**
	20%	16.40	17.12	**0.39**
	40%	15.40	17.70	**0.37**
	100%	12.00	17.42	**0.26**
Fly Ash 2	10%	16.60	17.20	**0.40**
	20%	17.60	17.65	**0.45**
	40%	16.80	17.44	**0.41**
	100%	15.20	16.77	**0.34**
Fly Ash 3	10%	15.97	16.76	**0.37**
	20%	16.46	16.88	**0.38**
	40%	15.60	16.44	**0.34**
	100%	22.00	13.34	**0.42**
Class C	10%	16.80	17.20	**0.41**
	20%	17.20	17.60	**0.43**
	40%	16.80	17.44	**0.41**
	100%	**15.00**	**16.96**	**0.34**

4.2 DEFORMATION PROPERTIES

The behavior of soil deformation under any form of loading is either elastic or elasto-plastic depending on whether the soil fully recovers to its original state or is partially deformed upon removal of the applied load. From the mechanical behavior of soils, soil can be considered as visco-elastic due to the time dependent of deformation under loading.

Deformation properties are determined commonly in the laboratory by one-dimensional consolidation tests, where deformation or settlement over a time period under a constant load is observed by means of expelling excess pore pressures from a saturated soil mass. As pore fluid is squeezed out soil grains rearrange forming a denser and stable medium. This process causes a decrease in volume causing settlement in engineering structures. Standard test method for one-dimensional consolidation (ASTM D 2435-03) was used in determining the deformation properties of the soil and the soil mixtures. Samples were prepared and placed in the consolidometer without delay. The remolded samples were preconsolidated over 24-hour period under a constant load of 24 kPa. All tests were performed in duplicates on the mixtures. In situations where the two tests on a mixture give results very different from each other, a third test on same mixture proportion was performed to compare to ensure consistency. The properties of interest in this experiment are the coefficient of compressibility (c_c), and the swelling coefficients (c_s) of the mixtures. This is used in assessing the deformation properties of the mixtures as a function of the fly ashes. Figures 4.6 shows the graphical summary of consolidation curves from the consolidation test of all the mixtures. The respective compression and swelling indices obtained from Figure 4.6 is analyzed with respect to fly ash content in the mixtures. This is presented in Figure 4.7.

According to the figure (Figures 4.7) the compressibility and swelling indices of the mixtures decreases with increasing fly ash content. Volume changes in saturated soils are due to the expansion and contraction of the clays in the soil. A soil with more clayey material is able to hold a lot of water which will cause the soil to swell. When the soil is loaded, the

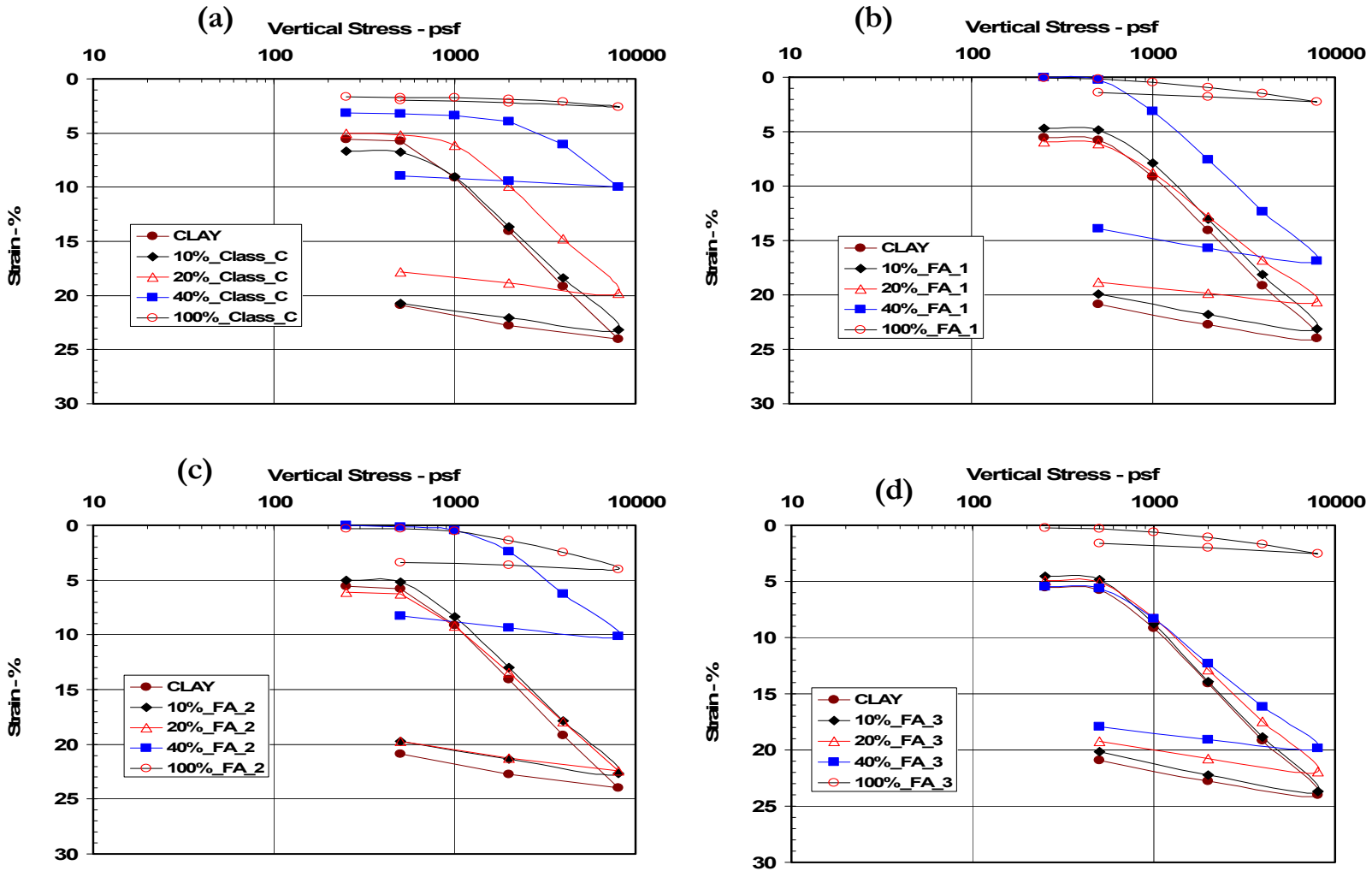

Figure 4.6 Consolidation Curves for Various Fly Ashes

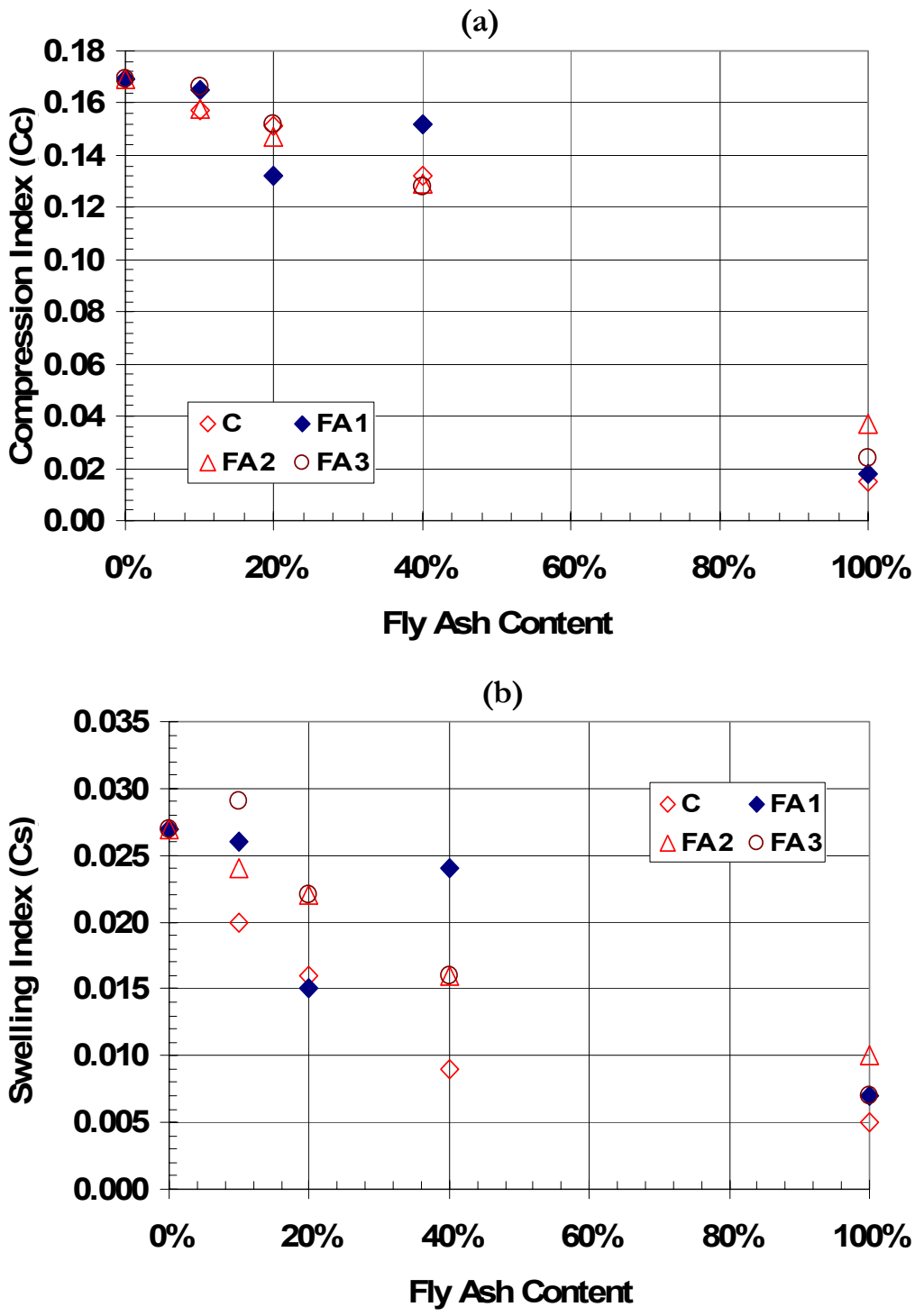

Figure 4.7 Effect of Fly Ash on Compression Index and Swelling Index of Various Fly Ashes

pore water dissipates causing a volume change. With a reduction in the clay content, the volume change or compressibility of the soil reduces since the clay particles available in holding water upon saturation is reduced. The reduction in clay fraction in the mixtures is due to the addition of the fly ashes, which replaces the clay particles with silt-sized particles. This further supports the argument made earlier with respect to plasticity and fly ash content. As the fly ash content increases, the plasticity decrease which in effect decreases the mixtures' ability to absorb enough water to swell. As observed in other parameters discussed above, both compression and swelling indices revealed a change in trend at 20% fly ash content.

The effect of fly ash on initial and final void ratios can be seen in Figure 4.8. It can be seen in the figure that the voids in the mixtures reduce as fly ash content increases. This is the case in both initial and final void ratios. In Class C ash, the final void ratios are greater than those in the corresponding Class F ash mixtures. This could be attributed to the high calcium oxide content in the Class C ash compared to the Class F ash. This causes the clay particles to flocculate more leaving more voids in the Class C mixtures. A summary of values obtained from the one dimensional consolidation experiments are presented in Table 4.5.

4.3 STRENGTH PROPERTIES

The standard test methods for consolidated undrained (CU) triaxial compression test for cohesive soils (ASTM D 4767-02) was used in determining strength properties of all mixtures. Samples were prepared and placed in the triaxial equipment without delay to begin sample saturation process. After saturation, the sample was consolidated for 24 hours at a

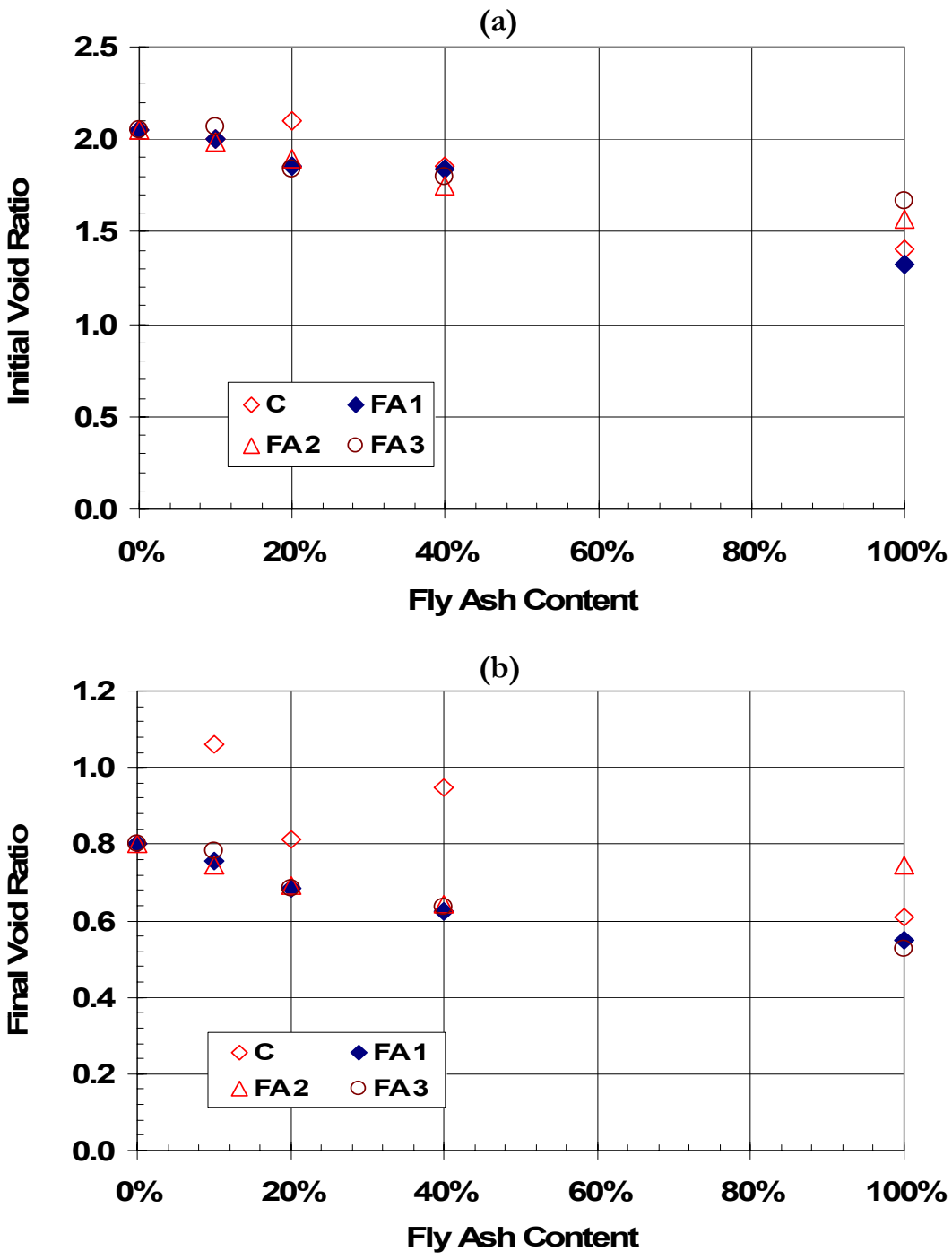

Figure 4.8 Effect of Fly Ash on Initial and Final Void Ratios

Table 4.5 Summary of Consolidation Results

Sample Description	Percent Fly Ash (%)	Initial Void Ratio (e_0)	Final Void Ratio (e_f)	Compression Index (c_c)	Swelling Index (c_s)
CLAY	0	2.053	0.803	0.165	0.026
	10	1.998	0.754	0.169	0.027
	20	1.857	0.683	0.132	0.015
	40	1.839	0.624	0.152	0.024
Fly Ash 1	100	1.323	0.549	0.018	0.007
	10	1.989	0.745	0.158	0.024
	20	1.899	0.693	0.147	0.022
	40	1.745	0.643	0.129	0.016
Fly Ash 2	100	1.572	0.745	0.037	0.010
	10	2.064	0.782	0.166	0.029
	20	1.841	0.683	0.152	0.022
	40	1.794	0.637	0.128	0.016
Fly Ash 3	100	1.669	0.527	0.024	0.007
	10	1.999	1.061	0.157	0.020
	20	2.098	0.811	0.151	0.016
	40	1.851	0.948	0.132	0.009
Class C	100	1.406	0.608	0.015	0.005

predetermined confining pressure, and volume change was recorded. The sample was then loaded until failure at a constant rate of 1 mm/min under undrained conditions. Vertical loads, vertical displacements, and pore pressures were recorded throughout the loading process. The procedure was repeated for three different confining pressures for each soil mixture. In this study, the peak stress a soil or soil mixture can sustain is defined as failure stress. The purpose of consolidated undrained (CU) test is to determine both drained and

undrained shear strength parameters (ϕ_p, ϕ_{cs}, s_u) of soils. The CU test yields both drained and undrained shear strength parameters, and it is less time consuming than that of consolidated drained (CD) test. The CU triaxial tests were performed for each fly ash-soil mixture as well as the pure clay and pure fly ashes at three different confining pressures. Figure 4.9 shows a stress strain plot of 20% Fly Ash 2 (FA 2) mixture from a typical compression test results from this study. The results are used in determining how the mixture composition affects the shear strength properties. The CU triaxial results for all mixtures can be found in Appendix E. Grain size distribution does not only affect density but also the shear strength of soil mixture (Fragaszy et al., 1992). In geotechnology, stability analysis uses effective stress parameters and this is because shear strength of soils is controlled by effective stresses. Laboratory results of the effective friction angles of the mixtures are shown in Table 4.6.

Mohr failure hypothesis is used in determining the shear strength parameters [cohesion (c), and ϕ]. It is noted that, usually in remolded soils as well as normally consolidated soils, cohesion is very small and therefore can be neglected (Head, 1986). Cohesion values observed in all the mixtures in this study were very small and therefore neglected as all samples were considered to be normally consolidated. Also, the failure hypothesis is only valid in terms of effective stresses, and therefore only effective stress parameters were obtained. Mohr circles and failure envelopes used in determining the effective stress parameters are presented in Figures 4.10 through 4.13. A combination of all the failure envelopes for the mixtures is presented in Figure 4.14. According to a study by Prabakar (2004), internal friction angle increases with increasing fly ash content regardless of the soil type used in the mixture. A similar trend was observed in this study, where effective friction

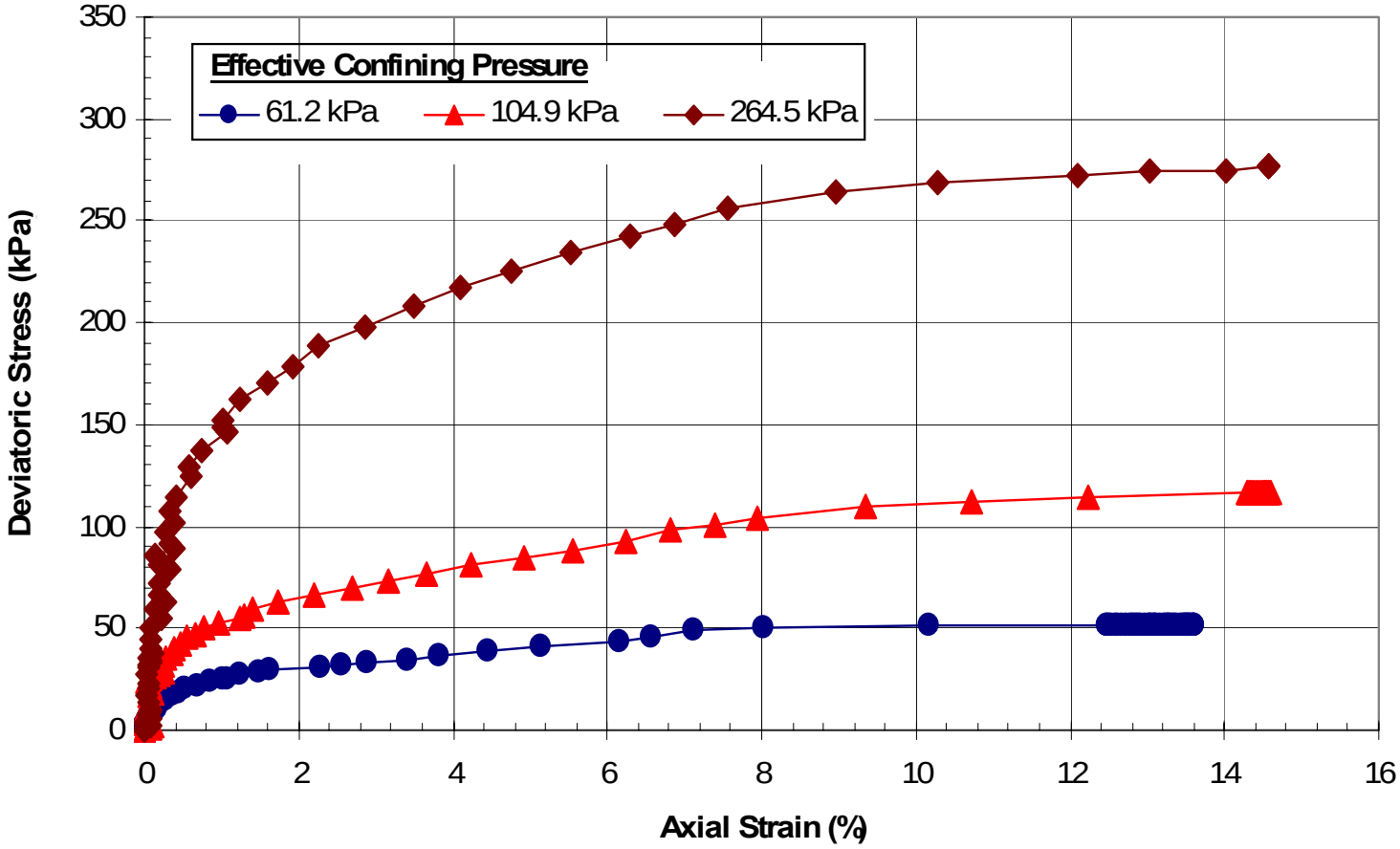

Figure 4.9 Stress-Strain Relationship of 20% Fly Ash 2 (FA 2) Mixture from One-Dimensional Triaxial Compression Test

Table 4.6 Effective Friction Angle and Void Ratios for all Mixtures

Sample Description	Percent Fly Ash (%)	Effective Friction Angle (ϕ') in degrees	Initial Void Ratio (e_i)	Final Void Ratio (e_f)
CLAY	0	17.8	1.45	1.11
Fly Ash 1	10	17.9	1.53	1.08
	20	19.2	1.42	1.02
	40	25.1	1.15	0.87
	100	31.1	0.96	0.84
Fly Ash 2	10	19.1	1.39	1.05
	20	19.2	1.29	0.99
	40	24.0	1.09	0.80
	100	28.8	0.90	0.60
Fly Ash 3	10	18.2	1.59	1.22
	20	22.2	1.29	0.95
	40	24.9	1.10	0.75
	100	31.1	0.63	0.58
Class C	10	20.3	1.44	0.97
	20	23.7	1.35	0.97
	40	28.2	1.42	0.94
	100	34.8	1.01	0.74

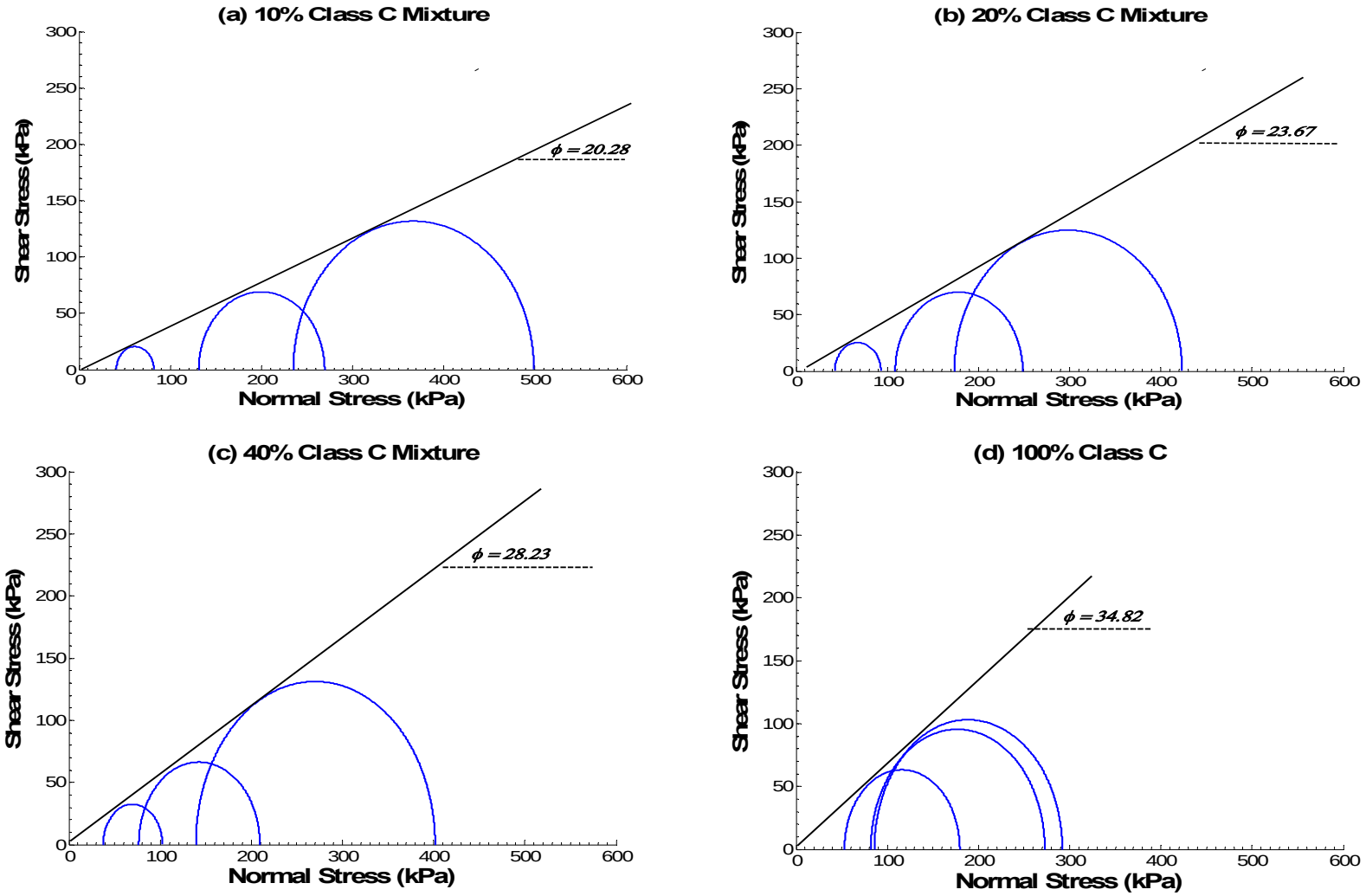

Figure 4.10 Mohr Circles and Effective Stress Failure Envelopes for Class C Fly Ash Mixtures

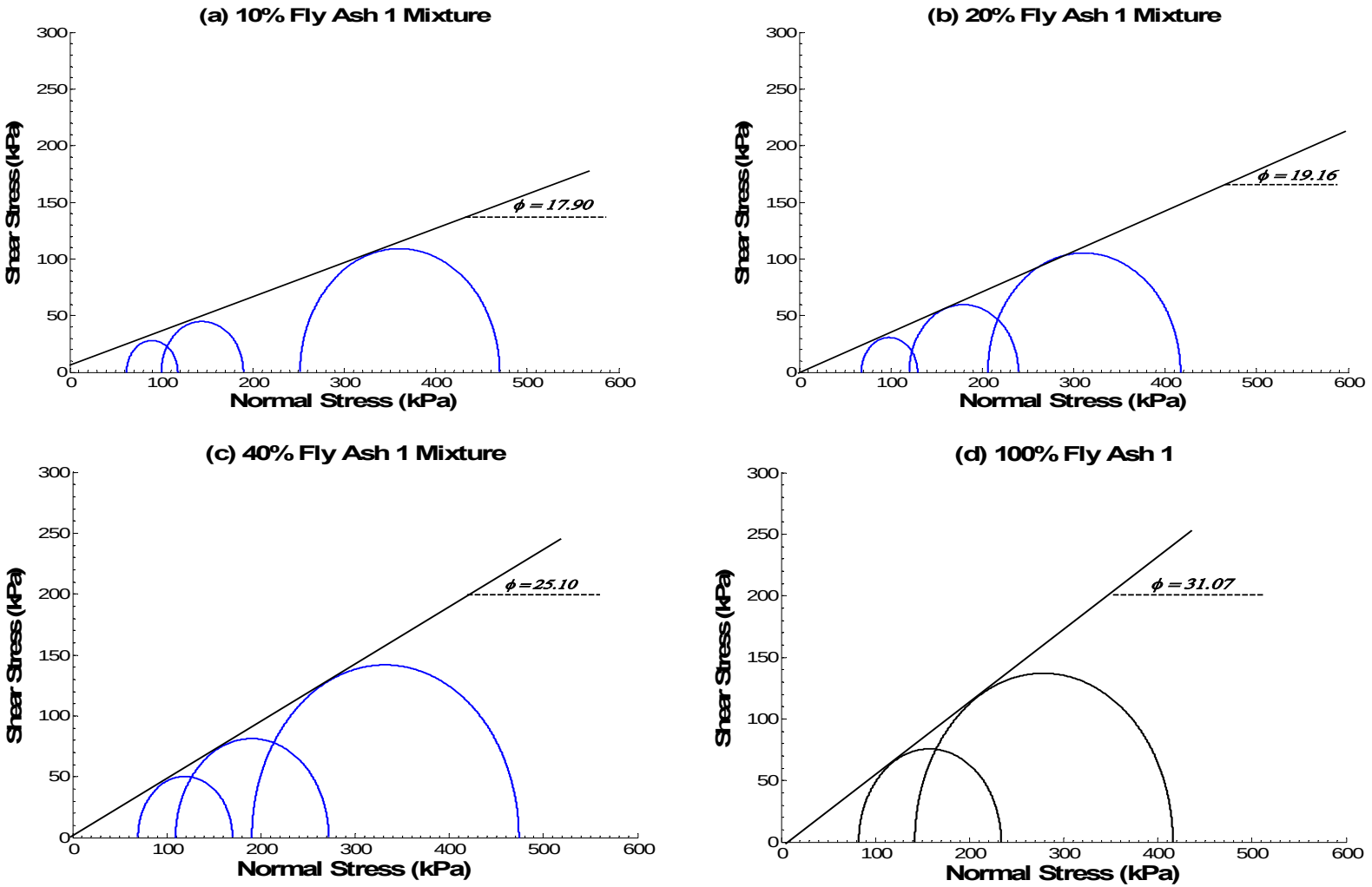

Figure 4.11 Mohr Circles and Effective Stress Failure Envelopes for Fly Ash 1 Mixtures

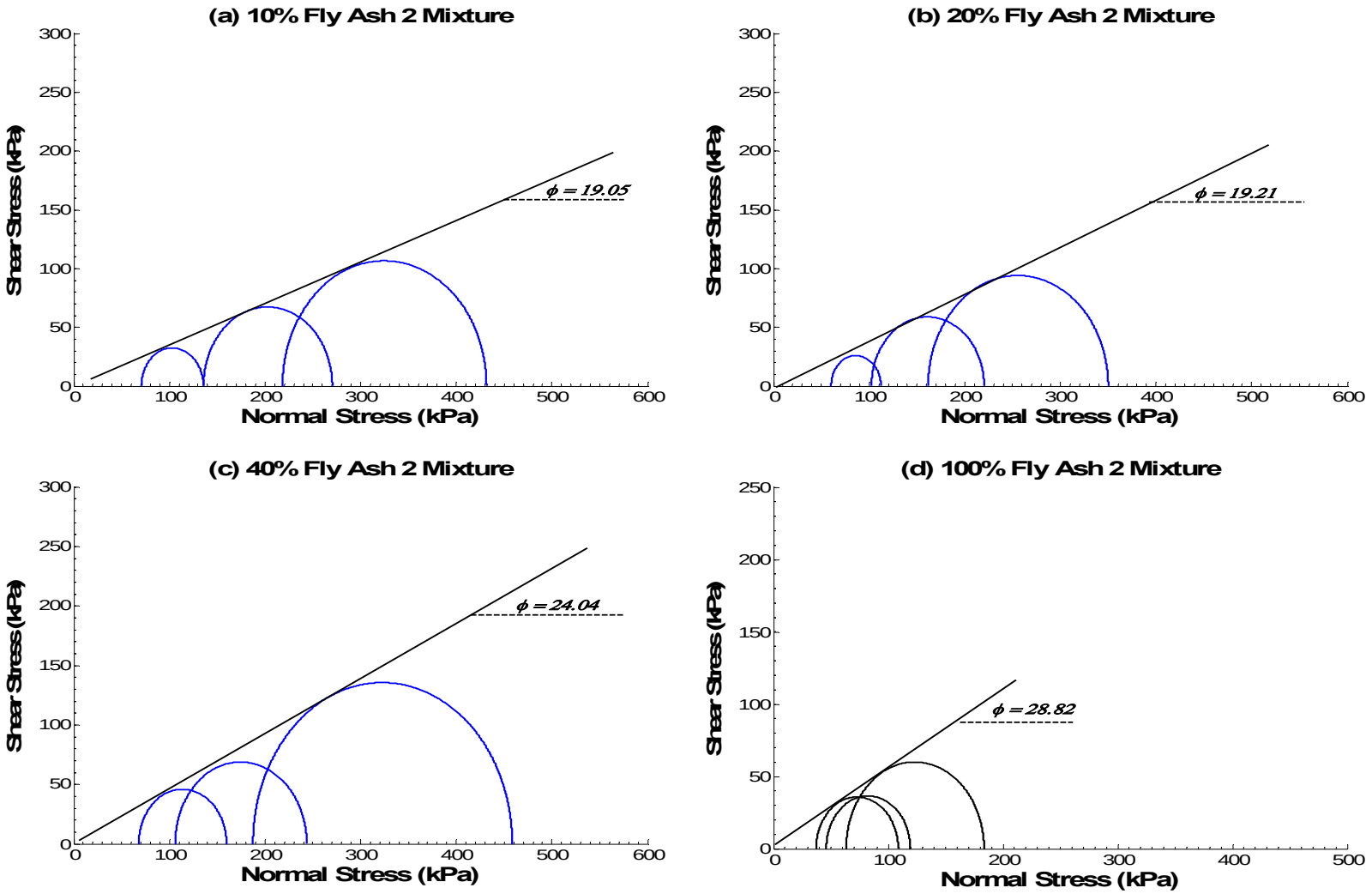

Figure 4.12 Mohr Circles and Effective Stress Failure Envelopes for Fly Ash 2 Mixtures

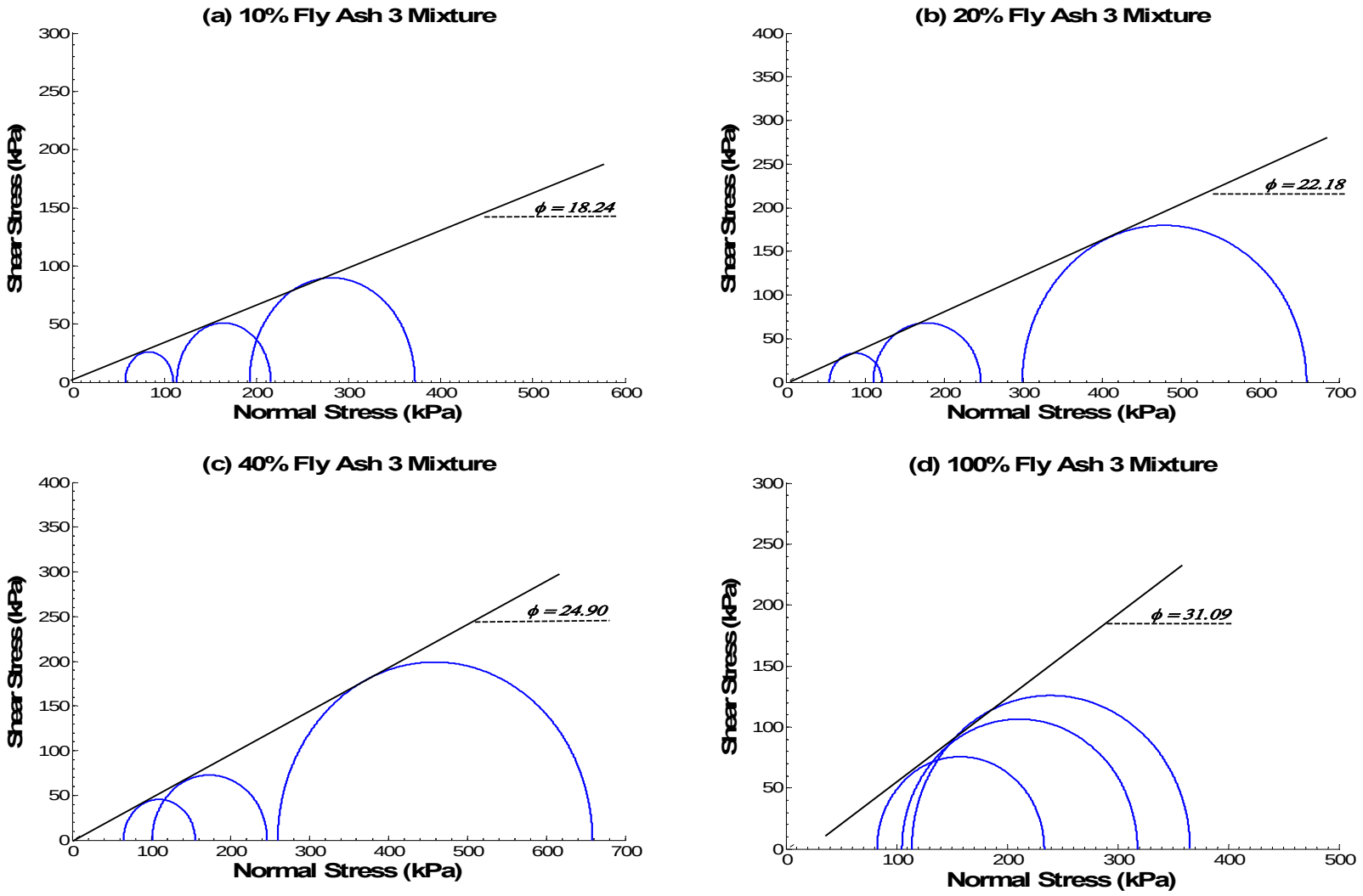

Figure 4.13 Mohr Circles and Effective Stress Failure Envelopes Fly Ash 3 Mixtures

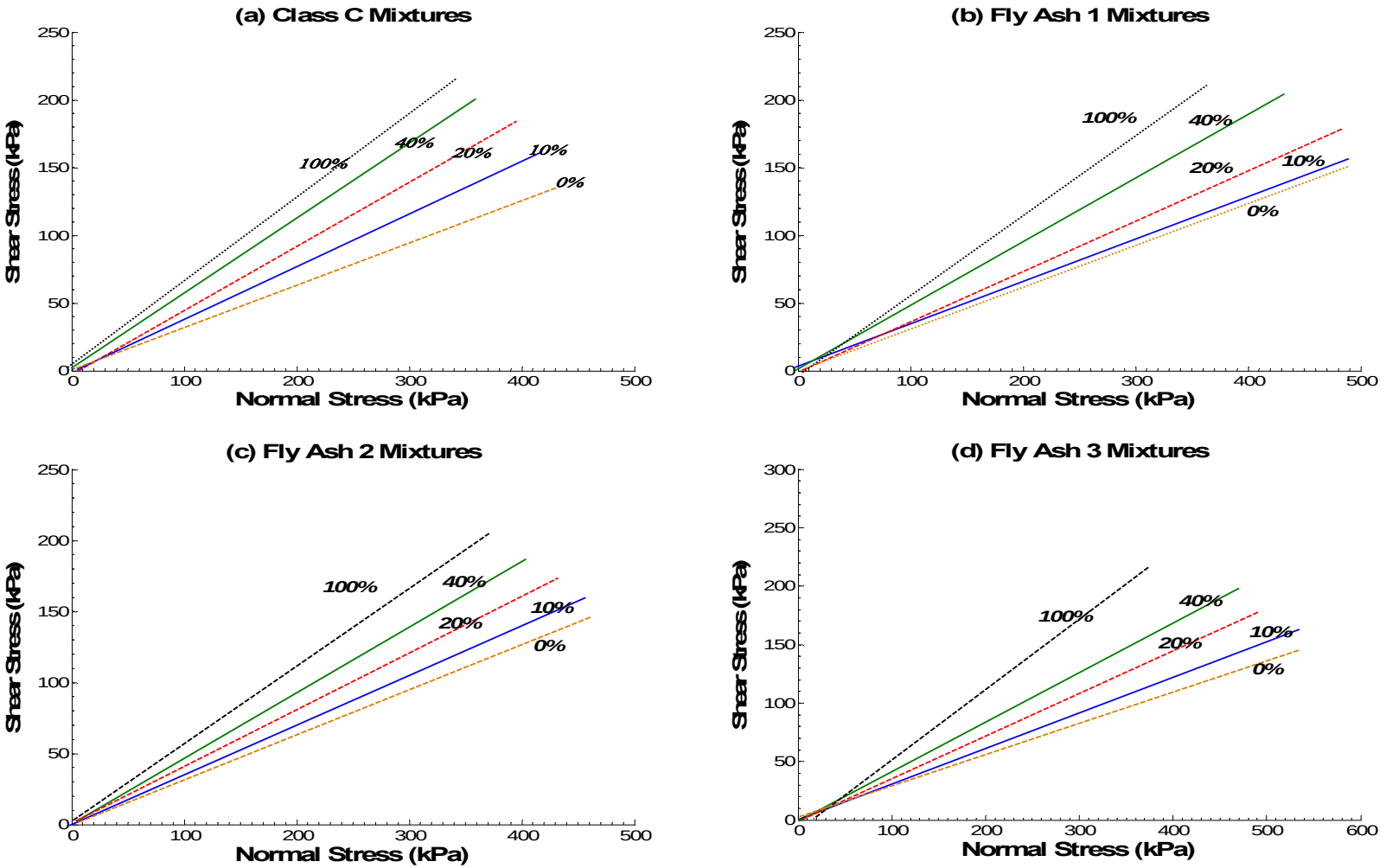

Figure 4.14 Combined Failure Envelopes All Fly Ash Mixture

angle increases with increasing friction angle regardless of the type of fly ash used (c.f. Figure 3.14). As discussed earlier in this chapter, the addition of fly ash decreases clay fraction resulting in a granular soil mixture compared to the pure clay. As mentioned by Fragaszy et al. (1992), grain size distribution affects effective stresses in soils and the more granular the higher the internal friction angle. The increased number of interlocking particles contributes to the increase in internal friction angle as the mixture becomes granular. As discussed earlier in Chapter 2, chemical reaction between soil and fly ash particles could also be a contributing factor to an increase in friction angle. This is because the reactions could lead to cementation, which amass the clay particles (Nalbantoglu, 2004) requiring an increased amount of energy to break these bond.

Undrained shear strength from unconfined compression tests was also analyzed. As observed by researchers such as Kumar and Sharma (2004), Acosta et al. (2003), and Misra (2000), undrained shear strength increases with increasing fly ash content. Zachary (2002) and Ferguson (1993) pointed out that since hydration process is a function of time, strength gain in fly ash modified soils will continue to increase with time as a result of hydration between soil and fly ash particles. This process makes the use of fly ash advantageous in improving soil properties for geotechnical purposes. The unconfined compression test results obtained from this study supports observations made by the researchers mentioned earlier on the subject. Figure 4.15 shows the unconfined compression test results for all mixtures. According to Figure 4.15, fly ash content increases the undrained shear strength in all the mixtures. Again, as observed by Acosta et al. (2003) and Misra (2000) that strength gain in fly-ash soil mixtures as fly ash content increases was independent of soil type, this

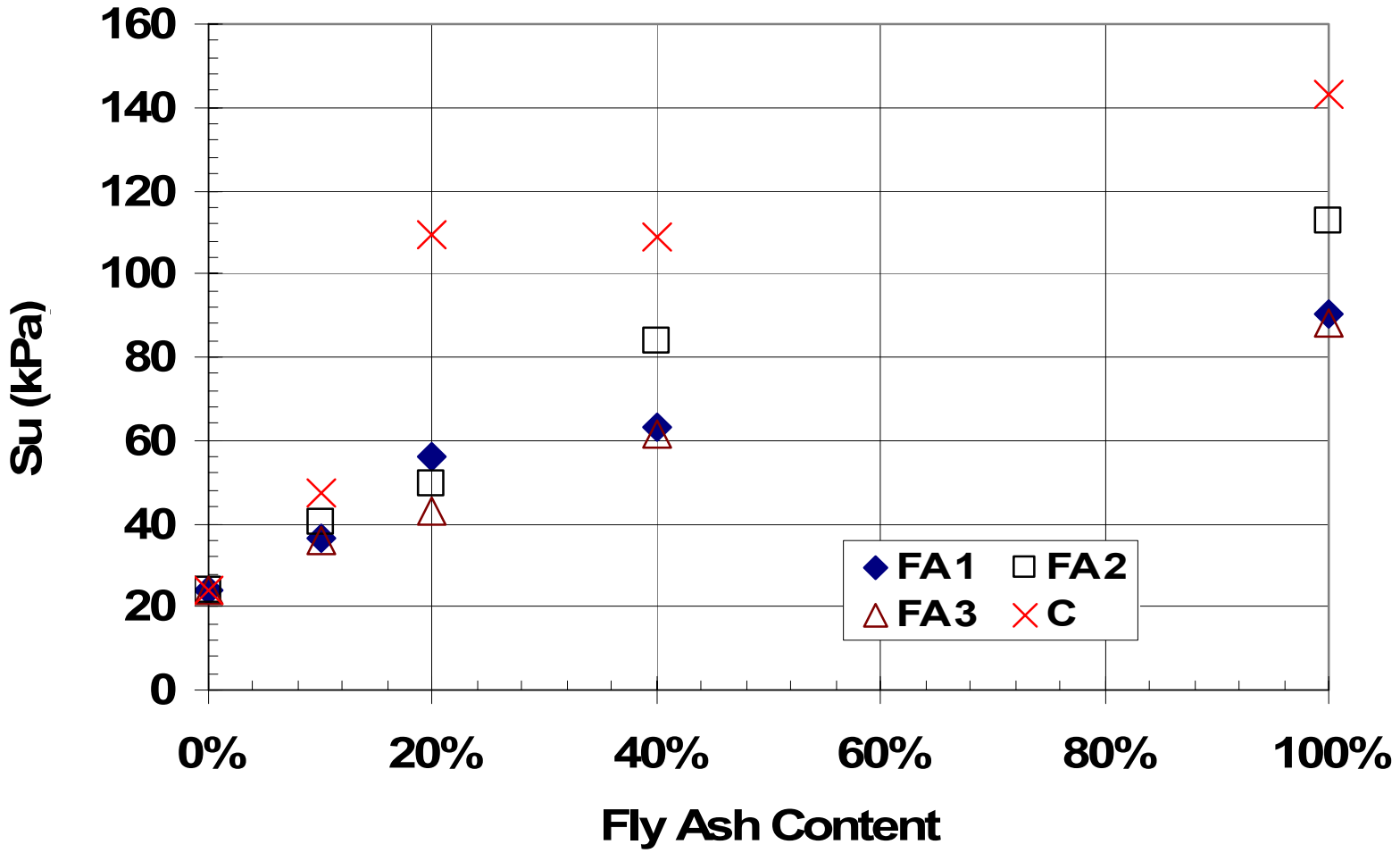

Figure 4.15 Effect of Fly Ash on Undrained Shear Strength (Su) of all Fly Ash Mixtures from Unconfined Compression Test

study revealed that strength gain in the mixtures with increasing fly ash content was independent of the fly ash type. However, a difference in the amount of strength gain was observed between fly ash types. This could be attributed to the difference in the chemical composition of the ashes.

4.4 SUMMARY

The salient points observed from the laboratory experiments are summarized here. According to the results, cation exchange capacity decreases with increasing fly ash content. The clay fraction was also found to decrease with increasing ash content. This is attributed to the introduction of silt sized particles to the mixture as the fly ash content increases at the expense of clay particles. Also, physicochemical interactions between the ash and clay particles cause flocculation of the particles making the resulting particles coarser and reducing the amount of clay fraction in the mixture.

Specific gravity in general, was found to decrease with increasing fly ash content. Again, the hollow nature of the fly ash particles that makes it lighter accounts for the decrease in the specific gravity of the mixtures. Liquid limit decreased with increasing fly ash content, but plasticity index increases to about 20% of fly ash content and then decreases. Fly ash had a similar effect on optimum moisture content as on liquid limit, and a similar effect on maximum dry density as on plasticity index. The behavior change of both the plasticity index and maximum dry density at around 20% fly ash content is attributed to the packing density concept where minimum porosity or void ratios are attained in mixtures within 20% to 40%

of proportion of inclusion. This in effect affects other engineering properties as well, as can be seen in the plasticity index in this case.

Deformation properties such as compression and swelling indices decreased with increasing fly ash content. This indicates that the addition of fly ash reduces the swelling potential of the soil mixtures and also reduces compressibility.

As the ash content increases the mixtures becomes coarser. This leads to an increase in particle interlocking which results in an increase in internal friction angle in the mixtures. Also, chemical interactions promote cementation between particles. These interactions increase with increasing fly ash content and as a result contribute to increase undrained shear strength of the mixtures.

CHAPTER 5 : THEORETICAL DEVELOPMENT

5.1 MODEL ASSESSMENT WITH RESEARCH DATA

The mixture theory models that were assessed in Chapter 3 are used in evaluating the results from this study. The models can be rewritten as

$$y_{mix} = f_{FA} y_{FA} + (1 - f_{FA}) y_C \tag{5.1}$$

$$y_{mix} = \frac{(b-1) f_{FA} + 1}{\frac{f_{FA} b}{y_{FA}} + \frac{(1 - f_{FA})}{y_C}} \tag{5.2}$$

where

$$b = \left(\frac{y_{FA}}{y_C} \right)^{1/2} \tag{5.3}$$

$$y_{mix} = y_C \left(\frac{y_{FA}}{y_C} \right)^{f_{FA}} \tag{5.4}$$

The aforementioned equations are the same as Equations 4.1 (Voigt, 1889), 4.2 (Omine et al., 1998), and 4.3 (Braem et al., 1987) with the exception that the subscripts *i* and *m* used in the original equations have been replaced with the subscripts FA and C denoting fly ash and clay, respectively. The parameter *y*, is the property of the soil to be determined and *f* is volume fraction. This is due to the fact that clay was considered to be the matrix and fly ash was treated as inclusion in this study.

The clay sample used for this study was classified as high plasticity clay (CH or A-6-7).

The existing models were used to predict and compare predicted engineering properties to actual laboratory engineering properties obtained from the research. The predictions were based on results from index properties (maximum dry density, optimum moisture content, and optimum void ratio), deformation properties, and strength properties. Since fly ash is usually non-plastic, the consistency limits were not determined, and therefore predictions of consistency limits with the mixture theory models were not possible. This is because predictions of properties of mixtures by the models are primarily based on the properties of the individual constituents and their mix proportions.

5.1.1 MOISTURE-DENSITY RELATIONS

As discussed in Chapter 3, the moisture-density relations are important in geotechnical engineering and the ability for the models to predict accurately will be useful in soil stabilization involving fly ash. Actual and predicted moisture-density parameters are compared and related to consistency plasticity index. The results are presented in Figures 5.1 through 5.3. In all the parameters, the models predicted closely to each other irrespective of the type of fly ash used. It can be seen from Figures 5.1 and 5.2 that the model predictions slightly over-predict the maximum dry density in some cases in both the relation with optimum moisture content and plasticity index. In the case of Figure 5.1, the results obtained are similar to that in Figure 3.1 (Chapter 3), where the maximum dry density was observed to decrease with increasing optimum moisture content with the exception of Fly Ash 3, which behaves somewhat like the mixtures with CL soils reported by Misra et al. (2000) (c.f. Figure 3.2). The predictions are slightly better with plasticity index than with optimum moisture content. Maximum dry density decreases with increasing plasticity index

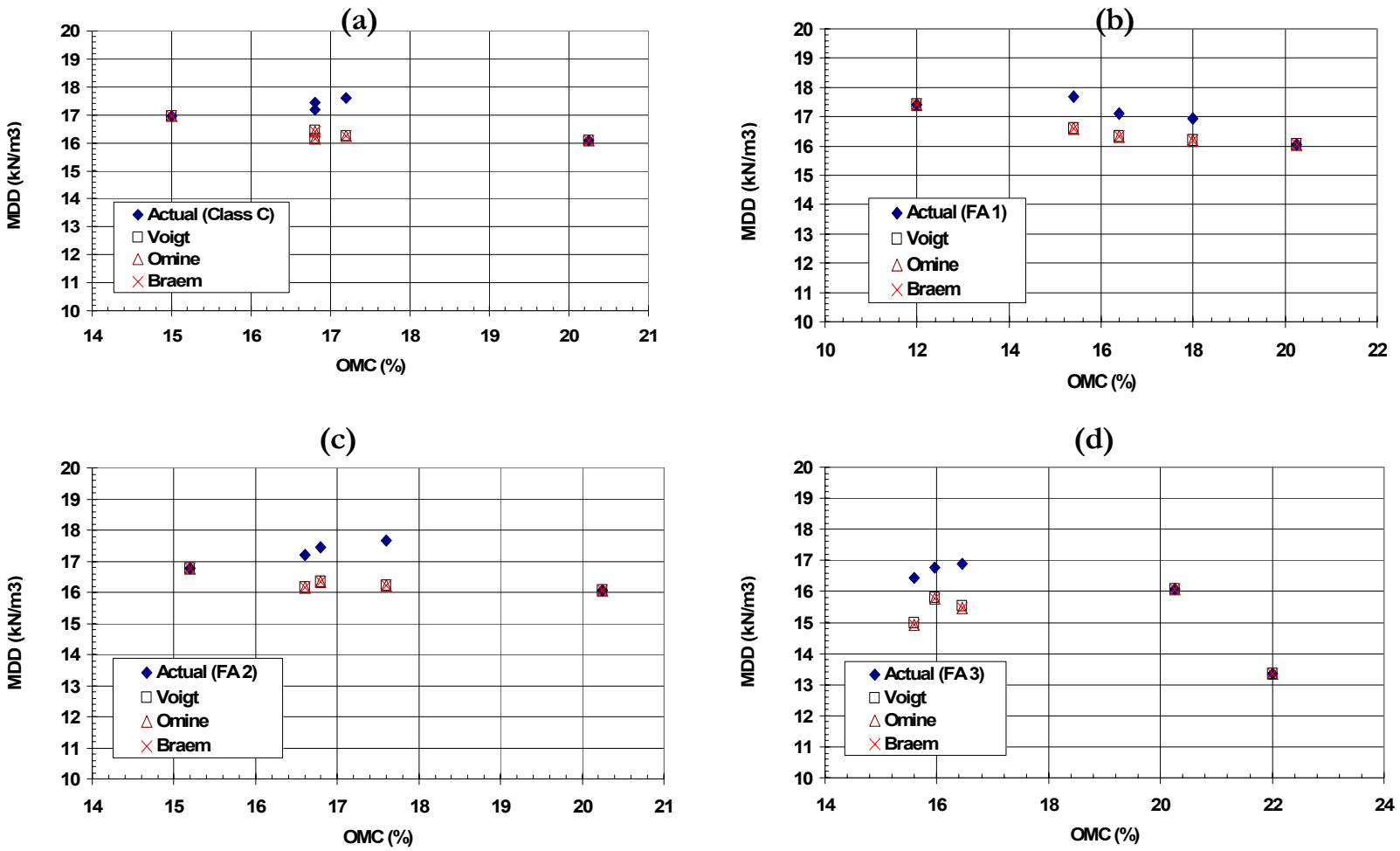

Figure 5.1 Effect of Optimum Moisture Content (OMC) on Actual and Predicted Maximum Dry Density (MDD)

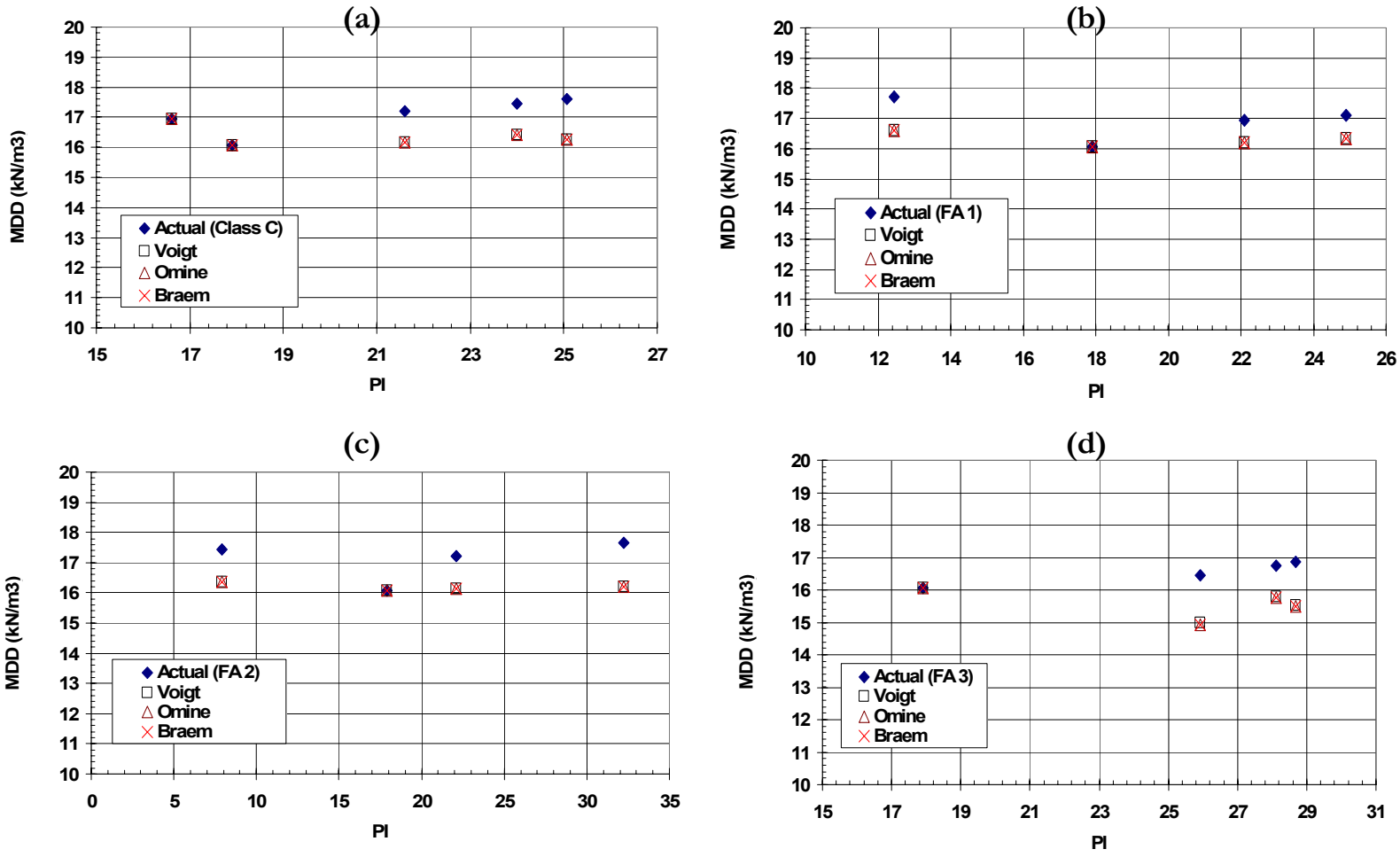

Figure 5.2 Relating Plasticity Index to Actual and Predicted Maximum Dry Density (MDD)

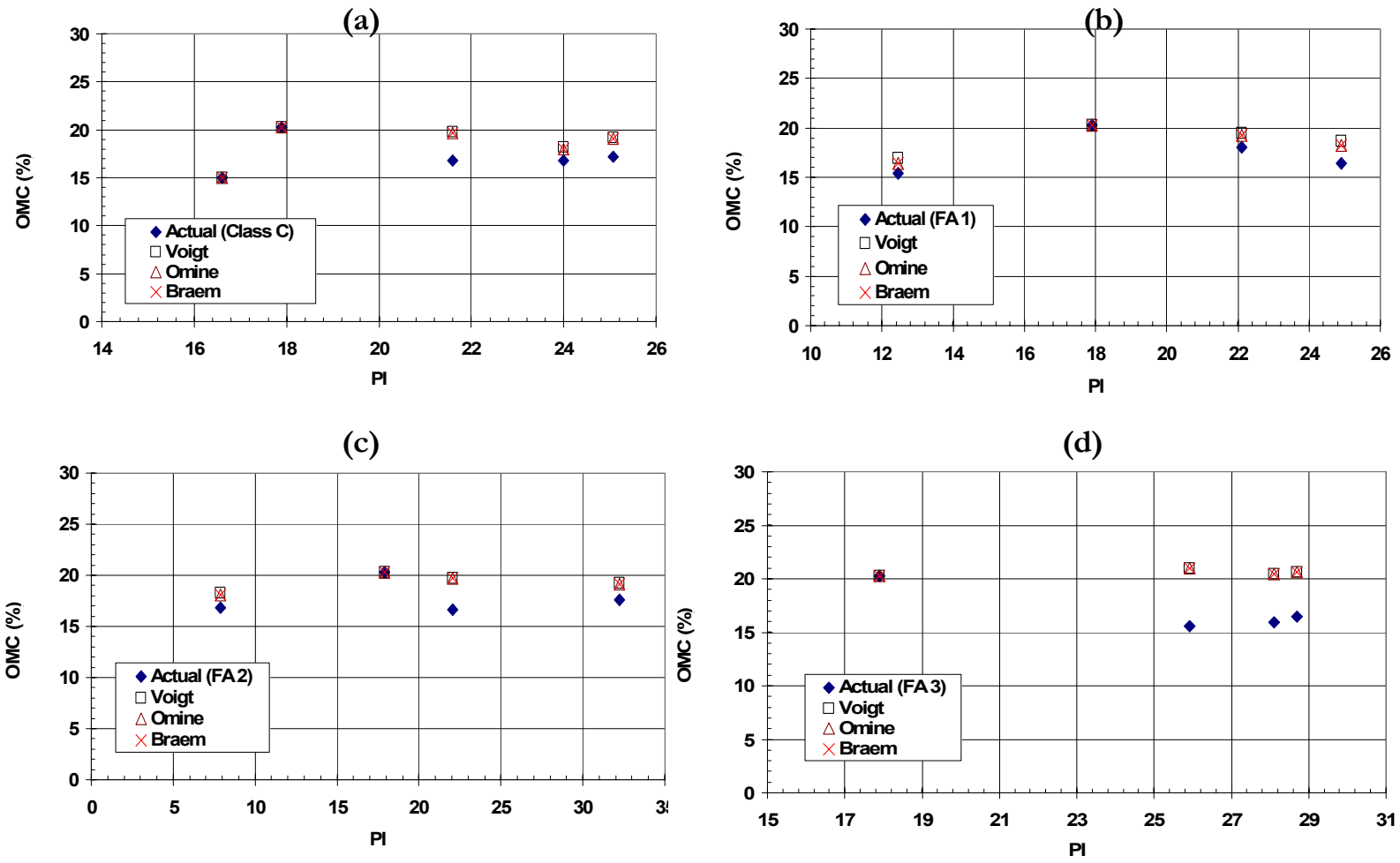

Figure 5.3 Relating Plasticity Index (PI) to Optimum Moisture Content (OMC)

for clay soils (Holtz and Kovacs, 1981). Soils becomes more plastic as plasticity index increases and as a result the tendency to for soil particles to reorient into a denser configuration with the application of compaction energy as moisture content increases is reduced leading to a decrease in maximum dry density. The behavior was observed in this study (Figure 5.2) as well as study reported in literature [see Figure 3.3 (c)]. A slight deviation from the behavior described above, as seen in Figure 5.2, could be due to the fact that, as fly ash content increases the mixtures behavior tends to be geared towards that of silt than clay due to the silt-sized nature of the fly ash particles. In Figure 5.3, predictions were closer to actual results in relating optimum moisture content to plasticity index. Prediction with Fly Ash 3 (FA 3) compared to actual gave the worst results in all cases. All the models predict closely to each other and the slight deviation of predicted from actual is similar to that observed in the data from literature presented in Chapter 3.

5.1.2 DEFORMATION PROPERTY RELATIONS

Figures 5.4 and 5.5 presents model predictions of deformation properties of all the mixtures. As discussed earlier in Chapter 4, the compression index is a function of other index properties of the soil. Plasticity index is plotted against both actual and predicted compression index to asses the models ability to predict deformation property. Although two of the models [Omine (1998) and Braem (1987)] predicted close to each other, Voigt (1889) yielded the best prediction among the three models with respect to compression index. A similar pattern of results was achieved with swelling index as well. The reason for the trend in predictions of the models could be explained by the fact that both compression and swelling indices are a function of void ratios or strain, the Voigt (1889) model is based

on the assumption of uniform distribution of strain in the mixture predicts better than the others with modifications from the earlier model based on the assumptions of uniform stresses (Omine et al., 1998) or a combination of both stresses and strain (Braem et al., 1987).

The relation between initial void ratio and compression index was assessed in Figure 5.5. From the discussion on deformation properties in Chapter 4, it was observed that initial void ratio and compression index decrease with increasing fly ash content. This implies that the higher the initial void ratio in the mixture the greater the compressibility of the soil mixture, hence the greater the compression index. This is the case in Figure 5.5. A similar trend of result with respect to model predictions as seen in Figure 5.4 was observed in Figure 5.5 as well with Voigt (1889) predicting better than the other two models. A similar pattern of relation and predictions is observed in final void ratio and compression index.

Analyses of swelling index yielded similar results as in compression index. As observed in Figures 5.4 and 5.5, the pattern in the model prediction was the same irrespective of the type of fly ash. The type of fly ash might play a role in how much the models prediction deviates from the actual results but not the trend.

5.1.3 STRENGTH PROPERTY RELATIONS

A change in index properties have been seen to affect other engineering properties of fly ash modified soils (Chapter 4) including strength properties. In view of this, the effect of liquid limit on shear strength and effective friction angle is assessed. According to Chapter 4, an increase in fly ash content decreases the liquid limit and increases the friction angle as well

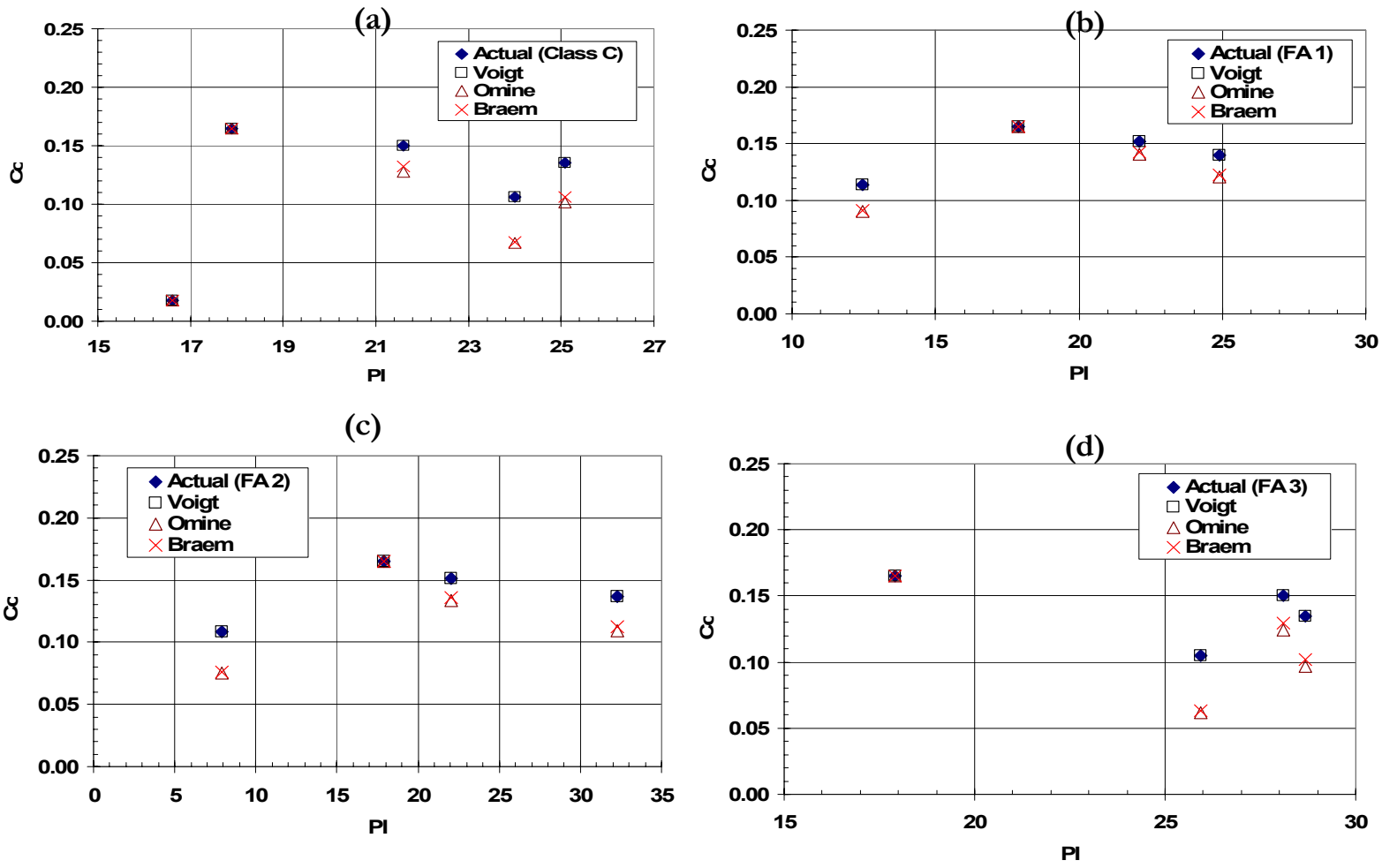

Figure 5.4 Relationship between Plasticity Index and Compression Index (both actual and predicted)

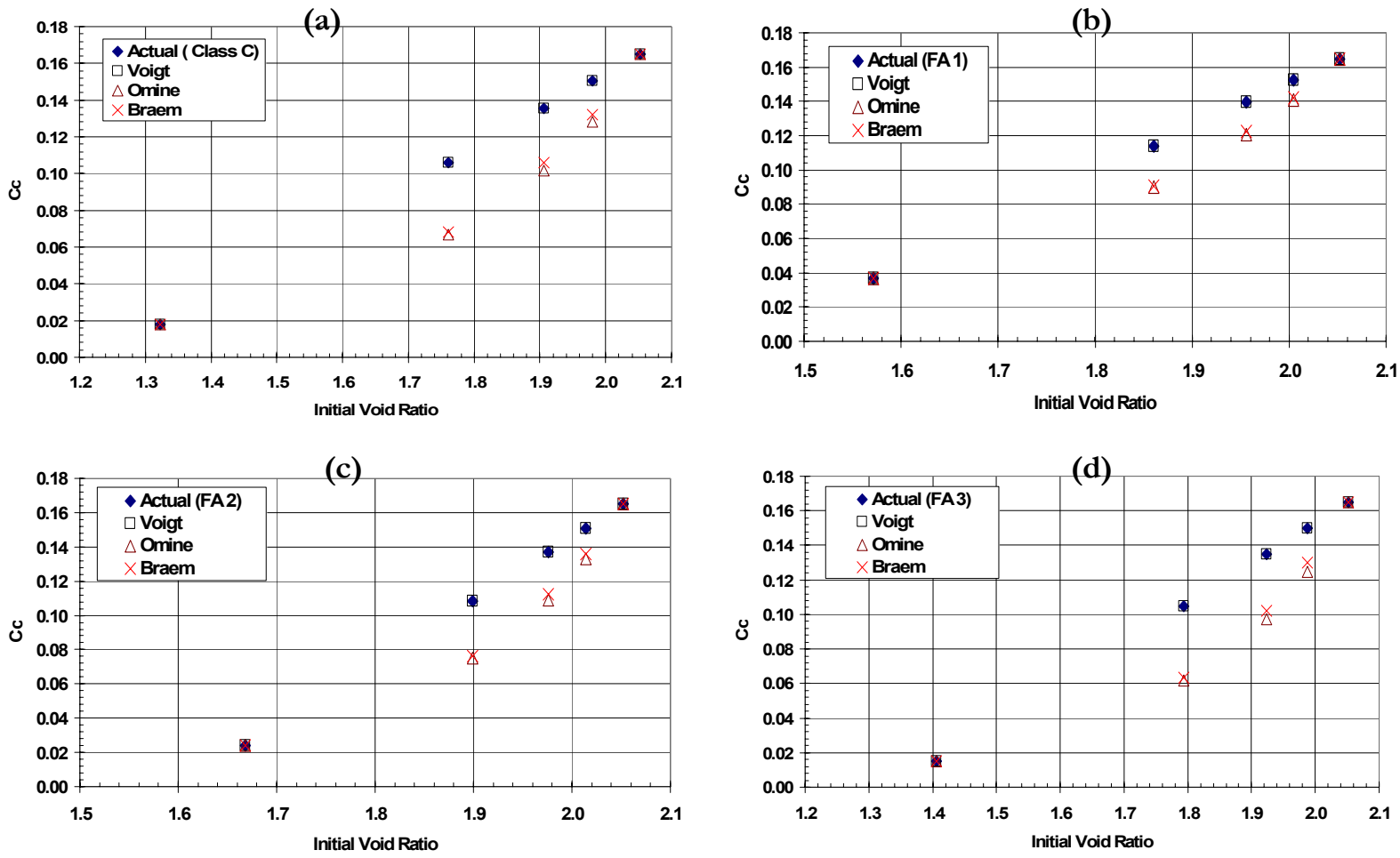

Figure 5.5 Relationship between Compression Index and Initial Void Ratio (both actual and predicted)

as shear strength. It can therefore be implied that, a decrease in liquid limit will result in an increase in both shear strength and effective friction angle or vice versa. From Figures 5.6 and 5.7, is observed that, in general, an increase in liquid limit decreases shear strength and effective friction angle in all soil mixtures considered. There is a scatter in the relation between liquid limit and undrained shear strength for the Class C ash [Figure 5.7 (a)] compared to other fly ashes. The scatter could be attributed to experimental errors or chemical interactions that take place between the Class C and clay particles.

Comparison of the model predictions revealed that, Voigt (1889) model predicts undrained shear strength better in all cases than the other two models (Figure 5.7). With respect to effective friction angle, Voigt's model gives a better prediction at lower liquid limits. As liquid limit increases, Omine (1998) and Braem (1987) models yields predictions similar to that of Voigt or slightly better in some cases. Other relations such as plasticity index and strength parameters yield similar pattern of results and predictions as discussed here. This probably could be due to the fundamental assumptions underlying the models development (see Section 2.3). The trend of predictions as observed in Figures 5.6 and 5.7, gives reason to believe that there is an additional factor or factors that accounts for behavior of the mixtures of which the models do not account for.

5.1.4 COMPARISON BETWEEN ACTUAL AND PREDICTED RESEARCH DATA

Assessment of the mixture theory models with data from literature in Chapter 3 continues here with data from this study. This is to determine the predictive accuracy of the models with respect to data from this study. The predicted results from the models and actual experimental results of index, deformation, and strength properties are compared for

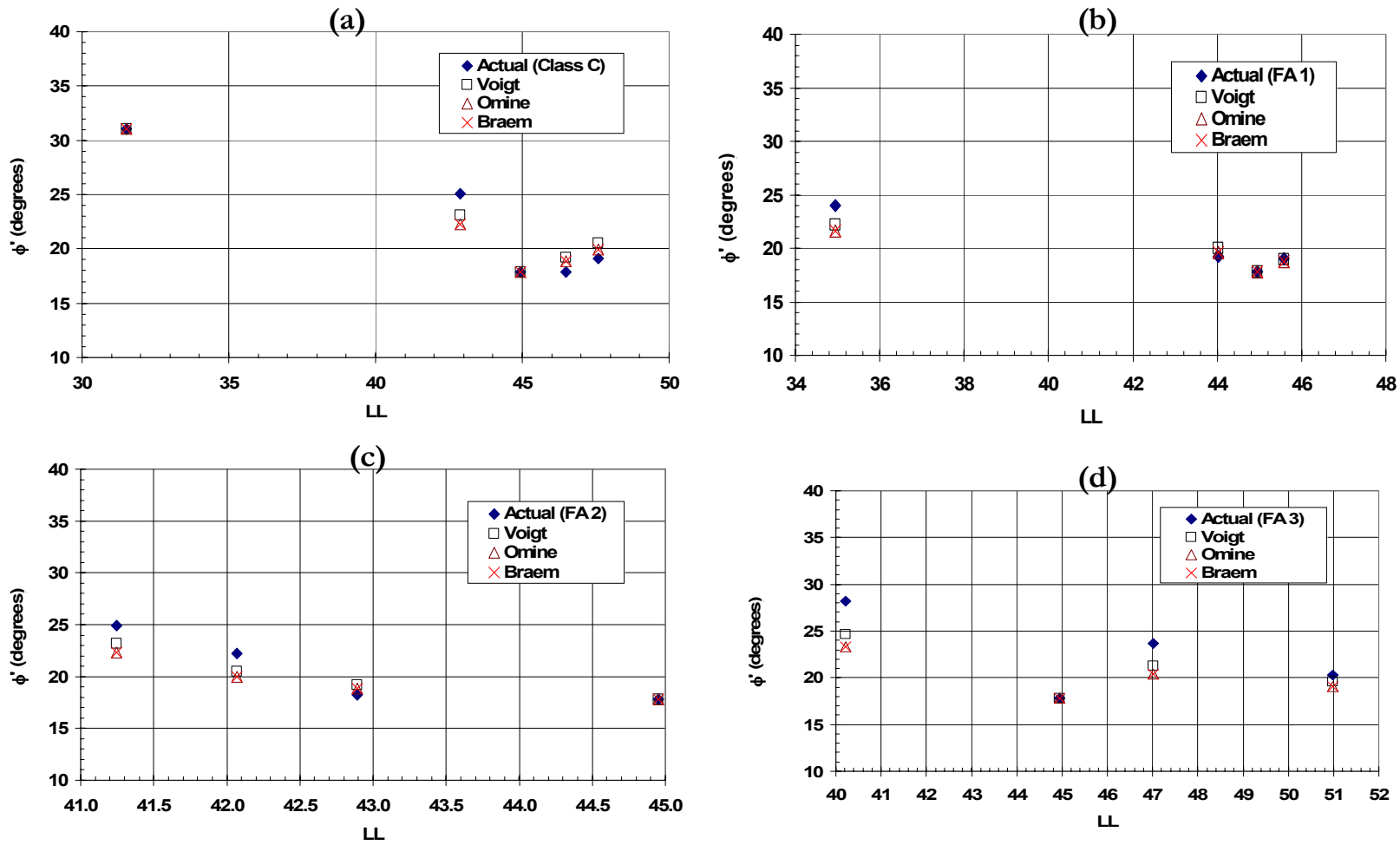

Figure 5.6 Relationship between Liquid Limit (LL) and Actual and Predicted Effective Internal Friction Angle (ϕ')

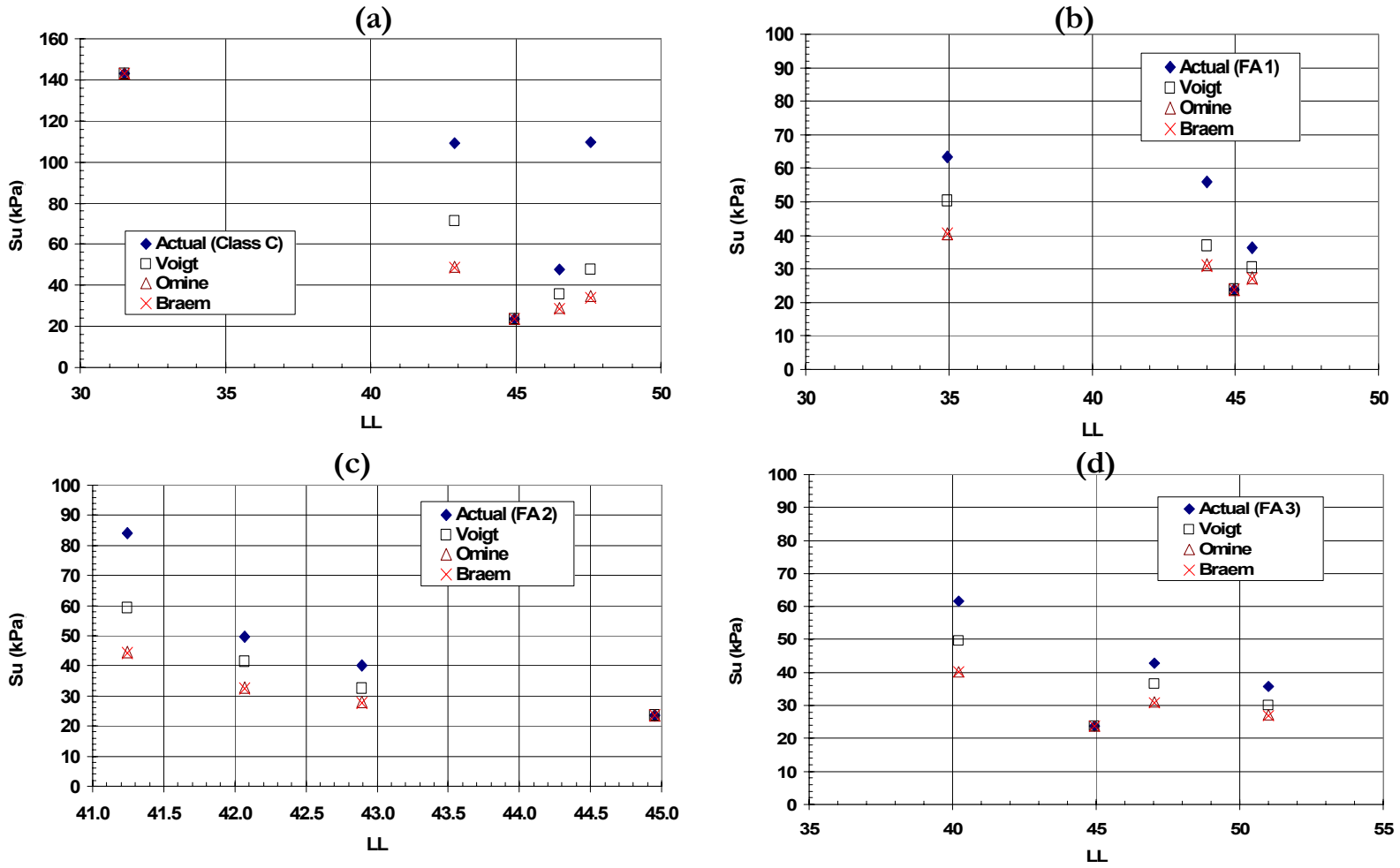

Figure 5.7 Relationships between Liquid Limit (LL) and Actual and Predicted Undrained Shear Strength (Su)

all mixtures. The results can be seen in Figures 5.8 through 5.10.

From Figure 5.8, it can be observed that all the models predicts very close to each other in all the parameters analyzed. Figures 5.8 (a) and (c) shows that the models over predicts the moisture content and the optimum void ratios, while it under predicts the maximum dry density [Figure 5.8 (b)]. Further observation shows that, with the exception of Fly Ash 3 (FA 3) the models predictions were fairly good with the moisture-density parameters.

Predictions of deformation properties are presented in Figure 5.9. There is a little scatter in the case of compression index [see Figure 5.9 (a)]. The figure indicates that, Voigt's model gives a better prediction of the compression index than the other two models. The prediction of the swelling index is presented in the adjacent figure [Figure 5.9 (b)]. Omine (1998) and Braem (1987) models gives better swelling index prediction compared to that of Voigt (1889). The pattern of scatter observed in the swelling index predictions indicates the models can give fairly average predictions.

In Figures 5.9 (c) and (d), all the models gave good predictions of both the initial and final void ratio. Prediction of the initial void ratio was better than the rest of the deformation data. This might be due to the fact that the initial void ratio is obtained right after sample preparation, and the remaining results obtained after a period of time of which certain activities such as chemical reactions might have taken place to affect the properties. This could also be the cause of deviations in some of the properties from predictions solely based on fractional contribution of individual constituents in the mixtures. The deviations in comparisons of actual versus predicted results are probably due to mechanisms not

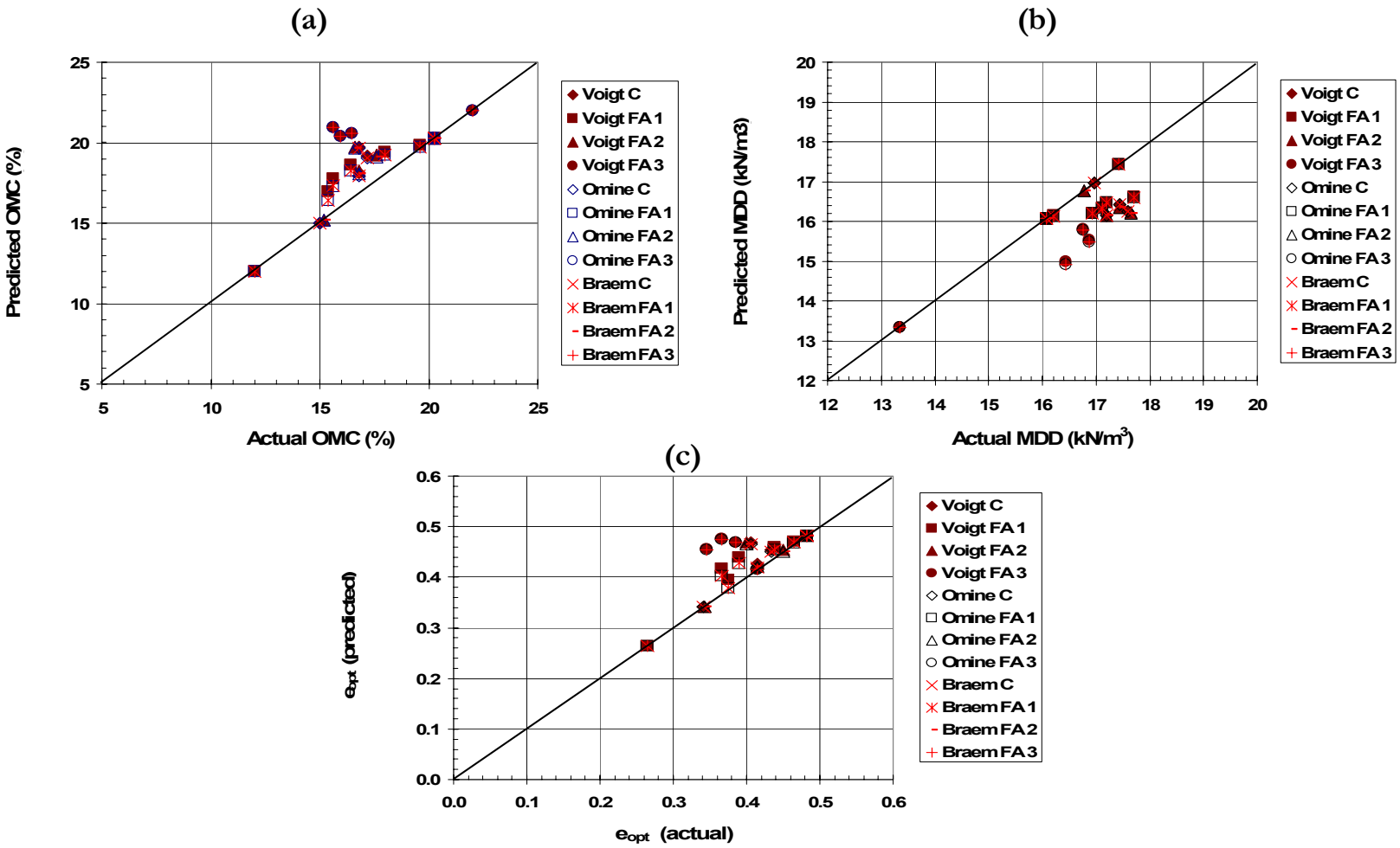

Figure 5.8 Comparisons of Actual and Predicted Moisture-Density Parameters from Research Data

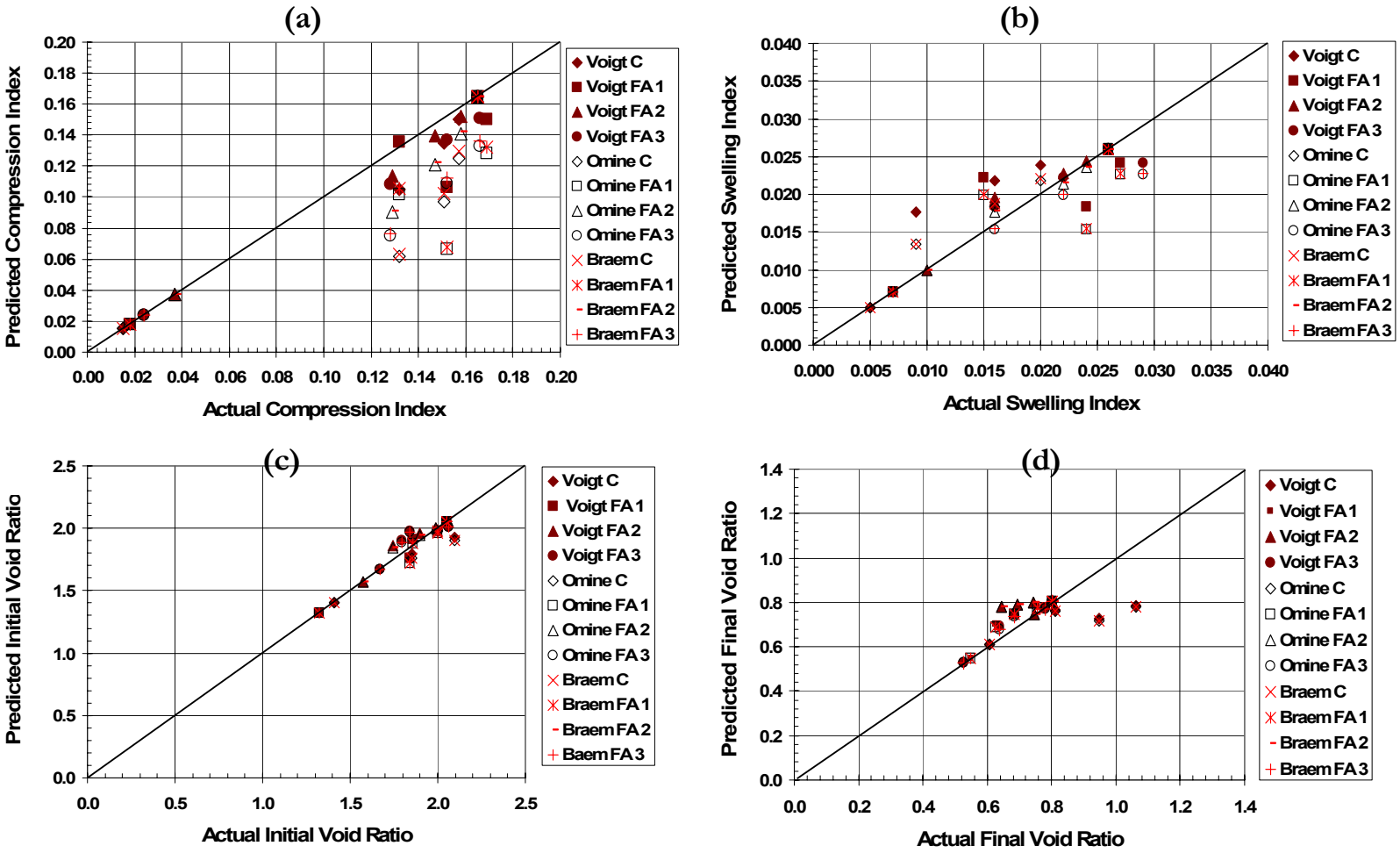

Figure 5.9 Comparisons of Actual and Predicted Deformation Parameters of Research Data

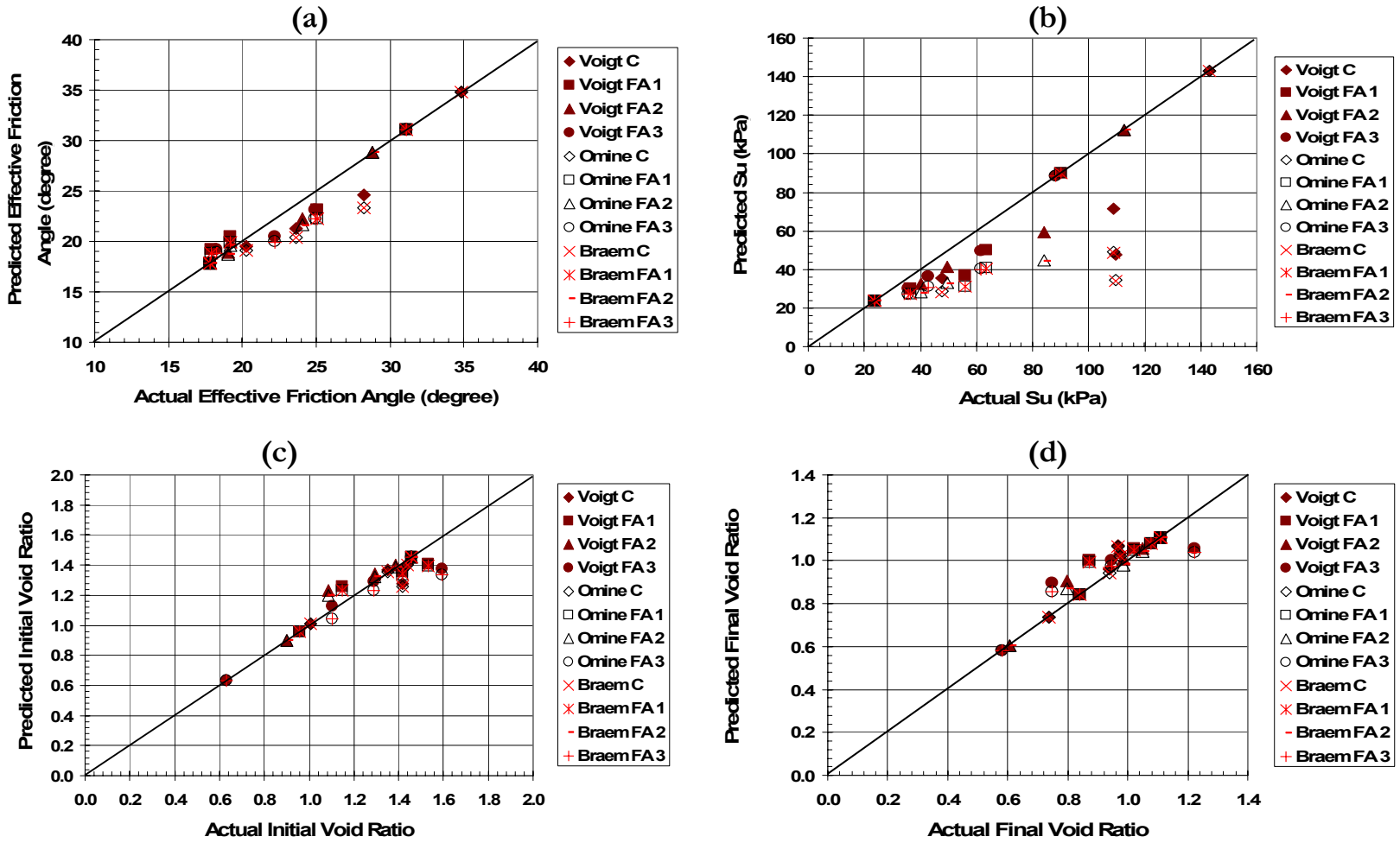

Figure 5.10 Comparisons of Actual and Predicted Strength Parameters from Research Data

accounted for in the mixture theory models.

In the case of strength properties, Voigt (1889) model gave a better prediction in both effective friction angle and undrained shear strength [Figure 5.10 (a) and (b)] similar to that of compression index in Figure 5.9 (a). The models did not give good friction angle and undrained shear strength predictions of Class C fly ash. With the exception of the Class C ash, all the models predicted fairly well with slight deviations. Again, predictions of initial and final void ratio were very good in all the models.

The void ratios (both initial and final) presented in Figure 5.9 were obtained from experiments for deformation property and those in Figure 5.10 were obtained from experiments for the strength properties of the mixtures in this study.

The intent of this research is to modify the existing theory or relation that is very simple to use in predicting engineering properties of fly ash-modified soils. Amongst the three models considered, Voigt (1889) model gives better results in many instances despite various modifications made by the authors of the other models considered. The determination coefficients of the models in predicting the engineering properties presented in Figures 5.8 through 5.10 are given in Table 5.1. This model (Voigt's model) will therefore be considered suitable for this study. Modification of the model to suit fly ash-modified soils will consider incorporating properties or mechanisms originally not accounted for by the model in order to improve predictive capabilities.

All the actual results and the predicted data from this study can be found in Appendix B

Table 5.1 Models Determination Coefficients (R^2) (in percentages) from Figures 5.8 through 5.10

Property	Voigt	Omine	Braem
Moisture-Density Parameters			
OMC	56.86	56.64	56.66
MDD	69.53	66.73	66.73
e_{opt}	58.16	57.29	57.32
Deformation Parameters			
Compression Index (C_c)	95.65	79.44	80.51
Swelling Index (C_s)	75.44	80.21	79.95
Initial Void Ratio	88.72	87.35	87.37
Final Void Ratio	39.22	39.5	39.5
Strength Parameters			
Effective Friciton Angle (ϕ')	93.05	89.81	89.78
Undrain Shear Strength (Su)	77.91	65.08	64.65
Initial Void Ratio	88.94	88.67	88.77
Final Void Ratio	83.38	85.22	85.27

5.2 PHYSICOCHEMICAL ANALYSIS OF RESEARCH DATA

As observed in the literature analysis, mineralogical composition of the fly ashes used in the research is analyzed with respect to the engineering properties of the mixtures. In this section, the physicochemical effects on the properties of the mixtures from this study are analyzed. Other physicochemical properties of the mixtures are also analyzed as well.

The major components considered in the classification of fly ashes are the sum of oxides (SiO_2, Al_2O_3, and Fe_2O_3) and calcium oxide contents available in a given fly ash. In view of this a relationship between the two components would be a good starting point in analyzing the physicochemical effects on the mixtures. A strong relation was found between the two components with the ashes used in this research and five (5) other fly ashes from other

researchers as can be seen in Figure 5.11. This strong relation gives reason to believe that the physicochemical effects could be attributed to either of the components or both.

As discussed earlier in previous chapters, cation exchange capacity (CEC) is affected by the amount of fly ash available in the mixtures. The amount of cations available from either the fly ash or the clay material or both is dependent on the mineralogical composition of the materials constituting the mixture. An important mineral available in both materials in this study is calcium (Ca). Specifically, calcium oxide (CaO) plays an important role in the cementation or flocculation of the clay materials in the presence of fly ash. This cementation process is due to exchange of ions. The effect of the amount of CaO present in the fly ash on CEC is investigated to see how it might have affected the behavior of the mixtures. Figure 5.12 presents how CaO from fly ashes used affects the CEC of the mixtures. From the figure, the high calcium oxide content fly ash revealed lower CEC with fly ash contents 20% and above. Below 20% fly ash, the distinction is not very clear. This is probably due to the fact that at lower fly ash percentage the reactions between the ash and the clay particles are not very pronounced to depict any significant pattern or trend.

In the case of deformation properties, the amount of CaO present did not seem to have any effect on the compression index in this study as can be seen in Figure 5.13. However, it does have an effect on the swelling index of the mixtures. It can be seen that the high calcium oxide content have the lowest swelling index. This indicates that the calcium oxide available leads to the cementation and flocculation of the clay materials making it less susceptible to swelling. The scatter in Fly Ash 1 (FA 1) particularly with the 20% fly ash could be due to

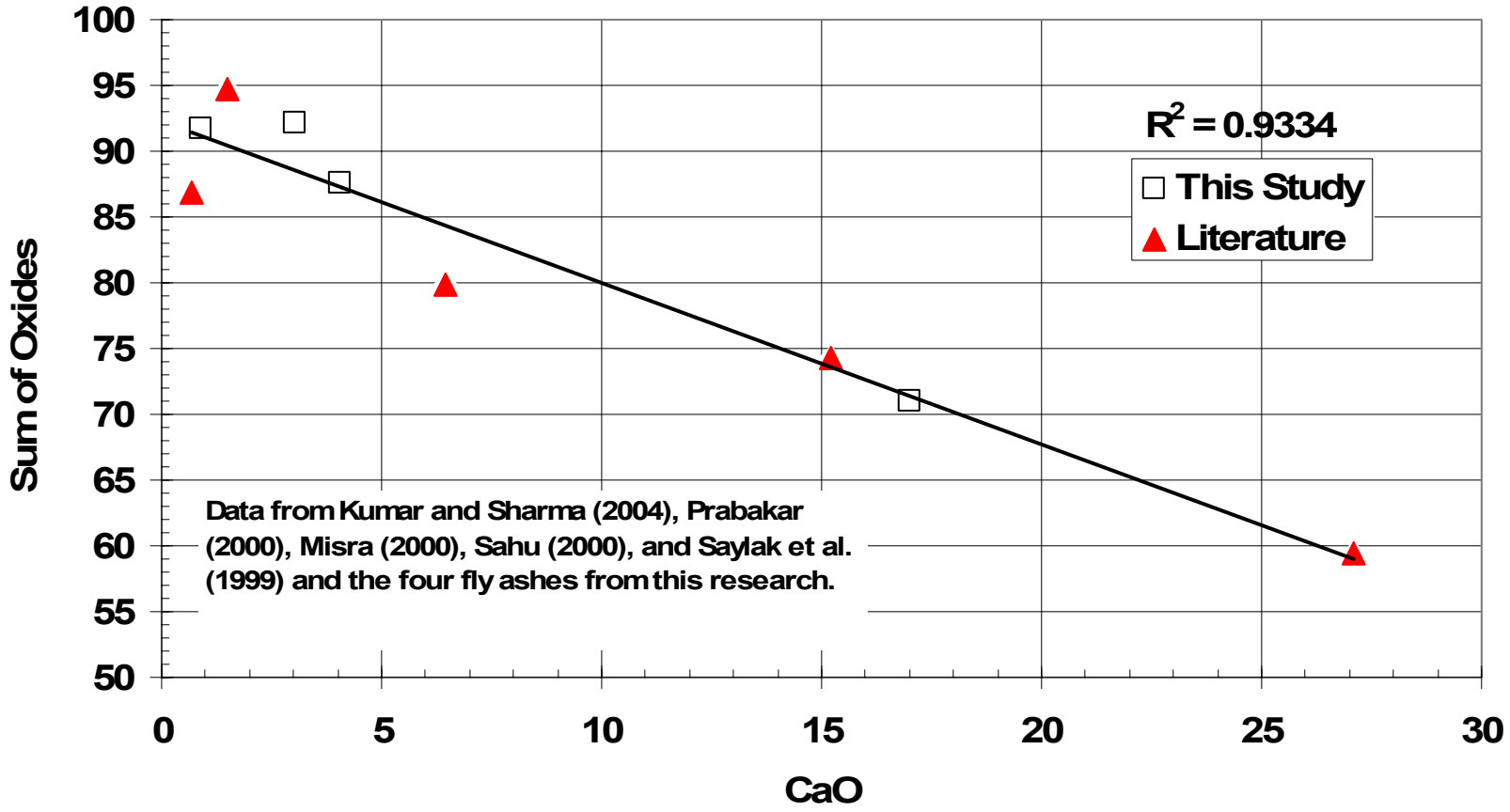

Figure 5.11 The Relationship between Calcium Oxide and the Sum of Oxides (SiO_2, Al_2O_3, and Fe_2O_3) from Nine Different Fly Ashes

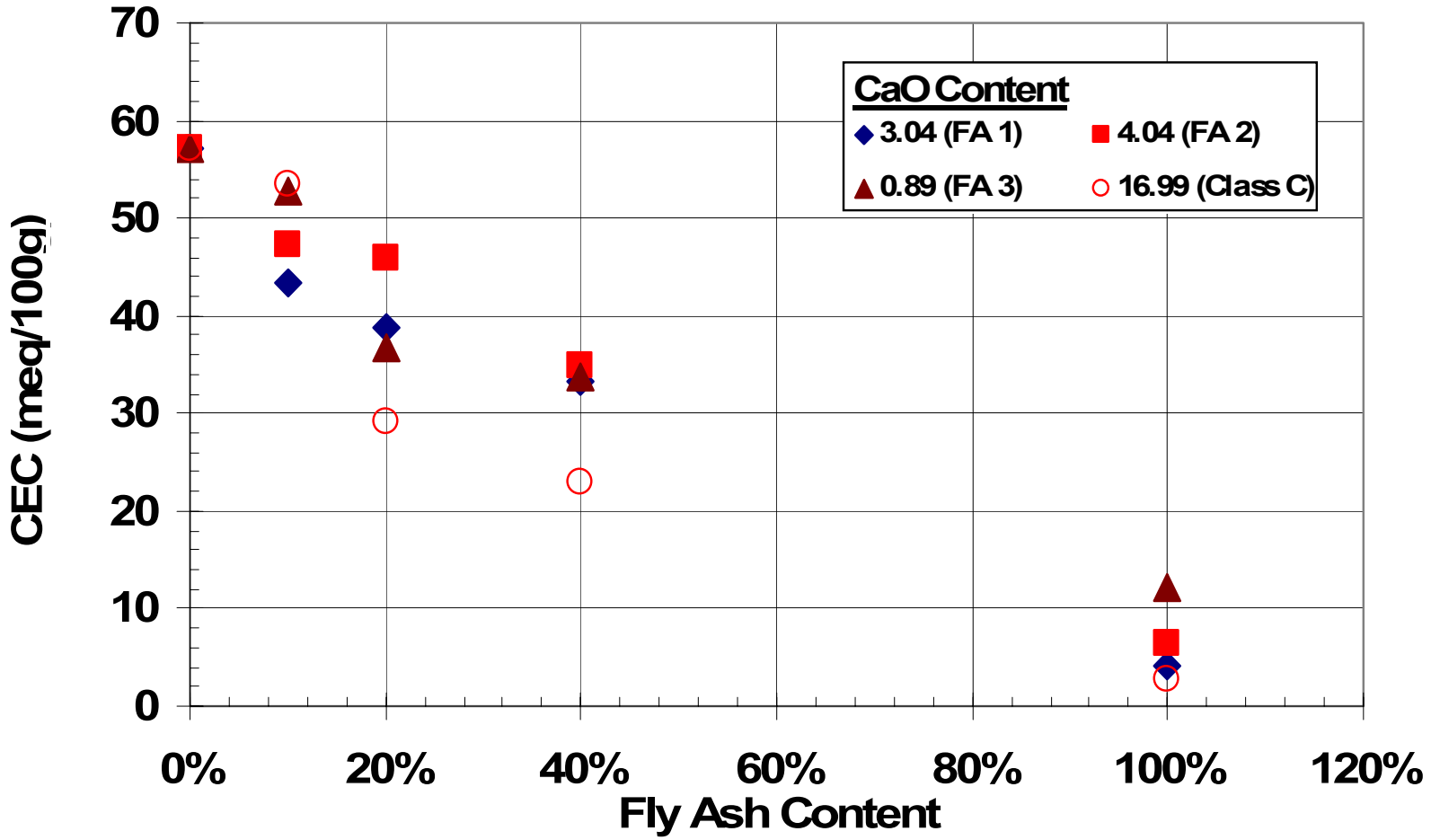

Figure 5.12 Effect of Calcium Oxide Content on Cation Exchange Capacity of the Mixtures

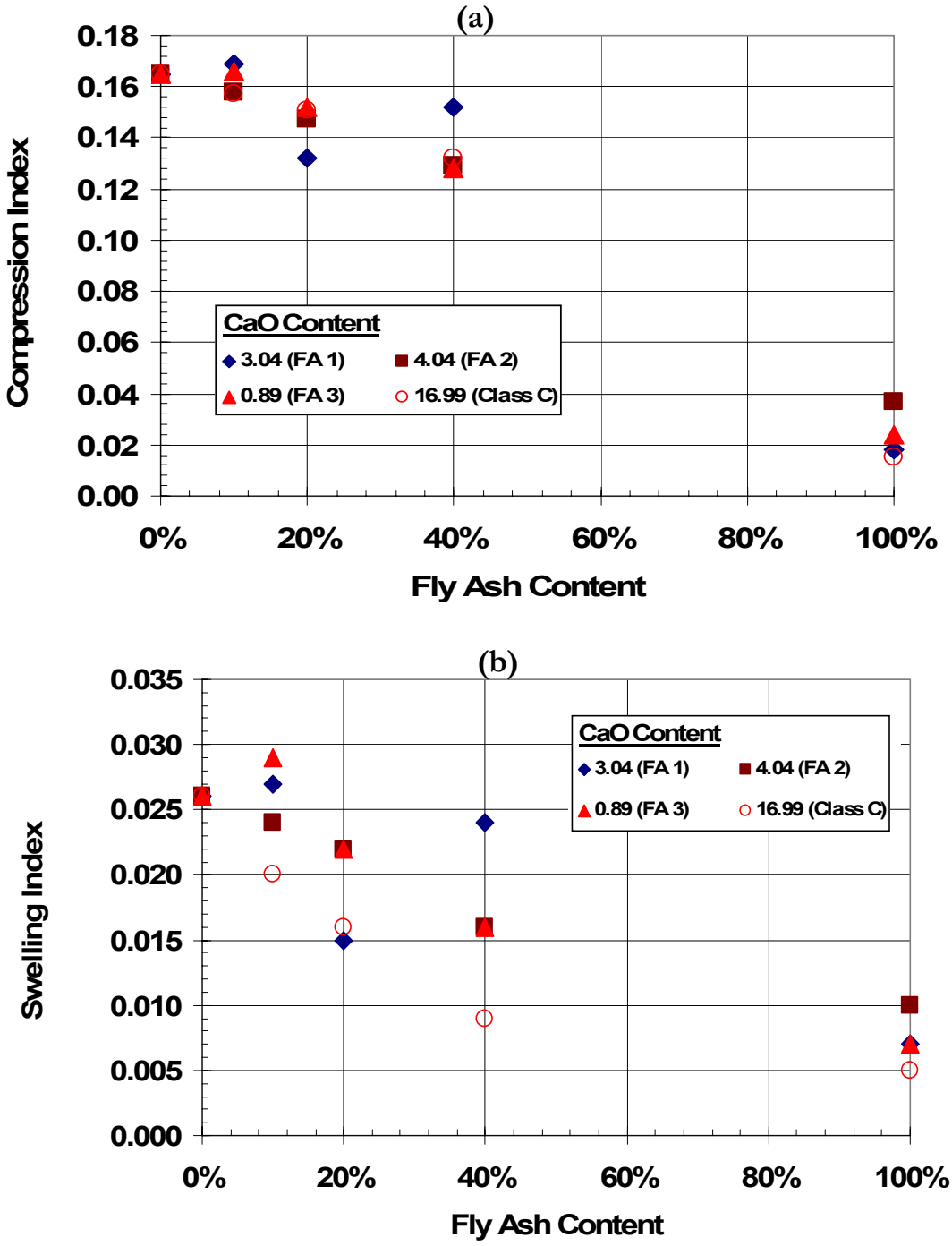

Figure 5.13 Effect of Calcium Oxide on Deformation Properties of Fly Ash Soil Mixtures

some other effects with respect to the ash or an outlier from the experiments.

According to Figure 5.14, high CaO in the mixtures leads to high strength properties. This could be due to the cementation process that takes place in the mixtures leading to stronger bonds in addition to interlocking between particles leading in an increase in internal friction as a result of the addition of silt-sized fly ash particles. The CaO effect is observed in both undrained shear strength and effective friction angle. Other physicochemical analysis from this study can be found in Appendix D.

The difference in trend in some cases with the fly ashes could be differences in the nature of the ashes. As mentioned by Ferguson (1993), an important unknown in physicochemical interactions in fly ash modified soils is the form of the calcium in the fly ash, which primarily governs physicochemical characteristics of fly ash modified soils. Boles (1986) also indicated that, the effect of soil stabilization (i.e. altering the engineering properties of the soil) prediction is based on the chemical properties of both the fly ash and the soil being stabilized. This could also explain why there are some slight behavior differences in some of the ash mixtures studied.

5.3 SUMMARY

From the discussions above, it was observed that all the models predicted closer to each other in all the mixtures, but the predictions deviates slightly from the actual results. The deviation suggests the need to modify the model to give good results.

A very good relation was observed between compression index and plasticity index.

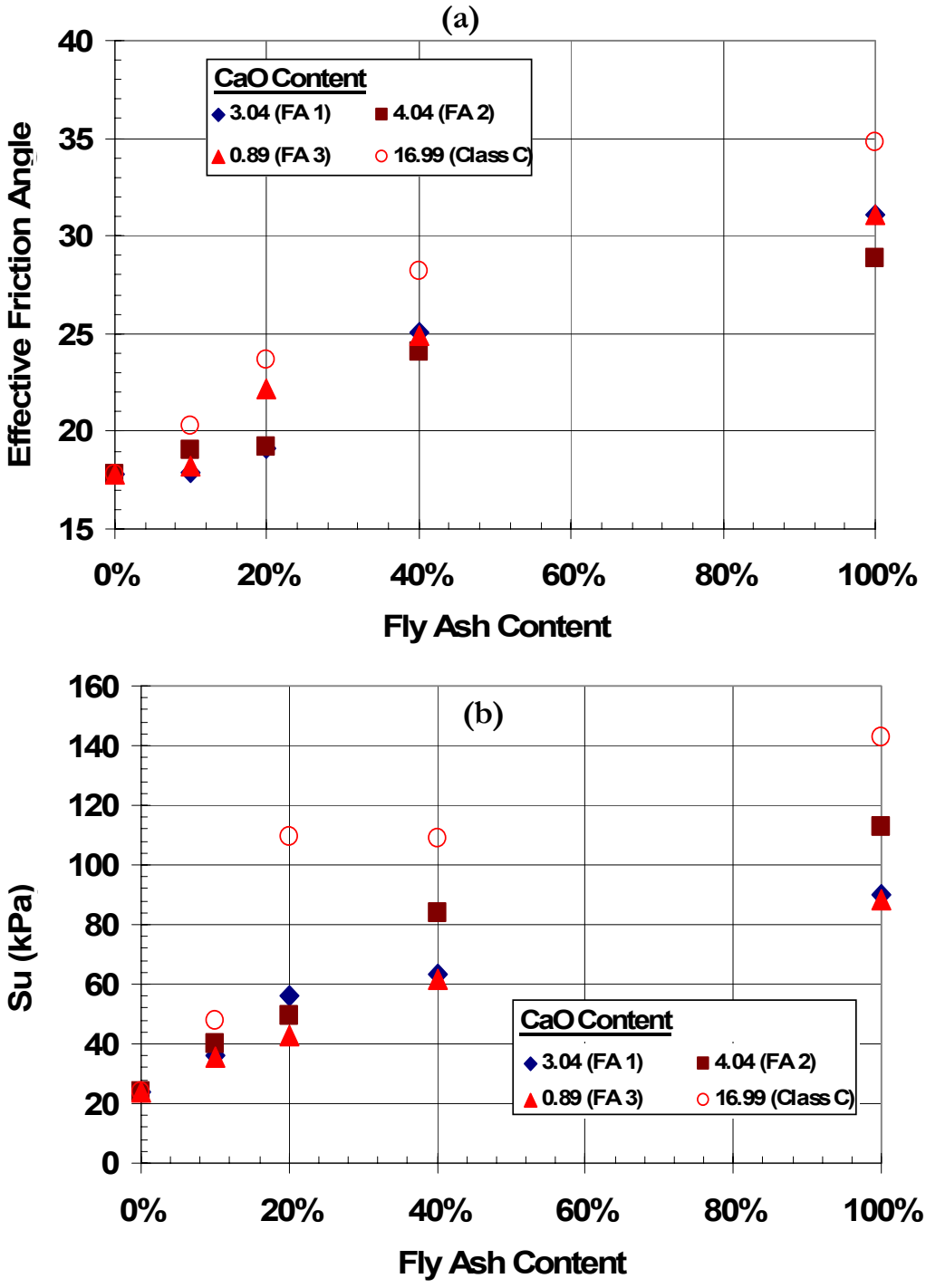

Figure 5.14 Effect of Calcium Oxide on Strength Properties of Fly Ash Soil Mixtures

Initial void ratio also correlates well with compression index. From these relationships, it was observed that Voigt's (1889) model gives a better prediction than that of Omine et al. (1998) and Braem (1987). There was a good relationship between consistency limits and strength parameters. At lower liquid limit, Voigt's model predicts better, and all the models predicts closer to each other at higher liquid limits in all mixtures.

In comparing actual and predicted results for all the engineering properties, again Voigt's model prediction was better than the other two models in almost all cases.

From the chemical composition perspective, a strong correlation was found between the sum of oxides and CaO with data from literature and this study. This gave a reason to base the modification on the two chemical properties of the ashes. The two chemical properties are also the main distinction between Class C and F ashes. Cation exchange capacity was found to decrease with increasing fly ash content. It was also observed that the higher the CaO content the lower the cation exchange capacity. The reverse effect of CaO oxide was observed with strength parameters such as effective friction angle and undrained shear strength. Unlike compression index, CaO significantly affect swelling index. This implies the chemical reaction that takes place due to the presence of CaO reduces the swelling ability of the mixtures.

In view of the above, the amount of CaO present in the fly ash was considered a necessary parameter that could help in modifying the mixture theory models.

CHAPTER 6 : MODEL MODIFICATION

6.1 MODIFICATION OF MODEL

As observed above and in previous discussions, the mixture theory models alone were unable to accurately predict some of the engineering properties. It has also been observed that physicochemical interactions between the soil and ash particles affect some of the engineering properties of the mixtures. As a result, a combination of both mixture theory and physicochemical properties could help improve upon engineering properties of mixture predictions.

Several forms of modifications were considered but the one that gave good results upon regression of the actual data and predicted data from the models indicated that, in almost all the mixtures, predicted results is a factor lower or higher than the actual laboratory results. In an attempt to modify the mixture theory models, first the modifications were applied to only the fly ash contributing part of the model in certain instances. The modifications applied only to the fly ash contributing part yielded results that were considered to be unreliable in the sense that, some of the modification factors were not comparable to others in the same mixture type, therefore the approach was abandoned. Modifications applied to the mixture theory model in its entirety gave a reasonable trend of results. The reason for the success of this form of modification can be attributed to the fact that, physicochemical interactions between the clay and fly ash particles were not addressed by the mixture theory alone. This physicochemical interaction is believed to only take place after both materials have been mixed and therefore a modification of the model in its entirety will be a fair

assessment of the chemical interactions that the original mixture theory models did not take into consideration. In view of this, the proposed modification can be presented in the form

$$y_{mix} = \alpha\left[f_{FA}y_{FA} + (1 - f_{FA})y_C\right] \tag{6.1}$$

where alpha(α) is the modification factor applied to the model. The remaining portion of the equation in parenthesis can be any of the mixture theory models discussed above. As before, subscripts FA and C represent fly ash and clay, respectively. The soil property to be determined is denoted by *y* and the volume fraction is denoted by *f* in Equation 6.1. The alpha factor is considered to be the contribution of the physicochemical interactions between particles to the engineering properties of the mixtures. The factor is therefore linked to the chemical composition of the fly ash in the mixture. As was mentioned in Section 5.2, it will be good to correlate the modification term to the calcium oxide and the sum of the oxides in the fly ash, since those are the major distinguishing components that are used in the classification of the ashes and therefore should have a significant impact on the chemical behavior of the ashes. The modification term, alpha, is computed through a power law relation involving the calcium oxide and the sum of oxides contents in the fly ash and is given as

$$\alpha = \left(\frac{CaO}{Sum\_of\_Oxides}\right)^x \tag{6.2}$$

where *x* is an index determined by regression. The modification factor in Equation 6.2 was arrived at after a series of combination of the chemical compounds in the fly ash to generate

factors to modify the models for each fly ash used. It was realized that no unique factor was suitable for the modification in all the ashes, however, a range of factors was found possible depending on the engineering property considered. That range of factors was also found to be dependent on the index (*x*) in Equation 6.2. Upon regression, different ranges of values of *x* for a given engineering property were determined and can be seen in Table 6.1.

Table 6.1 Range of Values for Index (*x*) in Equation 6.2

Property	Range of Index (*x*) Values
Optimum Moisture Content (OMC)	0.02 to 0.05
Maximum Dry Density (MDD)	-0.01 to 0.02
Effective Internal Frication Angle (ϕ')	-0.02 to 0.02
Undrained Shear Strength (Su)	-0.2 to -0.04
Compression Index (C_c)	-0.08 to -0.01
Swelling Index (C_s)	0 to 0.3

Mid-range values of the index (*x*) are used to calculate the alpha term in Equation 6.2 to modify the respective engineering properties. Graphical comparison of the modified and the actual model predictions with data from this study is presented in Figures 6.1 through 6.3. From the figures, it can be seen that modification of the mixture theory model by alpha (α) improved the relation between predicted and actual results in all the engineering properties investigated. This confirms that a combination of mixture theory model and

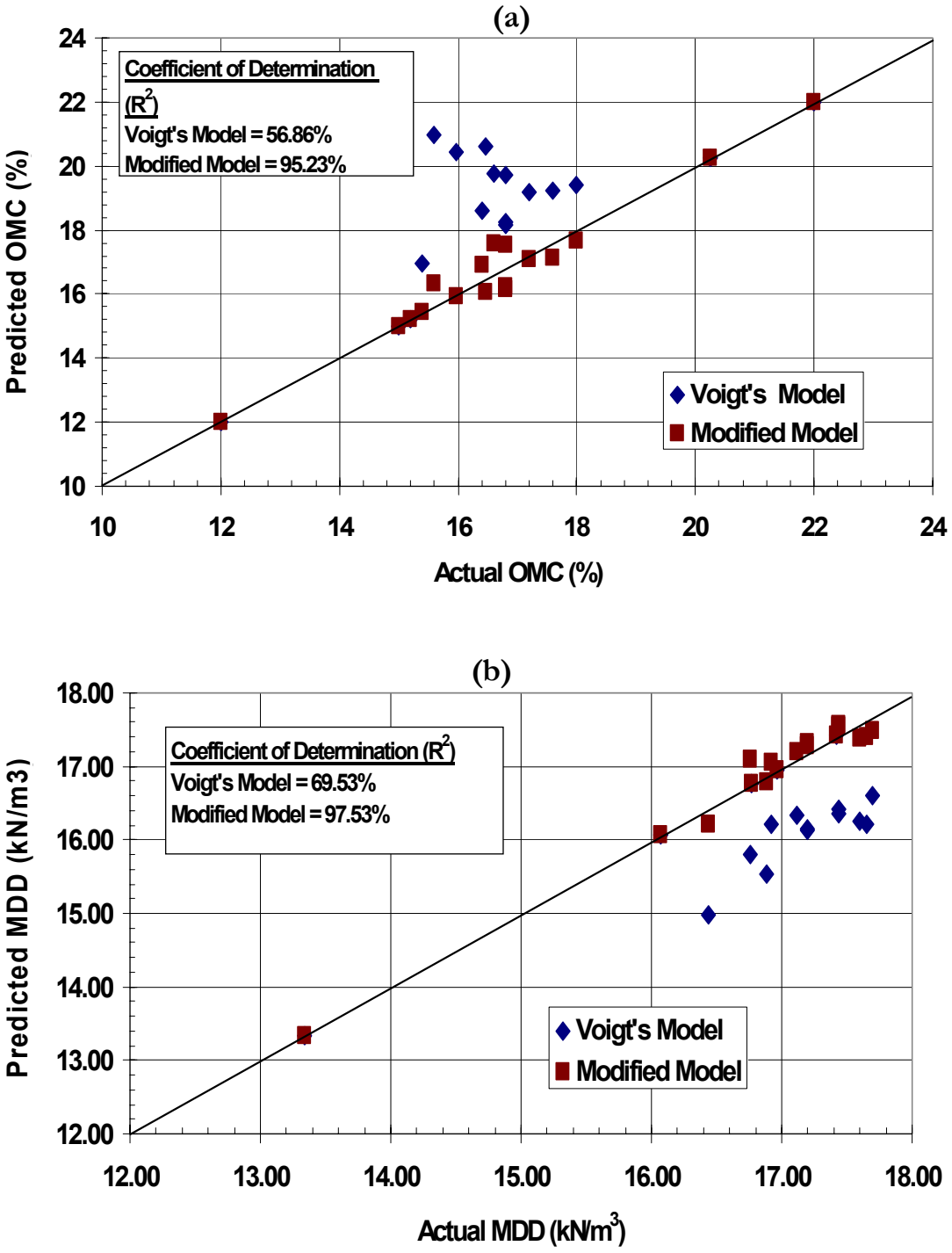

Figure 6.1 Comparisons of Actual and Modified Mixture Theory Model Predictions of Moisture-Density Parameters

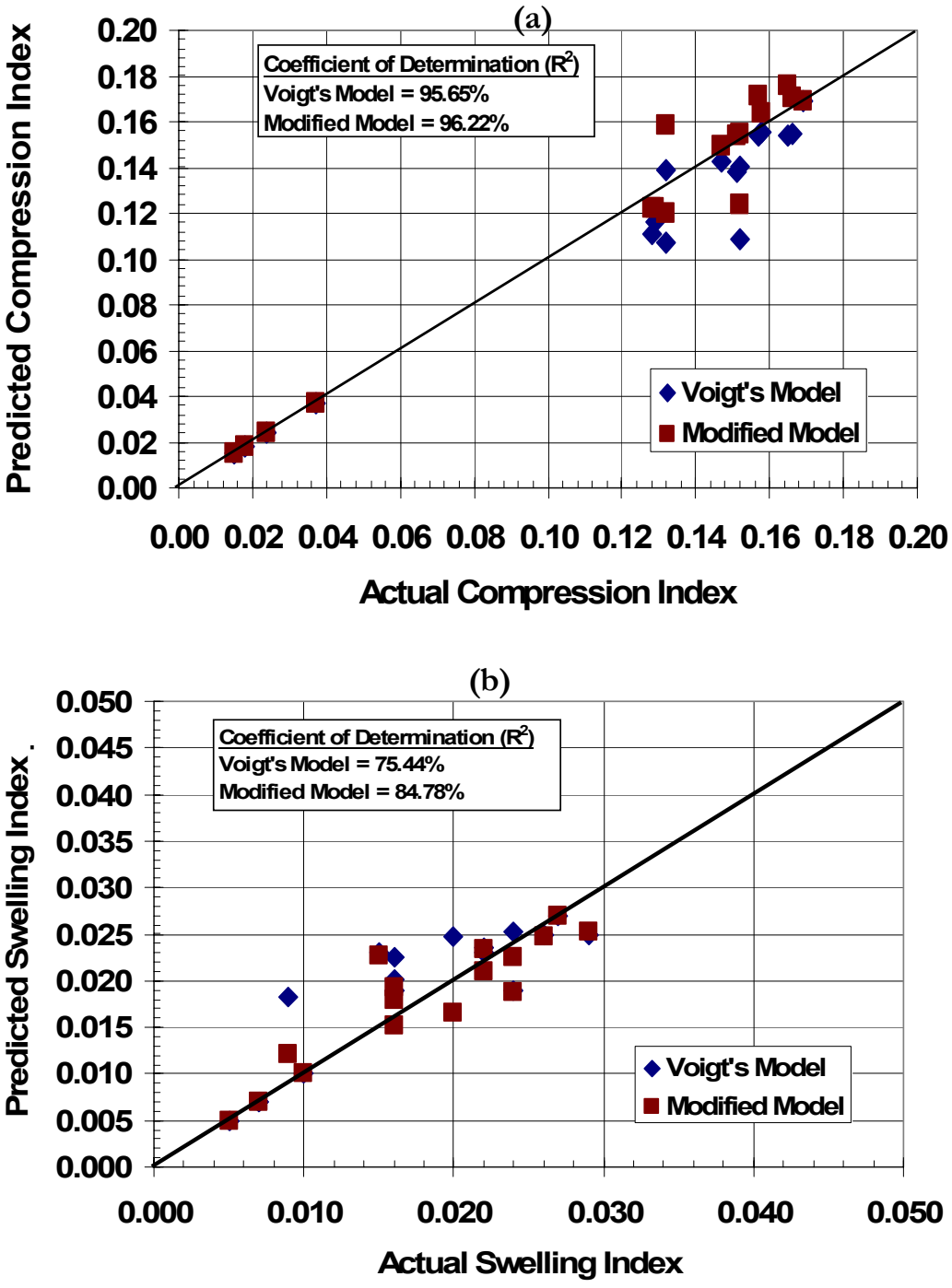

Figure 6.2 Comparisons of Actual and Modified Mixture Theory Model Predictions of Deformation Parameters

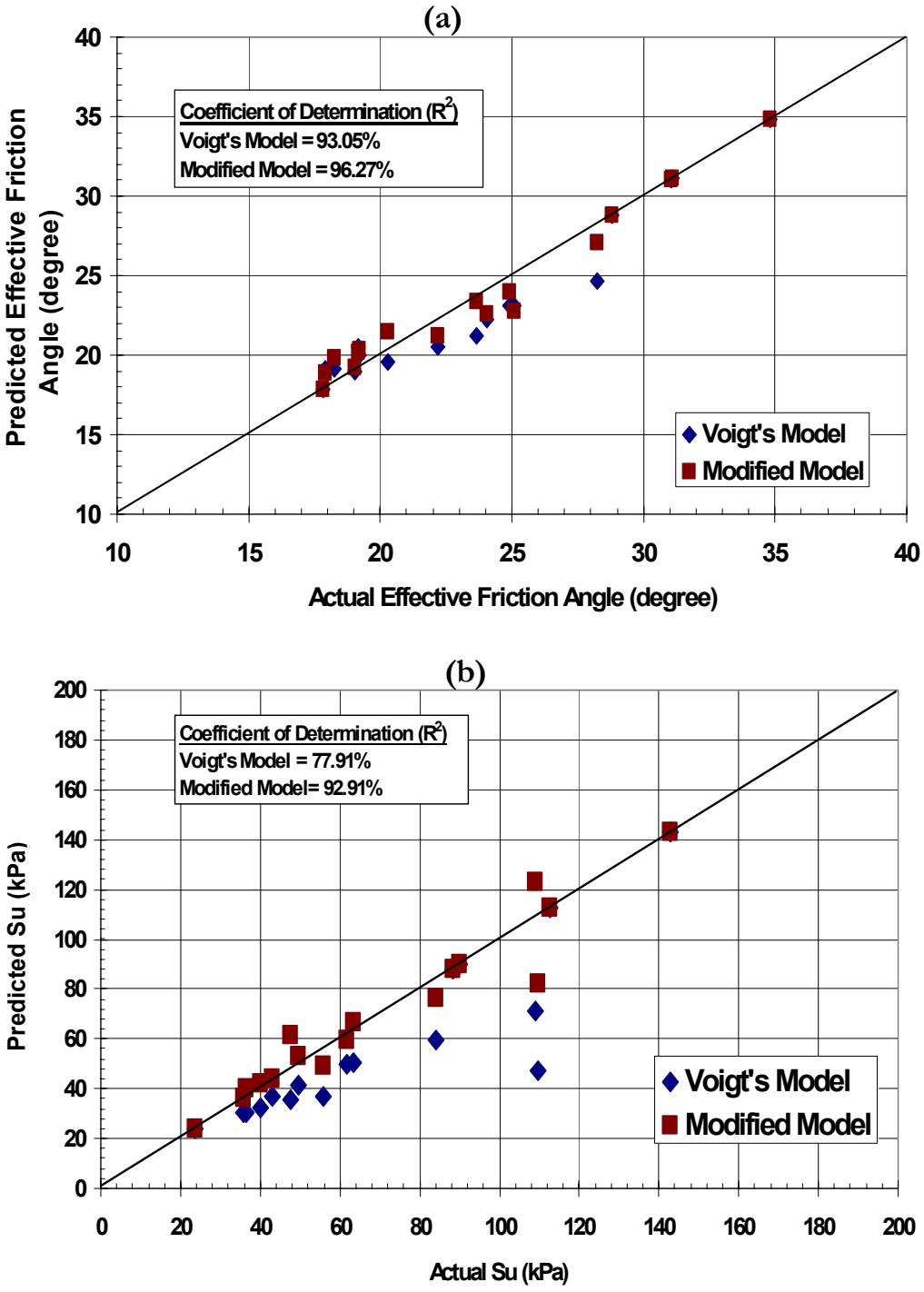

Figure 6.3 Comparisons of Actual and Modified Mixture Theory Model Predictions of Strength Parameters

physicochemical properties of fly ash is a good approach in predicting engineering properties of fly ash modified soils. The form of equation seen in Equation 6.2 and the range of values presented in Table 6.1 were obtained after multiple regression analyses with various combinations of the chemical composition in the fly ashes.

6.2 VALIDATION OF MODEL MODIFICATION

The method employed to improve predictions in Section 6.1 is applied to literature data to ascertain how best the model modification predicts engineering properties in fly ash modified soils from other researchers. As earlier discussed in Chapter 3, most of the research data do not have adequate information necessary to employ the method of mixture theory in predicting engineering properties. The little available data well suited to the mixture theory method of prediction was discussed in Chapter 3. Modifications of the models with the alpha term as seen in Section 6.1 is applied to data from literature, which was earlier presented in Chapter 3 and the outcome compared with predictions without modification.

Figure 6.4 through 6.6 shows graphs of moisture-density parameters and consistency limits of fly ash mixtures from different researchers (Prabakar, 2004, Kumar and Sharma, 2000, and Sahu and Piyo, 2000). The figures reveal that, the modified prediction is closer to the actual in all cases with all the researchers. The modification saw a slight deviation in Figure 6.4 (a), but the prediction was very close to the actual results. From Figure 6.5, predictions were seen to be good compared to actual results irrespective of the soil type used. A similar result is seen in the relationship between maximum dry density and plasticity index (see Figure 6.6).

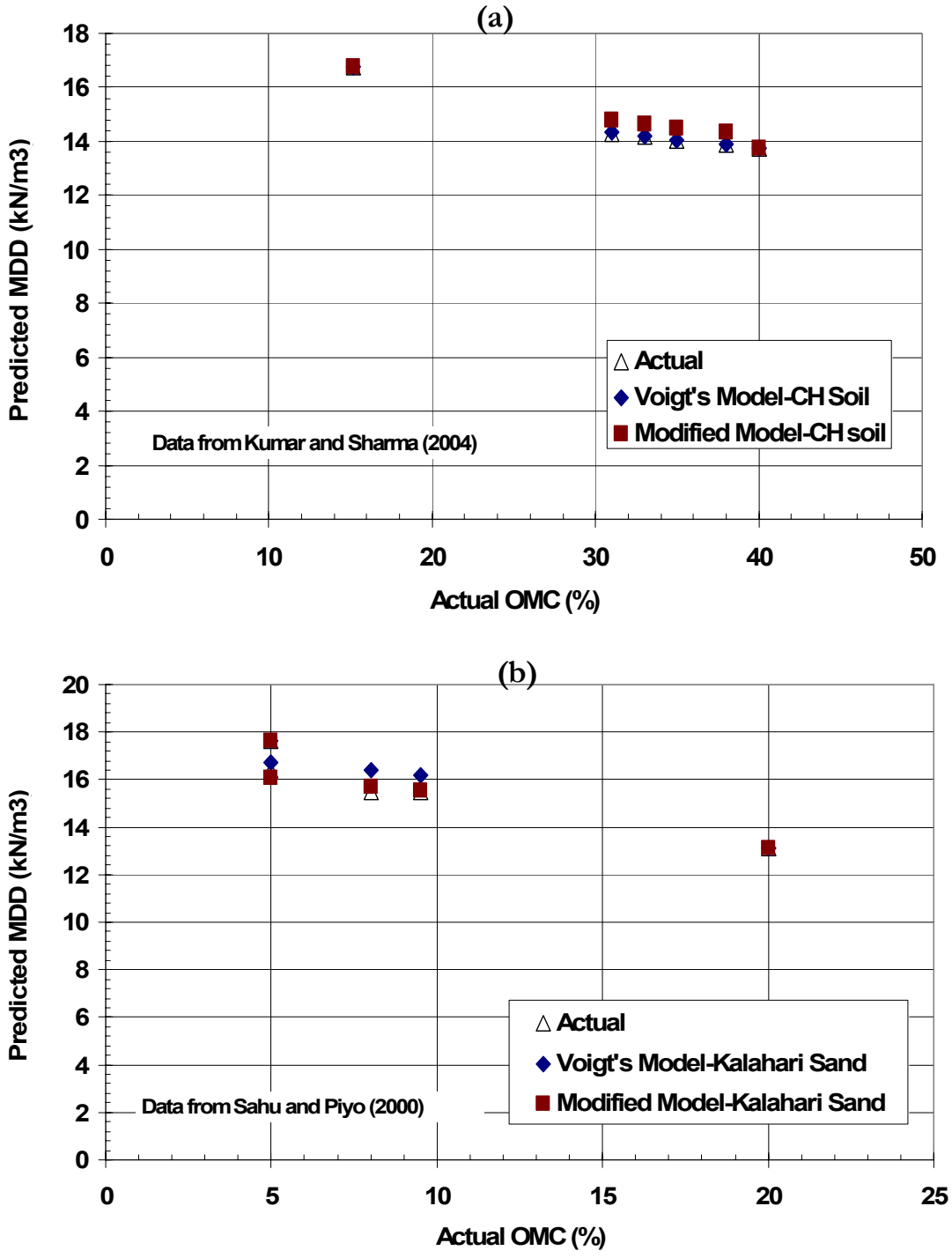

Figure 6.4 Comparing Modified and Unmodified Model Predictions and Relating Moisture-Density Parameter of CH Soil and Kalahari Sand

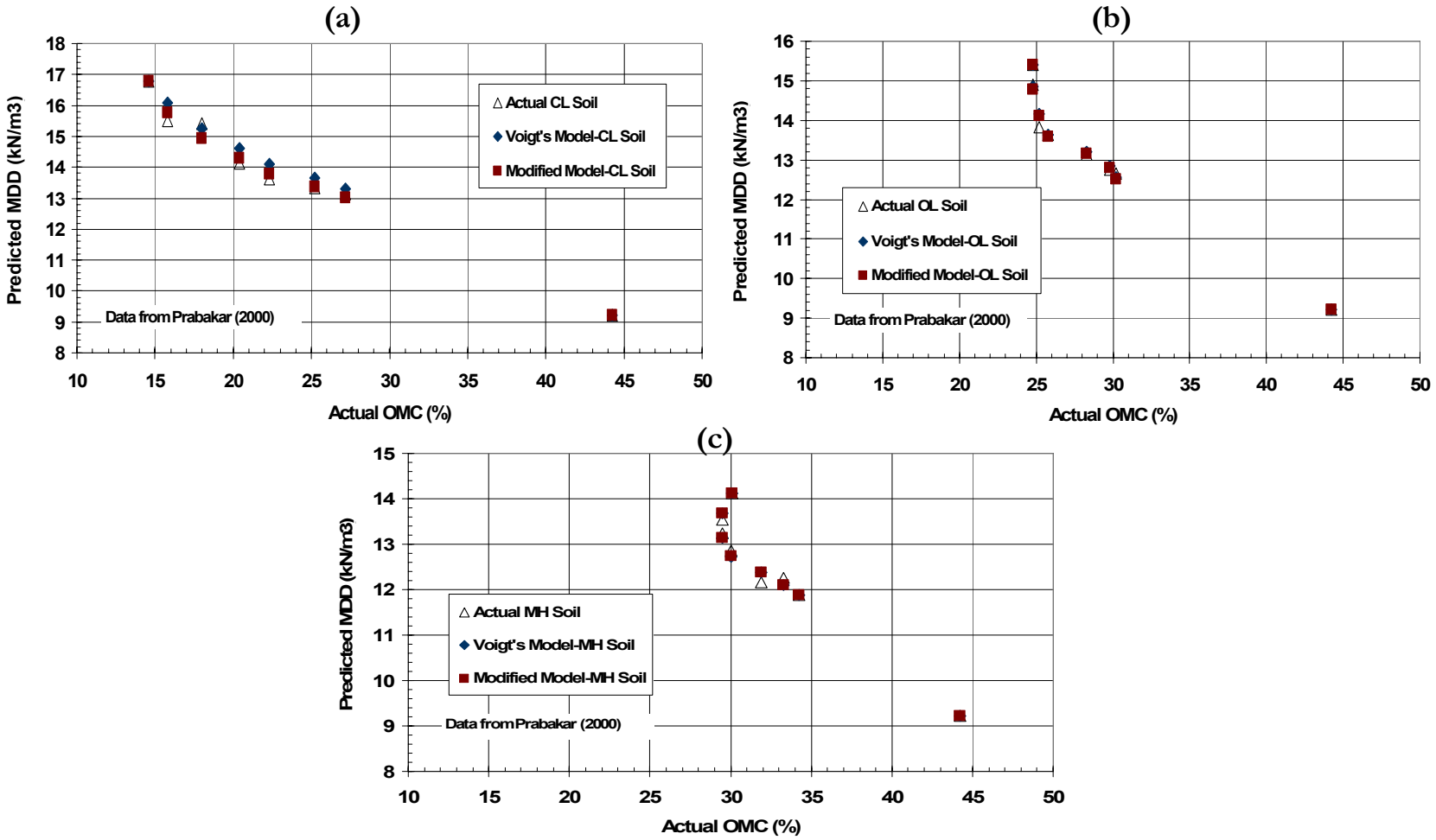

Figure 6.5 Comparing Modified and Unmodified Model Predictions and Relating Moisture-Density Parameter for CL, OL, and MH Soils

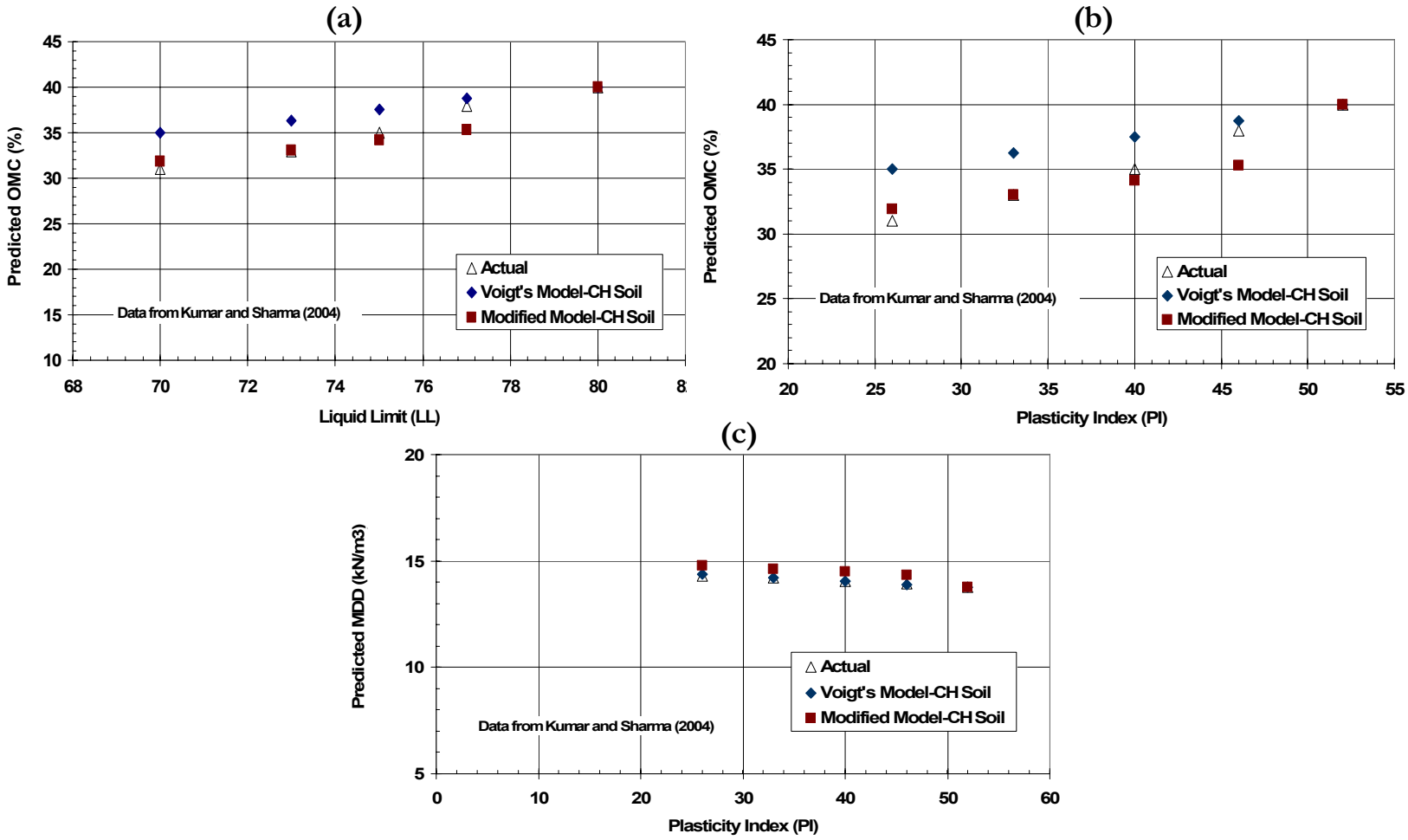

Figure 6.6 Comparing Modified and Unmodified Model Predictions and Relating Consistency Limits to Moisture-Density Parameters

Comparison of modified and unmodified models predictions can be seen in Figures 6.7 and 6.8. According to the figures, correlations between actual and the modified model predictions are higher than the unmodified results. This suggests that the modified model will give a more accurate prediction compared to the unmodified models as can be seen in the figures. It can be observed that model predictions as well as the modified predictions in the strength parameters are not as accurate as that of the moisture-density parameters, but in general the modified predictions give very good results.

6.3 FORMULATAION IN TERMS OF CRITICAL STATE PARAMETERS

The results obtained from the modified model can be transformed into critical state model. The essence of transforming the results into critical state is to be able to determine essential geotechnical parameters of fly ash modified soils with little information available.

The critical state line (CSL) representing failure state of soils is unique to soil types. In this study, the critical state lines for all the mixtures in *e-lnp'* space is presented in Figure 6.9 As can be observed in the figure, the failure state or behavior of all the mixtures at critical state can be categorized in three distinct sections. The distinction is in terms of the fly ash content. The failure behavior can be grouped into 0 to 20%, 20 to 40%, and then 100% fly ashes. With the exception of Fly Ash 1 (FA 1) and Fly Ash 3 (FA 3) where the 20% fly ash fall in the middle category, the remaining fly ashes have the middle category consisting of only the 40% fly ash mixtures. The reason for this distinction is that, as the fly ash content changes failure mechanism is controlled by either the clay particles alone, a combination of the fly ash and the clay particles or only the fly ah particles. This phenomenon is explained in

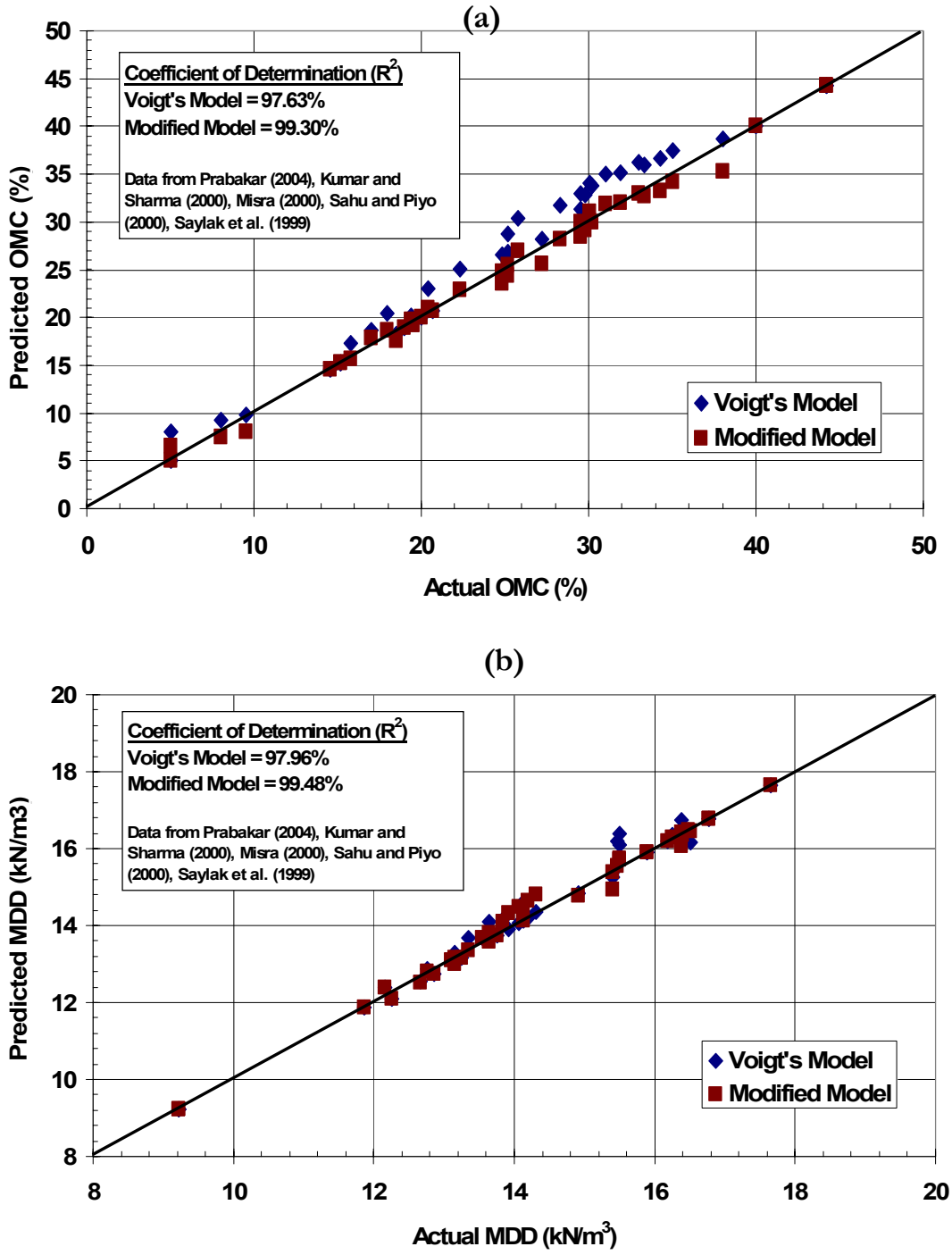

Figure 6.7 Comparisons of Modified and Unmodified Model Predictions of Moisture-Density Parameters to Actual Results

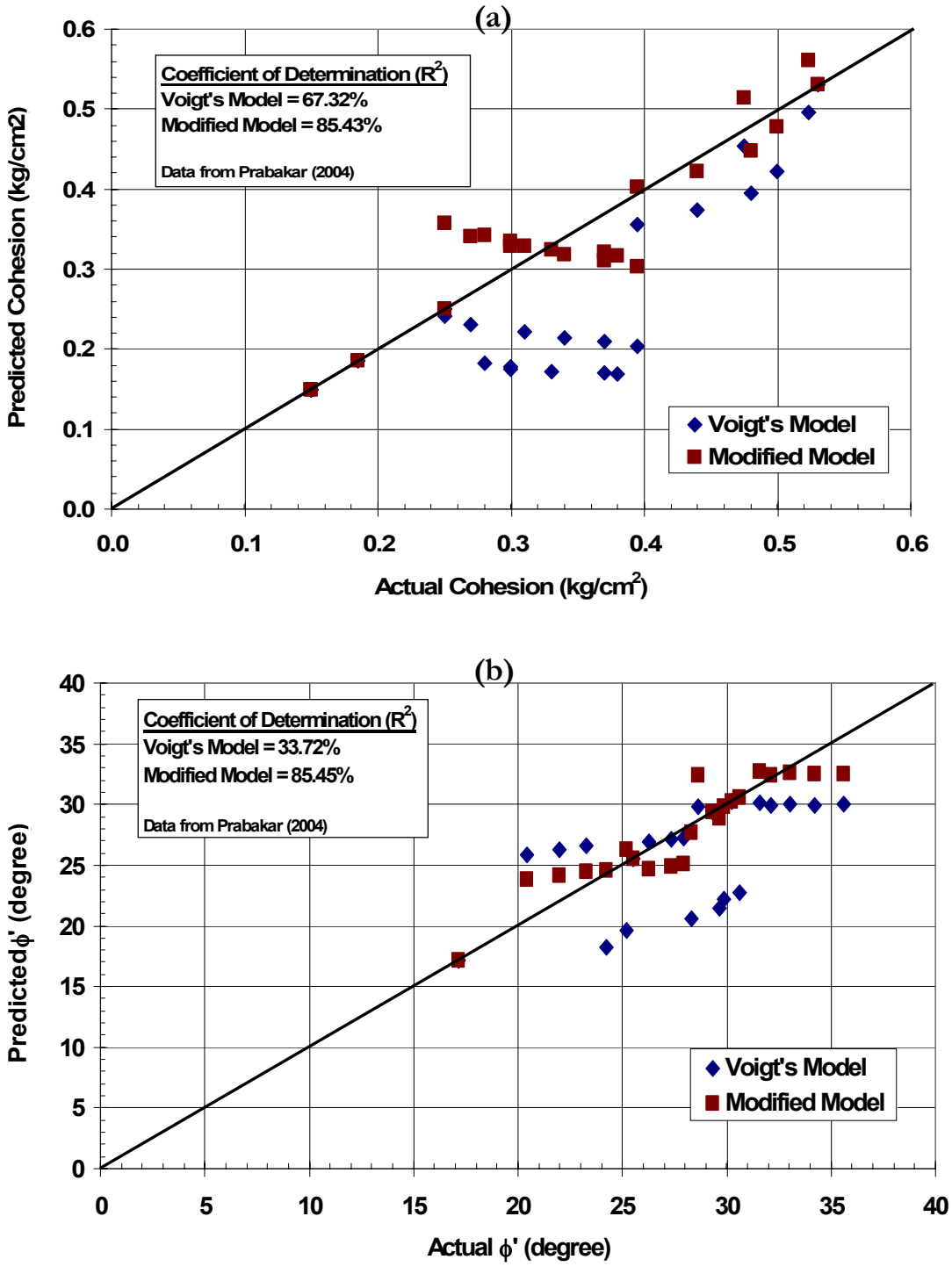

Figure 6.8 Comparisons of Modified and Unmodified Model Predictions of Strength Parameters to Actual Results

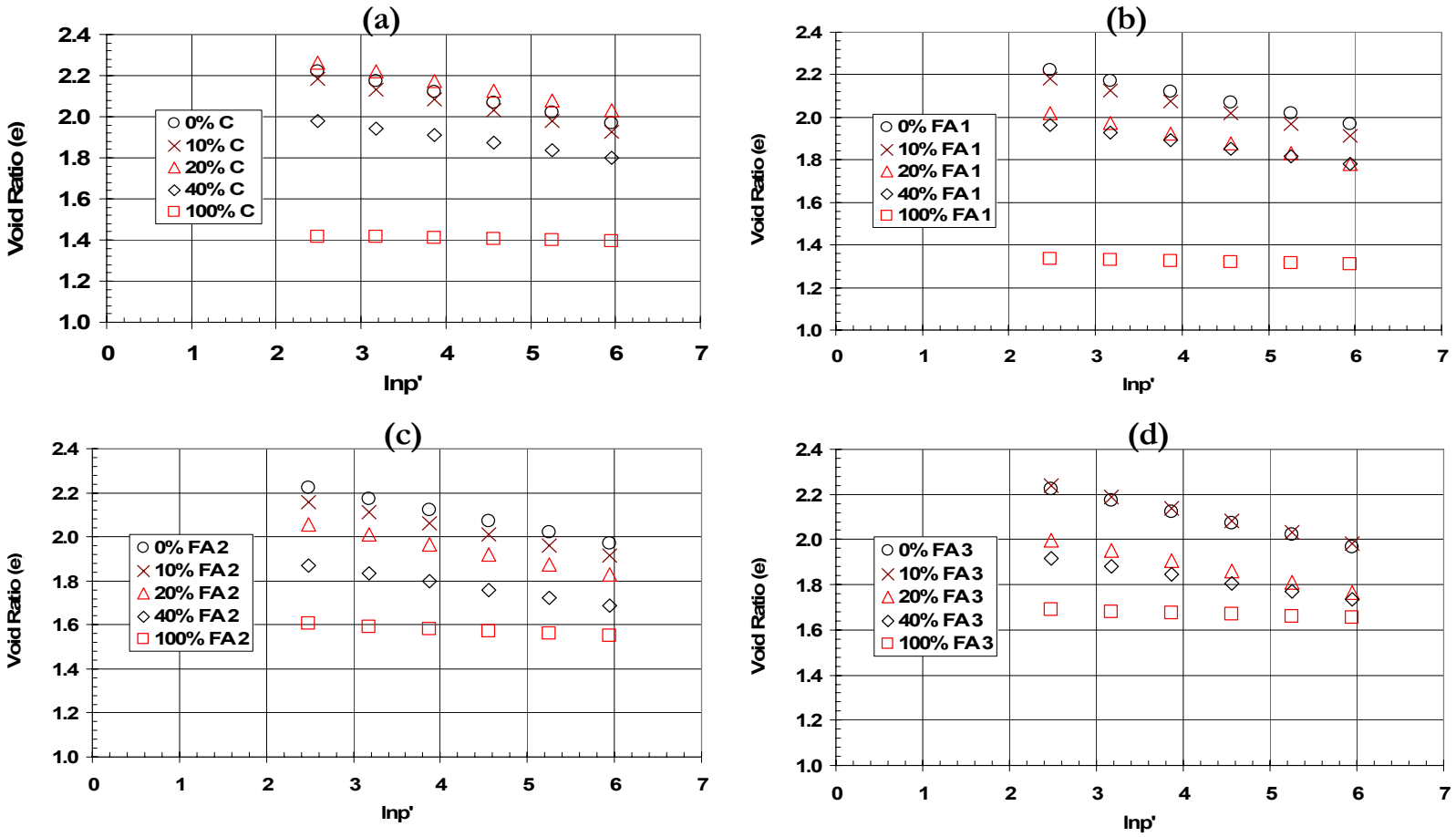

Figure 6.9 Critical State Lines in e-lnp' Space for All Fly Ash Mixtures

Section 2.2. It is observed that the failure behavior of mixtures from 20% to 40% (and probably beyond) fall between the clay controlled and fly ash controlled mixtures. This suggests that failure of mixtures within this range (20% to 40%) is governed by both materials. This further explains why the trend observed in most of the engineering properties analyzed in previous chapters' changes around 20% percent of fly ash in the mixtures.

The yield surface in stress space of soils is the stresses that separate elastic responses from plastic responses in the soil. As mentioned in Section 2.6.2, the yield surface in soils assumes the shape of an ellipse and the initial size is governed by the preconsolidation stress ($p_c^{'}$). In the study, all the samples were preconsolidated to a stress of 23.97 kPa and an initial effective stress ($p_0^{'}$) of 11.97 kPa was used. In Figure 6.10, the initial yield surfaces of the mixtures of fly ash 2 (FA 2) in *p'-q* space is presented. In the figure, CSL, IYS, and ESP denote critical state line, initial yield surface for compression, and effective stress path, respectively. Recalling from Section 2.6.2, the interception of the yield surface and the effective stress path gives the yield stresses. If the intersection is between the initial yield surface and the effective stress path, then the coordinates gives the initial yield stresses. Also, the interception between the critical state line and the effective stress path gives the failure stresses of the soil. According to the figure, as the fly ash content increases, the initial yield surface increases in the direction of the *q* axis. Since all samples were preconsolidated to the same stresses, the initial yield surfaces do not extend beyond the preconsolidated stress. Similarly, the slope of the critical state line increases as the fly ash content increases. The implication of this behavior is that, as the fly ash content increases, the deviatoric load

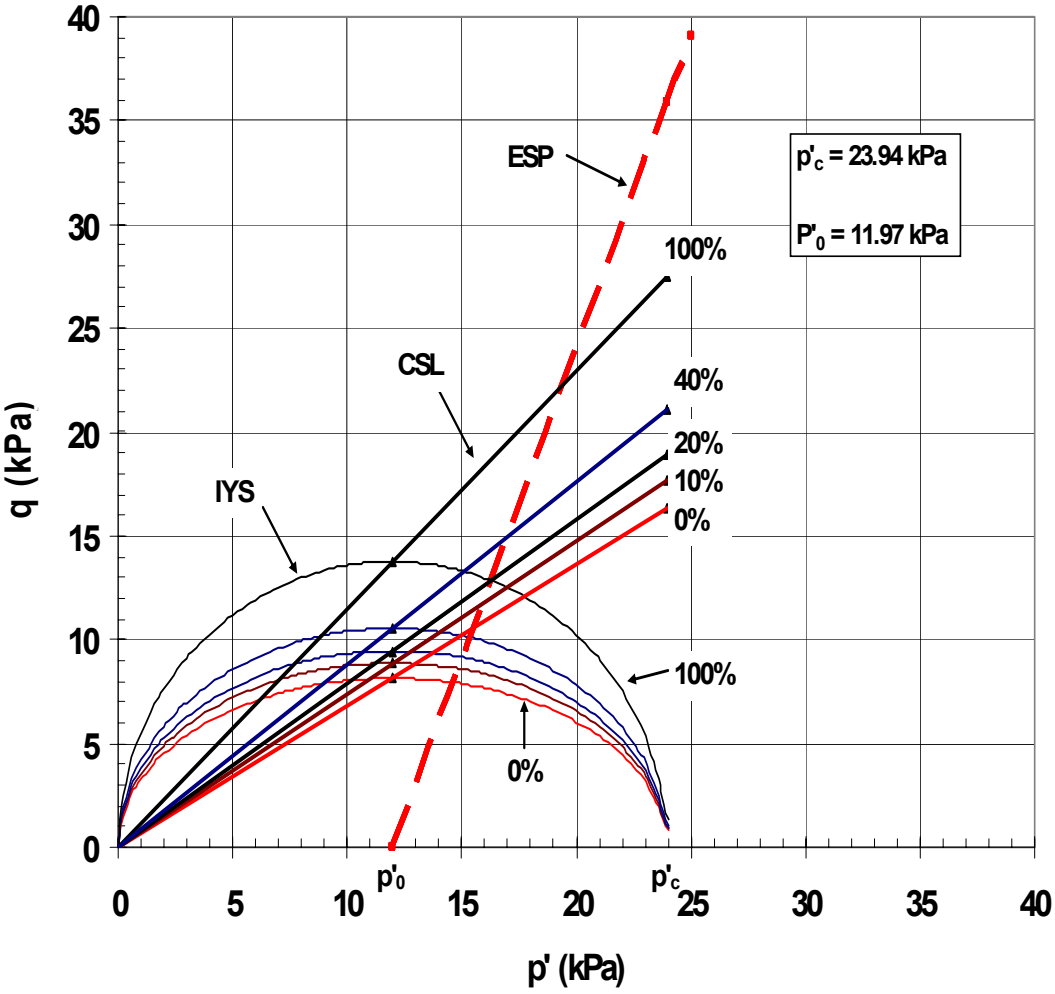

Fly Ash Content (%)	Yield Stresses p' (kPa)	Yield Stresses q (kPa)	Failure Stresses p' (kPa)	Failure Stresses q (kPa)
0	15.4	7.8	15.8	10.5
10	15	8.6	16	11.8
20	15.4	9.1	16.4	12.6
40	15.6	10	17	15
100	16.4	12.8	19.5	22.5

Figure 6.10 Effect of Fly Ash Content on Yield Surfaces for Fly Ash 2

required for the sample to get to yield and failure stresses also increases. The coordinates of the yield and failure stresses as the fly ash content increases is summarized in a tabular form and is presented in Figure 6.10. This trend of behavior is observed in all the fly ash mixtures in this study.

The soil mixtures behave elastically (full recovery when sample is unloaded) in all combinations of *p'* and *q* that fall within the initial yield surface of a given mixture. Combinations of *p'* and *q* falling outside the initial yield surface give the elastoplastic behavior of the mixtures. Thus the stresses experienced by the soil sample when a load is applied leads to partial deformation upon unloading. This usually occurs when the sample is loaded beyond the preconsolidated stress. In such situations, the initial yield surface expands, and the state of the soil is described by the expanded yield surface (EYS). Figure 6.11 demonstrates this behavior for 40% Class C soil mixture from this study. According to the figure, when the load application is such that q increases by 3 kPa beyond the initial yield surface, the yield surface expands beyond the preconsolidated stress. At this point, the soil behaves elastoplastically. When the sample is continuously loaded, the yield surface will continue to expand until it coincides with point B. This is the point where the sample failure is observed.

As earlier discussed, the critical state parameters presented here were obtained from experimental results and equations presented in Section 2.6. The parameters are presented in Table 6.2.

From the table, relationships between the critical state parameters and fly ash content

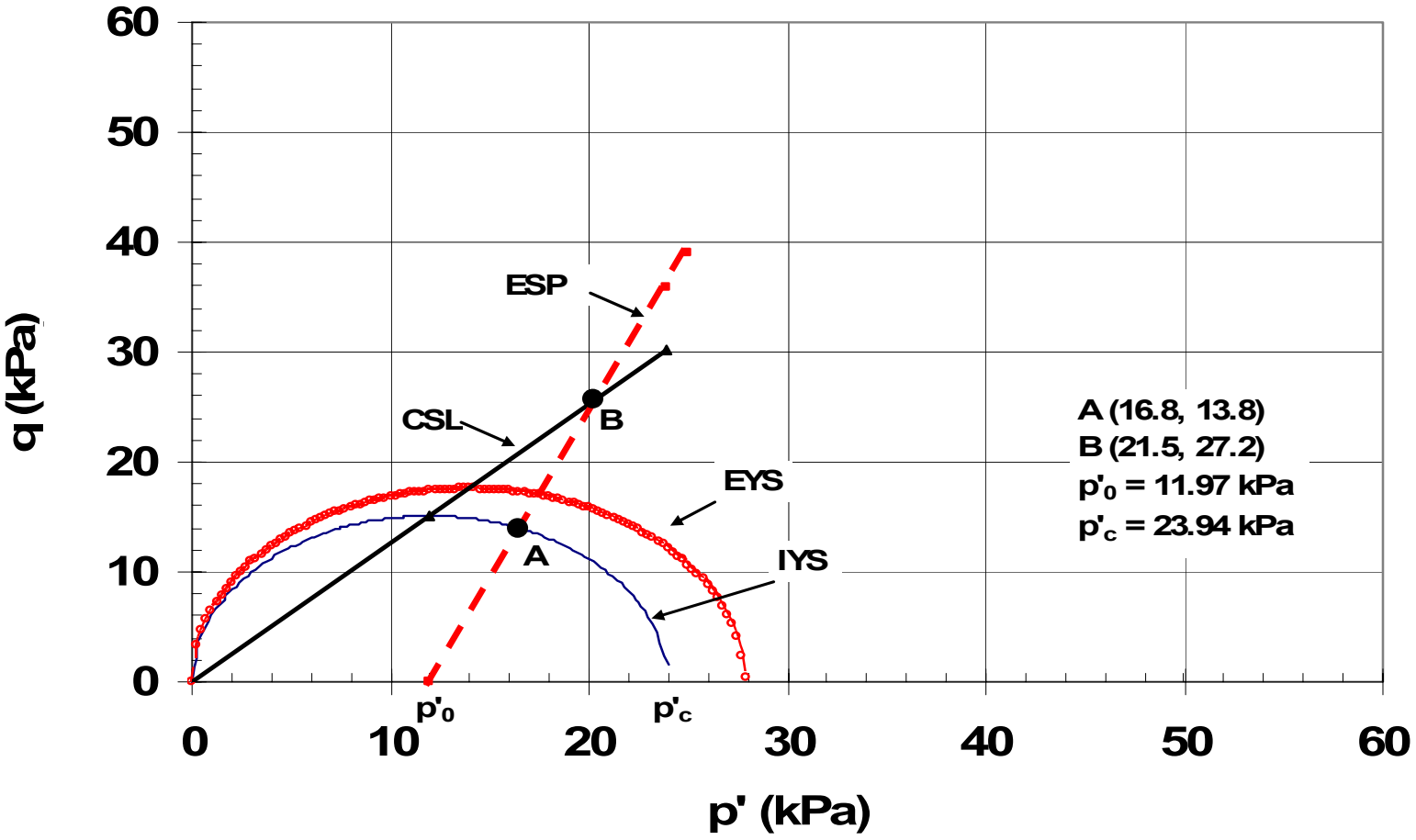

Figure 6.11 Demonstration of Elastoplastic Behavior in p'-q Space of 40% Class C Fly Ash

Table 6.2 Critical State Parameters for Soil Mixtures

Sample Description	% FA	Critical State Parameters			
		M	λ	κ	Γ
CLAY	0%	0.683	0.073	0.012	2.235
FA 1	10%	0.615	0.076	0.011	2.187
	20%	0.661	0.069	0.010	2.028
	40%	0.754	0.054	0.008	1.973
	100%	1.247	0.008	0.003	1.342
FA 2	10%	0.741	0.071	0.010	2.165
	20%	0.788	0.065	0.009	2.061
	40%	0.882	0.053	0.008	1.876
	100%	1.149	0.016	0.004	1.612
FA 3	10%	0.768	0.074	0.011	2.248
	20%	0.825	0.067	0.010	2.008
	40%	0.942	0.053	0.008	1.926
	100%	1.248	0.010	0.003	1.694
CLASS C	10%	0.979	0.074	0.007	2.183
	20%	1.072	0.067	0.007	2.264
	40%	1.259	0.052	0.005	1.980
	100%	1.410	0.007	0.002	1.422

can be obtained. The trend and relationships between fly ash content of the different fly ashes and critical state parameters can be seen in Figure 6.12 and Table 6.3, respectively. According to the figure, all the parameters relate linearly with the fly ash content irrespective of the fly ash type except in Figure 6.12 (a), where the relationship between the ash content in Class C and M is not strongly correlated linearly. This is presented in the form of equation in Table 6.3. A generalized relation was found that expresses the ash content in terms of the

critical state parameters regardless of the ash type. In the case of Figure 6.12 (a), the Class C ash was exempted in the formulation (see Table 6.3). The pattern observed in the figure reveals that, as the fly ash content increases, the parameter M also increases. Fly ash addition to the mixtures represents an addition of a coarse material to a fine material, thereby reducing the fine content in the mixture as the ash content increases. Kim et al. (2005) observed a similar trend of relationship between the amount of fines in soils and the critical state parameter M. He observed that as the fines increases, M decreases. He further pointed out that as the fine content increases, λ and κ increases accordingly indicating that the soil behaves as a cohesive soil. Bouckovalas et al. (2003) also reported a similar trend. The observations made by the above mentioned researchers were in agreement with the results from this study as well [see Figures 6.12 (b) and (c)].

The generalized relationship obtained from Figures 6.12 (b) and (c) are given as

$$\lambda = -0.0694(FA) + 0.0801 \tag{6.3}$$

$$\Gamma = -0.7353(FA) + 2.2474 \tag{6.4}$$

where *FA* is the percent fly ash by weight. The above equations have higher determination coefficients of 99% and 89% respectively. Combining Equations 6.3 and 6.4 gives a relation between the two parameters as

$$\Gamma = 10.6\lambda + 1.4 \tag{6.5}$$

From Equation 6.5, the critical state line in *v-lnp'* space can be written for the fly ash

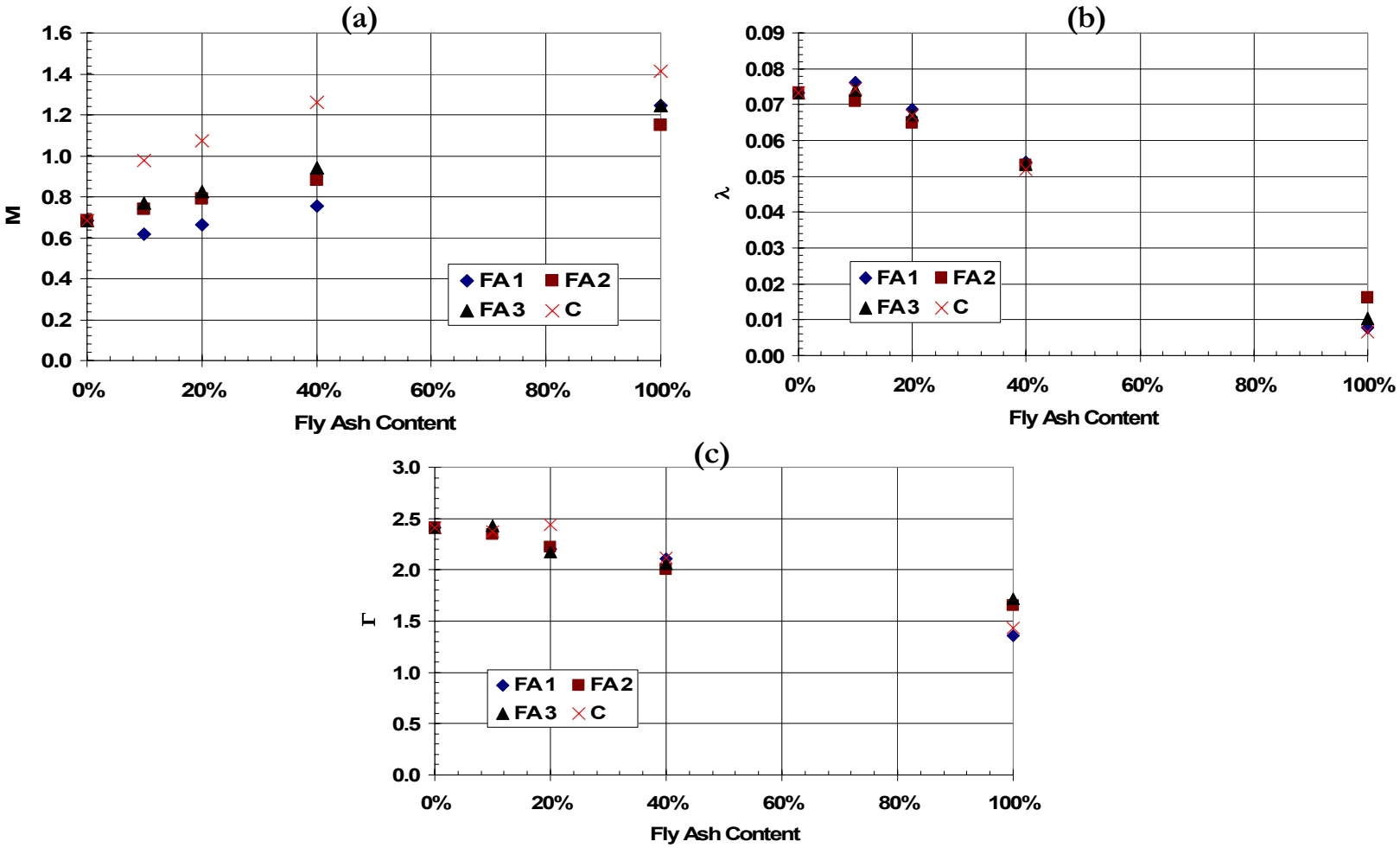

Figure 6.12 Relationships between Critical State Parameters and Fly Ash Content

Table 6.3 Equations Relating Critical State Parameters and Fly Ash Content and Their Corresponding R^2 Values

	Sample	FA 1	FA 2	FA 3	Class C	ALL Samples
M	Equation	0.6261(FA) + 0.579	0.4602(FA) + 0.6919	0.5508(FA) + 0.7057	0.6163(FA) + 0.871	0.5571(FA) + 0.6508 (only Class F)
	R^2 (%)	92.28	99.88	99.48	77.52	90.22
λ	Equation	-0.0704(FA) + 0.0799	-0.0591(FA) + 0.0758	-0.0666(FA) + 0.0783	-0.0708(FA) + 0.0787	-0.0694(FA) + 0.0801
	R^2 (%)	97.82	99.58	98.63	98.58	98.76
Γ	Equation	-0.8933(FA) + 2.2567	-0.6197(FA) + 2.2005	-0.5484(FA) + 2.2086	-0.8594(FA) + 2.3091	-0.7353(FA) + 2.2474
	R^2 (%)	98.2	96.46	89.14	95.06	89.37

modified soils in the study. Substituting Equation 6.5 into Equation 2.51 gives

$$\upsilon = \lambda(10.6 + \ln p') + 1.4 \qquad 6.6$$

From Equation 6.6, the specific volume and the void ratios at critical state under mean effective stress *p'* can be calculated for fly ash modified soils in this study. In view of the higher correlations obtained between the ash contents and the critical state parameters, the equations developed can be applicable to a wide range of fly ash modified soils at different ash percentages. Appendix C, gives the results of all the critical state parameters from this study.

6.4 SUMMARY

The model chosen to be modified is that of Voigt (1889) since it gave better prediction than the others in almost all cases. A modification term was determined to be better applied to the entire model than only the fly ash contributing part of the original model. The modification term was based on the ratio between the amount of CaO and sum of oxide (SiO_2+Al_2O_3+Fe_2O_3) present in the fly ash.

An experimental index was used to adjust the ratio to suit the specific engineering property. A range of values of the index was determined by regression based on the engineering property.

The modified form of the model was compared to the original, and in all cases the modified model performed better. The modified model was validated using data from literature, and this also gave good results compared to the original model. The performance

was irrespective of the ash or soil type. It is therefore believed that the modified model will be applicable to a wide variety of fly ash-modified soils.

The yield surface was found to depend on the amount of fly ash in the soil mixture. A relationship between critical state parameters and fly ash content was established. This helps in computing critical state parameters and modeling behavior of the fly ash mixtures given the ash type and the percentage of the ash in the mixture.

CHAPTER 7 : CONCLUSIONS AND RECOMMENDATIONS

7.1 CONCLUSIONS

The motivation behind this study was to find a generalized model that can predict the behavior of fly ash modified soils. Fly ash from the same source with the same burning technique produced at different times behaves differently when used in soil stabilization. This behavior has limited the wide application of fly ash in soil stabilization. A model that predicts behavior of fly ash modified soils with a considerably high degree of accuracy irrespective of the ash type would help reduce uncertainty in behavior and increase the use of fly ash in soil improvement. The main issues and findings from this study leading to the development of a generalized model applicable to fly ash modified soils are summarized below.

The procedures followed in achieving the objectives in this study are as follows:

1. A comprehensive literature review on the subject was made to establish the state of the art scenario which will serve as a guide in the direction of the study.

2. Data from literature were extracted and manipulated to examine trends and data gaps of which the study will attempt to fill.

3. Based on the results from the literature, laboratory tests were performed on mixtures made from three different fly ashes. The engineering properties as well as the necessary physicochemical properties on the mixtures at various fly ash percentages in the mixtures were determined.

4. The results were analyzed with respect to physicochemical effects and trends compared to traditional soil behaviors.

5. Three mixture theory models were employed to predict actual results. Upon analysis of the predicted results, one of the models was selected as the best model and this was modified based on the physicochemical influence on the mixtures. This modified model is the final product of this research and is expected to be applicable to a wide variety of fly ash-modified soils.

The conclusions drawn from the study based on the models and its application to binary mixtures are summarized below.

- The concept of mixture theory model is based on the properties of the individual constituents and their respective volume or gravimetric fractions. Based on the principles governing the development of the models, it can be used in the theory of mixtures to predict any property of mixtures regardless of the nature of the materials as long as those properties of the individual constituents are known. Different forms and modifications of mixture theory models have been developed. Three models were considered among the lot of existing models. The three models considered are Voigt (1889), Braem et al. (1987), and Omine et al. (1998).

- It was ascertained from the literature that, in binary mixtures, a minimum porosity or void ratio is reached where maximum or minimum engineering

properties of the mixture are realized. This minimum porosity or void ratio is dependent on the shape of the materials constituting the binary mixture and usually occurs within 20% to 40% of the inclusion in the mixture. This is believed to be the case where both materials control the properties of the mixture. Outside this range of minimum void ratio is where one of the constituents of the binary mixture dominates the mixture properties. This phenomenon is always realized regardless of whether the inclusion is coarse and the matrix is fine or vice versa as demonstrated by Santamarina (2001), Vallejo (2000), and Kumar and Wood (1997). The particle sizes differential in the materials used in the study (fly ash and clay), makes the concept of minimum porosity and void ratio applicable to the mixtures. Fly ash is considered the inclusion, and clay is the matrix. In almost all the engineering properties investigated, a change in trend was observed at around 20% of fly ash content in the mixtures, irrespective of the fly ash type.

The fly ash tend affects the behavior of the mixtures. Below is a summary of the influence of fly ash on the mixtures.

- Specific gravity, in general, was found to decrease with increasing fly ash content. The hollow nature of the fly ash particles makes it lighter, accounting for the decrease in the specific gravity of the mixtures as the ash replaces the clay particles. This led to a decrease in the maximum dry density of all the mixtures as fly ash content increases. In general, this trend was similar to what has been

reported in literature. Liquid limit decreased with increasing fly ash content, but plasticity index increases to about 20% of fly ash content and then decreases. Fly ash had a similar effect on optimum moisture content as was on liquid limit, and a similar effect on maximum dry density as it was on plasticity index. The behavior change of both the plasticity index and maximum dry density at around 20% fly ash content is attributed to the packing density concept where minimum porosity or void ratios are attained in mixtures within 20% to 40% of proportion of inclusion. This in effect affects other engineering properties as well, as can be seen in plasticity index in this case.

- Deformation properties such as compression and swelling indices decrease with increasing fly ash content. This indicates that the addition of fly ash reduces the swelling potential of the soil mixtures and also reduces compressibility.

- As the ash content increases the mixtures becomes coarser. This leads to an increase in particle interlocking which results in an increase in internal friction angle in the mixtures. Also chemical interactions promote cementation between particles. These interactions increase with increasing fly ash content and as a result contribute to increases undrained shear strength of the mixtures.

Based on the behavior of model predictions the following conclusions were made;

- In certain cases the models either overpredict or underpredict the actual results. This could be due to other factors that the models do not take into

consideration, such as the influence of chemical composition of the materials forming the mixtures and chemical reactions between particles. There was a good relation between deformation parameters, strength parameters and consistency limits, such as between compression index and plasticity index. From these relationships and the comparison between actual and predicted results, it was observed that Voigt's (1889) model gives a better prediction than that of Omine et al. (1998) and Braem (1987).

- In general, predictions from the models were observed to deviate slightly from the actual results, even in the case of Voigt's model which was observed to predict better. The deviations suggest the need to modify the model to yield good results.

The materials considered are fly ash and clay, and due to their chemical compositions, physicochemical activities can be analyzed and compared to results from the literature. The improvement in engineering properties of fly ash modified soils is partially attributed to physicochemical interactions between the fly ash and the soil. The extent of improvement could be dependent on the chemical composition of the fly ash or the soil type, or both. A summary of observations and conclusions based on physicochemical interactions is as follows:

- Chemical properties such as cation exchange capacity of soils are influenced by the addition of fly ash. The availability of multivalent cations (particularly Ca^{++}, Si^{++}, Fe^{++}, and Al^{++}) present in fly ashes influences the cation exchanges in fly

ash-soil mixtures. The ability to exchange cations among soil and fly ash particles depending on the chemical compositions lead to pozzolanic reactions, which contributes to the improvement in strength and index properties. Cation exchange capacity was found to decrease with increasing fly ash content. The clay fraction was also found to decrease with increasing ash content. This is attributed to the introduction of silt sized particles to the mixture as the fly ash content increases at the expense of clay particles. Also, physicochemical interactions between the ash and clay particles cause flocculation of the particles making the resulting particles coarser and reducing the amount of clay fraction in the mixture.

- Calcium oxide (CaO) was found to play a major role in the behavior of fly ash-modified soils and it affects most of its engineering properties. Findings from literature and this study revealed that regardless of soil type fly ash is capable of improving engineering properties when mixed with soils. Calcium oxide was found to influence consistency limits. The higher the CaO, the lower the consistency limit for a given mixture of same fly ash proportion. Compressive strength is also found to increase with increasing fly ash content due to the chemical interaction that renders the particles to be coarser and also increasing bonding between particles. This could be a result of pozzolanic reactions promoted by the presence of CaO in a mixture of clay and fly ashes.

- From chemical composition perspective, a strong correlation was found between the sum of oxides and CaO with data from literature and this study. Also, CaO was found to affect most of the engineering properties investigated. The two chemical properties are also the main distinction between Class C and F ashes. This gave a reason to base the modification on these two chemical properties of the ashes.

Based on the findings from physicochemical point of view and predictions from the mixture theory models, it was deemed important to combine both concepts to improve upon the predictive capabilities of the model. The resulting findings are as follows:

- Voigt (1889) model was chosen to be modified since it gave better predictions than the others in almost all cases. The modified form of the model is given by $y_{mix} = \alpha\left(f_{FA}y_{FA} + (1 - f_{FA})y_C\right)$. Where y is the property of the soil to be determined, and f is the volume fraction of the constituents. The subscripts FA and C represent fly ash and clay, respectively.

- The modification term (α) was based on the ratio between the amount of CaO and sum of oxides (SiO_2+Al_2O_3+Fe_2O_3) present in the fly ash and is given as $\alpha = \left(\frac{CaO}{Sum\_of\_Oxides}\right)^x$. These compounds are considered to be the primary compounds that distinguish Class C fly ash from Class F.

- An experimental index (x) was used to adjust the ratio for specific engineering properties. Depending on the ratio and the engineering property considered, different values of x were determined. As a result, a range of values of the index was determined by regression based on the engineering properties.

- The modified form of the model was compared to the original, and in all cases the modified model performed better. In certain cases, the modification improved the predictions by about 40% where the original model performs poorly. Lower improvements averaging about 3% were observed in situations where the original model performs very well. The modified model was validated with data from literature. The performance was irrespective of the ash or soil type. It is therefore believed that the modified model will be applicable to a wide variety of fly ash-modified soils.

The laboratory results were transformed into critical state terms. The transformation into critical state can help in predicting behavior based on limited data on the soil or soil mixture. It can be used to predict yield and failure stresses in soils. Yield surface was found to depend on the amount of fly ash in the soil mixture, and both yield and failure stresses were dependent on the amount of fly ash in the mixture. A relationship between critical state parameters and fly ash content was established. This helps in computing critical state parameters and modeling behavior of the fly ash mixtures given the ash type and the percentage of the ash in the mixture.

The results obtained in this study can be useful for assessment of predictive methods to estimate engineering properties of fly ash mixtures irrespective of the source of the ash.

7.2 RECOMMENDATIONS

According to the results from this study a few recommendations listed below in future studies would help strengthen the proposed model performance in a wide variety of applications in fly ash modified soil. The recommendations are as follows:

- It is believed that the index factor in the term used in modifying the model is a function of some property of the mixture. Further investigation is therefore needed to relate and ascertain the dependence of the index on some property or properties of the mixture. This might narrow the range of values determined in this study.

- An investigation into the influence of the soil mineralogy on fly ash soil mixture behavior is necessary to understand some of the behaviors observed in this study.

- Because of the pozzolanic reactions that take place in fly ash modified soils, the effect of time on the modified model's predictability needs to be investigated to be able to apply it to mixtures irrespective of the age of sample.

- Similar experimentation with a different variety of fly ashes is needed to strengthen the proposed model, particularly in the case of the index factor in the

definition of the modification term. The variety of the fly ashes should include higher calcium oxide ashes.

- Thorough chemical analysis such as the crystallinity of the chemical compositions on both fly ash and soil types are necessary in any further studies, since the form of the compounds might influence the chemical interactions between particles.

REFERENCES

Acosta H. A., Edil, T. B., and Benson, C. H. (2003), "Soil Stabilization and Drying Using Fly Ash," *Geotechnical Engineering Report No. 03*, University of Wisconsin, Madison, WI.

Adams, B. A., and Wulfsohn, D., (1996), "Variation of Critical State Boundaries of an Agricultural Soil," *American Society of Agricultural Engineers*, St. Joseph, MI., ASAE Paper, pp. 96-1065.

American Coal Ash Association, http://www.acaa-usa.org/PDF/2004_CCP_Survey(9-9-05).pdf, 2004.

American Society for Testing and Materials (ASTM). (1998), "Standard Test Method for Particle-Size Analysis of Soils," *Designation D422–63(1998)*, Philadelphia.

American Society for Testing and Materials (ASTM). (2000), "Standard Test Methods for Laboratory Compaction Characteristics of Soil Using Standard Effort (12,400 ft-lbf/ft^3 (600 kN-m/m^3)," *Designation D698–00a*, Philadelphia.

American Society for Testing and Materials (ASTM). (2000), "Standard Test Method for Unconfined Compressive Strength of Cohesive Soil," *Designation D2166–00*, Philadelphia.

American Society for Testing and Materials (ASTM). (2000), "Standard Test Methods for Liquid Limit, Plastic Limit, and Plasticity Index of Soils," *Designation D4318–00*, Philadelphia.

American Society for Testing and Materials (ASTM). (2000), "Standard Test Methods for Specific Gravity of Soil Solids by Water Pycnometer," *Designation D854-00*, Philadelphia.

American Society for Testing and Materials (ASTM). (2002), "Standard Test Method for Consolidated Undrained Triaxial Compression Test for Cohesive Soils," *Designation D4767–02*, Philadelphia.

American Society for Testing and Materials (ASTM). (2003), "Standard Test Method for One-Dimensional Consolidation Properties of Soils," *Designation D2435–03*, Philadelphia.

Atkinson, J. (1993), *An Introduction to The Mechanics of Soils and Foundations*, McGraw-Hill, London, U.K.

Bedford, A., and Drumheller, D. S. (1983), "Theories of Immiscible and Structured Mixtures," *International Journal of Engineering Science*, Vol. 21, pp. 863-960.

Boles, W. F., (1986), "Fly Ash Facts for Highway Engineers: Technology Transfer," *Federal Highway Administration, FHWA-DP-59-8,* Washington, D. C.

Bouckovalas, G. D., Andrianopoulos, K. I., and Papadimitriou, A. G. (2003), "A Critical State Interpretation for Cyclic Liquefacion Resistance of Silty Sands," *Soil Dynamics and Earthquake Engineering*, Vol. 23, No. 3, pp. 115-125.

Braem, M., Van Doren, V. E., Lambrechts, P. and Vanherle, G. (1987), "Determination of Young's Modulus of Dental Composites: A Phenomenological Model," *Journal of Material Science*, Vol. 22, pp. 2037 – 2042.

Budhu, M. (2000), *Soil Mechanics and Foundations*, Wiley and Sons Inc., New York.

Chantler, P. M., Hu, X.. and Boyd, N. M. (1999), "An Extension of a Phenomenological Model for Dental Composites," *Dental Materials*, Vol. 15, No. 2, pp. 144 – 149.

Cokca, E. (2001), "Use of Class C Fly Ashes for the Stabilization of an Expansive Soil," *Journal of Geotechnical and Geoenvironmental Engineering*, Vol. 127, No. 7, pp. 568-573.

Dorban, F. (1985), "Theory of Multiphase Mixtures (a Thermodynamic Formulation)," *International Journal of Multiphase Flow*, Vol. 11, No. 1, pp. 1-30.

Drumheller, D. S., and Bedford, A. (1980), "A Thermodynamical Theory of Reacting Immiscible Mixtures," *Archive for Rational Mechanics and Analysis*, Vol. 73, pp. 257-284.

Eko, R. M. (2005), "Use of Triaxial Stress State Framework to Evaluate the Mechanical Behavior of an Agricultural Clay Soil," *Soil and Tillage Research*, No. 1, Vol. 81, pp. 71-85.

Ferguson, G. (1993), "Use of Self-Cementing Fly Ash as a Soil Stabilizing Agent," *Geotechnical Special Publication*, No. 36, ASCE New York, N.Y.

Fragaszy, R. J., Su, W., Siddiqui, F. and Ho, C. (1992), "Modeling Strength of Sandy Gravel," *Journal of Geotechnical Engineering*, Vol. 118, No. 6, pp. 920 – 935.

Georgiannou, V. N., Burland, J. B. and Hight, D. W. (1990), "The Undrained Behavior of Clayey Sands in Triaxial Compression and Extension," *Geotechnique*, Vol. 40, No. 3, pp. 431-449.

Goodman, M. A., and Cowin, S. C. (1971), "A Continuum Theory for Granular Materials," *Archive for Rational Mechanics and Analysis*, Vol. 44, pp. 248-266.

Goodman, M. A., and Cowin, S. C. (1971), "Two Problems in the Gravity Flow of Granular Materials," Journal of Fluid Mechanics, Vol. 45, No. 2, pp. 321-339.

Hansen, A. C. (1989), "Reexamining Some Basic Definitions of Modern Mixture Theory," *International Journal of Engineering Science*, Vol. 27, No. 12, pp. 1531-1544.

Hansen, A. C., Crane, R. L., Damson, M. H., Donovan, R. P., Horning, D. T., and Walker J. L. (1991), "Some Notes on a Volume Fraction Mixture Theory and Comparison with the

Kinetic Theory of Gases," *International Journal of Engineering Science*, Vol. 29, No. 5, pp. 561-573.

Hashin, Z. (1983), "Analysis of Composite Materials – A Survey," *Journal of Applied Mechanics*, Vol. 50, pp. 481-505.

Hashin, Z. and Shtrikman, S. (1962), "A Variational Approach to the Theory of the Elastic Behavior of Polycrystals," *Journal of the Mechanics and Physics of Solids*, Vol. 10, pp. 343-352.

Hashin, Z. and Shtrikman, S. (1963), "A Variational Approach to the Theory of the Elastic Behavior of Multiphase Materials," *Journal of the Mechanics and Physics of Solids*, Vol. 11, pp. 127-140.

Head, K. H. (1986), *Manual of Soil Laboratory Testing, Effective Stress Tests*, Vol. 3, Pentach Press, London, U.K.

Holtz, R. D., and Kovacs, W. D. (1981), *An Introduction to Geotechnical Engineering*, Prentice-Hall, Englewood Cliffs, N.J.

Hwang, K., Noguchi, T., and Tomosawa, F. (2004), "Prediction Model of Compressive Strength Development of Fly-Ash Concrete," *Cement and Concrete Research*, Vol. 34, No. 12, pp. 2269-2276.

Kaniraj, S. R. and Gayathri, V. (2004), "Permeability and Consolidation Characteristics of Compacted Fly Ash," *Journal of Energy Engineering*, Vol. 130, No. 1, pp. 18-43.

Kaniraj, S. R. and Havanagi, V. G. (2001), "Correlation Analysis of Laboratory Compaction Fly Ashes," *Practice Periodical of Hazardous, Toxic, and Radioactive Waste Management*, Vol. 5, No. 1, pp 25-32.

Kim, B., Prezzi, M., and Salgado, R. (2005), "Geotechnical Properties of Fly and Bottom Ash Mixtures for Use in Highway Embankment," *Journal of Geotechnical and Geoenvironmental Engineering*, Vol. 131, No. 7, pp. 914-924.

Kim, D., Sagong, M., and Lee, Y. (2005), "Effects of Fine Aggregate Content on the Mechanical Properties of the Compacted Decomposed Granitic Soils," *Construction and Building Materials*, Vol. 19, No. 3, pp. 189-196.

Kirby, J. M., O'Sullivan, M. F., and Wood, J. T. (1998), "Estimating Critical State Soil Mechanics Paramters from Constant Cell Volume Triaxial Tests," *European Journal of Soil Science*, Vol. 49. No. 1, pp. 85-93.

Krishnan, J. M., and Rao, C. L. (2000), "Mechanics of Air Voids Reduction of Asphalt Concrete using Mixture Theory," *International Journal of Engineering Science*, Vol. 17, pp. 419-432.

Krishnan, J. M., and Rao, C. L. (2001), "Permeability and Bleeding of Asphalt Concrete using Mixture Theory," *International Journal of Engineering Science*, Vol. 39, No. 6 pp. 611-627.

Kumar, P. B. R. and Sharma, R. S. (2004), "Effect of Fly Ash on Engineering Properties of Expansive Soils," *Journal of Geotechnical and Geoenvironmental Engineering*, Vol. 130, No. 7, pp. 764-767.

Kumar, V. G. and Wood, M. D. (1997), "Mechanical Behavior of Mixtures of Kaolin and Coarse Sand," *IUTAM Symposium on Mechanics of Granular and Porous Materials*, pp. 57 - 68.

Lav, A. H. and Lav, M. A. (2000), "Microstructural Development of Stabilized Fly Ash as Pavement Base Material," Journal of Materials in Civil Engineering, Vol. 12, No. 2, pp. 157-163.

Lingling, X., Wei, G., Tao, W., and Nanru, Y. (2005), "Study of Fired Bricks with Replacing Clay by Fly Ash in High Volume Ratio," *Construction and Building Materials*, Vol. 19, No. 3, pp. 243-247.

Lu, S. and Zhu, L. (2004), "Effect of Fly Ash on Physical Properties of Ultisols from Subtropical China," *Communication in Soil Science and Plant Analysis*, Vol. 35, No. 5 and 6, pp. 703-717.

Mesri, G. and Olsen, E. E. (1971), "Mechanism Controlling the Permeability of Clays," *Clays and Clay Minerals*, Vol. 19, pp. 151-158.

Misra A. (2000), "Utilization of Western Coal Fly Ash in Construction of Highways in the Midwest," *Mid-American Transportation Center*, MATC Project No. MATC UMC 96-2.

Misra, A., Biswas, D., and Upadhyaya, S. (2005), "Physico-mechanical Behavior of Self-Cementing Class C Fly Ash-Clay Mixtures," *Fuel*, Vol. 84, No. 11, pp. 1410-1422.

Mitchell, J. K. (1993), *Fundamentals of Soil Behavior*, 2nd Edition, Wiley and Sons, New York.

Morland, L. W. (1978), "A Theory of Slow Fluid Flow through a Porous Thermoelastic Matrix," *Geophysical Journal of Royal Astronomical Society*, Vol. 55, pp. 393-410.

Morland, L. W., Foulser, R., Garg, S. K. (2004), "Mixture Theory for a Fluid-Saturated Isotropic Matrix," *International Journal of Geomechanics*, Vol. 4, No. 3, pp. 207-215.

Muller. (1968), "A Thermodynamic Theory of Mixtures of Fluids," *Archive for Rational Mechanics and Analysis*, Vol. 28, pp. 1-39.

Naik, T. R., Singh, S. S., and Ramme, B. W. (2002), "Effect of Source of Fly Ash on Abrasion Resistance of Concrete," *Journal of Materials in Civil Engineering*, Vol. 14, No. 5, pp. 417-427.

Nalbantoglu, Z. (2004), "Effectiveness of Class C Fly Ash as an Expansive Soil Stabilizer," *Construction and Building Materials*, Vol. 18, No. 6, pp. 377-381.

Narasimha, R. S. and Mathew, P. (1995), "Effects of Exchangeable Cations on Hydraulic Conductivity of a Marine Clay," *Clays and Clay Minerals*, Vol. 43, pp. 433-437.

O'Sullivan, M. F., Campbell, D. J., and Hettiarachi, D. R. P. (1996), "Critical State Parameters Derived from Constant Cell Volume Triaxial Tests," *European Journal of Soil Science*, Vol. 47, pp. 249-256.

Omine, K., Ochiai, H. and Yoshida, N. (1998), "Estimation of In-situ Strength of Cement-Treated Soils Based on a Two-Phase Mixture Model," *Soils and Foundation*, Vol. 38, No. 4, pp. 17 – 29.

Passman, S. L., (1977), "Mixtures of Granular Materials," *International Journal of Engineering Science*, Vol. 15, pp. 117-129.

Porbaha, A., Pradhan, T. B. S. and Yamane, N. (2000), "Time Effect on Shear Strength and Permeability of Fly Ash," *Journal of Energy Engineering*, Vol. 126, No. 1, pp. 15-31.

Prabakar, J. Dendorkar, N. and Morchale, R. K. (2004), "Influence of Fly Ash on Strength Behavior of Typical Soils," *Construction and Building Materials*, Vol. 18, No. 4, pp 263-267.

Reuss, A., and Angew, Z. (1929), "Berechnung der Fliessgrenze von Mishkristallen auf Grund der Plastiztatsbeding fur Einkristalle," *Mathematical Mechanics*, Vol. 9, pp. 49-58.

Sahu, B. K. and Piyo, P. M. (2000), "Improvement in Strength Characteristics of White Kalahari Sands by Fly Ash," *Botswana Journal of Technology*.

Santamarina, J. C., Klein, K. A., and Fam, A. M. (2001), *Soils and Waves-Particulate Materials Behavior, Characterization and Process Monitoring*, Wiley and Sons Inc., New York.

Santamarina, J. C., Klein, K. A., Wang, Y. H. and Prencke, E. (2002), "Specific Surface: Determination and Relevance," *Canadian Geotechnical Journal*, Vol. 39, No. 1, pp. 233-241.

Saskaguchi, R. L., Wiltbank, B. D. and Murchison, C. F. (2004), "Prediction of Composite Elastic Modulus and Polymerization Shrinkage by Computational Micromechanics," *Dental Materials*, Vol. 20, No. 4, pp. 397 – 401.

Sieg, C. and Bergman, B. (2005), "Analysis of Fly Ash for Ohio University," *Headwaters Resources Testing Materials Testing and Research Facility*, Report No. 57TS-05.

Sridharan, A., Rao, S. M. and Murphy, N. S. (1986), "Liquid Limit of Montimorillonit Soils," *Geotechnical Testing Journal*, Vol. 9, No. 3, pp. 156-159.

Stovall, T., De Larrard, F. and Buil, M. (1996), "Linear Packing Density Model of Grain Mixtures," *Powder Technology*, Vol. 48, pp. 1-12.

Tien, Y. M., Wu, P. L., Chuang, W. S. and Wu, L. H. (2004), "Micromechanics Model for Compaction Characteristics of Bentonite-Sand Mixtures," *Applied Clay Science*, Vol. 26, No. 1-4, pp. 489-498.

Tiwari, B. and Marui, H. (2005), "A New Method for the Correlation of Residual Shear Strength of the Soil with Mineralogical Composition," *Journal of Geotechnical and Geoenvironmental Engineering*, Vol. 131, No. 9, pp. 1139-1150.

Tsimas, S. and Moutsatsou-Tsima, A. (2005), "High-Calcium Fly Ash as the Fourth Constituent in Concrete: Problems, Solutions, and Perspectives," *Cement and Concrete Composites*, Vol. 27, No. 2, pp. 231-237.

Twiss, R. J. (1975), "Theory of Mixtures for Micromorphic Materials-II, Elastic Constitutive Equations," *International Journal of Engineering Science*, Vol. 10, pp. 437-465.

Twiss, R. J., and Eringen, A. C. (1974), "Theory of Mixtures for Micromorphic Materials-I, Balance Laws," *International Journal of Engineering Science*, Vol. 9, pp. 1019-1044.

Usmen, M. A. and Bowers, J. J. (1990), "Stabilization Characteristics of Class F Fly Ash," *Transportation Research Record 1288*, Transportation Research Board, National Academy of Science, Washington D.C., pp. 59-69.

Vallejo, E. L. (2001), "Interpretation of the Limits in Shear Strength in Binary Granular Mixtures," *Canadian Geotechnical Journal*, Vol. 38, No. 5, pp. 1097-1104.

Vallejo, E. L. and Mawby, R. (2000), "Porosity Influence on the Shear Strength of Granular Material-Clay Mixtures," *Engineering Geology*, Vol. 58, No. 2, pp. 125-136.

Voigt, W. (1889), "Uber die Bezichungen zwischen den beiden Elastizitaskonstanen Isotroper Korper," *Wield Ann* Vol. 38, pp. 573-587.

Wang, L., Wang, X., Louay, M., and Wang, Y. (2004), "Application of Mixture Theory in the Evaluation of Mechanical Properties of Asphalt Concrete," *Journal of Materials in Civil Engineering*, Vol. 16, No. 2, pp. 167 – 174.

Wang, Q., Pufahl, D. E., and Fredlund, D. G. (2002), "A Study of Critical State on an Unsaturated Silty Soil," *Canadian Geotechnical Journal*, Vol. 39, No. 1, pp. 213-218.

Wartman, J. and Riemer, M. F. (2002), "The Use of Fly Ash to Alter the Geotechnical Properties of Artificial "model" Clay," *Proc. to Physical Modeling in Geotechnics, ICPMG 2002, St. John's, Canada.*

Watt, J. P. and O'Connell, R. J. (1980), "An Experimental investigation of Hashin-Shtrikman Bounds on Two-phase Aggregate Elastic Properties," *Physics of the Earth and Planetary Interiors*, No. 21, pp. 359-370.

Wong, P. K., and Mitchell, R. J. (1975), "Yielding and Plastic Flow of Sensitive Cemented Clays," Geotechnique, Vol. 25, No. 4, pp. 763 – 782.

Wood, D. M. (1990), *Soil Behavior and Critical State Soil Mechanics,* Cambridge University Press.

Wood, D. M., and Graham, J. (1990), "Anisotropic Elasticity and Yielding of Natuarl Plastic Clay," *International Journal of Plasticity*, Vol. 6, pp. 377-388.

Wroth, C. P., and Wood, D. M. (1978), "The Correlation of Index Propeties with Some Basic Engineering Properties of Soils," *Canadian Geotechnical Journal*, Vol. 15, pp.137-145.

Zachary, G. T. (2002), "Engineering Properties of Fly Ash Subgrade Mixtures," *Midwest Transportation Consortium*, Ames, Iowa.

APPENDIX A: CHEMICAL COMPOSITION OF FLY ASHES, ACTUAL AND MODELS PREDICTION DATA FROM LITERATURE

Chemical Compostion of Fly Ashes from Research and Literature

Reference		Compounds					
		SiO_2 (%)	Al_2O_3 (%)	Fe_2O_3 (%)	$SiO_2+Al_2O_3+Fe_2O_3$ (%)	CaO (%)	LOI (%)
Research	FA 1	41.57	20.66	29.97	92.2	3.04	1.45
	FA 2	40.62	19.87	27.06	87.55	4.04	1.86
	FA 3	58.76	29.14	3.81	91.71	0.89	2.7
	Class C	40.21	21.74	9.08	71.03	16.99	2.89
Literature	Prabakar (2000)	58	32	4.7	94.7	1.5	1.7
	Sahu and Piyo (2000)	41.2	33.6	5.08	79.88	6.45	-
	Kumar and Sharma (2004)	63.17	19.36	4.32	86.85	0.67	0.23
	Anil Misra	48.5	19.6	6.2	74.3	15.2	0.5
	Saylak et. al.	33.63	19.03	6.73	59.39	27.1	0.25

HEADWATERS RESOURCES

Adding Value to Energy ™

Analysis of Fly Ash for Ohio University

Headwaters Resources Materials Testing and Research Facility
Report No. 57TS-05
April 20, 2005

for

Headwaters Resources
Attention: Dr. Sebastian Bryson

Prepared by:

Christy Sieg
Chemist II

Approved By:

Bobby Bergman
MTRF Manager

Materials Testing & Research Facility
2650 Highway 113 S.W.
Taylorsville, Georgia 30178
P: 770.684.0102
F: 770.684.5114
www.headwaters.com

Scope:

Samples of fly ash from Ohio University (MTRF Sample No.636TS-639TS) were received at the MTRF on 4/18/05 for chemical composition including carbon and loss on ignition.

The chemical analysis was performed on a dry, ignited basis using a Bruker S4 X-ray fluorescence spectrometer according to ASTM D4326. Carbon content was measured with a Leco SC444DR Carbon/Sulfur Analyzer. The LOI was performed according to ASTM C-311. The chemical analysis is reported in the following table.

Test Results:

The chemical properties of the fly ash are as follows:

Sample Label	Fly Ash #1	Fly Ash #2	Fly Ash #3	Fly Ash #4
MTRF ID	636TS	637TS	638TS	639TS
Silicon Dioxide, SiO_2	41.57 %	40.62 %	58.76 %	40.21 %
Aluminum Oxide, Al_2O_3	20.66 %	19.87 %	29.14 %	21.74 %
Iron Oxide, Fe_2O_3	29.97 %	27.06 %	3.81 %	9.08 %
Sum of SiO_2 , Al_2O_3 , Fe_2O_3	92.20 %	87.55 %	91.71 %	71.03 %
Sulfur Trioxide, SO_3	0.78 %	2.33 %	0.13 %	2.15 %
Calcium Oxide, CaO	3.04 %	4.04 %	0.89 %	16.99 %
Sodium Oxide, Na_2O	0.41 %	0.38 %	0.24 %	1.22 %
Magnesium Oxide, MgO	0.64 %	2.86 %	0.85 %	4.52 %
Potassium Oxide, K_2O	1.67 %	1.66 %	2.82 %	1.41 %
Phosphorus Pentoxide, P_2O_5	0.24 %	0.21 %	0.10 %	1.30 %
Titanium Dioxide, TiO_2	1.03 %	0.97 %	1.70 %	1.33 %
Carbon	1.19 %	0.63 %	2.13 %	2.19 %
Loss on Ignition	1.45 %	1.86 %	2.70 %	2.89 %

Actual and Voigt's Model Prediction Data for Moisture-Density Paramters from Literature

Reference	Description		Actual		Voigt Prediction		Modified Voigt Prediction	
		% Fly Ash	OMC (%)	MDD (kN/m^3)	OMC (%)	MDD (kN/m^3)	OMC (%)	MDD (kN/m^3)
Prabakar et al. (2000)	SOIL A (CL)	0	14.57	16.78	14.57	16.78	14.57	16.78
		9	15.8	15.50	17.24	16.10	15.69	15.75
		20	17.98	15.40	20.50	15.26	18.66	14.94
		28.5	20.4	14.13	23.03	14.62	20.95	14.31
		35.5	22.3	13.64	25.10	14.09	22.84	13.79
		41.2	25.2	13.34	26.79	13.66	24.38	13.37
		46	27.2	13.15	28.22	13.30	25.68	13.01
		100	44.24	9.22	44.24	9.22	44.24	9.22
Prabakar et al. (2000)	SOIL B (OL)	0	24.81	15.40	24.81	15.40	24.81	15.40
		9	24.8	14.91	26.56	14.85	23.64	14.78
		20	25.2	13.83	28.70	14.17	25.54	14.11
		28.5	25.76	13.64	30.35	13.64	27.01	13.58
		35.5	28.3	13.15	31.71	13.21	28.22	13.15
		41.2	29.8	12.75	32.82	12.86	29.21	12.80
		46	30.2	12.65	33.75	12.56	30.04	12.51
		100	44.24	9.22	44.24	9.22	44.24	9.22
Prabakar et al. (2000)	Soil C (MH)	0	30.09	14.13	30.09	14.13	30.09	14.13
		9	29.5	13.54	31.36	13.68	28.54	13.69
		20	29.5	13.24	32.92	13.15	29.96	13.15
		28.5	30.05	12.85	34.12	12.73	31.05	12.73
		35.5	31.9	12.16	35.11	12.39	31.95	12.39
		41.2	33.3	12.26	35.92	12.11	32.69	12.11
		46	34.26	11.87	36.60	11.87	33.31	11.87
		100	44.24	9.22	44.24	9.22	44.24	9.22
Sahu and Piyo (2000)	Kalahari Sand	0	5.00	17.66	5.00	17.66	5.00	17.66
		20	5.00	16.38	8.00	16.75	6.56	16.07
		28	8.00	15.50	9.20	16.38	7.54	15.72
		32	9.50	15.46	9.80	16.20	8.04	15.54
		100	20.00	13.10	20.00	13.10	20.00	13.10
Kumar and Sharma (2004)	CH Soil	0	40.00	13.75	40.00	13.75	40.00	13.75
		5	38.00	13.91	38.76	13.90	35.27	14.33
		10	35.00	14.06	37.52	14.06	34.14	14.48
		15	33.00	14.20	36.28	14.21	33.01	14.64
		20	31.00	14.30	35.04	14.36	31.89	14.79
		100	15.20	16.77	15.20	16.77	15.20	16.77
Anil Misra (2000)	SOIL A (CL)	0	19.00	16.19	19.00	16.19	19.00	16.19
		10	17.00	16.51	18.62	16.16	17.88	16.45
		20	18.50	16.37	18.24	16.13	17.51	16.42
		100	15.2	15.89	15.20	15.89	15.20	15.89
Anil Misra (2000)	SOIL B (CH)	0	20.70	16.48	20.70	16.48	20.70	16.48
		10	19.40	16.40	20.15	16.42	19.75	16.36
		20	19.50	16.26	19.60	16.36	19.21	16.30
		100	15.2	15.89	15.20	15.89	15.20	15.89

Actual and Omine's Model Prediction Data for Moisture-Density Paramters from Literature

Reference	Description		Actual		Omine Prediction		Modified Omine Prediction	
		% Fly Ash	OMC (%)	MDD (kN/m^3)	OMC (%)	MDD (kN/m^3)	OMC (%)	MDD (kN/m^3)
Prabakar et al. (2000)	SOIL A (CL)	0	14.57	16.78	14.57	16.78	14.57	16.78
		9	15.8	15.50	16.16	15.89	15.80	15.50
		20	17.98	15.40	18.29	14.87	17.98	15.40
		28.5	20.4	14.13	20.09	14.13	20.40	14.13
		35.5	22.3	13.64	21.69	13.56	22.30	13.64
		41.2	25.2	13.34	23.08	13.10	25.20	13.34
		46	27.2	13.15	24.31	12.74	27.20	13.15
		100	44.24	9.22	44.24	9.22	44.24	9.22
Prabakar et al. (2000)	SOIL B (OL)	0	24.81	15.40	24.81	15.40	24.81	15.40
		9	24.8	14.91	26.15	14.70	24.80	14.91
		20	25.2	13.83	27.87	13.89	25.20	13.83
		28.5	25.76	13.64	29.28	13.30	25.76	13.64
		35.5	28.3	13.15	30.48	12.83	28.30	13.15
		41.2	29.8	12.75	31.50	12.46	29.80	12.75
		46	30.2	12.65	32.38	12.16	30.20	12.65
		100	44.24	9.22	44.24	9.22	44.24	9.22
Prabakar et al. (2000)	Soil C (MH)	0	30.09	14.13	30.09	14.13	30.09	14.13
		9	29.5	13.54	31.16	13.59	29.50	13.54
		20	29.5	13.24	32.51	12.97	29.50	13.24
		28.5	30.05	12.85	33.59	12.51	30.05	12.85
		35.5	31.9	12.16	34.51	12.14	31.90	12.16
		41.2	33.3	12.26	35.27	11.85	33.30	12.26
		46	34.26	11.87	35.93	11.61	34.26	11.87
		100	44.24	9.22	44.24	9.22	44.24	9.22
Sahu and Piyo (2000)	Kalahari Sand	0	5.00	17.66	5.00	17.66	5.00	17.66
		20	5.00	16.38	6.67	16.63	5.00	16.38
		28	8.00	15.50	7.44	16.24	8.00	15.50
		32	9.50	15.46	7.86	16.05	9.50	15.46
		100	20.00	13.10	20.00	13.10	20.00	13.10
Kumar and Sharma (2004)	CH Soil	0	40.00	13.75	40.00	13.75	40.00	13.75
		5	38.00	13.91	38.81	13.73	38.00	13.91
		10	35.00	14.06	37.65	13.71	35.00	14.06
		15	33.00	14.20	36.54	13.69	33.00	14.20
		20	31.00	14.30	35.46	13.67	31.00	14.30
		100	15.20	16.77	22.00	13.34	22.00	13.34
Anil Misra (2000)	SOIL A (CL)	0	19.00	16.19	19.00	16.19	19.00	16.19
		10	17.00	16.51	18.58	16.16	17.00	16.51
		20	18.50	16.37	18.17	16.13	18.50	16.37
		100	15.2	15.89	15.20	15.89	15.20	15.89
Anil Misra (2000)	SOIL B (CH)	0	20.70	16.48	20.70	16.48	20.70	16.48
		10	19.40	16.40	20.07	16.42	19.40	16.40
		20	19.50	16.26	19.46	16.36	19.50	16.26
		100	15.2	15.89	15.20	15.89	15.20	15.89

Actual and Braem's Model Prediction Data for Moisture-Density Paramters from Literature

Reference	Description		Actual		Braem Prediction		Modified Braem Prediction	
		% Fly Ash	OMC (%)	MDD (kN/m^3)	OMC (%)	MDD (kN/m^3)	OMC (%)	MDD (kN/m^3)
Prabakar et al. (2000)	SOIL A (CL)	0	14.57	16.78	14.57	16.78	14.57	16.78
		9	15.8	15.50	16.10	15.90	15.80	15.50
		20	17.98	15.40	18.19	14.88	17.98	15.40
		28.5	20.4	14.13	20.00	14.14	20.40	14.13
		35.5	22.3	13.64	21.61	13.56	22.30	13.64
		41.2	25.2	13.34	23.02	13.11	25.20	13.34
		46	27.2	13.15	24.29	12.74	27.20	13.15
		100	44.24	9.22	44.24	9.22	44.24	9.22
Prabakar et al. (2000)	SOIL B (OL)	0	24.81	15.40	24.81	15.40	24.81	15.40
		9	24.8	14.91	26.14	14.71	24.80	14.91
		20	25.2	13.83	27.85	13.90	25.20	13.83
		28.5	25.76	13.64	29.26	13.31	25.76	13.64
		35.5	28.3	13.15	30.46	12.84	28.30	13.15
		41.2	29.8	12.75	31.49	12.47	29.80	12.75
		46	30.2	12.65	32.37	12.16	30.20	12.65
		100	44.24	9.22	44.24	9.22	44.24	9.22
Prabakar et al. (2000)	Soil C (MH)	0	30.09	14.13	30.09	14.13	30.09	14.13
		9	29.5	13.54	31.15	13.59	29.50	13.54
		20	29.5	13.24	32.50	12.97	29.50	13.24
		28.5	30.05	12.85	33.58	12.51	30.05	12.85
		35.5	31.9	12.16	34.50	12.14	31.90	12.16
		41.2	33.3	12.26	35.27	11.85	33.30	12.26
		46	34.26	11.87	35.93	11.61	34.26	11.87
		100	44.24	9.22	44.24	9.22	44.24	9.22
Sahu and Piyo (2000)	Kalahari Sand	0	5.00	17.66	5.00	17.66	5.00	17.66
		20	5.00	16.38	6.60	16.63	5.00	16.38
		28	8.00	15.50	7.37	16.24	8.00	15.50
		32	9.50	15.46	7.79	16.05	9.50	15.46
		100	20.00	13.10	20.00	13.10	20.00	13.10
Kumar and Sharma (2004)	CH Soil	0	40.00	13.75	40.00	13.75	40.00	13.75
		5	38.00	13.91	38.82	13.73	38.00	13.91
		10	35.00	14.06	37.68	13.71	35.00	14.06
		15	33.00	14.20	36.57	13.69	33.00	14.20
		20	31.00	14.30	35.49	13.67	31.00	14.30
		100	15.20	16.77	22.00	13.34	22.00	13.34
Anil Misra (2000)	SOIL A (CL)	0	19.00	16.19	19.00	16.19	19.00	16.19
		10	17.00	16.51	18.58	16.16	17.00	16.51
		20	18.50	16.37	18.17	16.13	18.50	16.37
		100	15.2	15.89	15.20	15.89	15.20	15.89
Anil Misra (2000)	SOIL B (CH)	0	20.70	16.48	20.70	16.48	20.70	16.48
		10	19.40	16.40	20.07	16.42	19.40	16.40
		20	19.50	16.26	19.46	16.36	19.50	16.26
		100	15.2	15.89	15.20	15.89	15.20	15.89

Actual and Voigt's Model Prediction Data for Strength Paramters from Literature

Reference	Description		Actual		Voigt Prediction		Modified Voigt Prediction	
		% Fly Ash	Cohesion (kg/cm^2)	Friction Angle	Cohesion (kg/cm^2)	Friction Angle	Cohesion (kg/cm^2)	Friction Angle
Prabakar et al. (2000)	SOIL A (CL)	0	0.25	30.25	0.250	30.25	0.250	30.25
		9	0.25	31.60	0.241	30.17	0.358	32.73
		20	0.27	33.02	0.230	30.07	0.341	32.62
		28.5	0.31	35.60	0.222	29.99	0.329	32.54
		35.5	0.34	34.20	0.215	29.93	0.318	32.47
		41.2	0.37	32.10	0.209	29.88	0.310	32.41
		46	0.40	28.63	0.204	29.84	0.303	32.37
		100	0.15	29.35	0.150	29.35	0.150	29.35
Prabakar et al. (2000)	SOIL B (OL)	0	0.19	17.17	0.185	17.17	0.185	17.17
		9	0.28	24.22	0.182	18.26	0.342	24.51
		20	0.30	25.20	0.178	19.60	0.334	26.31
		28.5	0.30	28.30	0.175	20.64	0.329	27.70
		35.5	0.33	29.63	0.173	21.49	0.324	28.85
		41.2	0.37	29.88	0.171	22.19	0.320	29.78
		46	0.38	30.63	0.169	22.77	0.317	30.56
		100	0.15	29.35	0.150	29.35	0.150	29.35
Prabakar et al. (2000)	Soil C (MH)	0	0.53	25.53	0.530	25.53	0.530	25.53
		9	0.52	20.43	0.496	25.88	0.561	23.76
		20	0.48	21.97	0.454	26.30	0.514	24.14
		28.5	0.50	23.25	0.422	26.62	0.477	24.44
		35.5	0.48	26.28	0.395	26.89	0.447	24.69
		41.2	0.44	27.37	0.373	27.11	0.423	24.89
		46	0.40	27.93	0.355	27.29	0.402	25.06
		100	0.15	29.35	0.150	29.35	0.150	29.35

Actual and Omine's Model Prediction Data for Strength Paramters from Literature

Reference	Description		Actual		Omine Prediction		Modified Omine Prediction	
		% Fly Ash	Cohesion (kg/cm^2)	Friction Angle	Cohesion (kg/cm^2)	Friction Angle	Cohesion (kg/cm^2)	Friction Angle
Prabakar et al. (2000)	SOIL A (CL)	0	0.25	30.25	0.250	30.25	0.250	30.25
		9	0.25	31.60	0.239	30.17	0.250	31.60
		20	0.27	33.02	0.226	30.07	0.270	33.02
		28.5	0.31	35.60	0.216	29.99	0.310	35.60
		35.5	0.34	34.20	0.208	29.93	0.340	34.20
		41.2	0.37	32.10	0.203	29.88	0.370	32.10
		46	0.40	28.63	0.198	29.83	0.400	28.63
		100	0.15	29.35	0.150	29.35	0.150	29.35
Prabakar et al. (2000)	SOIL B (OL)	0	0.19	17.17	0.185	17.17	0.185	17.17
		9	0.28	24.22	0.182	18.02	0.280	24.22
		20	0.30	25.20	0.177	19.12	0.300	25.20
		28.5	0.30	28.30	0.174	20.01	0.300	28.30
		35.5	0.33	29.63	0.172	20.78	0.330	29.63
		41.2	0.37	29.88	0.170	21.42	0.370	29.88
		46	0.38	30.63	0.168	21.97	0.380	30.63
		100	0.15	29.35	0.150	29.35	0.150	29.35
Prabakar et al. (2000)	Soil C (MH)	0	0.53	25.53	0.530	25.53	0.530	25.53
		9	0.52	20.43	0.470	25.86	0.520	20.43
		20	0.48	21.97	0.409	26.26	0.480	21.97
		28.5	0.50	23.25	0.367	26.57	0.500	23.25
		35.5	0.48	26.28	0.337	26.83	0.480	26.28
		41.2	0.44	27.37	0.314	27.04	0.440	27.37
		46	0.40	27.93	0.296	27.22	0.400	27.93
		100	0.15	29.35	0.150	29.35	0.150	29.35

Actual and Braem's Model Prediction Data for Strength Paramters from Literature

Reference	Description		Actual		Braem Prediction		Modified Braem Prediction	
		% Fly Ash	Cohesion (kg/cm^2)	Friction Angle	Cohesion (kg/cm^2)	Friction Angle	Cohesion (kg/cm^2)	Friction Angle
Prabakar et al. (2000)	SOIL A (CL)	0	0.25	30.25	0.250	30.25	0.250	30.25
		9	0.25	31.60	0.239	30.17	0.363	32.73
		20	0.27	33.02	0.226	30.07	0.344	32.62
		28.5	0.31	35.60	0.216	29.99	0.329	32.54
		35.5	0.34	34.20	0.209	29.93	0.317	32.47
		41.2	0.37	32.10	0.203	29.88	0.308	32.41
		46	0.40	28.63	0.198	29.83	0.301	32.37
		100	0.15	29.35	0.150	29.35	0.150	29.35
Prabakar et al. (2000)	SOIL B (OL)	0	0.19	17.17	0.185	17.17	0.185	23.73
		9	0.28	24.22	0.182	18.02	0.342	24.91
		20	0.30	25.20	0.177	19.11	0.335	26.42
		28.5	0.30	28.30	0.174	20.00	0.329	27.65
		35.5	0.33	29.63	0.172	20.77	0.324	28.71
		41.2	0.37	29.88	0.170	21.41	0.320	29.60
		46	0.38	30.63	0.168	21.97	0.317	30.37
		100	0.15	29.35	0.150	29.35	0.150	29.35
Prabakar et al. (2000)	Soil C (MH)	0	0.53	25.53	0.530	25.53	0.530	23.49
		9	0.52	20.43	0.473	25.86	0.612	23.79
		20	0.48	21.97	0.412	26.25	0.532	24.15
		28.5	0.50	23.25	0.370	26.57	0.478	24.44
		35.5	0.48	26.28	0.339	26.83	0.438	24.68
		41.2	0.44	27.37	0.315	27.04	0.407	24.88
		46	0.40	27.93	0.297	27.22	0.383	25.04
		100	0.15	29.35	0.150	29.35	0.150	29.35

Actual and Models Prediction Data for Strength Paramters from Literature

Reference	Description	% Fly Ash	Actual CBR	Voigt Prediction CBR	Modified Voigt Prediction CBR	Omine Prediction CBR	Modified Omine Prediction CBR	Braem Prediction CBR	Modified Braem Prediction CBR
Prabakar et al. (2000)	SOIL A (CL)	0	4.7	4.70	4.70	4.70	4.70	4.70	4.70
		9	7	5.39	7.02	5.14	7.00	5.13	7.70
		20	8.84	6.24	8.35	5.73	8.84	5.71	8.56
		28.5	9.24	6.89	9.38	6.22	9.24	6.20	9.30
		35.5	9.93	7.43	10.22	6.65	9.93	6.63	9.95
		41.2	10.67	7.87	10.91	7.02	10.67	7.01	10.52
		46	11.6	8.24	11.49	7.35	11.60	7.34	11.02
		100	12.4	12.40	12.40	12.40	12.40	12.40	12.40
Prabakar et al. (2000)	SOIL B (OL)	0	2.03	2.03	2.03	2.03	2.03	2.03	2.03
		9	5.47	2.96	7.14	2.43	5.47	2.39	5.37
		20	6.12	4.10	7.71	2.98	6.12	2.92	6.32
		28.5	7.26	4.99	8.15	3.47	7.26	3.40	7.72
		35.5	9.05	5.71	8.52	3.92	9.05	3.86	9.00
		41.2	10.84	6.30	8.82	4.32	10.84	4.28	10.22
		46	11.41	6.80	9.07	4.69	11.41	4.67	11.33
		100	12.4	12.40	12.40	12.40	12.40	12.40	12.40
Prabakar et al. (2000)	Soil C (MH)	0	3.53	3.53	3.53	3.53	3.53	3.53	3.53
		9	4.4	4.33	5.77	3.97	4.40	3.95	4.79
		20	5.3	5.30	6.05	4.57	5.30	4.54	5.50
		28.5	5.83	6.06	6.27	5.09	5.83	5.05	6.11
		35.5	6.7	6.68	6.46	5.54	6.70	5.51	6.68
		41.2	7.73	7.18	6.61	5.94	7.73	5.92	7.17
		46	8.24	7.61	6.73	6.30	8.24	6.29	7.62
		100	12.4	12.40	12.40	12.40	12.40	12.40	12.40

APPENDIX B: ACTUAL AND MODELS PREDICITON DATA FROM STUDY

Actual Data and Models Predictions of Optimum Moisture Content

Description	% Fly Ash	Optimum Moisture Content (%)						
	(%)	Actual	Voigt Prediction	Modified Voigt Prediction	Omine Prediction	Modified Omine Prediction	Braem Prediction	Modified Braem Prediction
CLAY	0	20.25	20.25	20.25	20.25	20.25	20.25	20.25
	10	16.80	19.73	17.56	19.65	16.80	19.65	16.80
	20	17.20	19.20	17.09	19.07	17.20	19.07	17.20
	40	16.80	18.15	16.15	17.96	16.80	17.95	16.80
Class C	100	15.00	15.00	15.00	15.00	15.00	15.00	15.00
	10	18.00	19.43	17.68	19.21	18.00	19.21	18.00
	20	16.40	18.60	16.93	18.23	16.40	18.22	16.40
	40	15.40	16.95	15.42	16.42	15.40	16.41	15.40
Fly Ash 1	100	12.00	12.00	12.00	12.00	12.00	12.00	12.00
	10	16.60	19.75	17.57	19.68	16.60	19.68	16.60
	20	17.60	19.24	17.12	19.12	17.60	19.11	17.60
	40	16.80	18.23	16.22	18.05	16.80	18.06	16.80
Fly Ash 2	100	15.20	15.20	15.20	15.20	15.20	15.20	15.20
	10	15.97	20.43	15.93	20.42	15.97	20.41	15.97
	20	16.46	20.60	16.07	20.59	16.46	20.58	16.46
	40	15.60	20.95	16.34	20.93	15.60	20.93	15.60
Fly Ash 3	100	22.00	22.00	22.00	22.00	22.00	22.00	22.00

Actual Data and Models Predictions of Maximum Dry Density

Description	% Fly Ash (%)	Maximum Dry Density (kN/m^3)						
		Actual	Voigt Prediction	Modified Voigt Prediction	Omine Prediction	Modified Omine Prediction	Braem Prediction	Modified Braem Prediction
CLAY	0	16.07	16.07	16.07	16.07	16.07	16.07	16.07
	10	17.20	16.16	17.29	16.16	17.29	16.16	17.29
	20	17.60	16.25	17.38	16.24	17.38	16.23	17.38
	40	17.44	16.43	17.57	16.42	17.57	16.41	17.57
Class C	100	16.96	16.96	16.96	16.96	16.96	16.96	16.96
	10	16.92	16.21	17.06	16.20	17.06	16.20	17.06
	20	17.12	16.34	17.20	16.33	17.20	16.32	17.20
	40	17.70	16.61	17.48	16.60	17.48	16.60	17.48
Fly Ash 1	100	17.42	17.42	17.42	17.42	17.42	17.42	17.42
	10	17.20	16.14	17.33	16.14	17.33	16.13	17.33
	20	17.65	16.21	17.41	16.21	17.41	16.21	17.41
	40	17.44	16.35	17.56	16.35	17.55	16.34	17.55
Fly Ash 2	100	16.77	16.77	16.77	16.77	16.77	16.77	16.77
	10	16.76	15.80	17.09	15.77	17.11	15.77	17.11
	20	16.88	15.52	16.80	15.48	16.80	15.47	16.80
	40	16.44	14.98	16.21	14.92	16.18	14.92	16.18
Fly Ash 3	100	13.34	13.34	13.34	13.34	13.34	13.34	13.34

Actual Data and Models Predictions of Undrained Shear Strength

Description	% Fly Ash	Undrained Shear Strength (kPa)						
	(%)	Actual	Voigt Prediction	Modified Voigt Prediction	Omine Prediction	Modified Omine Prediction	Braem Prediction	Modified Braem Prediction
CLAY	0	23.688	23.688	23.688	23.69	23.69	23.688	23.688
	10	36.337	30.334	40.152	27.27	56.73	27.075	57.132
	20	55.935	36.979	48.948	31.24	87.32	30.947	87.945
	40	63.366	50.269	66.540	40.61	98.92	40.429	99.629
FA 1	100	90.140	90.140	90.140	90.14	90.14	90.140	90.140
	10	40.217	32.576	41.822	28.00	64.86	27.684	65.561
	20	49.679	41.463	53.232	32.83	80.12	32.352	80.984
	40	84.047	59.237	76.052	44.50	135.54	44.185	137.011
FA 2	100	112.560	112.560	112.560	112.56	112.56	112.560	112.560
	10	35.769	30.152	36.224	27.21	50.40	27.020	50.736
	20	42.941	36.615	43.989	31.10	60.51	30.821	60.909
	40	61.682	49.542	59.519	40.28	86.91	40.101	87.491
FA 3	100	88.322	88.322	88.322	88.32	88.32	88.322	88.322
	10	47.572	35.611	61.376	28.85	111.45	28.352	113.420
	20	109.619	47.534	81.925	34.70	256.80	33.935	261.349
	40	109.104	71.379	123.022	49.14	255.60	48.613	260.121
Class C	100	142.916	142.916	142.916	142.92	142.92	142.916	142.916

Actual Data and Models Predictions of Effective Friciton Angle

Description	% Fly Ash	Effective Friction Angle (degrees)						
	(%)	Actual	Voigt Prediction	Modified Voigt Prediction	Omine Prediction	Modified Omine Prediction	Braem Prediction	Modified Braem Prediction
CLAY	0	17.84	17.84	17.84	17.84	17.84	17.84	17.84
	10	17.90	19.17	18.87	18.87	19.09	18.86	19.09
	20	19.16	20.49	20.18	19.95	20.18	19.94	20.18
	40	25.10	23.14	22.78	22.28	22.54	22.27	22.54
Class C	100	31.07	31.07	31.07	31.07	31.07	31.07	31.07
	10	19.05	18.94	19.23	18.73	19.39	18.72	19.39
	20	19.21	20.04	20.34	19.65	20.35	19.65	20.35
	40	24.04	22.24	22.57	21.62	22.39	21.61	22.39
Fly Ash 1	100	28.82	28.82	28.82	28.82	28.82	28.82	28.82
	10	18.24	19.17	19.87	18.87	20.10	18.87	20.10
	20	22.18	20.49	21.24	19.95	21.25	19.94	21.25
	40	24.90	23.14	23.99	22.29	23.74	22.28	23.74
Fly Ash 2	100	31.09	31.09	31.09	31.09	31.09	31.09	31.09
	10	20.28	19.54	21.48	19.09	21.84	19.09	21.84
	20	23.67	21.24	23.35	20.42	23.35	20.43	23.35
	40	28.23	24.63	27.08	23.33	26.68	23.34	26.68
Fly Ash 3	100	34.82	34.82	34.82	34.82	34.82	34.82	34.82

Actual Data and Models Predictions of Compression Index

Description	% Fly Ash	Compression Index (C_c)						
	(%)	Actual	Voigt Prediction	Modified Voigt Prediction	Omine Prediction	Modified Omine Prediction	Braem Prediction	Modified Braem Prediction
CLAY	0	0.169	0.169	0.169	0.17	0.17	0.169	0.169
	10	0.165	0.154	0.176	0.13	0.21	0.135	0.209
	20	0.132	0.139	0.158	0.10	0.17	0.108	0.167
	40	0.152	0.109	0.124	0.07	0.11	0.069	0.107
Class C	100	0.018	0.018	0.018	0.02	0.02	0.018	0.018
	10	0.158	0.156	0.164	0.14	0.18	0.145	0.178
	20	0.147	0.143	0.150	0.12	0.15	0.125	0.153
	40	0.129	0.116	0.122	0.09	0.11	0.092	0.113
Fly Ash 1	100	0.037	0.037	0.037	0.04	0.04	0.037	0.037
	10	0.166	0.155	0.171	0.14	0.19	0.139	0.194
	20	0.152	0.140	0.155	0.11	0.16	0.114	0.159
	40	0.128	0.111	0.123	0.08	0.11	0.077	0.108
Fly Ash 2	100	0.024	0.024	0.024	0.02	0.02	0.024	0.024
	10	0.157	0.154	0.171	0.13	0.21	0.133	0.207
	20	0.151	0.138	0.154	0.10	0.16	0.104	0.163
	40	0.132	0.107	0.120	0.06	0.10	0.064	0.100
Fly Ash 3	100	0.015	0.015	0.015	0.02	0.02	0.015	0.015

Actual Data and Models Predictions of Swelling Index

Description	% Fly Ash	Swelling Index (C_s)						
	(%)	Actual	Voigt Prediction	Modified Voigt Prediction	Omine Prediction	Modified Omine Prediction	Braem Prediction	Modified Braem Prediction
CLAY	0	0.027	0.027	0.027	0.03	0.03	0.027	0.027
	10	0.026	0.025	0.025	0.02	0.03	0.024	0.026
	20	0.015	0.023	0.023	0.02	0.02	0.021	0.023
	40	0.024	0.019	0.019	0.02	0.02	0.016	0.018
Class C	100	0.007	0.007	0.007	0.01	0.01	0.007	0.007
	10	0.024	0.025	0.023	0.02	0.02	0.024	0.024
	20	0.022	0.024	0.021	0.02	0.02	0.022	0.021
	40	0.016	0.020	0.018	0.02	0.02	0.018	0.017
Fly Ash 1	100	0.010	0.010	0.010	0.01	0.01	0.010	0.010
	10	0.029	0.025	0.025	0.02	0.03	0.024	0.026
	20	0.022	0.023	0.023	0.02	0.02	0.021	0.023
	40	0.016	0.019	0.019	0.02	0.02	0.016	0.017
Fly Ash 2	100	0.007	0.007	0.007	0.01	0.01	0.007	0.007
	10	0.020	0.025	0.017	0.02	0.02	0.023	0.018
	20	0.016	0.023	0.015	0.02	0.02	0.019	0.015
	40	0.009	0.018	0.012	0.01	0.01	0.014	0.011
Fly Ash 3	100	0.005	0.005	0.005	0.01	0.01	0.005	0.005

APPENDIX C: CRITICAL STATE DATA FROM STUDY

Data for Critical State Lines in in *e - lnp' space*

Sample Description	p' (kPa)	11.97	23.94	47.88	95.76	191.52	383.04
	lnp'	**2.48**	**3.18**	**3.87**	**4.56**	**5.25**	**5.95**
	% Fly Ash	**Void Ratio (e)**					
CLAY	0%	2.22	2.17	2.12	2.07	2.02	1.97
	10%	2.18	2.13	2.07	2.02	1.97	1.92
	20%	2.02	1.97	1.93	1.88	1.83	1.78
	40%	1.97	1.93	1.89	1.85	1.82	1.78
FA 1	100%	1.34	1.33	1.32	1.32	1.31	1.31
	10%	2.16	2.11	2.06	2.01	1.96	1.91
	20%	2.05	2.01	1.96	1.92	1.87	1.83
	40%	1.87	1.83	1.80	1.76	1.72	1.69
FA 2	100%	1.60	1.59	1.58	1.57	1.56	1.55
	10%	2.24	2.19	2.14	2.09	2.03	1.98
	20%	2.00	1.95	1.91	1.86	1.81	1.77
	40%	1.92	1.88	1.84	1.81	1.77	1.73
FA 3	100%	1.69	1.68	1.67	1.67	1.66	1.65
	10%	2.18	2.13	2.08	2.03	1.98	1.93
	20%	2.27	2.22	2.17	2.13	2.08	2.03
	40%	1.98	1.94	1.91	1.87	1.84	1.80
Class C	100%	1.42	1.41	1.41	1.40	1.40	1.40

Data for Critical State Lines in in *p' - q space*

Sample Description	p' (kPa)	**11.97**	**23.94**	**47.88**	**95.76**	**191.52**	**383.04**
	% Fly Ash	**q**					
CLAY	0%	8.17	16.34	32.68	65.36	130.73	261.45
	10%	7.37	14.73	29.47	58.93	117.86	235.72
	20%	7.91	15.83	31.66	63.31	126.62	253.25
	40%	9.02	18.04	36.09	72.17	144.35	288.70
FA 1	100%	14.92	29.85	59.69	119.39	238.77	477.54
	10%	8.87	17.74	35.49	70.97	141.95	283.89
	20%	9.43	18.86	37.72	75.43	150.87	301.73
	40%	10.56	21.11	42.22	84.44	168.88	337.77
FA 2	100%	13.75	27.50	55.00	110.01	220.01	440.03
	10%	9.19	18.38	36.75	73.51	147.02	294.04
	20%	9.88	19.76	39.52	79.03	158.06	316.12
	40%	11.27	22.55	45.10	90.20	180.39	360.79
FA 3	100%	14.93	29.87	59.74	119.48	238.95	477.91
	10%	11.71	23.43	46.86	93.71	187.42	374.85
	20%	12.83	25.65	51.31	102.62	205.23	410.46
	40%	15.07	30.15	60.30	120.60	241.19	482.38
Class C	100%	16.88	33.77	67.53	135.06	270.13	540.26

Critical State Parameters

Sample Description	% Fly Ash	M	λ	κ	Γ
CLAY	0%	0.683	0.073	0.012	2.406
	10%	0.615	0.076	0.011	2.369
	20%	0.661	0.069	0.010	2.191
	40%	0.754	0.054	0.008	2.100
FA 1	100%	1.247	0.008	0.003	1.355
	10%	0.741	0.071	0.010	2.335
	20%	0.788	0.065	0.009	2.216
	40%	0.882	0.053	0.008	2.002
FA 2	100%	1.149	0.016	0.004	1.644
	10%	0.768	0.074	0.011	2.423
	20%	0.825	0.067	0.010	2.166
	40%	0.942	0.053	0.008	2.050
FA 3	100%	1.248	0.010	0.003	1.715
	10%	0.979	0.074	0.007	2.369
	20%	1.072	0.067	0.007	2.432
	40%	1.259	0.052	0.005	2.109
Class C	100%	1.410	0.007	0.002	1.434

APPENDIX D: FIGURES ON PHYSICOCHEMICAL ANALYSES FROM STUDY

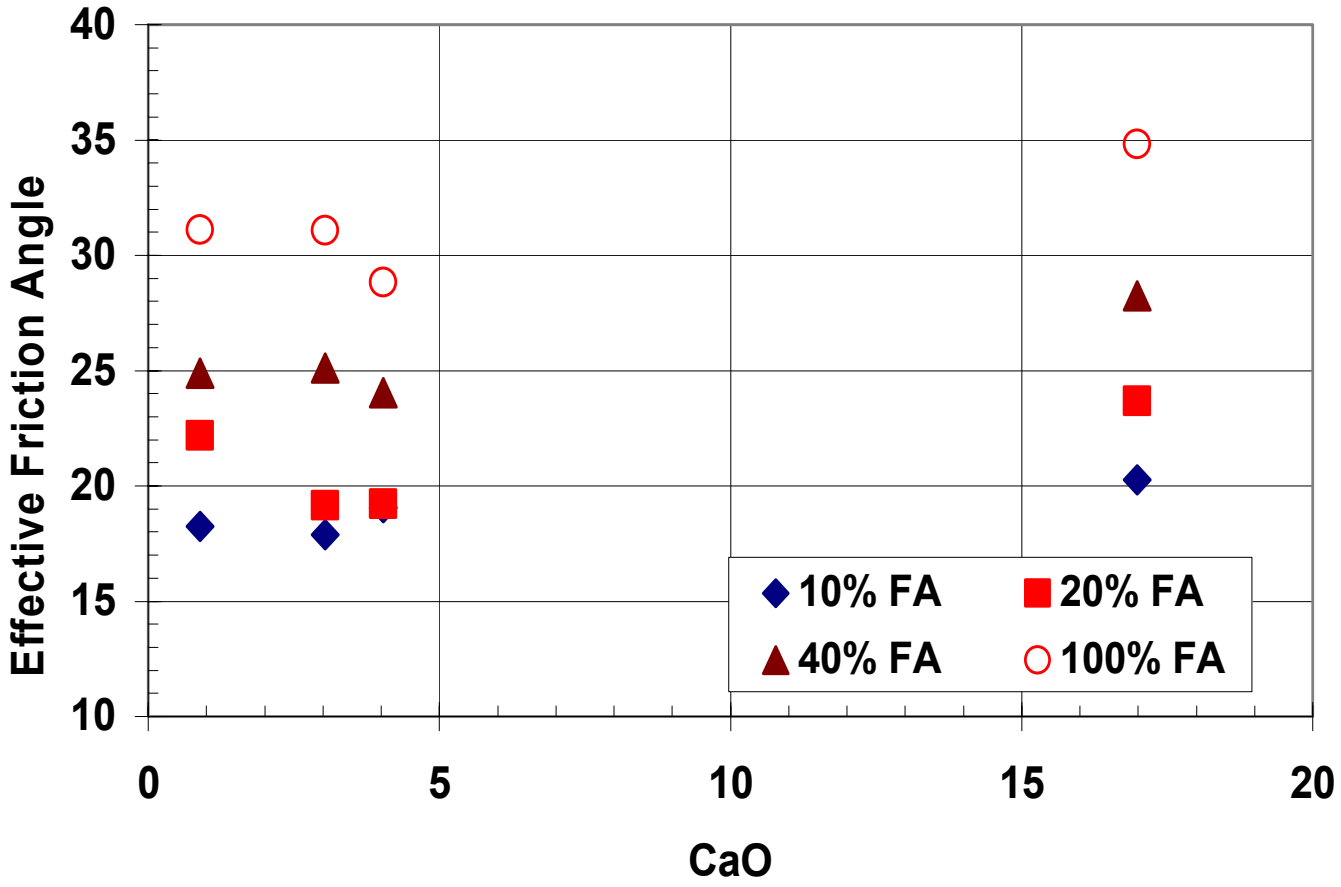

Effect of Calcium Oxide (CaO) on Effective Friction Angle

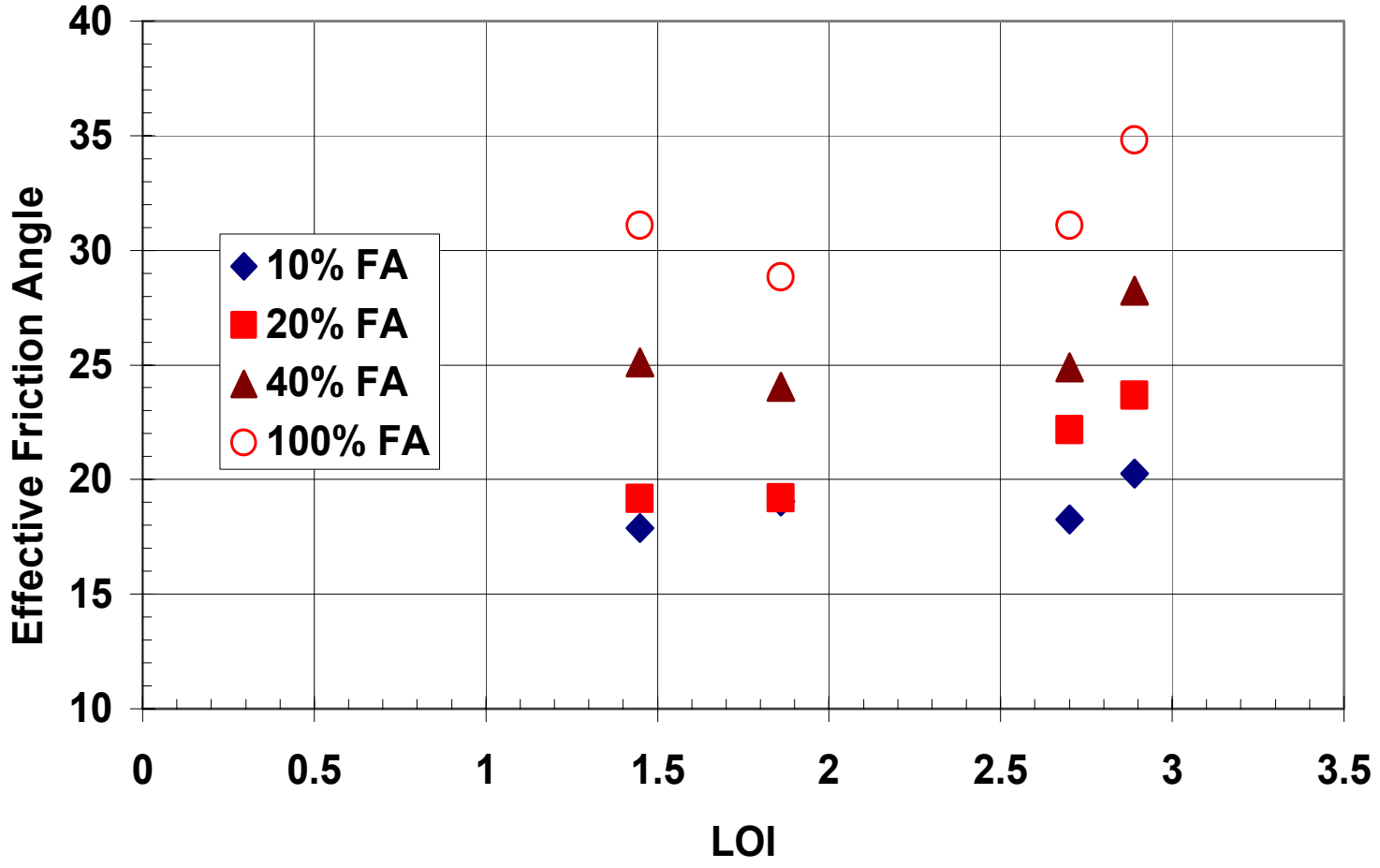

Effect of Calcium Oxide (CaO) on Effective Friction Angle

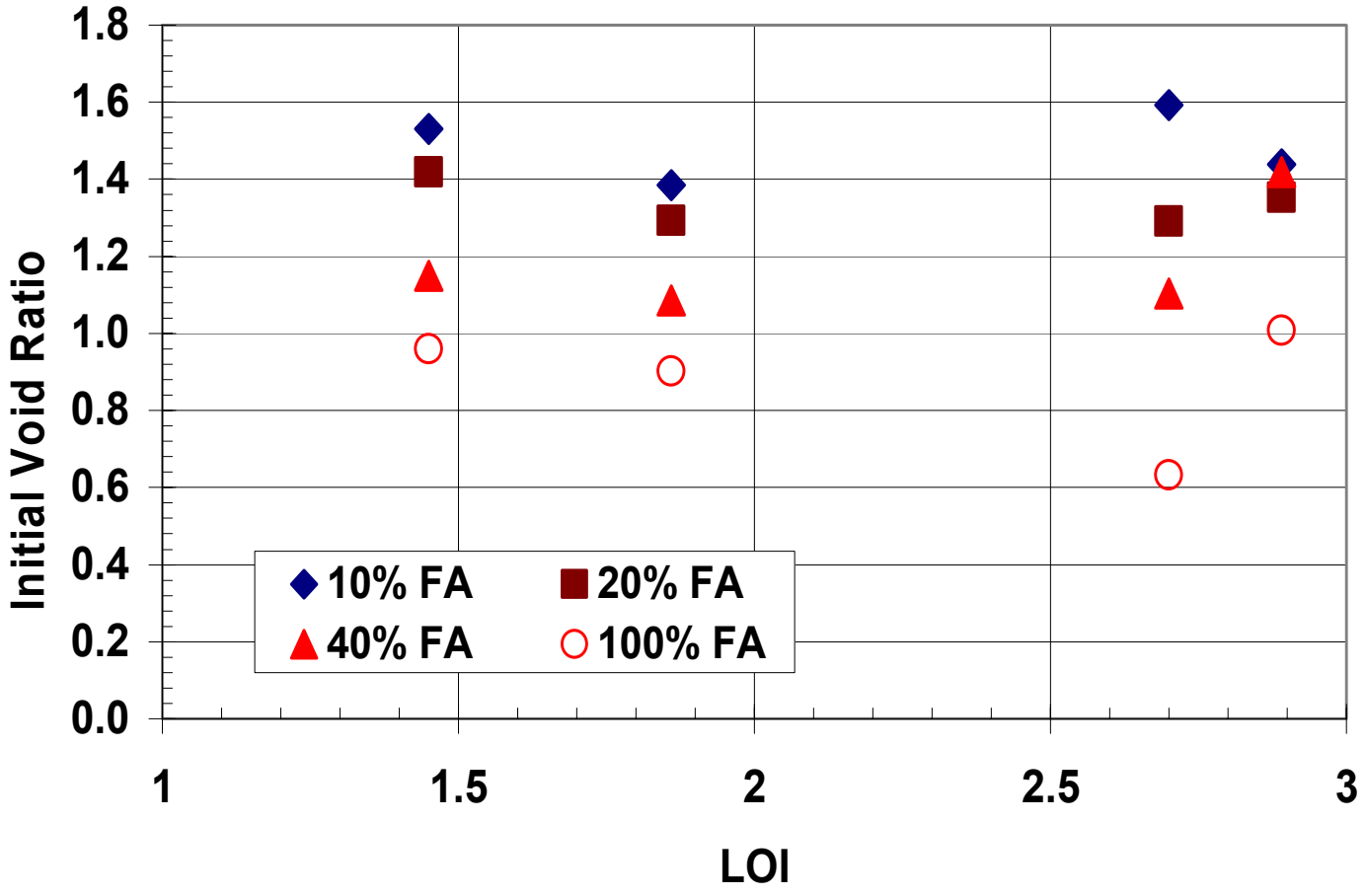

Effect of Loss of Ignition (LOI) on Initial Void Ratio

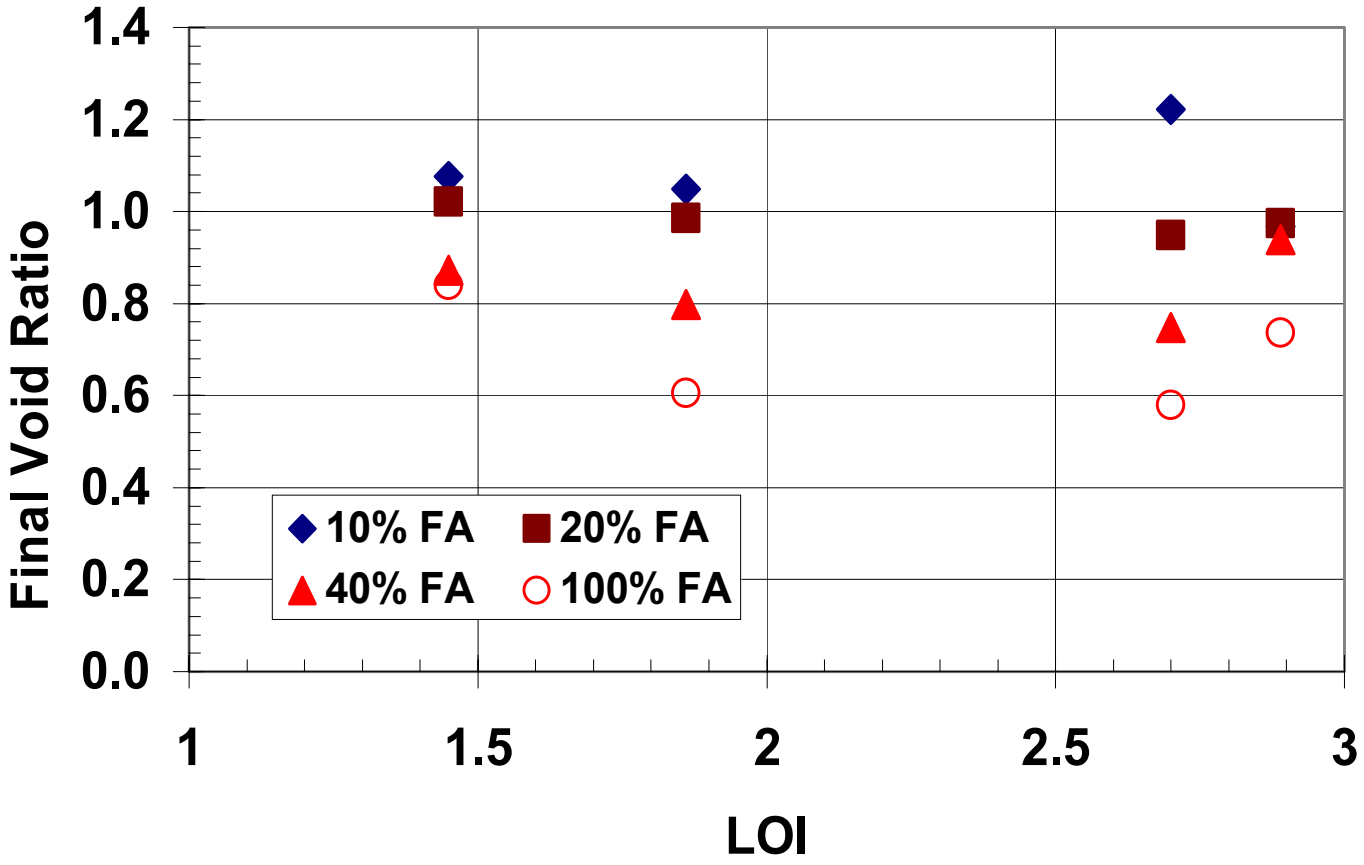

Effect of Loss of Ignition (LOI) on Final Void Ratio

APPENDIX E: FIGURES FROM TRIAXIAL ANALYSES FROM STUDY

Confining Pressure (σ_3) (kPa)	96.53	193.16	386.22
Back Pressure (kPa)	89.63	89.63	89.63
Sample Height (cm)	14.00	14.00	14.00
Sample Diameter (cm)	7.00	7.00	7.00
Area of Sample (cm^2)	38.48	38.48	38.48
Volume Before Consolidation, V_0 (cm^3)	538.78	538.78	538.78
Volume Change After Consolidation, ΔV_c (cm^3)	45.40	51.30	77.80
Volume After Consolidation, V_c (cm^3)	493.38	487.48	460.98
Area After Consolidation, A_c (cm^2)	35.24	34.82	32.93

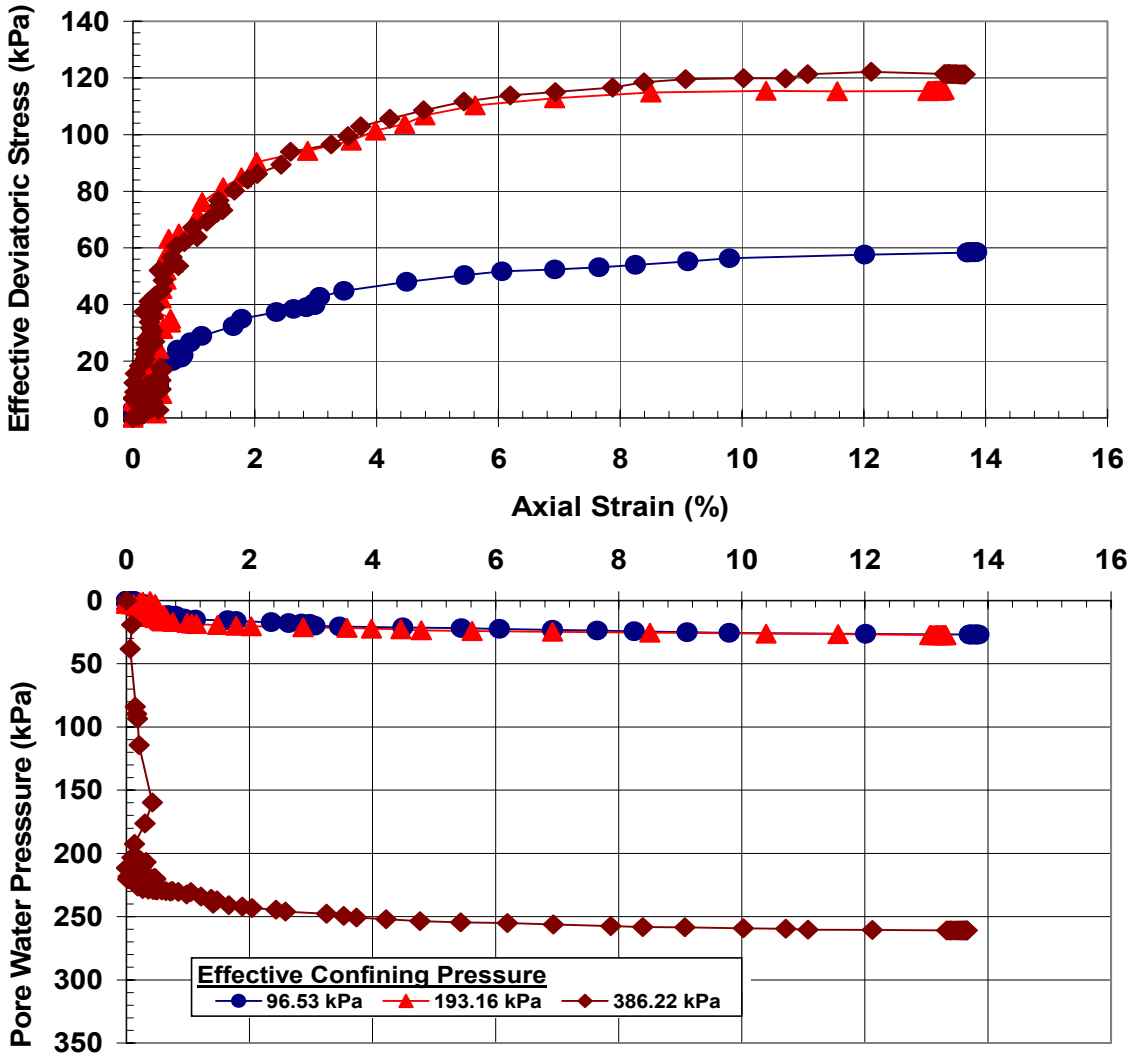

Stress-Strain and Pore Water-Strain Relationships from Triaxial Tests for **CLAY**

Confining Pressure (σ_3) (kPa)	96.53	193.16	386.22
Back Pressure (kPa)	89.63	89.63	89.63
Sample Height (cm)	14.00	14.00	14.00
Sample Diameter (cm)	7.00	7.00	7.00
Area of Sample (cm^2)	38.48	38.48	38.48
Volume Before Consolidation, V_0 (cm^3)	538.78	538.78	538.78
Volume Change After Consolidation, ΔV_c (cm^3)	45.40	51.30	77.80
Volume After Consolidation, V_c (cm^3)	493.38	487.48	460.98
Area After Consolidation, A_c (cm^2)	35.24	34.82	32.93

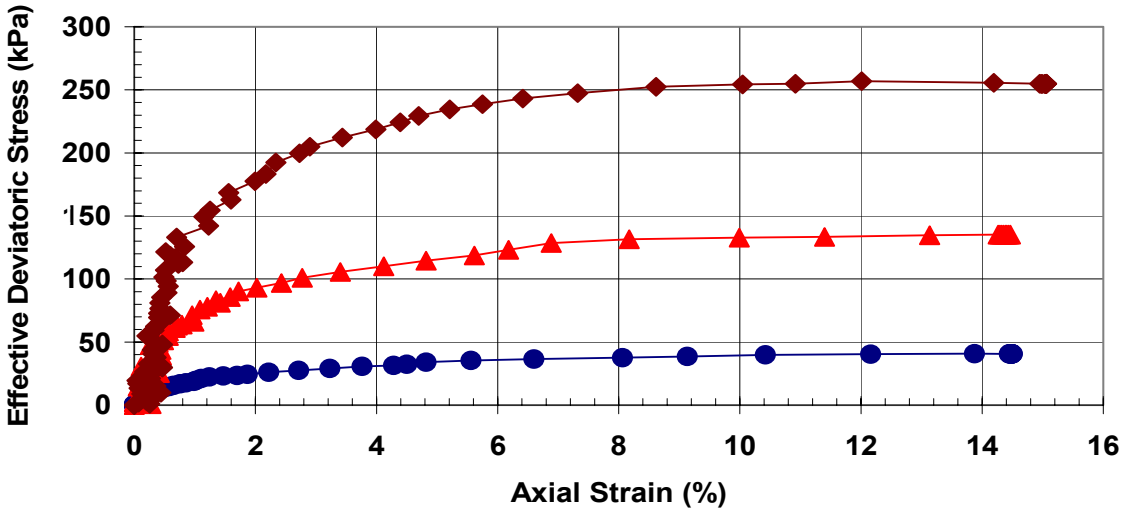

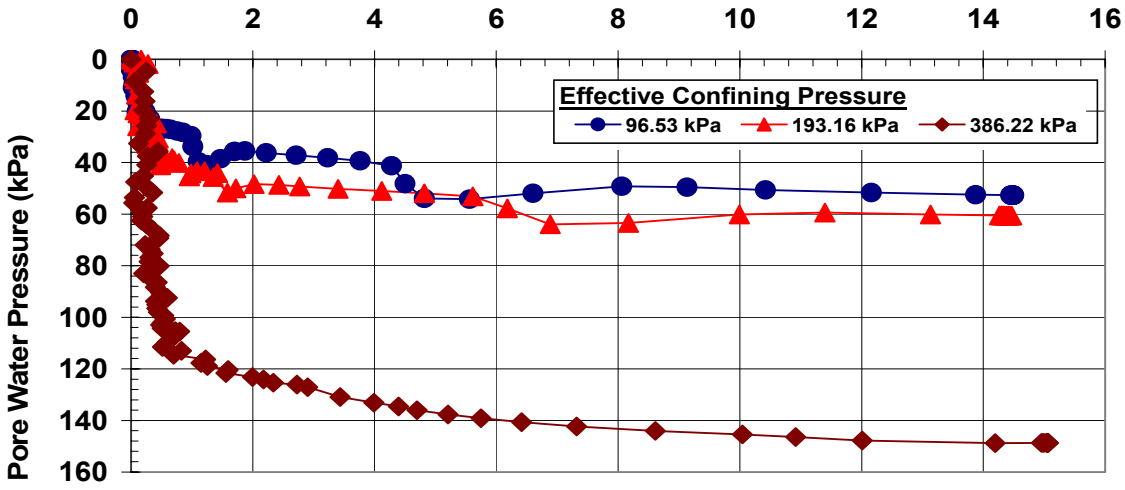

Stress-Strain and Pore Water-Strain Relationships from Triaxial Tests for **10% Class C** Fly Ash

Confining Pressure (σ_3) (kPa)	96.53	193.16	386.22
Back Pressure (kPa)	89.63	89.63	89.63
Sample Height (cm)	14.00	14.00	14.00
Sample Diameter (cm)	7.00	7.00	7.00
Area of Sample (cm^2)	38.48	38.48	38.48
Volume Before Consolidation, V_0 (cm^3)	538.78	538.78	538.78
Volume Change After Consolidation, ΔV_c (cm^3)	45.40	51.30	77.80
Volume After Consolidation, V_c (cm^3)	493.38	487.48	460.98
Area After Consolidation, A_c (cm^2)	35.24	34.82	32.93

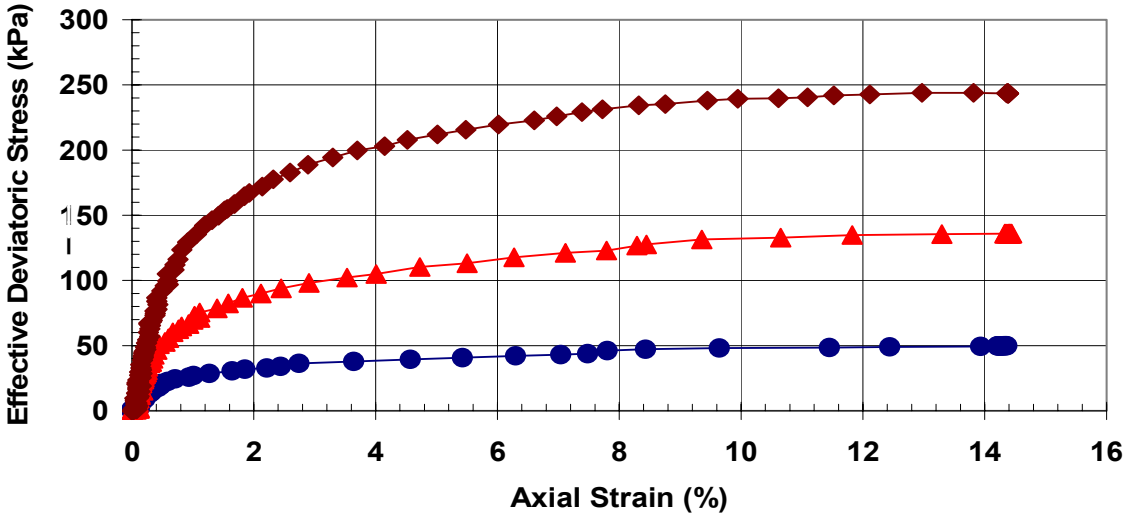

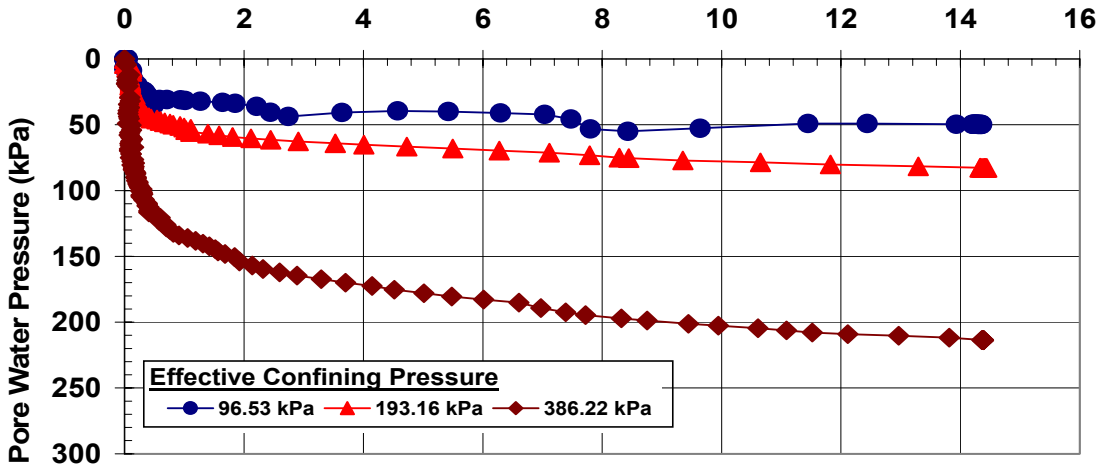

Stress-Strain and Pore Water-Strain Relationships from Triaxial Tests for **20% Class C** Fly Ash

Confining Pressure (σ_3) (kPa)	96.53	193.16	386.22
Back Pressure (kPa)	89.63	89.63	89.63
Sample Height (cm)	14.00	14.00	14.00
Sample Diameter (cm)	7.00	7.00	7.00
Area of Sample (cm^2)	38.48	38.48	38.48
Volume Before Consolidation, V_0 (cm^3)	538.78	538.78	538.78
Volume Change After Consolidation, ΔV_c (cm^3)	45.40	51.30	77.80
Volume After Consolidation, V_c (cm^3)	493.38	487.48	460.98
Area After Consolidation, A_c (cm^2)	35.24	34.82	32.93

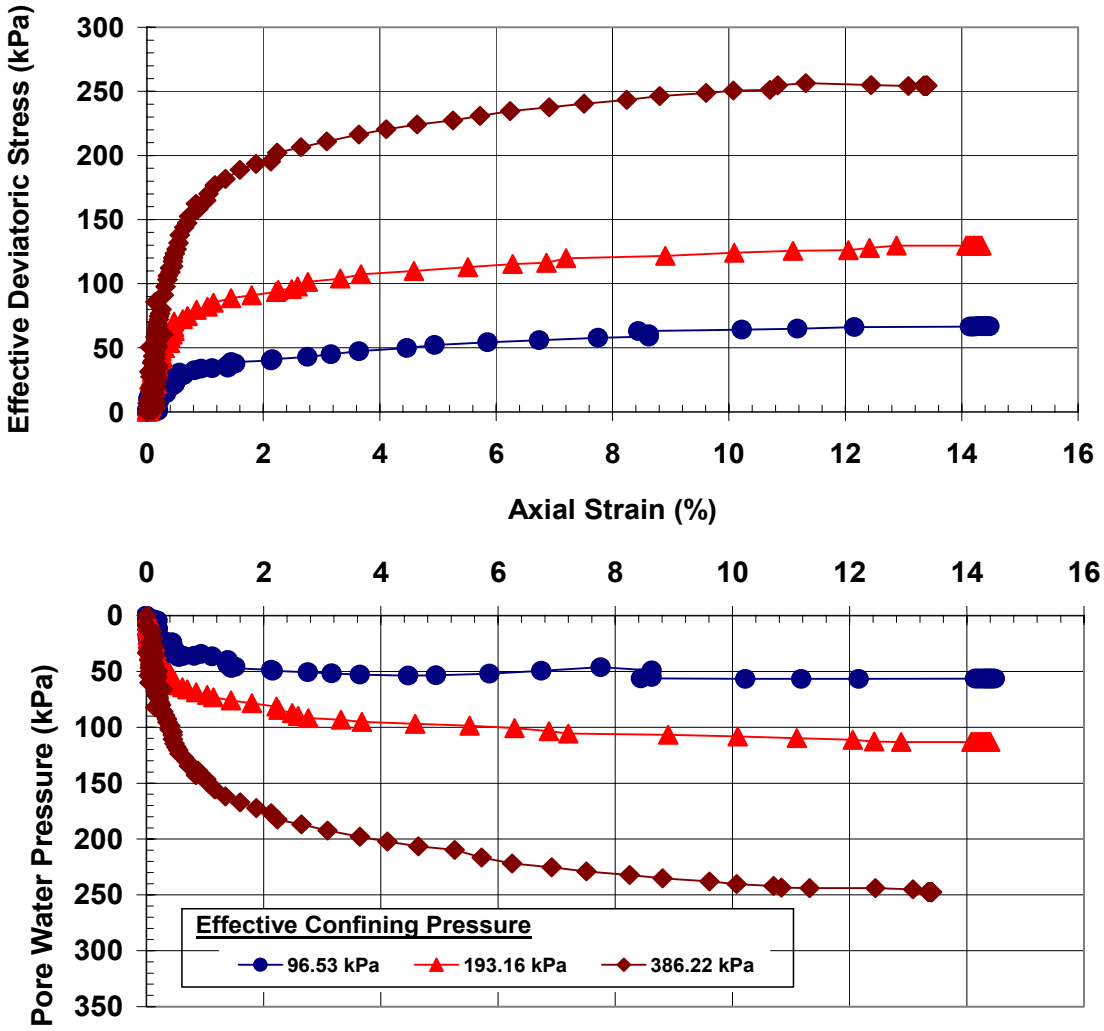

Stress-Strain and Pore Water-Strain Relationships from Triaxial Tests for **40% Class C** Fly Ash

Confining Pressure (σ_3) (kPa)	27.57	48.27	68.96
Back Pressure (kPa)	0.00	0.00	0.00
Sample Height (cm)	14.00	14.00	14.00
Sample Diameter (cm)	7.00	7.00	7.00
Area of Sample (cm^2)	38.48	38.48	38.48
Volume Before Consolidation, V_0 (cm^3)	538.78	538.78	538.78
Volume Change After Consolidation, ΔV_c (cm^3)	0.60	13.50	5.10
Volume After Consolidation, V_c (cm^3)	538.18	525.28	533.68
Area After Consolidation, A_c (cm^2)	38.44	37.52	38.12

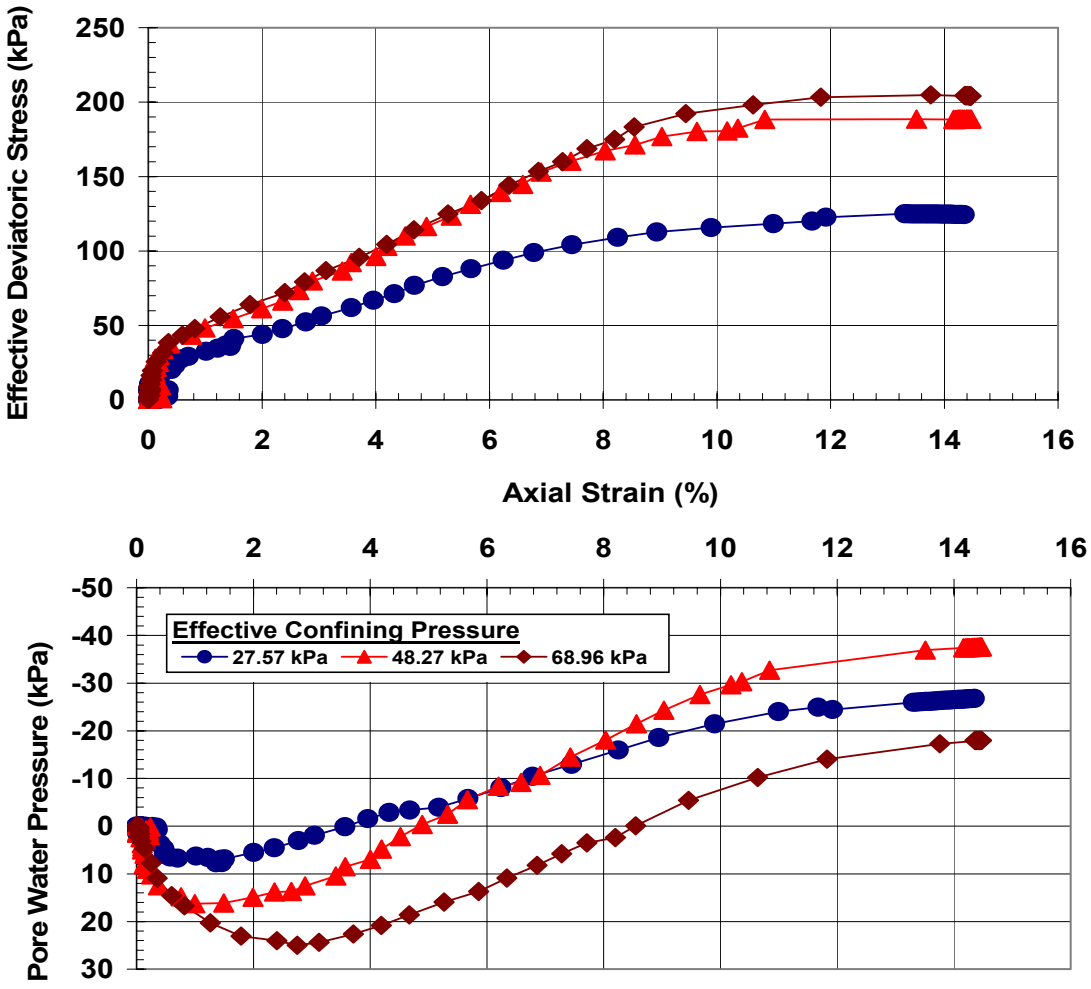

Stress-Strain and Pore Water-Strain Relationships from Triaxial Tests for **100% Class C** Fly Ash

Confining Pressure (σ_3) (kPa)	96.53	193.16	386.22
Back Pressure (kPa)	89.63	89.63	89.63
Sample Height (cm)	14.00	14.00	14.00
Sample Diameter (cm)	7.00	7.00	7.00
Area of Sample (cm^2)	38.48	38.48	38.48
Volume Before Consolidation, V_0 (cm^3)	538.78	538.78	538.78
Volume Change After Consolidation, ΔV_c (cm^3)	45.40	51.30	77.80
Volume After Consolidation, V_c (cm^3)	493.38	487.48	460.98
Area After Consolidation, A_c (cm^2)	35.24	34.82	32.93

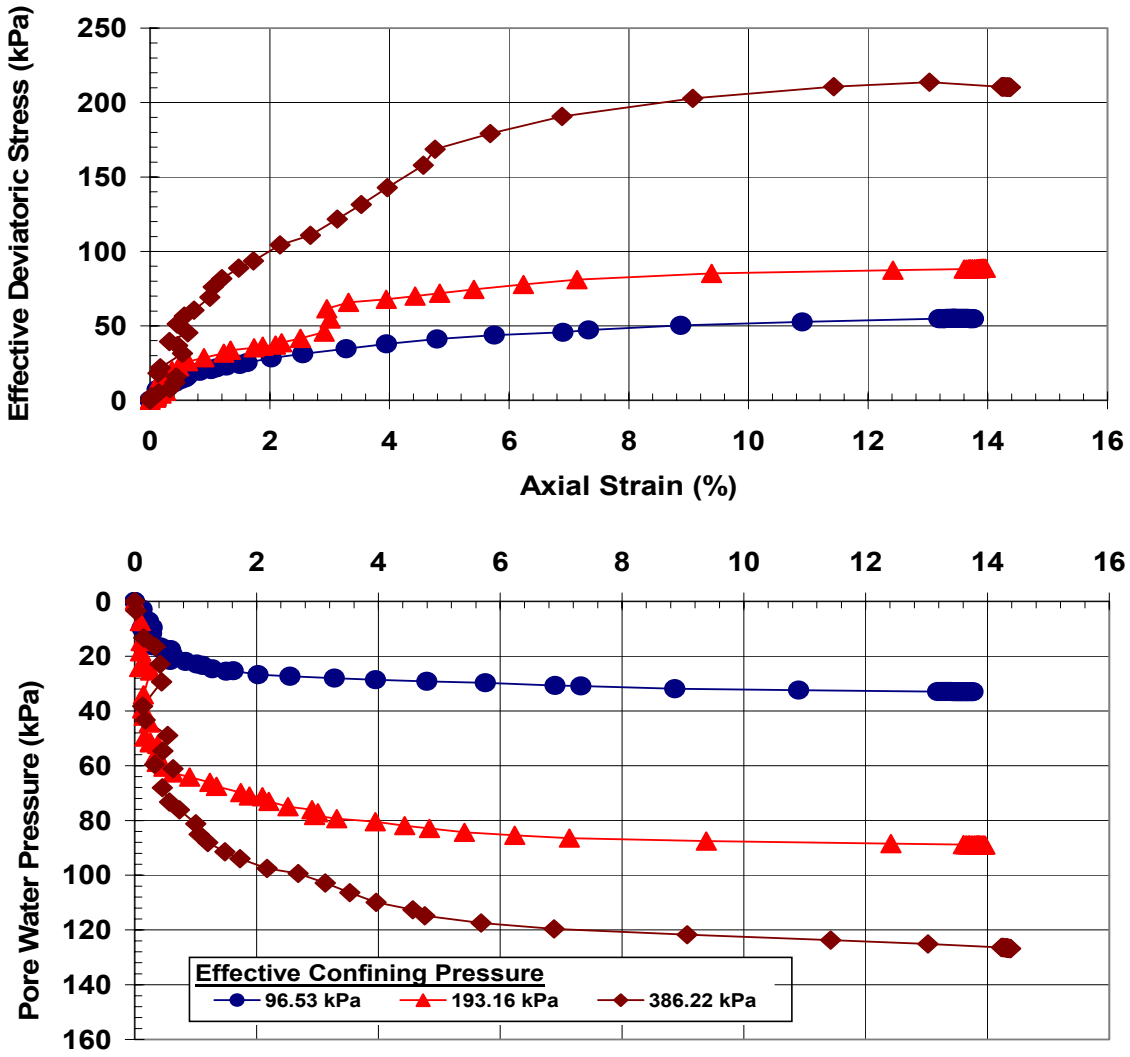

Stress-Strain and Pore Water-Strain Relationships from Triaxial Tests for **10% Fly Ash 1 (FA 1)**

Confining Pressure (σ_3) (kPa)	96.53	193.16	386.22
Back Pressure (kPa)	89.63	89.63	89.63
Sample Height (cm)	14.00	14.00	14.00
Sample Diameter (cm)	7.00	7.00	7.00
Area of Sample (cm^2)	38.48	38.48	38.48
Volume Before Consolidation, V_0 (cm^3)	538.78	538.78	538.78
Volume Change After Consolidation, ΔV_c (cm^3)	45.40	51.30	77.80
Volume After Consolidation, V_c (cm^3)	493.38	487.48	460.98
Area After Consolidation, A_c (cm^2)	35.24	34.82	32.93

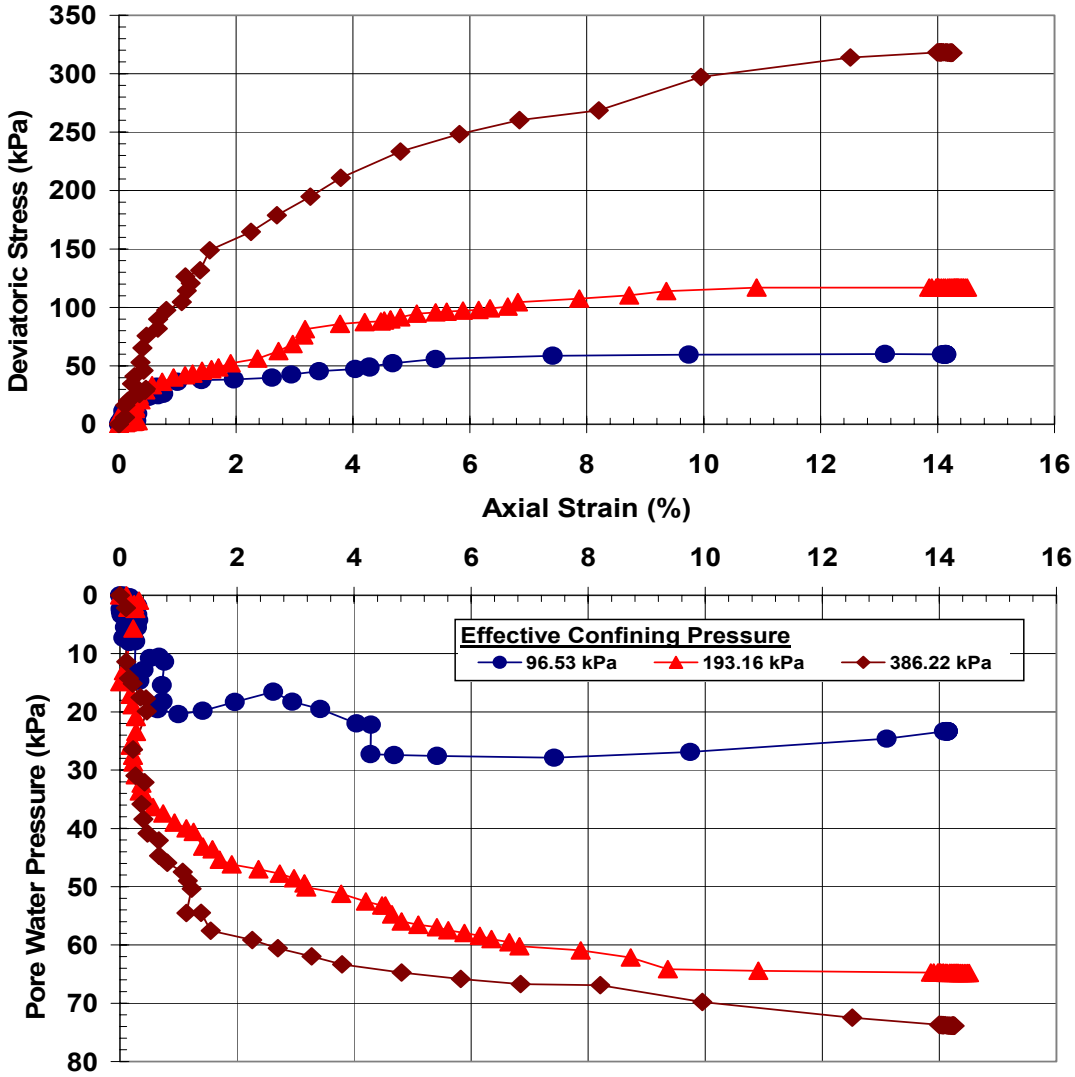

Stress-Strain and Pore Water-Strain Relationships from Triaxial Tests for **20% Fly Ash 1 (FA 1)**

Confining Pressure (σ_3) (kPa)	96.53	193.16	386.22
Back Pressure (kPa)	89.63	89.63	89.63
Sample Height (cm)	14.00	14.00	14.00
Sample Diameter (cm)	7.00	7.00	7.00
Area of Sample (cm^2)	38.48	38.48	38.48
Volume Before Consolidation, V_0 (cm^3)	538.78	538.78	538.78
Volume Change After Consolidation, ΔV_c (cm^3)	45.40	51.30	77.80
Volume After Consolidation, V_c (cm^3)	493.38	487.48	460.98
Area After Consolidation, A_c (cm^2)	35.24	34.82	32.93

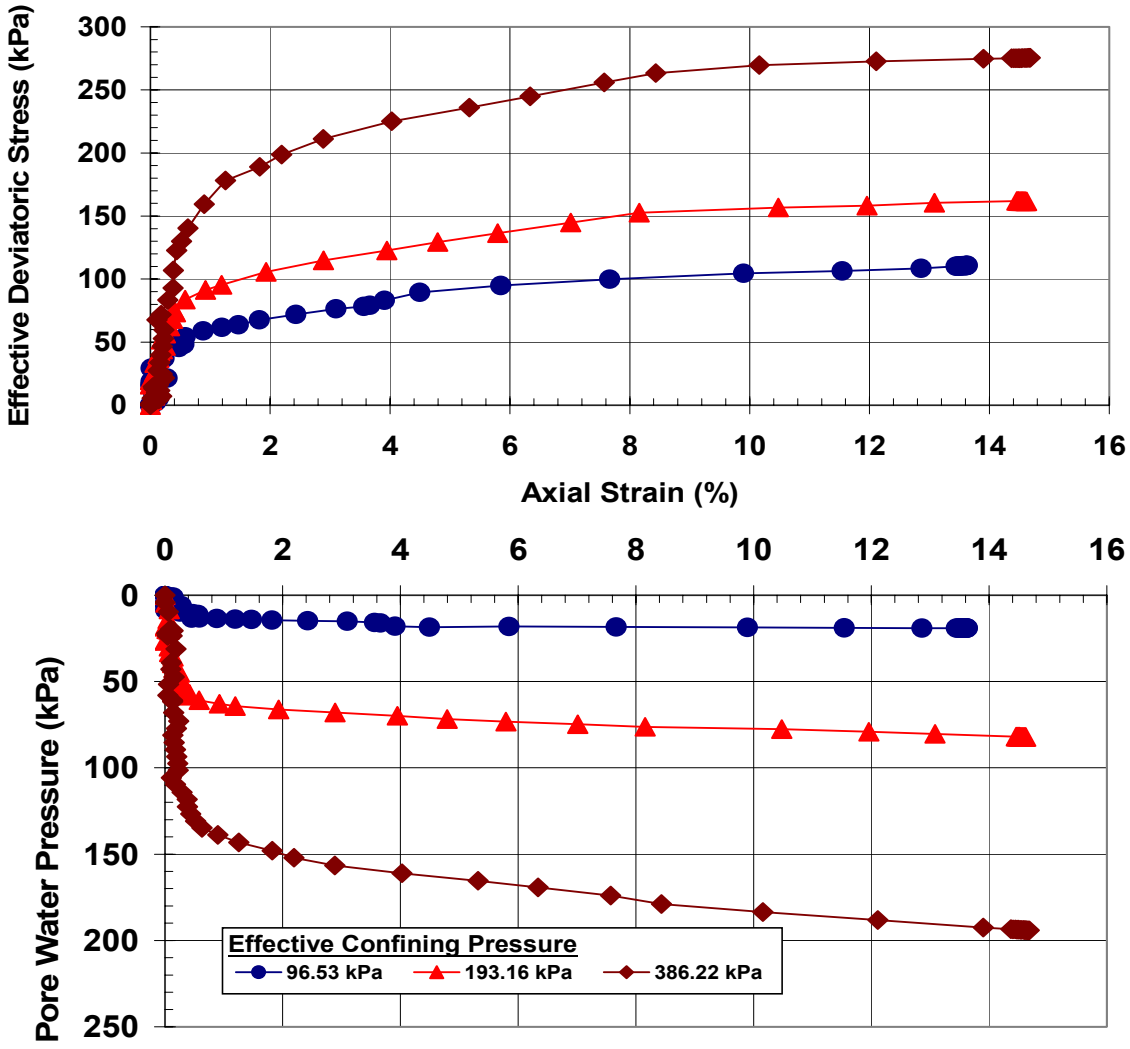

Stress-Strain and Pore Water-Strain Relationships from Triaxial Tests for **40% Fly Ash 1 (FA 1)**

Confining Pressure (σ_3) (kPa)	48.27	96.53	193.16
Back Pressure (kPa)	0.00	0.00	0.00
Sample Height (cm)	14.00	14.00	14.00
Sample Diameter (cm)	7.00	7.00	7.00
Area of Sample (cm^2)	38.48	38.48	38.48
Volume Before Consolidation, V_0 (cm^3)	538.78	538.78	538.78
Volume Change After Consolidation, ΔV_c (cm^3)	4.30	40.30	42.50
Volume After Consolidation, V_c (cm^3)	534.48	498.48	496.28
Area After Consolidation, A_c (cm^2)	38.18	35.61	35.45

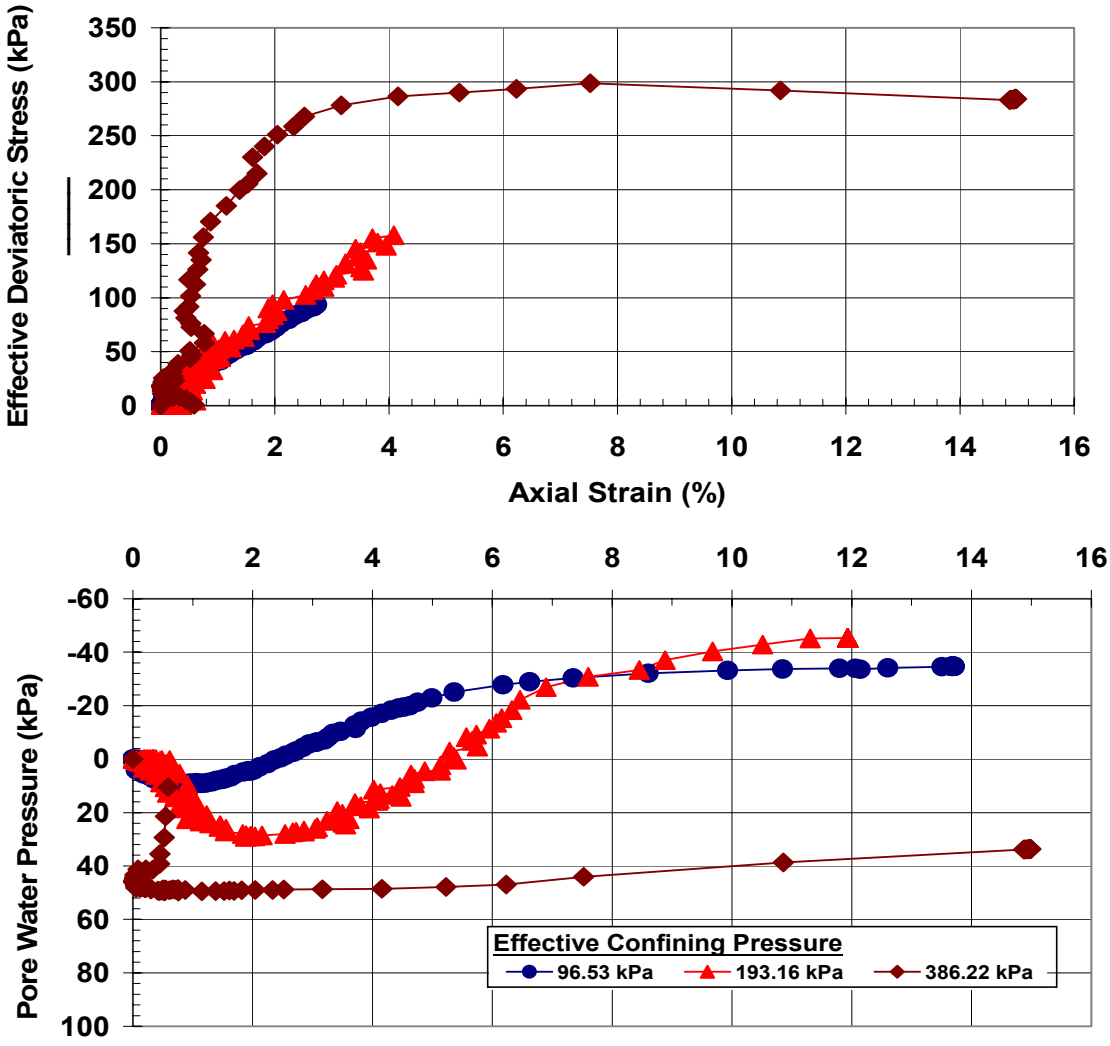

Stress-Strain and Pore Water-Strain Relationships from Triaxial Tests for **100% Fly Ash 1 (FA 1)**

Confining Pressure (σ_3) (kPa)	96.53	193.16	386.22
Back Pressure (kPa)	89.63	89.63	89.63
Sample Height (cm)	14.00	14.00	14.00
Sample Diameter (cm)	7.00	7.00	7.00
Area of Sample (cm^2)	38.48	38.48	38.48
Volume Before Consolidation, V_0 (cm^3)	538.78	538.78	538.78
Volume Change After Consolidation, ΔV_c (cm^3)	45.40	51.30	77.80
Volume After Consolidation, V_c (cm^3)	493.38	487.48	460.98
Area After Consolidation, A_c (cm^2)	35.24	34.82	32.93

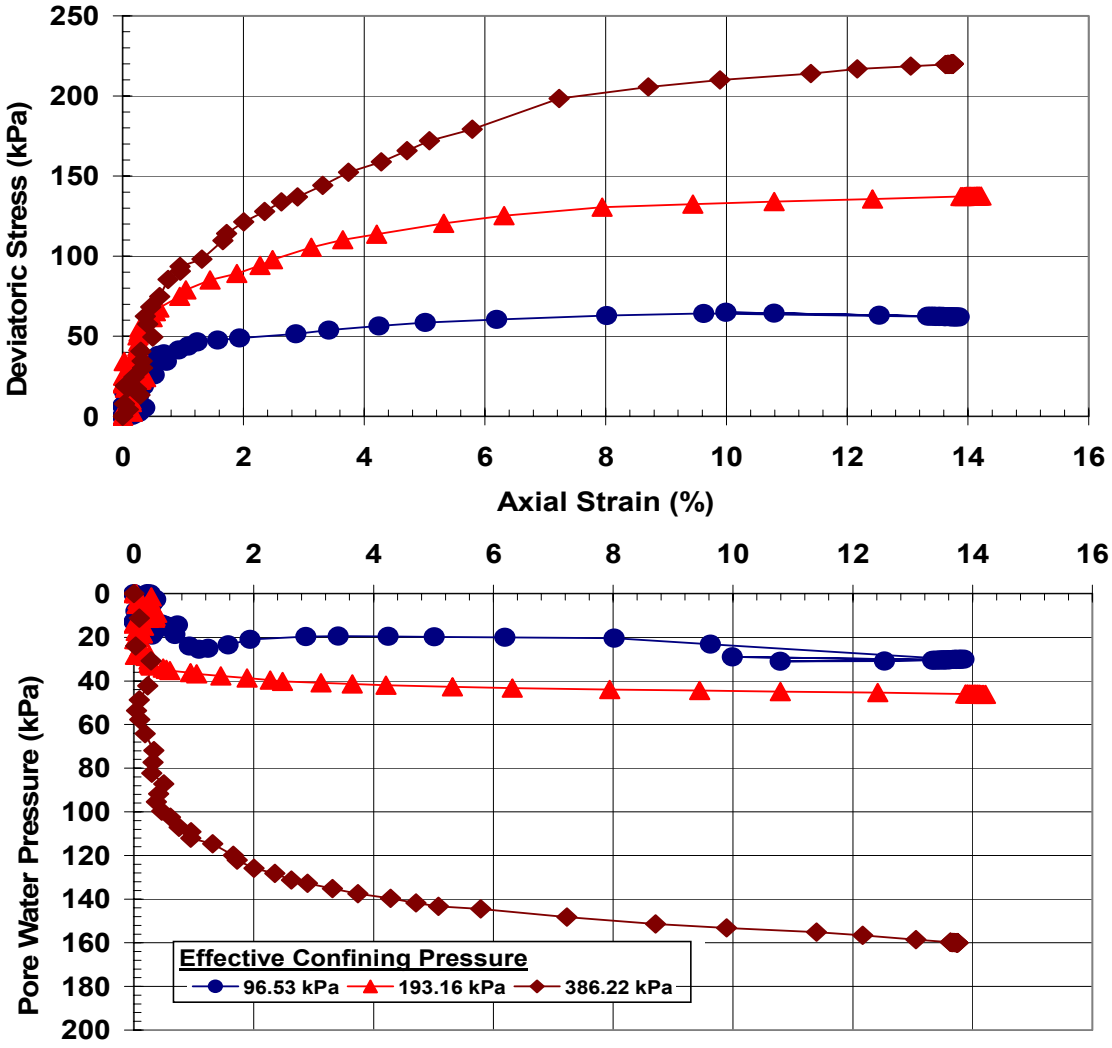

Stress-Strain and Pore Water-Strain Relationships from Triaxial Tests for **10% Fly Ash 2 (FA 2)**

Confining Pressure (σ_3) (kPa)	96.53	193.16	386.22
Back Pressure (kPa)	89.63	89.63	89.63
Sample Height (cm)	14.00	14.00	14.00
Sample Diameter (cm)	7.00	7.00	7.00
Area of Sample (cm^2)	38.48	38.48	38.48
Volume Before Consolidation, V_0 (cm^3)	538.78	538.78	538.78
Volume Change After Consolidation, ΔV_c (cm^3)	45.40	51.30	77.80
Volume After Consolidation, V_c (cm^3)	493.38	487.48	460.98
Area After Consolidation, A_c (cm^2)	35.24	34.82	32.93

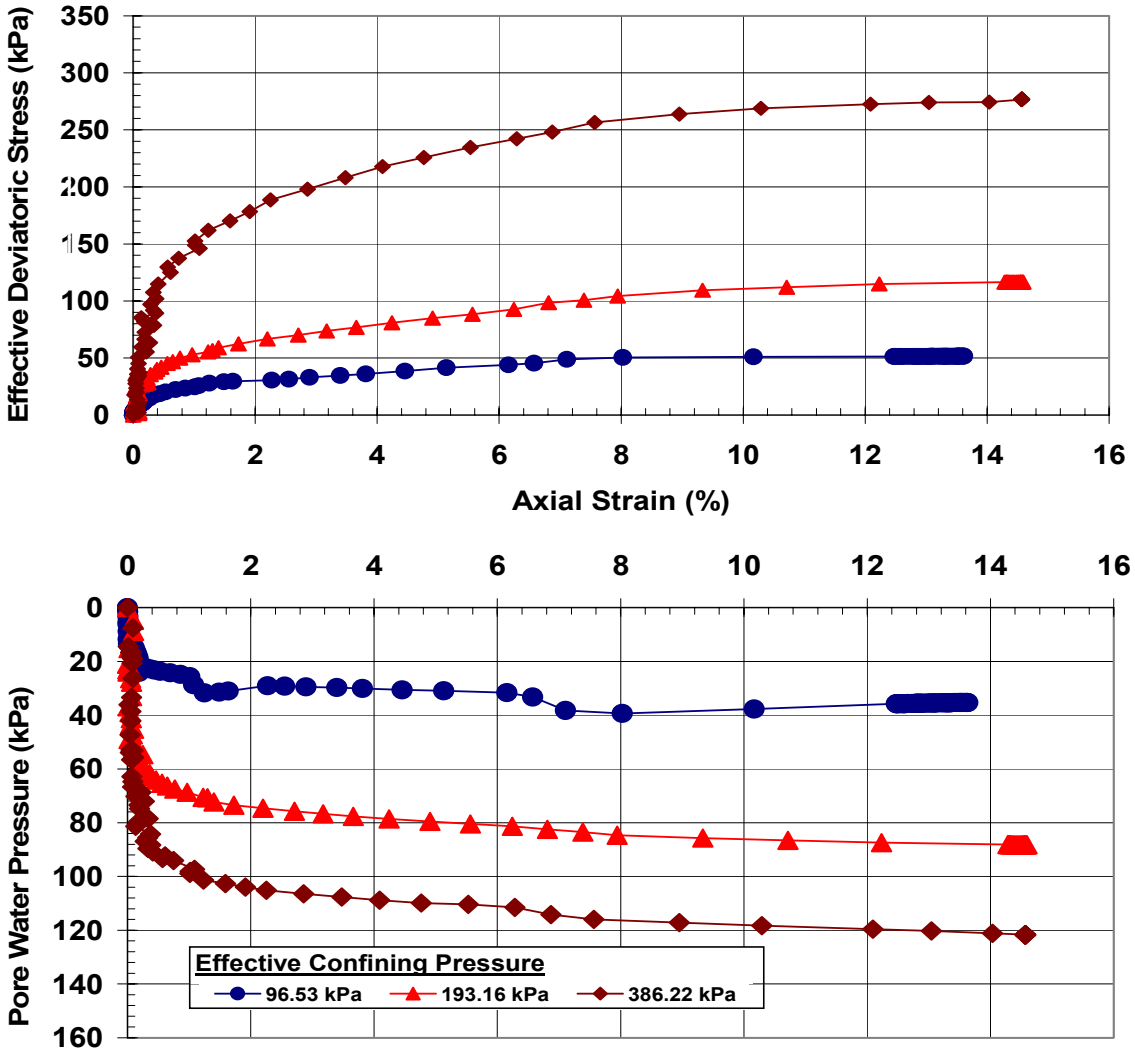

Stress-Strain and Pore Water-Strain Relationships from Triaxial Tests for **20% Fly Ash 2 (FA 2)**

Confining Pressure (σ_3) (kPa)	48.27	68.96	96.53
Back Pressure (kPa)	0.00	0.00	0.00
Sample Height (cm)	14.00	14.00	14.00
Sample Diameter (cm)	7.00	7.00	7.00
Area of Sample (cm^2)	38.48	38.48	38.48
Volume Before Consolidation, V_0 (cm^3)	538.78	538.78	538.78
Volume Change After Consolidation, ΔV_c (cm^3)	3.00	17.40	19.10
Volume After Consolidation, V_c (cm^3)	535.78	521.38	519.68
Area After Consolidation, A_c (cm^2)	38.27	37.24	37.12

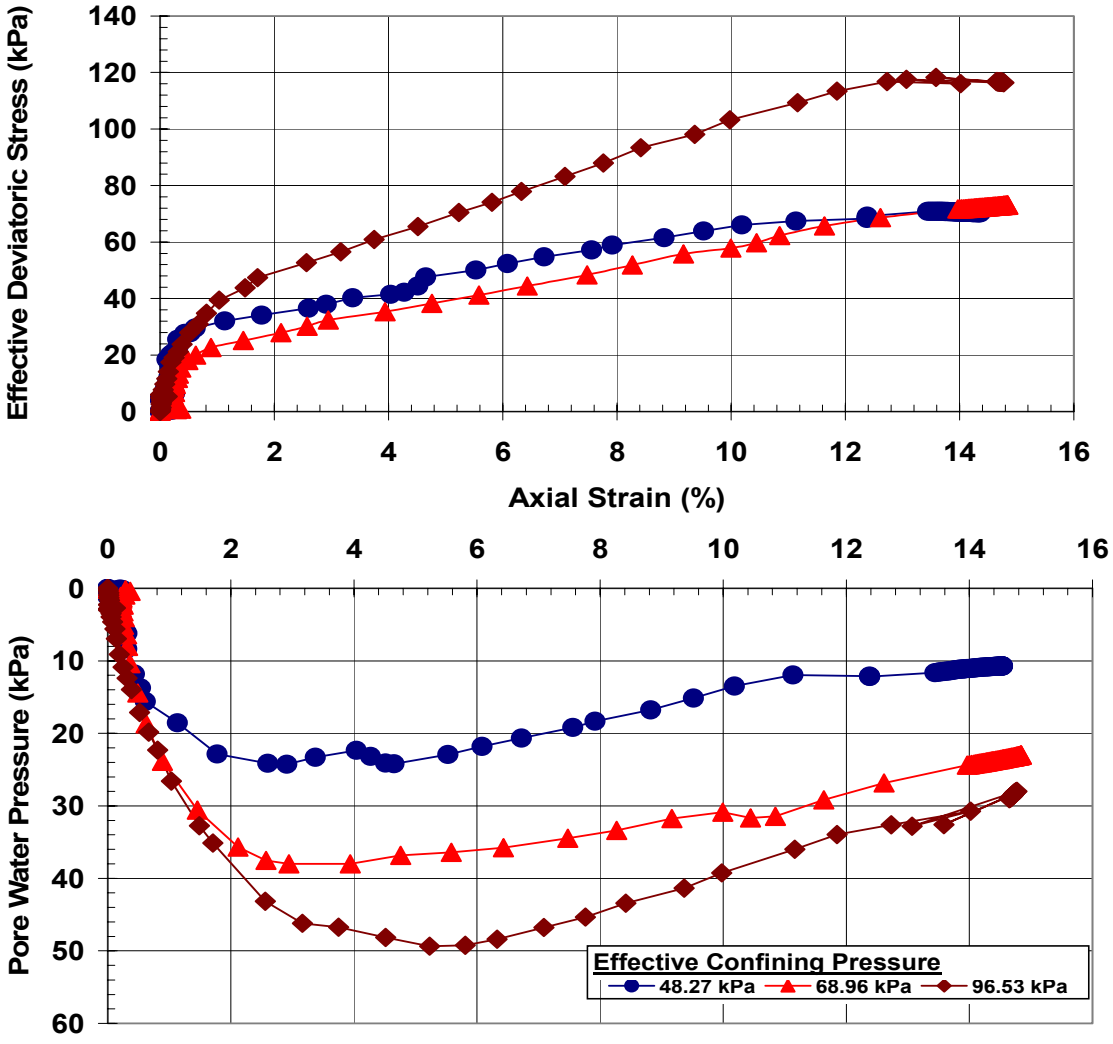

Stress-Strain and Pore Water-Strain Relationships from Triaxial Tests for **100% Fly Ash 2 (FA 2)**

Confining Pressure (σ_3) (kPa)	96.53	193.16	386.22
Back Pressure (kPa)	89.63	89.63	89.63
Sample Height (cm)	14.00	14.00	14.00
Sample Diameter (cm)	7.00	7.00	7.00
Area of Sample (cm^2)	38.48	38.48	38.48
Volume Before Consolidation, V_0 (cm^3)	538.78	538.78	538.78
Volume Change After Consolidation, ΔV_c (cm^3)	45.40	51.30	77.80
Volume After Consolidation, V_c (cm^3)	493.38	487.48	460.98
Area After Consolidation, A_c (cm^2)	35.24	34.82	32.93

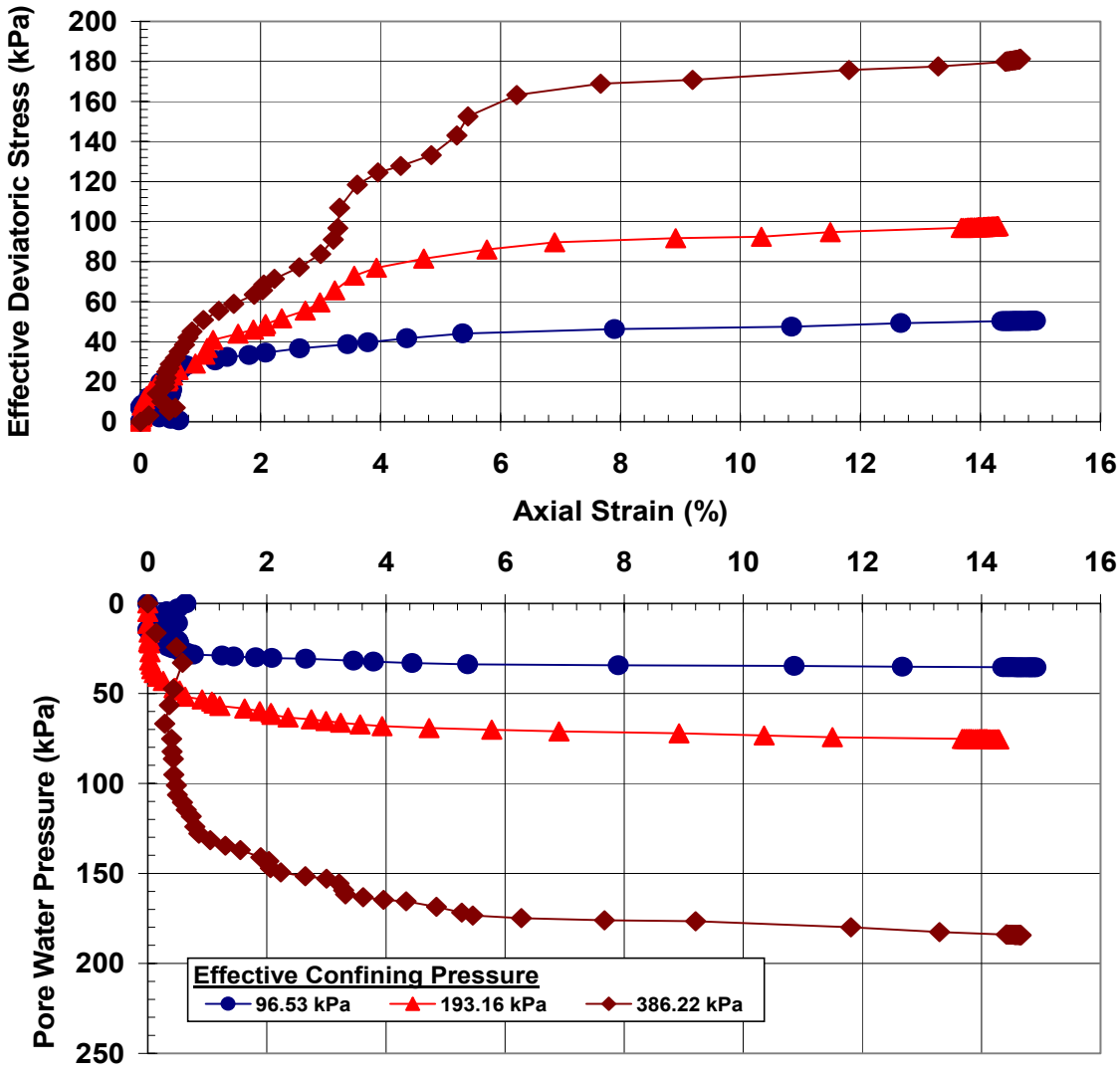

Stress-Strain and Pore Water-Strain Relationships from Triaxial Tests for **10% Fly Ash 3 (FA 3)**

Confining Pressure (σ_3) (kPa)	96.53	193.16	386.22
Back Pressure (kPa)	89.63	89.63	89.63
Sample Height (cm)	14.00	14.00	14.00
Sample Diameter (cm)	7.00	7.00	7.00
Area of Sample (cm^2)	38.48	38.48	38.48
Volume Before Consolidation, V_0 (cm^3)	538.78	538.78	538.78
Volume Change After Consolidation, ΔV_c (cm^3)	45.40	51.30	77.80
Volume After Consolidation, V_c (cm^3)	493.38	487.48	460.98
Area After Consolidation, A_c (cm^2)	35.24	34.82	32.93

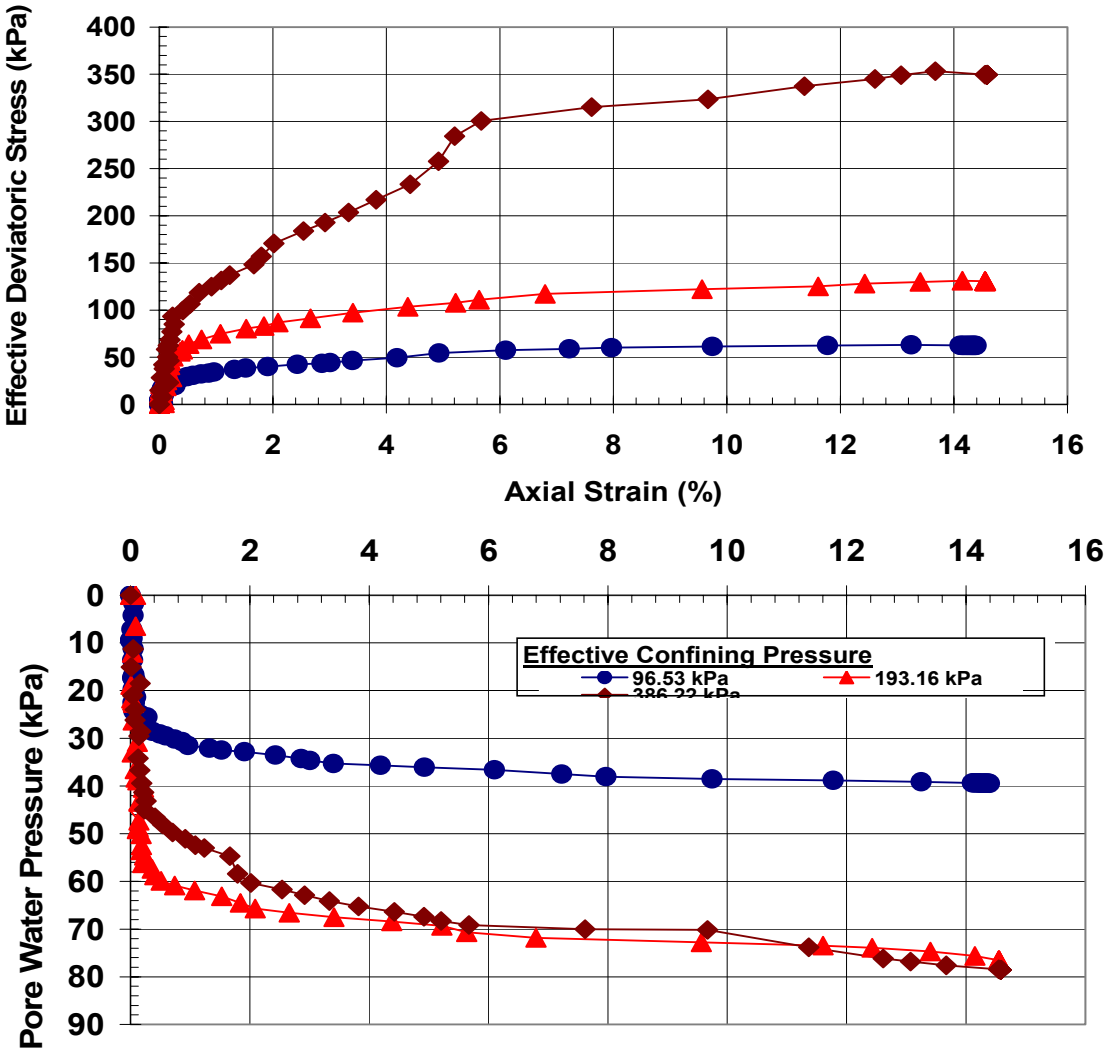

Stress-Strain and Pore Water-Strain Relationships from Triaxial Tests for **20% Fly Ash 3 (FA 3)**

Confining Pressure (σ_3) (kPa)	96.53	193.16	386.22
Back Pressure (kPa)	89.63	89.63	89.63
Sample Height (cm)	14.00	14.00	14.00
Sample Diameter (cm)	7.00	7.00	7.00
Area of Sample (cm^2)	38.48	38.48	38.48
Volume Before Consolidation, V_0 (cm^3)	538.78	538.78	538.78
Volume Change After Consolidation, ΔV_c (cm^3)	45.40	51.30	77.80
Volume After Consolidation, V_c (cm^3)	493.38	487.48	460.98
Area After Consolidation, A_c (cm^2)	35.24	34.82	32.93

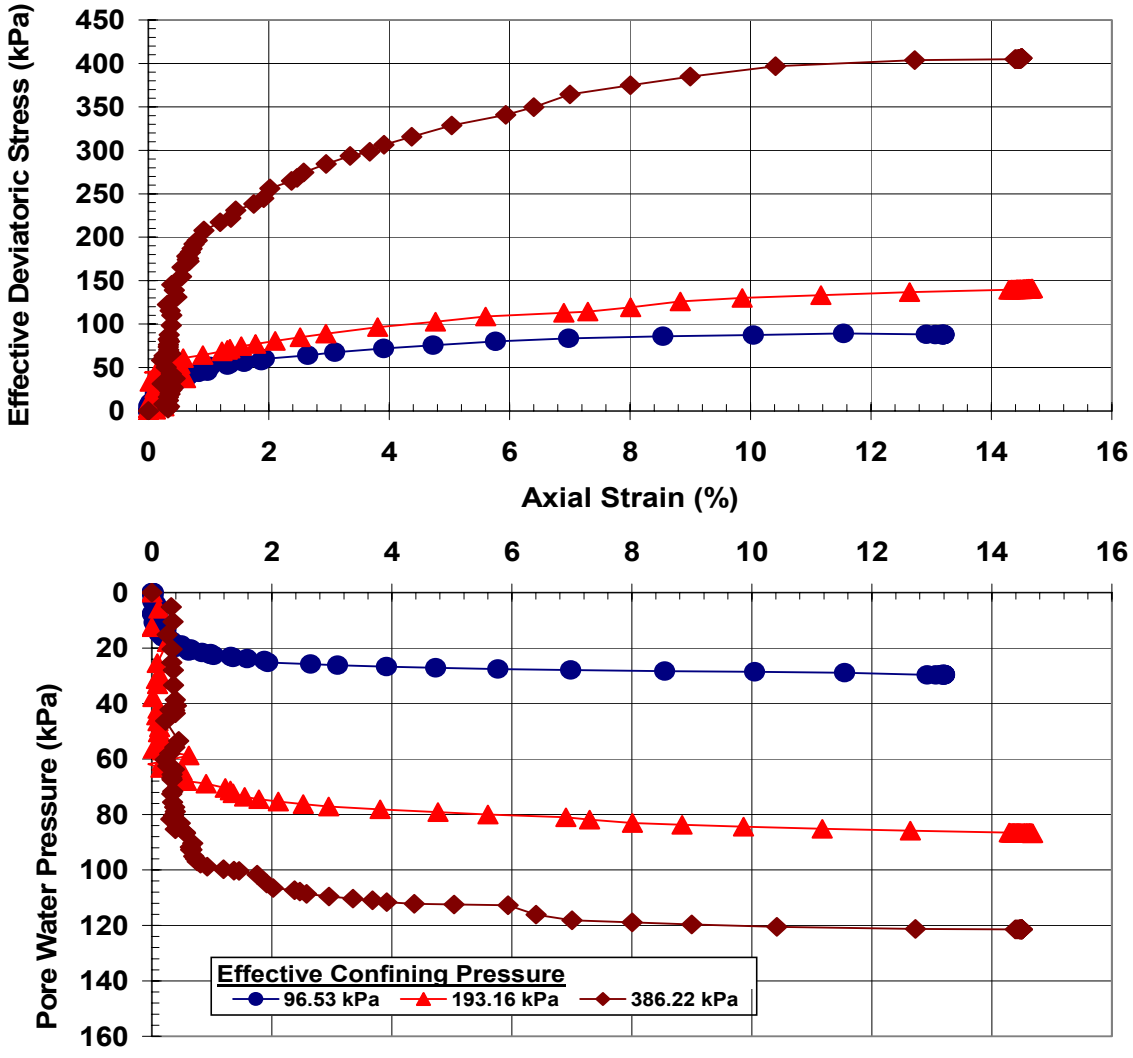

Stress-Strain and Pore Water-Strain Relationships from Triaxial Tests for **40% Fly Ash 3 (FA 3)**

Confining Pressure (σ_3) (kPa)	48.27	68.96	96.53
Back Pressure (kPa)	0.00	0.00	0.00
Sample Height (cm)	14.00	14.00	14.00
Sample Diameter (cm)	7.00	7.00	7.00
Area of Sample (cm^2)	38.48	38.48	38.48
Volume Before Consolidation, V_0 (cm^3)	538.78	538.78	538.78
Volume Change After Consolidation, ΔV_c (cm^3)	3.00	14.60	74.50
Volume After Consolidation, V_c (cm^3)	535.78	524.18	464.28
Area After Consolidation, A_c (cm^2)	38.27	37.44	33.16

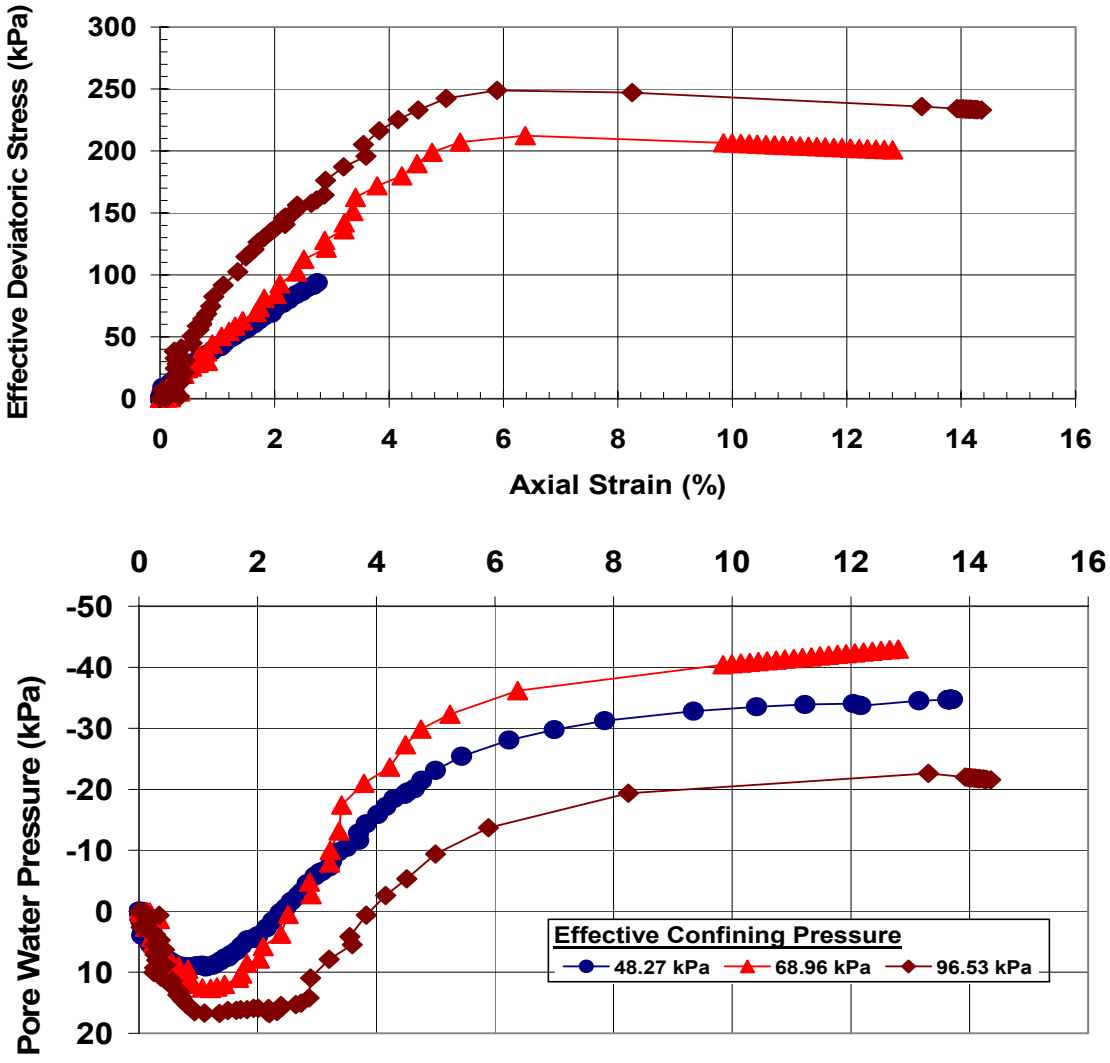

Stress-Strain and Pore Water-Strain Relationships from Triaxial Tests for **100% Fly Ash 3 (FA 3)**